ΠΑΝΕΠΙΣΤΗΜΙΟ ΚΡΗΤΗΣ
ΤΜΗΜΑ ΙΑΤΡΙΚΗΣ
ΤΟΜΕΑΣ ΒΑΣΙΚΩΝ ΕΠΙΣΤΗΜΩΝ

Διδακτορική Διατριβή

Ο ρόλος της απολιποπρωτεΐνης A-I στις αθηροπροστατευτικές δράσεις της λιποπρωτεΐνης υψηλής πυκνότητας (HDL)

Ιωάννα Τηνιακού

Επιβλέπων Καθηγητής: Δημήτρης Καρδάσης

Ηράκλειο, 2015

UNIVERSITY OF CRETE
FACULTY OF MEDICINE
DIVISION OF BASIC SCIENCES

Ph.D. Thesis

The role of apolipoprotein A-I in the atheroprotective functions of high-density lipoprotein (HDL)

Ioanna Tiniakou

Supervisor: Prof. Dimitris Kardassis

Heraklion, 2015

Table of Contents

Abstract

Numerous epidemiological and clinical studies have demonstrated an inverse correlation between plasma high-density lipoprotein (HDL) cholesterol levels and the risk for coronary heart disease in humans. Apolipoprotein A-I (apoA-I) constitutes the major protein component of HDL and possesses a central role in HDL biogenesis, structure and function. ApoA-I interacts with several receptors and enzymes (ABCA1, ABCG1, SR-BI, LCAT) that participate in HDL metabolism and functions. The above interactions lead to the activation of atheroprotective mechanisms such as cholesterol efflux, maintenance of endothelial integrity as well as mechanisms involving anti-oxidative, anti-inflammatory and anti-apoptotic actions. The aim of this PhD thesis was to study the role of apoA-I in the anti-inflammatory and atheroprotective functions of HDL *in vivo.*

Rheumatoid arthritis (RA) is a chronic inflammatory autoimmune disease that is associated with increased cardiovascular morbidity and mortality. In addition, low HDL cholesterol levels are considered a marker for various chronic inflammatory conditions, while the levels of pro-inflammatory HDL are increased in RA patients.

In Chapter I we studied the role of HDL in RA. For this purpose, we used a model of antigen-induced arthritis in wild-type and in apoA-I$^{-/-}$ mice to investigate the effect of HDL deficiency on the pathogenesis of RA as well as the effect of chronic inflammation on HDL levels and atheroprotective functions. Moreover, we assessed HDL's ability to modulate the immune system and attenuate the inflammatory response. Following induction of arthritis, wild-type mice demonstrated moderate to severe inflammation while the majority of apoA-I$^{-/-}$ mice exhibited a more severe phenotype which was associated with pannus formation. In order to study the effect of HDL on Th1 and Th17 immune responses which are implicated in RA development, the antigen-specific proliferation and differentiation of Th cells in the presence of increasing amounts of reconstituted HDL was determined in draining lymph nodes (dLNs) from ovalbumin-immunized wild-type mice. The induction and proliferation of autoreactive T cells was determined by measuring cytokine levels (IFN-γ, IL-17, IL-2) in culture medium. According to these results

treatment of dLN cells with rHDL led to a dose-dependent suppression of cytokine secretion. Next, we studied the effect of rHDL treatment on bone-marrow-derived dendritic cells (BMDCs) and concluded that rHDL suppressed pro-inflammatory cytokine secretion (IL-6, IL-12, IL-23, IL-8, TNF-α) and downregulated co-stimulatory molecules (CD40, CD80, CD86, MHC-II) in these cells. Finally, we showed that the suppressive effect of rHDL was attenuated in BMDCs lacking either ABCA1 or SR-BI, thus providing evidence for an important role of these two membrane lipid transporters in the HDL-mediated anti-inflammatory functions on DCs.

In Chapter II we investigated the effect of two naturally occurring mutations of human apoA-I, apoA-I(L141R)$_{Pisa}$ and apoA-I(L159R)$_{FIN}$, on HDL biogenesis and atherosclerosis development *in vivo*. Humans that are heterozygotes for either of these apoA-I mutations exhibit very low levels of plasma HDL cholesterol and some of them develop premature atherosclerosis.

In order to study the properties of the above mutations *in vivo* we generated transgenic mice that express either wild-type or mutant human apoA-I in the liver. Briefly, wild-type and mutant forms of apoA-I were cloned downstream of the mouse transthyretin promoter (TTR1). The TTR1-apoA-I fragments were excised and used to inject male pronucleus of C57BL6/CBA F2 fertilized eggs for transgenesis purposes. Selected founder animals were crossed with apoA-I$^{-/-}$ mice to obtain human apoA-I transgenic mice on an apoA-I deficient background. The human apoA-I transgenic mice were analyzed for abnormalities in their lipid and lipoprotein profile, in HDL structure and functionality as well as for predisposition to atherosclerosis. Transgenic mice expressing either mutant apoA-I form were characterized by very low serum total and HDL-cholesterol, as well as serum apoA-I levels. Moreover, these mice generated only few small spherical HDL particles with pre-β2 and α3, α4 electrophoretic mobility. HDL particles containing either apoA-I mutant exhibited attenuated anti-oxidative properties but increased capacity to promote ABCA1-dependent cholesterol efflux and endothelial cell migration. Finally, the expression of human apoA-I(L141R)$_{Pisa}$ or apoA-I(L159R)$_{FIN}$ in mice was associated with increased diet-induced

atherosclerosis compared to mice expressing wild-type apoA-I and apoA-I deficient mice.

Recent studies suggest that the normally atheroprotective HDL can be rendered atherogenic as a result of the myeloperoxidase (MPO)-mediated oxidative modifications in apoA-I. It has been shown that MPO-dependent chlorination of Tyr-192 combined with oxidation of Met-148 residues of apoA-I inhibit its ability to promote ABCA1-mediated cholesterol efflux. Moreover, *in vitro* studies have demonstrated that oxidation of Met-148 by MPO impairs the ability of apoA-I to activate LCAT. However, the mechanisms underlying formation of dysfunctional HDL particles remain largely unknown.

In Chapter III we aimed at investigating the mechanisms of apoA-I modification by MPO leading to the generation of dysfunctional HDL *in vivo*. For this purpose, we generated recombinant adenoviruses carrying either wild-type (apoA-I WT) or mutant forms of apoA-I [apoA-I(Met148Ala) και apoA-I(Tyr192Ala)] as well as adenovirus expressing human MPO. The above mutations in the human apoA-I gene were generated by site-directed mutagenesis, while the human MPO cDNA sequence was cloned from neutrophils isolated from human peripheral blood. All sequences were subcloned into the pAdTrack-CMV vector and recombinant adenoviruses were generated according to the AdEasy protocol, purified by CsCl gradient ultracentrifugation and titrated by performing the plaque assay. The titrated adenoviruses were used to infect cells to determine efficient production and secretion of the corresponding protein. The adenoviruses expressing the above apoA-I mutants will be used either separately or in combination with the adenovirus expressing MPO to infect apoA-I$^{-/-}$ mice, and allow the investigation of the *in vivo* effect of MPO on lipids concentration, HDL structure and functions.

Genome-wide association studies have identified new genetic loci, including the GALNT2 (GalNAc Transferase 2) gene, that are associated with low HDL levels. GALNT2 is an enzyme that participates in O-glycosylation of proteins by catalyzing the transfer an N-acetyl galactosamine to serine/threonine residues. Since O-glycosylation possesses a regulatory role in protein function, it is possible that GALNT2 affects lipid concentration by modifying several of the proteins that participate in the HDL pathway.

In Chapter IV we aimed at investigating the role of GALNT2 in HDL metabolism *in vivo* by performing adenovirus-mediated gene transfer in apoA-I transgenic mice. To this end, the sequence of human GALNT2 cDNA was cloned from HepG2 cells and then subcloned into an appropriate vector which was used to generate a recombinant adenovirus expressing GALNT2 (Ad-GALNT2) according to the AdEasy methodology. The generated adenovirus was subsequently amplified, purified and titrated as aforementioned. Adenovirus-mediated gene transfer will be performed in transgenic mice that express the human apoA-I gene under the control of its proximal promoter and enhancer in an apoA-I deficient background. Following infection, a series of analyses will be performed in order to determine serum lipids concentration, enzyme activities (LPL, LCAT) as well as HDL structure and functionality. The above experiments will provide insights on the effect of GALNT2 on HDL structure and metabolism *in vivo*

.

Περίληψη

Επιδημιολογικές και κλινικές μελέτες έχουν καταδείξει μια αντιστρόφως ανάλογη συσχέτιση μεταξύ των επίπεδων της HDL χοληστερόλης και του κινδύνου εμφάνισης στεφανιαίας νόσου στον άνθρωπο. Κύριο πρωτεϊνικό συστατικό των λιποπρωτεϊνών υψηλής πυκνότητας (HDL) αποτελεί η απολιποπρωτεΐνη A-I (αποA-I), η οποία και κατέχει σημαντικό ρόλο στη βιογένεση, τη δομή, καθώς και τις λειτουργίες της HDL. Η αποA-I αλληλεπιδρά με πλήθος υποδοχέων και ενζύμων (ABCA1, ABCG1, SR-BI, LCAT) που συμμετέχουν ενεργά στην βιογένεση, τον καταβολισμό και τις λειτουργίες της HDL. Αποτέλεσμα αυτών των αλληλεπιδράσεων είναι η ενεργοποίηση μηχανισμών, όπως η εκροή χοηστερόλης, η διατήρηση της ακεραιότητας του ενδοθηλίου καθώς και αντι-οξειδωτικοί, αντι-φλεγμονώδεις και αντι-αποπτωτικοί μηχανισμοί, οι οποίοι συμβάλλουν στην προστασία από την αθηρωμάτωση. Σκοπός της παρούσας διδακτορικής διατριβής ήταν η μελέτη του ρόλου της αποA-I στις αντιφλεγμονώδεις και τις αθηροπροστατευτικές δράσεις της HDL *in vivo.*

Η ρευματοειδής αρθρίτιδα (PA) είναι μια χρόνια αυτοάνοση νόσος με αυξημένη θνητότητα, η οποία οφείλεται μερικώς σε καρδιαγγειακά αίτια. Επιπλέον, τα χαμηλά επίπεδα HDL χοληστερόλης αποτελούν δείκτη για διάφορες φλεγμονώδεις νόσους, ενώ τα επίπεδα προφλεγμονώδους HDL βρίσκονται αυξημένα σε ασθενείς με PA.

Στόχος της πρώτης ενότητας της παρούσας διατριβής ήταν η μελέτη του ρόλου της HDL στη ρευματοειδή αρθρίτιδα. Για το σκοπό αυτό εφαρμόσθηκε ένα μοντέλο της ασθένειας σε αγρίου τύπου ποντικούς και ποντικούς με έλλειψη σε αποA-I (apoA-I$^{-/-}$) και μελετήθηκε σε αυτό η επίδραση της έλλειψης της HDL στην παθογένεση της PA, η επίδραση της χρόνιας φλεγμονής στα επίπεδα και τις αθηροπροστατευτικές δράσεις της HDL, καθώς και κατά πόσο η HDL μπορεί να δράσει στο ανοσοποιητικό σύστημα οδηγώντας σε μείωση της φλεγμονής. Έπειτα από την επαγωγή της αρθρίτιδας οι ποντικοί αγρίου τύπου εμφάνισαν κατά κύριο λόγο μέτρια έως σοβαρή φλεγμονή, ενώ η πλειοψηφία των apoA-I$^{-/-}$ ποντικών εμφάνισαν το βαρύτερο φαινότυπο που χαρακτηρίζεται από το σχηματισμό πάννου. Προκειμένου να μελετηθεί η επίδραση της HDL στις Th1 και Th17 ανοσοαπόκρισεις, οι οποίες εμπλέκονται

στην ανάπτυξη της PA, πραγματοποιήθηκε ανοσοποίηση αγρίου τύπου ποντικών με οβαλβουμίνη και προσδιορίστηκε ο αντιγονο-ειδικός πολλαπλασιασμός και η διαφοροποίηση των Th λεμφοκυττάρων παρουσία αυξανόμενων συγκεντρώσεων συνθετικής HDL (rHDL). Η επαγωγή και ο πολλαπλασιασμός των αυτοδραστικών Τ λεμφοκυττάρων προσδιορίστηκε με βάση τα εκκρινόμενα επίπεδα κυτταροκινών (IFN-γ, IL-17, IL-2) στα θρεπτικά μέσα των καλλιεργειών. Τα αποτελέσματα αυτών των πειραμάτων κατέδειξαν μια δοσο-εξαρτώμενη αναστολή στη σύνθεση των κυτταροκινών σαν αποτέλεσμα της χορήγησης αυξανόμενων συγκεντρώσεων rHDL στα κύτταρα. Στη συνέχεια, μελετήθηκε η επίδραση της rHDL σε καλλιέργεια δενδριτικών κυττάρων, στα οποία η επώαση με rHDL οδήγησε σε μείωση της έκκρισης προ-φλεγμονωδών κυτταροκινών (IL-6, IL-12, IL-23, IL-8, TNF-α) και της έκφρασης συν-διεγερτικών μορίων (CD40, CD80, CD86, MHC-II). Τέλος, μελετήθηκε η επίδραση της rHDL σε καλλιέργεια δενδριτικών κυττάρων με έλλειψη σε καθέναν από τους υποδοχείς της HDL (ABCG1, ABCA1, SR-BI). Στην περίπτωση των δενδριτκών κυττάρων με έλλειψη στον ABCA1 ή τον SR-BI, η rHDL δε μπόρεσε να καταστείλλει την ενεργοποίηση τους καταδεικνύοντας τη συμμετοχή των δύο αυτών υποδοχέων στον μηχανισμό δράσης της.

Το δεύτερο μέρος της παρούσας διατριβής αφορά στη μελέτη της επίδρασης δύο φυσικά απαντώμενων μεταλλάξεων της αποA-I, των αποA-I(L141R)$_{Pisa}$ και αποA-I(L159R)$_{FIN}$ στη βιογένεση της HDL και την ανάπττυξη αθηροσκλήρωσης *in vivo*. Ετεροζυγώτες για οποιαδήποτε από τις δύο παραπάνω μεταλλάξεις παρουσιάζουν πολύ χαμηλά επίπεδα HDL χοληστερόλης στο πλάσμα και ορισμένοι από αυτούς εμφανίζουν πρόωρη αθηροσκλήρωση.

Για τη μελέτη των ιδιοτήτων των συγκεκριμένων μεταλλάξεων *in vivo* δημιούργηθηκαν διαγονιδιακοί ποντικοί οι οποίοι εκφράζουν την ανθρώπινη αποA-I στο ήπαρ. Για το σκοπό αυτό, η αγρίου τύπου (WT) και τα παραπάνω μεταλλάγματα της ανθρώπινης αποA-I κλωνοποιήθηκαν σε κατάλληλο φορέα καθοδικά του υποκινητή του γονιδίου της τρανσθυρετίνης (TTR1). Από την ανάλυση αυτή προέκυψαν τα ζώα «ιδρυτές», τα οποία διασταυρώθηκαν με apoA-I$^{-/-}$ ποντικούς για τη δημιουργία διαγονιδιακών ποντικών που εκφράζουν μόνο την αντίστοιχη, είτε αγρίου τύπου είτε μεταλλαγμένη,

ανθρώπινη αποA-I. Τα ζώα που προέκυψαν χαρακτηρίστηκαν ως προς το λιπιδικό και λιποπρωτεϊνικό τους προφίλ, τη δομή και τη λειτουργικότητα της HDL και την ανάπτυξη αθηροσκλήρωσης. Οι διαγονιδιακοί ποντικοί που εξέφραζαν οποιοδήποτε εκ των δύο μεταλλαγμάτων της αποA-I εμφάνισαν πολύ χαμηλά επίπεδα ολικής και HDL χοληστερόλης, καθώς και αποA-I στον ορό. Επιπλέον, στον ορό αυτών των ποντικών ανιχνεύθηκαν λίγα μικρού μεγέθους HDL σωματίδια με preβ2 και α3, α4 ηλεκτροφοριτική κινητικότητα. Επιπλέον, τα HDL σωματιδία που έφεραν τις μεταλλαγμένες μορφές της αποA-I εμφάνισαν μειωμένες αντι-οξειδωτικές ιδιότητες αλλά αυξημένη ικανότητα ABCA1-εξαρτώμενης εκροής χοληστερόλης από τα μακροφάγα, καθώς και αυξημένη ικανότητα να προωθούν τη μετανάστευση των ενδοθηλιακών κυττάρων. Τέλος, έπειτα από 14 εβδομάδες σε δίαιτα υψηλής περιεκτικότητας σε λίπη, η ανάπτυξη αθηρωματικών πλακών στην αορτή ήταν σημαντικά υψηλότερη στους διαγονιδιακούς ποντικούς που εξέφραζαν τις μεταλλαγμένες μορφές της αποA-I σε σχέση με αυτούς που είτε εξέφραζαν την αγρίου τύπου αποA-I είτε εμφάνιζαν παντελή έλλειψη της αποA-I (apoA-I$^{-/-}$).

Πρόσφατες έρευνες υποστηρίζουν πως η φυσιολογικά αθηροπροστατευτική HDL μπορεί να μετατραπεί σε αθηρογόνο ως αποτέλεσμα των οξειδωτικών τροποποιήσεων που υφίσταται η αποA-I από το ένζυμο μυελοπεροξειδάση (MPO). Συγκεκριμένα, έχει προταθεί πως ο συνδυασμός χλωρίωσης της τυροσίνης-192 και οξείδωσης της μεθειονίνης-148 μειώνει την ικανότητα της αποA-I να επάγει έξοδο χοληστερόλης μέσω του μεταφορέα ABCA1. Επιπλέον, *in vitro* πειράματα έχουν δείξει πως η οξείδωση της μεθειονίνης-148 από την MPO οδηγεί σε απώλεια της ικανότητας της αποA-I να ενεργοποιήσει το ένζυμο LCAT. Τα αίτια, καθώς και οι μηχανισμοί δημιουργίας δυσλειτουργικών μορίων HDL παραμένουν αδιευκρίνιστα.

Στόχος του τρίτου μέρους της διατριβής ήταν η μελέτη των μηχανισμών με τους οποίους η μυελοπεροξειδάση επιδρά στην αποA-I και παράγει δυσλειτουργικά HDL σωματίδια *in vivo*. Για το σκοπό αυτό δημιουργήθηκαν ανασυνδυασμένοι αδενοϊοί που εκφράζουν την αγρίου τύπου αποA-I (apoA-I WT), τις μεταλλαγμένες μορφές apoA-I(Met148Ala) και apoA-I(Tyr192Ala), καθώς και την ανθρώπινη μυελοπεροξειδάση. Αρχικά, χρησιμοποιήθηκε η

μέθοδος κατευθυνόμενης μεταλλαξιγένεσης για τη δημιουργία των παραπάνω μεταλλάξεων στο γονίδιο της ανθρώπινης αποA-I. Παράλληλα, ουδετερόφιλα κύτταρα απομονώθηκαν από ανθρώπινο ολικό αίμα και το RNA που απομονώθηκε από αυτά χρησιμοποιήθηκε για την κλωνοποίηση του cDNA της MPO. Οι αλληλουχίες που προέκυψαν κλωνοποιήθηκαν στο φορέα pAdTrack-CMV και οι αντίστοιχοι ανασυνδυασμένοι αδενοϊοί παρήχθησαν σε μεγάλη κλίμακα με τη μέθοδο AdEasy, απομονώθηκαν με υπερφυγοκέντρηση σε διαβάθμιση χλωριούχου καισίου και τιτλοδοτήθηκαν με τη δοκιμασία σχηματισμού μολυσματικών πλακών. Οι τιτλοδοτημένοι αδενοϊοί ελέγχθηκαν ως προς τη μολυσματικότητά τους και την παραγωγή της αντίστοιχης πρωτεΐνης. Οι παραπάνω αδενοϊοί που εκφράζουν τις διάφορες μορφές αποA-I μπορούν μελλοντικά να χρησιμοποιηθούν είτε μεμονωμένα είτε σε συνδυασμό με τον αδενοϊό που εκφράζει MPO για την επιμόλυνση apoA-I$^{-/-}$ ποντικών. Με τον τρόπο αυτό θα μπορέσει να προσδιοριστεί *in vivo* η επίδραση του ενζύμου αυτού στα επίπεδα των λιπιδίων του πλάσματος, το σχήμα, το μέγεθος και τη λειτουργικότητα της HDL.

Πρόσφατες γονιδιωματικές μελέτες μεγάλης κλίμακας έχουν αναδείξει νέους γενετικούς τόπους, μεταξύ των οποίων το γονίδιο GALNT2 (GalNAc Transferase 2), που σχετίζονται με χαμηλά επίπεδα HDL. Η GALNT2 είναι ένα ένζυμο που συμμετέχει στην O-γλυκοζυλίωση και καταλύει τη μεταφορά σακχάρων σε κατάλοιπα σερίνης ή θρεονίνης πρωτεϊνών. Δεδομένου ότι η O-γλυκοζυλίωση κατέχει ρυθμιστικό ρόλο για πληθώρα πρωτεϊνών, είναι πιθανό η GALNT2 να επηρεάζει τις συγκεντρώσεις των λιπιδίων τροποποιώντας διάφορες πρωτεΐνες που συμμετέχουν στο μεταβολισμό της HDL.

Η τελευταία ενότητα αφορά τη μελέτη του ρόλου της GALNT2 στο μεταβολισμό της HDL *in vivo* με χρήση της γονιδιακής μεταφοράς μέσω αδενοϊών σε apoA-I διαγονιδιακούς ποντικούς. Για το σκοπό αυτό αρχικά απομονώθηκε από κύτταρα HepG2 το cDNA της ανθρώπινης GALNT2 το οποίο κλωνοποιήθηκε σε κατάλληλο φορέα, και στη συνέχεια χρησιμοποιήθηκε για την παραγωγή του αδενοϊού Ad-GALNT2 σύμφωνα με το πρωτόκολλο AdEasy. Ο αδενοϊός παρήχθη σε μεγάλη κλίμακα, απομονώθηκε και τιτλοδοτήθηκε όπως αναφέρθηκε παραπάνω. Ο τιτλοδοτημένος αδενοϊός πρόκειται μελλοντικά να χορηγηθεί σε ποντικούς από τους οποίους έχει απαλειφεί το γονίδιο της αποA-I, ενώ ταυτόχρονα

φέρουν το ανθρώπινο γονίδιο της αποA-I υπό τον έλεγχο του φυσικού υποκινητή και ενισχυτή του. Στους μολυσμένους ποντικούς θα πραγματοποιηθεί μια σειρά αναλύσεων προκειμένου να προσδιοριστούν τα επίπεδα λιπιδίων στο πλάσμα, η δραστικότητα συγκεκριμένων ενζύμων (LPL, LCAT), καθώς και η δομή και η λειτουργικότητα των HDL σωματιδίων που θα προκύψουν. Με τον τρόπο αυτό θα μπορέσει να εκτιμηθεί η επίδραση της GALNT2 τόσο στη δομή όσο και το μεταβολισμό της HDL *in vivo*.

1. INTRODUCTION

1.1 Biological role and classification of lipoproteins

Cholesterol is an essential component of mammalian cell membranes that is required for maintenance of membrane permeability and regulation of membrane fluidity. It participates in various biological functions including intracellular transport, cell signaling by being an essential component of lipid rafts and neuronal transduction (1) while it also serves as a precursor molecule in several biochemical pathways (steroid hormone and bile acid synthesis) (2, 3). The importance of cholesterol is highlighted by the fact that abnormal plasma cholesterol levels have been associated with the pathogenesis of atherosclerosis and other diseases (4-7).

Lipids, such as cholesterol and triglycerides, are insoluble in plasma and their transport through the bloodstream and distribution to various tissues is achieved by their packaging in lipoproteins. Lipoproteins are macromolecular structures formed by the association of proteins and lipids, and are either spherical or discoidal particles. The spherical particles are composed of a hydrophobic core and a hydrophilic surface layer (Fig. 1.1). The non-polar core mainly consists of cholesteryl esters and triglycerides while the hydrophilic surface is formed by phospholipids, free cholesterol and proteins.

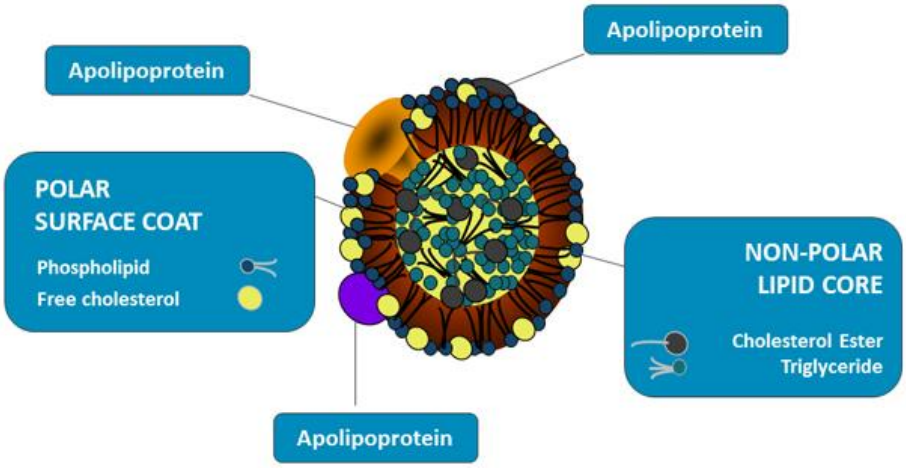

Figure 1.1 Schematic illustration of a lipoprotein particle (Modified from Medscape; Advanced Lipoprotein Analysis).

The discoidal particles consist of mostly polar lipids and proteins in a bilayer conformation. The proteins that bind to lipids to form the lipoproteins are called apolipoproteins. The composition and ratio of protein to lipids determines the size and density of the lipoproteins (Table 1.1). Based on their buoyant density, plasma lipoproteins are grouped into the following five major classes: chylomicrons (CM), very low density lipoproteins (VLDL), intermediate-density lipoproteins (IDL), low-density lipoproteins (LDL), and high-density lipoproteins (HDL) (Fig. 1.2) (8).

Table 1.1 Properties and lipid composition of major human plasma lipoproteins (modified from (9)).

Particles	Source	Density (g/mL)	Protein (%)	TG (%)	PL (%)	free CH (%)	CE (%)
Chylomicrons	Intestine	<0.94	1-2	80-95	3-6	1-3	2-4
VLDL	Liver	0.94 -1.006	6-10	45-65	15-20	4-8	16-22
IDL	VLDL	1.006-1.019	10-12	25-30	25-27	8-10	32-35
LDL	VLDL	1.019-1.063	18-22	4-8	18-24	6-8	45-50
HDL	Liver, intestine	1.063-1.210	45-55	2-7	26-32	3-5	15-20
Lp(a)	Liver	1.040-1.090	~32	~1	~22	~8	~37

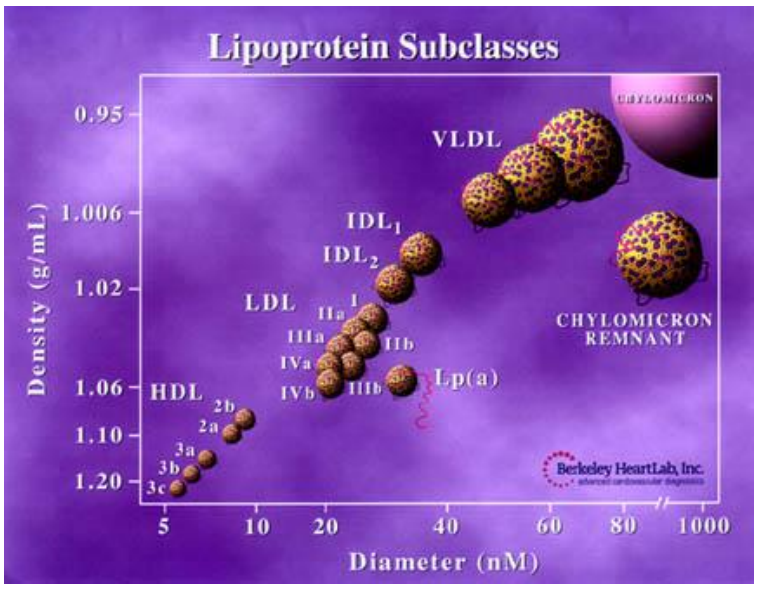

Figure 1.2 An illustration of the different plasma lipoprotein subclasses separated according to their density (g/mL) and size (nm) ((Berkley HeartLab, Inc.).

Lipoproteins undergo multiple rounds of metabolic remodeling during lipid transport and numerous different factors including lipoprotein receptors, lipid transporters and plasma enzymes participate in this process. Lipoprotein metabolism occurs through three distinct, yet interconnected pathways: the chylomicron pathway, the VLDL/IDL/LDL pathway and the HDL pathway (Fig. 1.3) (10-13). The role of the chylomicron pathway is to transport dietary lipids from the intestine to peripheral tissues. Briefly, chylomicrons are synthesized in the intestine where dietary lipids assemble with apolipoprotein B (apoB) isoform B48. The synthesized lipoprotein particles are then transported to peripheral tissues through the bloodstream. In muscle and adipose tissues, the enzyme lipoprotein lipase (LPL) catalyzes the hydrolysis of chylomicrons, and releases glycerol and free fatty acids which are absorbed by the tissues. The chylomicron remnants are subsequently taken up by the liver. In the liver lipids are packaged with apoB isoform B100 and secreted as VLDLs, which undergo sequential hydrolysis by LPL and hepatic lipase (HL) to form initially IDLs and finally LDLs. LDLs are then taken up by the liver through binding to the LDL receptor (LDLR), as well as through other processes. The role of the VLDL/IDL/LDL pathway is the transport of lipids from the liver to peripheral tissues where it is required. In contrast, HDLs are generated extracellularly following secretion of lipid-free apoA-I by the liver and the intestine. The formation of mature HDL particles requires several remodeling steps. The HDL pathway serves to facilitate delivery of cholesterol from peripheral tissues back to the liver, a process known as reverse cholesterol transport (RCT). However, studies over the last decade have unraveled multiple beneficial roles of HDL which include anti-inflammatory, anti-oxidant, anti-apoptotic and anti-thrombotic functions among others. The details of HDL metabolism and functions are discussed at length in subsequent sections.

There are many human diseases associated with perturbations and genetic alterations in different steps of each of the above pathways (9). Numerous epidemiological and clinical studies have established an inverse correlation between HDL levels and the risk for coronary heart disease (CHD) (14). In the context of this thesis we will focus on HDL metabolism and protective functions as well as the contribution of apoA-I, HDL's major protein component, on atheroprotection.

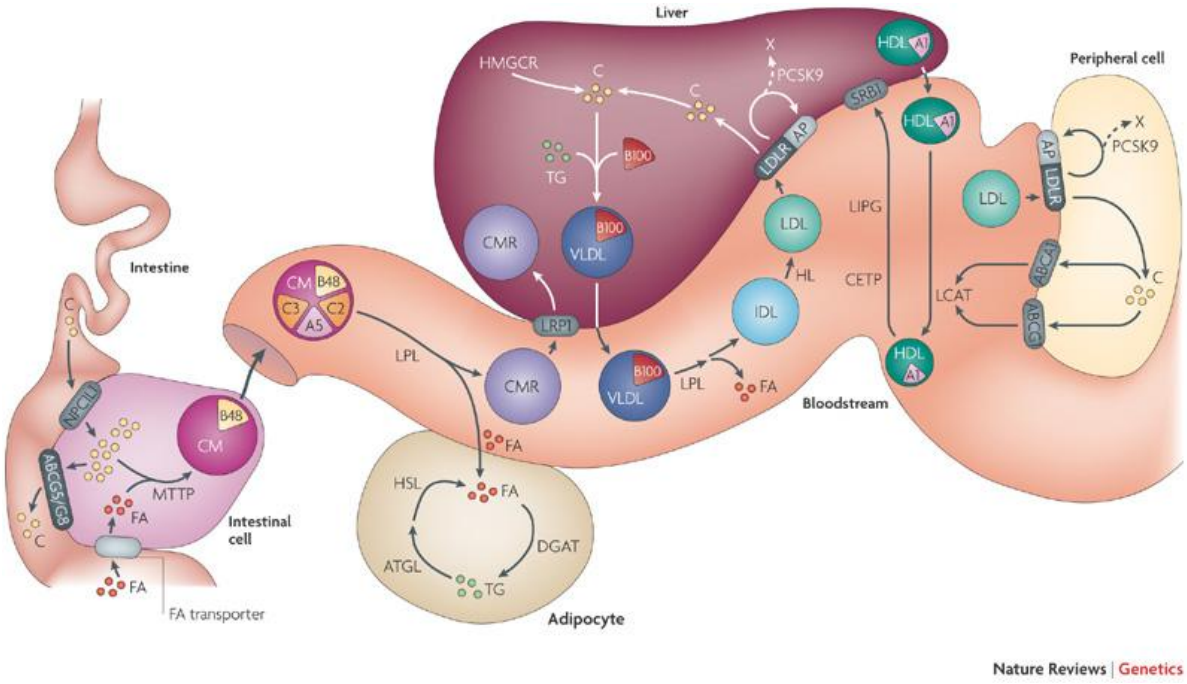

Figure 1.3 An overview of the lipoprotein metabolism (see text for details) (15).

1.2 HDL biogenesis, remodeling and catabolism

HDL metabolism is a complex process that involves multiple steps requiring the action of several membrane-bound and plasma proteins (Fig. 1.4). As a result HDLs constitute a very heterogeneous group of macromolecules in terms of structure, composition and functionality.

HDL biogenesis is initiated by the synthesis and the secretion of apoA-I mainly by the liver and to a lesser extent by the intestine (16). Lipid-free or minimally lipidated apoA-I then acquires cellular phospholipids and cholesterol via its interactions with the ATP-binding cassette A1 (ABCA1) lipid transporter and becomes gradually lipidated to form nascent discoidal-shaped HDL particles enriched in unesterified cholesterol (13, 17). Maturation of nascent HDL is achieved by the action of the enzyme lecithin:cholesterol acyltransferase (LCAT) which is activated by apoA-I and catalyzes the esterification of free cholesterol (13, 17). The esterified cholesterol is packaged into the HDL non-polar core, thus creating spherical HDL particles. Mutations in either apoA-I, ABCA1 or LCAT have been shown to prevent the

formation of apoA-I-containing HDL particles and lead to low HDL disorders (18). Similar to apoA-I, apoE and apoA-IV can also interact with the above mediators and participate in the biogenesis of HDL (19, 20).

The spherical HDL particles are further remodeled by the action of the ABCG1 transporter in macrophages and various plasma lipases. By interacting with ABCG1, HDL acquires cholesterol from peripheral tissues (21) while the transfer of phospholipids from VLDL/LDL to HDL is achieved by the action of phospholipid transfer protein (PLTP) (22). The above interactions result in the formation of mature spherical cholesteryl ester-enriched HDL particles. These particles interact functionally with the scavenger receptor class B type I (SR-BI) which mediates the selective transfer of HDL cholesteryl esters (CE) to the liver for excretion into the bile (23). By the action of cholesterol ester transfer protein (CETP) cholesteryl esters are also transferred from HDL to VLDL/LDL particles in exchange for triglycerides for eventual catabolism by the LDLR (24). Finally, the hydrolysis of phospholipids and residual triglycerides of HDL is mediated by various lipases (lipoprotein, hepatic and endothelial lipase) resulting in lipid-poor apoA-I (25-27). Lipid-poor apoA-I is then catabolized by the kidney or reutilized for HDL synthesis.

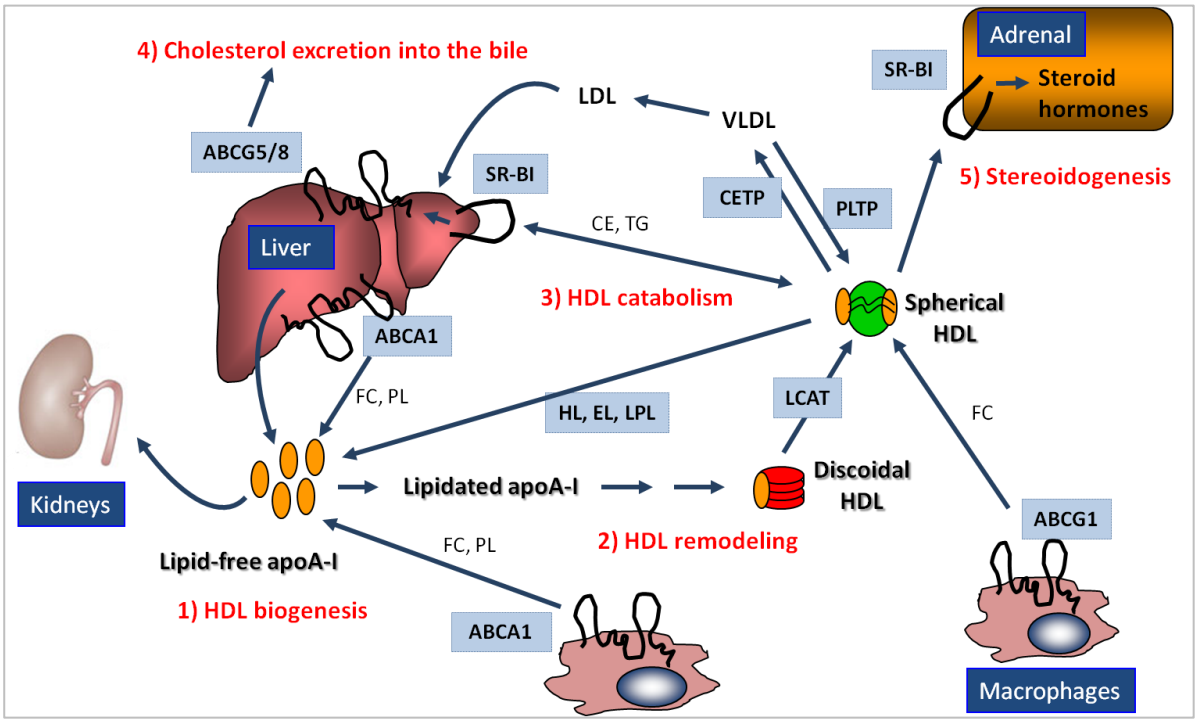

Figure 1.4 Schematic representation of the HDL pathway (see text for details).

1.3 HDL subpopulations

HDL in human plasma constitutes a very heterogeneous population of particles in terms of shape, size, density, lipid and protein composition, and surface charge (Fig. 1.5) (28).

As mentioned above, during the initial steps of HDL biogenesis, discoidal HDL particles are initially formed which then undergo extensive remodeling to form mature spherical HDL particles. Under normal conditions, most HDL particles are present in the spherical form (Fig. 1.5A) (29). Based on their density, HDL particles can be separated by ultracentrifugation into two major subfractions, the larger and less dense HDL_2 fraction (1.063-1.125 g/ml) and the smaller HDL_3 fraction (1.125-1.21 g/ml) particles (Fig. 1.5B). Non-denaturing polyacrylamide gradient gel electrophoresis separates HDL by particle size into five distinct subpopulations: HDL_{2b} (~10.6 nm), HDL_{2a} (~9.2 nm), HDL_{3a} (~8.4 nm), HDL_{3b} (~8.0 nm), HDL_{3c} (~7.6 nm) (Fig. 1.5C) (30).

Classification of HDL on the basis of apolipoprotein content by immunoaffinity chromatography, divides HDL particles into two main subpopulations; HDL that contains apoA-I but no apoA-II (A-I HDL), or HDL particles that contain both apoA-I and apoA-II (A-I/A-II HDL) (Fig. 1.5D) (31, 32). In most human subjects, apoA-I is distributed approximately equally between A-I HDL and A-I/A-II HDL, while almost all of the apoA-II is in A-I/A-II HDL. Most of the A-I/A-II HDL are found in the small HDL_3 density range, while A-I HDL are prominent components of both HDL_2 and HDL_3. Epidemiological and transgenic animal studies have raised the possibility that A-I HDL possesses a more potent atheroprotective role compared to A-I/A-II HDL (33, 34), while other studies have suggested that the protection conferred by A-I HDL and by A-I/A-II HDL is comparable (35).

Based on surface charge, HDL can be separated by agarose gel electrophoresis into three subpopulations (γ-, preβ- and α- migrating particles) (Fig. 1.5E). Most spherical HDLs (HDL_2 and HDL_3 subfractions and A-I HDL and A-I/A-II HDL subpopulations) are α-migrating particles whereas discoidal HDL and lipid-poor apoA-I comprise the preβ-migrating particles. The γ-migrating particles consist only of large, spherical apoE-containing HDL particles (36, 37). Finally, HDL classification by both

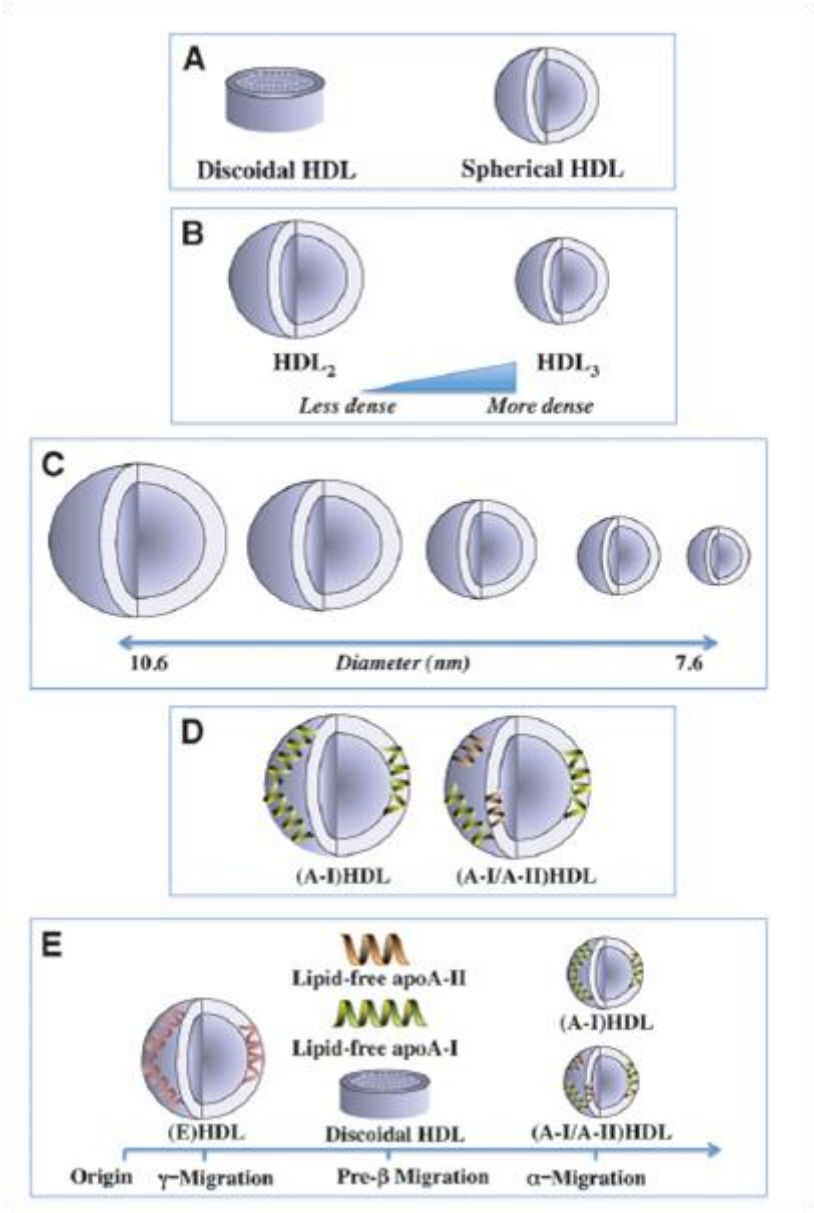

Figure 1.5 Heterogeneity of HDL (29). Human plasma HDL is classified into several subpopulations depending on shape (**A**), density (**B**), size (**C**), apolipoprotein composition (**D**), and surface charge (**E**).

size and surface charge is achieved by non-denaturing two-dimensional gel electrophoresis (Fig. 1.6) (38). Similarly to the above, in the first (horizontal) dimension HDL particles are separated by surface charge into three subpopulations and characterized according to their electrophoretic mobilities relative to albumin. The derived subpopulations designated as preβ-HDL (mobility slower than albumin), α-HDL (mobility similar to albumin) and preα-

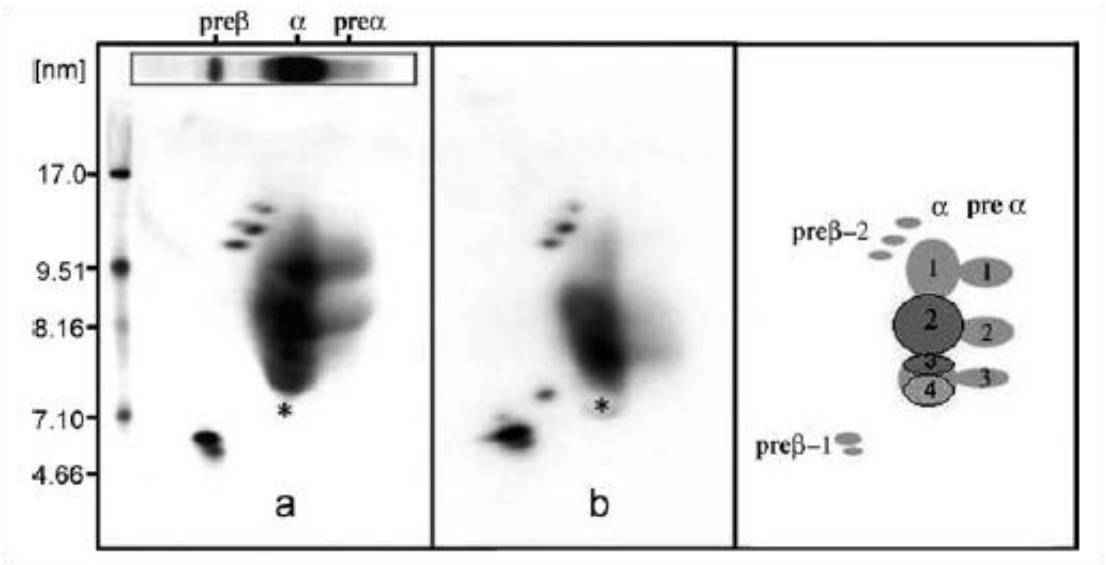

Figure 1.6 Two-dimensional gel patterns of apoA-I-containing HDL particles as detected in whole plasma as shown in **(a)** a normal subject, and **(b)** a patient with premature coronary artery disease with rearrangements in certain HDL subpopulations. The asterisk depicts the location of human plasma albumin. Locations of the apoA-I containing HDL particles are shown in the picture on the right (39).

HDL (mobility faster than albumin) are then further separated in the vertical dimension according to size and give rise to a total of twelve subpopulations: preβ-1a, preβ-1b, preβ-2a, preβ-2b, preβ-2c, α1, α2, α3, α4, preα-1, preα-2 and preα-3 (Fig. 1.6).

Previous studies have suggested that lipid-poor apoA-I and small HDL subpopulations consisting of discoidal, preβ-migrating HDL, are the preferred acceptors of ABCA1-mediated cholesterol efflux while also efficiently promoting cholesterol efflux via ABCG1 (40-42) and are more cardioprotective. However, contradicting evidence has been obtained from CHD subjects characterized by deficiencies in the large, a-migrating spherical HDL (α1, preα-1, preα-2, and preα-3 subpopulations) and high concentrations of α3 and preβ-1 particles (Fig. 1.6) (39, 43-45). Overall, the evidence linking specific HDL subpopulations to atheroprotection in humans remains conflicting. Characterizing distinct HDL subpopulations in terms of functionality might provide the answer.

1.4 Apolipoprotein A-I

ApoA-I is a key-player in HDL biogenesis and catabolism (17). By functioning as the scaffold protein that acquires lipids through interactions with the ABCA1 and ABCG1 transporters and as an obligatory cofactor of the enzyme LCAT (46), apoA-I is inevitably a major participant in the regulation of RCT. Since this pathway is considered to be atheroprotective, apoA-I deficiencies are associated with abnormalities in lipoprotein metabolism resulting in low plasma HDL levels and predisposition to atherosclerosis (47). In contrast, *in vivo* studies have shown that apoA-I overexpression increases plasma HDL levels (48, 49) and attenuates atherosclerotic plaque formation in animal models of atherosclerosis (50-52).

1.4.1 Transcriptional regulation of the human apoA-I gene

In humans, the apoA-I gene is expressed abundantly in the liver and intestine and to a lesser extent in other tissues (16). It has a length of 1870 bp and consists of 4 exons and 3 introns (53, 54). Regional mapping has localized the human apoA-I gene on the long arm of chromosome 11q23-q24 (55, 56) in close physical linkage with the apoC-III and apoA-IV genes (57, 58). The three genes are arranged in a ~17 kb DNA region in tandem (Fig. 1.7).

The regulation of apolipoprotein gene expression is known to primarily occur at the level of transcription initiation (59, 60). The proximal human apoA-I promoter comprises of multitude of nuclear factor binding sites that respond to various ligands (Fig. 1.8) (39, 61-63). As shown in Fig. 1.8, there are two hormone response elements (HREs) that play a prominent role in the regulation of the apoA-I promoter. These HREs bind several orphan nuclear receptors, such as Hepatocyte Nuclear Factor-4 (HNF-4), Regulatory Protein 1 (ARP-1) and Liver Receptor Homologue 1 (LRH-1) as well as ligand-dependent receptors such as Retinoid X Receptor (RXRα), Retinoic Acid Receptor (RAR), Farnesoid X Receptor (FXR), Peroxisome Proliferator-Activated Receptor (PPAR) and Thyroid Hormone Receptor (TR) (64-69).

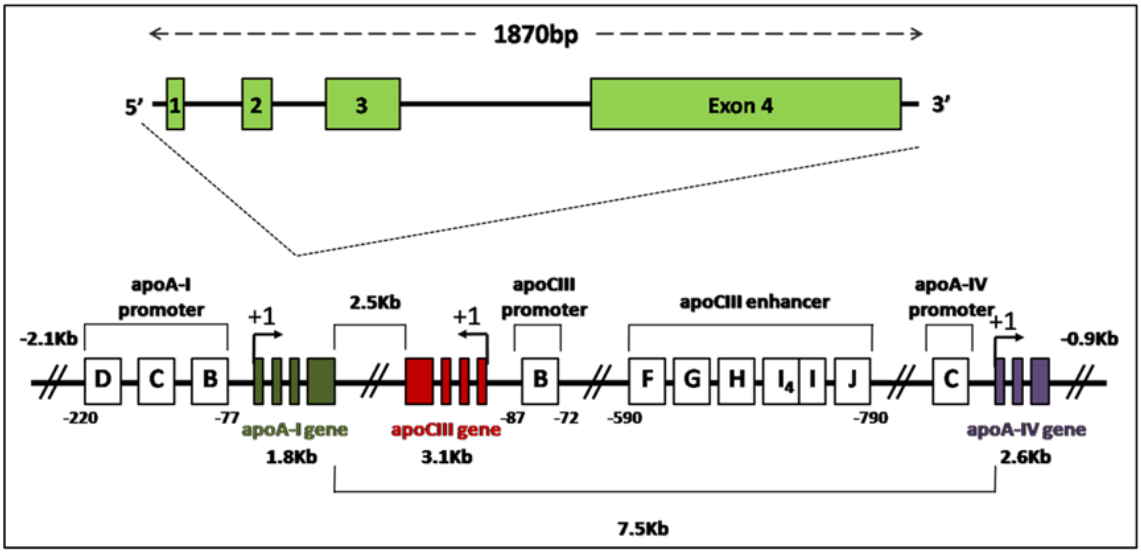

Figure 1.7 Schematic representation of the human apoA-I/apoC-III/apoA-IV gene cluster. Modified from (39).

Animal and cell culture studies have revealed that PPARα plays a prominent role in apoA-I gene regulation in the liver and the intestine (64, 70). In response to fibrates PPARα binds to the proximal apoA-I promoter as a heterodimer with RXRα and increases human apoA-I gene transcription (71). On the other hand, LXR has been recognized as a negative regulator of apoA-I transcription and HDL synthesis human hepatocytes (72). Furthermore, ARP-1 and LRH-1 bind the two HREs of the proximal apoA-I promoter and lead to repression and activation of the promoter, respectively (65, 66). Finally, FXR downregulates apoA-I either by direct binding to the apoA-I promoter or indirectly, by inducing small heterodimers partner (SHP), which in turn represses the activity of LRH-1 (65).

Although early studies had established that the proximal human apoA-I promoter is sufficient to drive the liver-specific gene expression (64, 73, 74) its effect is very weak. Linkage of the apoA-I promoter to an enhancer element located upstream of the apoC-III gene increased the strength of this promoter by several fold (75). This apoC-III enhancer is believed to coordinate gene expression in the apoA-I/apoC-III/apoA-IV cluster and contains two HREs and three binding sites of the transcription factor Specificity Protein 1 (SP1) (76, 77). The contribution of each site to the

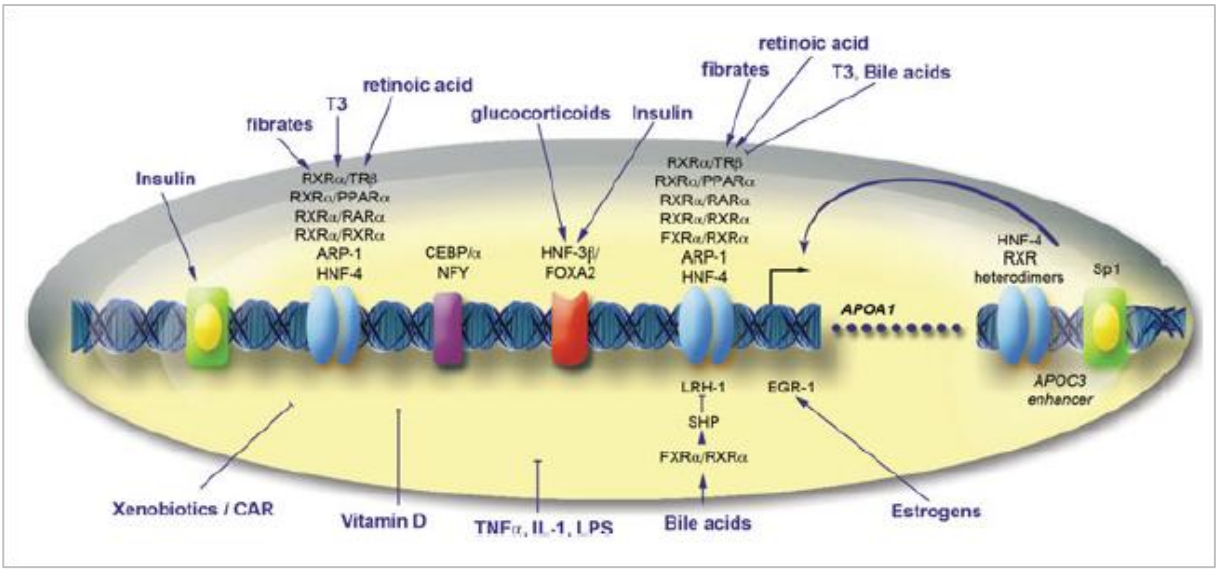

Figure 1.8 Regulatory elements and transcription factors that control the expression of the apoA-I gene (78). Arrows and block lines denote activation and repression, respectively. The mechanisms are described in detail in the text.

expression of the apoA-I gene has been evaluated with a series of *in vitro* and *in vivo* experiments (60). Mutagenesis of the apoA-I promoter/apoCIII enhancer cluster showed that mutations in the two HREs of the apoA-I promoter significantly reduced apoA-I expression, while combined mutations in two HREs of the apoA-I promoter and the I_4 HRE of the apoCIII enhancer completely abolished the hepatic and intestinal expression of the apoA-I gene (48, 64). Moreover, the I_4 HRE of the apoCIII enhancer was shown to be required for the intestinal expression and to contributes to the hepatic expression of the apoA-I gene (48). Studies in cell cultures have established that the combined action of the regulatory elements of the cluster is required to achieve optimal activation of transcription (79). According to the proposed model, the synergy between the apoA-I promoter and the enhancer requires the physical interaction of the HNF-4 and Sp1 factors (Fig. 1.9). Finally, apart from the aforementioned nuclear receptors, there is a variety of other factors such as cytokines, hormonal and pharmacological factors that influence apoA-I gene expression and are reviewed in (78).

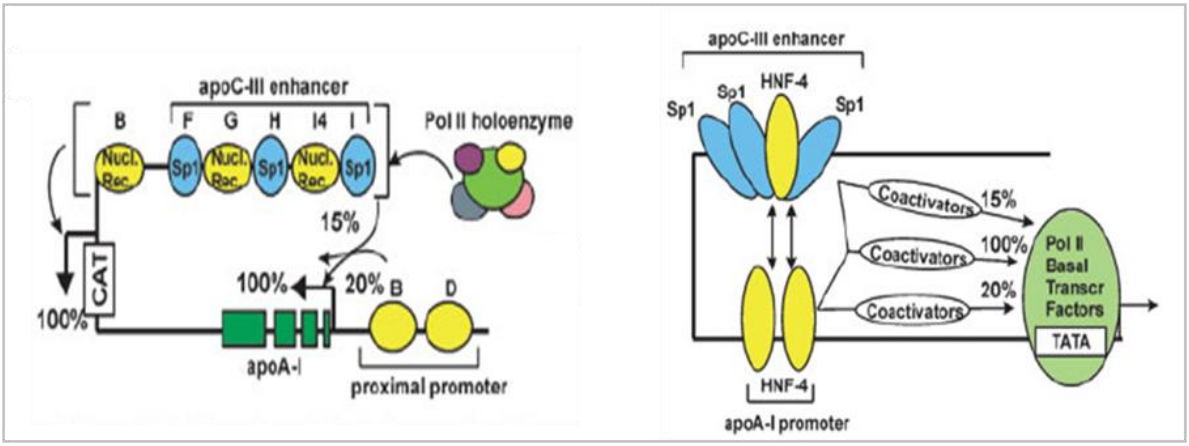

Figure 1.9 Model of transcriptional synergism in the apoA-I gene. The contribution of each of the apoA-I promoter and the apoC-III enhancer alone to the transcription of apoA-I is 20% and 15%, respectively. Normal (100%) hepatic and intestinal expression of the apoA-I gene requires synergistic activation of the two regulatory elements which may be attributed to protein-protein interactions of the promoter and enhancer complexes via coactivators with the proteins of the basal transcription complex (39).

1.4.2 ApoA-I and HDL structure

ApoA-I is the major structural and functional component of HDL and accounts for approximately 70 % of total HDL protein. As for many plasma apolipoproteins, the main sites for apoA-I synthesis are the liver and small intestine. ApoA-I is synthesized and secreted in a precursor form which undergoes proteolytic processing to attain the major isoform observed in the plasma (Fig. 1.10) (80, 81). The coding region of the mature apoA-I mRNA specifies a 267-amino acid primary translation product (prepoapoA-I) (Fig. 1.11) (82). During translocation of prepro-apoA-I through the endoplasmic reticulum, the first 18 amino acids of the prepropeptide are intracellularly cleaved off by the signal peptidase and the remaining pro-apoA-I is secreted into plasma or lymph. The maturation of apoA-I involves the extracellular hydrolysis of the 6-amino-acid-long prosegment (RHFWQQ) by the C-terminal procollagen endoproteinase/bone morphogenetic protein-1 (BMP-1) (83). The mature apoA-I is a 243-residue single polypeptide with a calculated mass of 28079.

Many of HDL's atheroprotective activities are exerted through apoA-I. The ability of apoA-I to exert distinct functions by interacting with different receptors and enzymes presumes conformational plasticity of the protein. Therefore, the physical state and domain structure of apoA-I significantly contribute to its functionality.

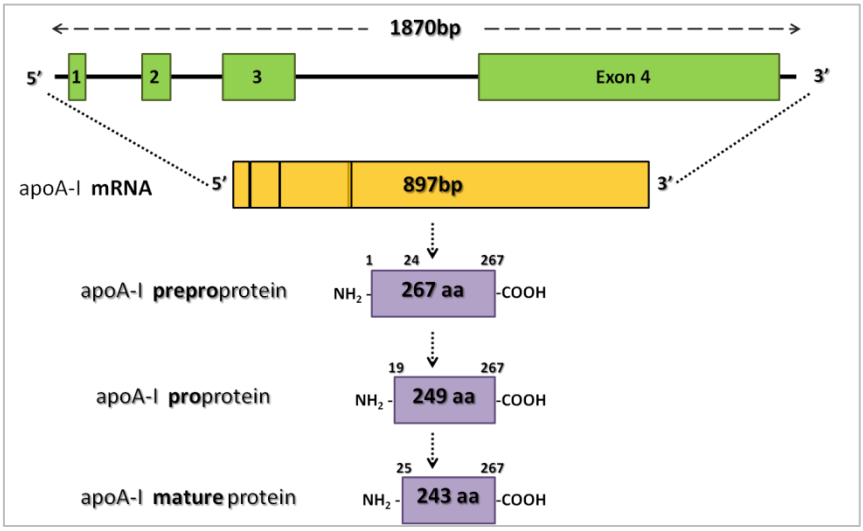

Figure 1.10 Proteolytic processing of human apoA-I precursor protein to form the 243-residue mature apoA-I.

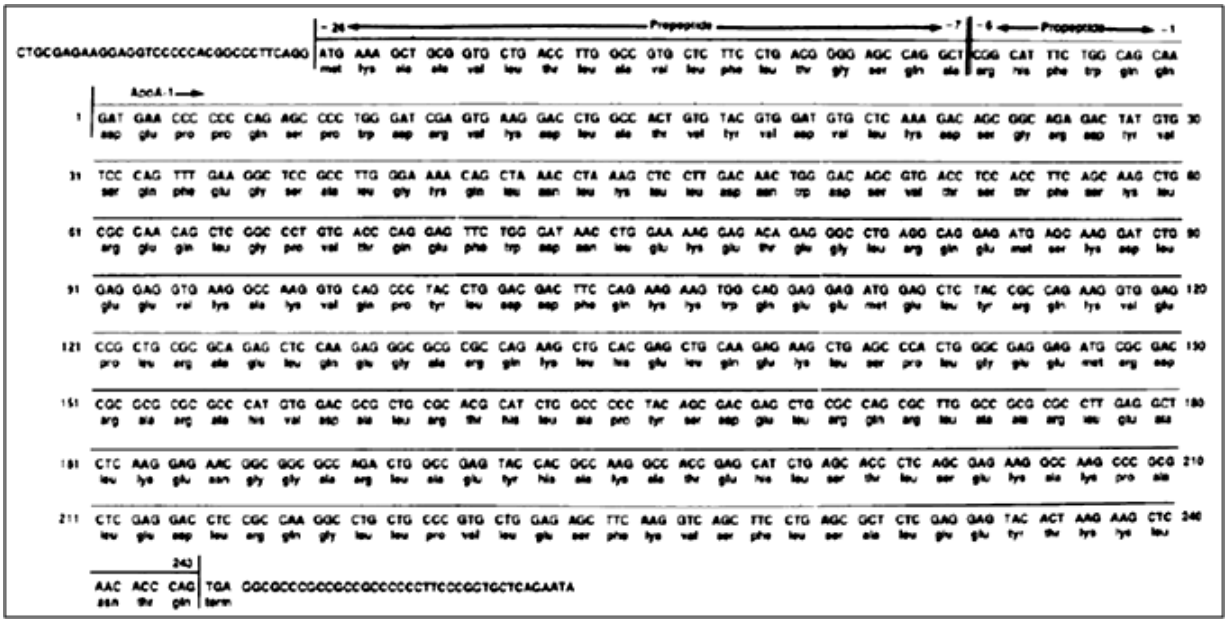

Figure 1.11 The complete nucleotide and inferred 267-amino-acid sequence of human preproapoA-I mRNA as determined from analysis of cloned apoA-I cDNA (82).

Primary and secondary structure of apoA-I

In human apoA-I, exon 3 encodes for the N-terminal residues 1-43 while exon 4 codes for a primary structure of eight 22- and two 11-amino acid tandem repeats that span the remaining region of apoA-I (residues 44-243). With respect to the secondary structure of the protein, each of these repeats is organized in an amphipathic α-helix with the majority of the helices separated by proline residues (Fig. 1.12) (84, 85). This secondary structure allows the molecule to adopt a horseshoe shape with dimensions of 125×80×40 Å (86, 87). The N- (residues 1-43, 44–65) and C-terminal (residues 220–241) α-helices exhibit the greatest lipid affinity (88) and therefore contribute significantly to the lipid-binding properties (89, 90) of apoA-I. Moreover, as shown in Fig. 1.12 different regions of the protein have been assigned to distinct functions of apoA-I through specific interactions with proteins involved in HDL metabolism.

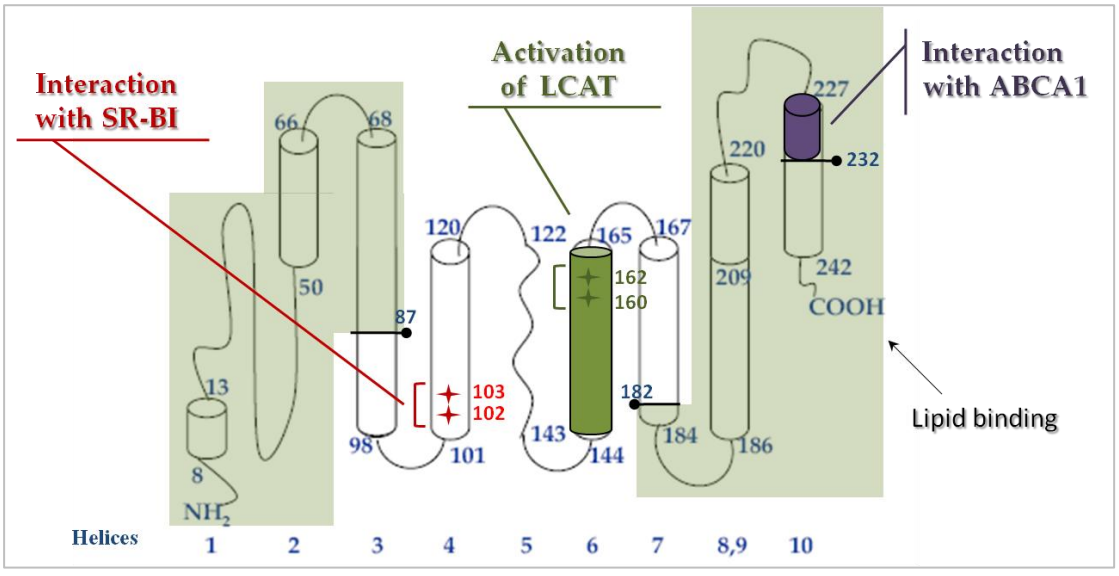

Figure 1.12 The secondary structure and the properties of human apoA-I (adapted from (13)). Cylinders represent amphipathic α-helices and grey shading indicates the N- and C-terminus of the protein. Purple and green colors indicate regions that affect interactions of apoA-I with ABCA1 and LCAT, respectively. Red asterisks indicate amino acids that are involved in interactions of apoA-I with SR-BI.

Tertiary structure of lipid-free apoA-I

Only a small percentage of human plasma apoA-I exists in a lipid-free state. Regardless of the state of apoA-I (lipid-free or lipidated), it appears that the driving force of protein folding lies in the effort to minimize the aqueous exposure of the non-polar helical surfaces. So far, attempts to obtain a crystal structure of full length lipid-free apoA-I have failed. However, physical-biochemical measurements of apoA-I in aqueous solution suggest that apoA-I folds into a compact two-domain tertiary structure that comprises of an N-terminal anti-parallel four helix bundle domain and a distinct less organized C-terminal domain (Fig. 1.13) (91-95). The non-polar surfaces of the amphipathic α-helices are retained in the interior of the bundle which is stabilized mainly by hydrophobic interactions (96). However, the apoA-I N-terminal domain does not possess fixed and specific inter-helix interactions, thus allowing for a high degree of flexibility of this protein which can readily adopt different conformations. This low stability structure facilitates functional remodeling of HDL particles (97). In contrast to the N-terminal domain of apoA-I, the C-terminal domain lacks a well-structured three-dimensional fold and forms α-helix when it either self-associates or interacts with a phospholipid surface. Studies have indicated that the apoA-I C-terminal domain also participates in intramolecular interactions (salt bridges and hydrogen bonds) that stabilize the N-terminal helix bundle domain (98). The

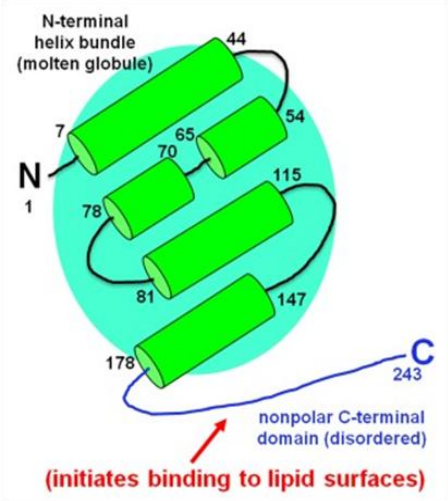

Figure 1.13 The structure of human apoA-I in the lipid-free monomeric state (adapted from (99)). In the two-domain tertiary structure of the protein the N-terminal two thirds is folded into an anti-parallel helix bundle, and the C-terminal region forms a distinct domain.

stability of the N-terminal helix bundle along with the hydrophobicity and α-helix content of the C-terminal domain are to a significant extent responsible for determining the overall functionality of apoA-I (100).

Lipid-bound apoA-I: discoidal and spherical HDL

Over the past decades multiple efforts have been made to solve the lipid-bound conformation of apoA-I (99, 101). Based on several structural studies, detailed belt and hairpin models have been proposed to describe the binding of apoA-I in discoidal and spherical HDL particles (102, 103).

In an attempt to describe the lipid-free structure of apoA-I, Borhani's crystal structure (87) introduced the idea of a belt-like orientation for apoA-I. In the studies that followed, such an organization of the apoA-I molecules in discoidal HDL particles was strongly supported (96, 104-106). According to the "double belt" model for discoidal HDL particle (~10 nm diameter), a small discoidal phospholipid bilayer structure consisting of 160 lipid molecules are stabilized by two ring-shaped apoA-I molecules (Fig. 1.14). The apoA-I molecules are arranged in an anti-parallel, double-belt conformation around the edge of the disc thus shielding the hydrophobic phospholipid acyl chains from exposure to water. Upon interaction with phospholipids the α-helix content of the apoA-I molecule increases (~40%) thus in the lipid-bound state nearly the entire apoA-I molecule (except for the N-terminal 1–6 and the C-terminal 237–243 amino acids) forms a continuous helical structure (107). This apoA-I organization is also consistent with a similar conformation recently observed in a 2.2 Å resolution crystal structure of a C-terminally truncated variant of human apoA-I in the lipid-free state (108). Discoidal HDL particles of greater than 10 nm diameter can associate with apoA-I molecules where at least one of them adopts a helical hairpin conformation (102, 109). According to cross-linking and mass spectrometry studies, apoA-II in discoidal HDL particles is also arranged in a similar hairpin structure (110).

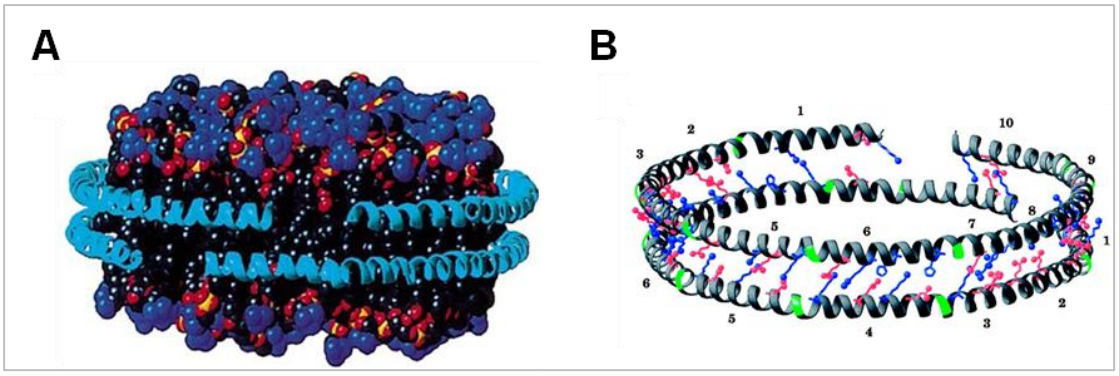

Figure 1.14 The “double belt” model of discoidal HDL (106). (**A**) Two apoA-I molecules, displayed as light blue helical ribbons, are docked around a 85Å diameter patch of phospholipid bilayer. (**B**) Structure and inter-helical salt bridges of the double belt model. The apoA-I backbone is shown as a helical ribbon diagram in which prolines are colored green. The charged residues that form the proposed inter-helical salt bridges are depicted in extended conformation. The amphipathic α-helices (1–10) are labeled.

The conversion of discoidal HDL into a spherical particle postulates the readjustment of the apoA-I structure on the helical surface to allow the transition to a spherical form. However, studies so far support the notion that the double-belt model represents a common structural model for apoA-I in both discs and spheres, regardless of the size and number of apoA-I molecules present (111). According to the proposed “trefoil model” for spherical HDL depicted in Fig. 1.15 half of each apoA-I molecule in the double-belt arrangement is bent 60° out of the plane of the particle and the spherical geometry is achieved by addition of a third apoA-I molecule bent in the same fashion (111, 112). An alternative arrangement involving two apoA-I molecules forming a twisted helical dimer and a third molecule forming a helical hairpin has also been suggested (113). Furthermore, it is possible that both the trefoil and helical dimer/hairpin structures co-exist on the surface of spherical HDL particles. Studies on the structure of apoA-I in human A-I HDL has revealed that this fraction consisted of 8.8 to 11.2 nm particles carrying 3–7 apoA-I molecules that had identical cross-linking pattern (114). Based on the trefoil model changes in spherical HDL particle size and lipid content can be accommodated by twisting of the apoA-I molecules (113). An open

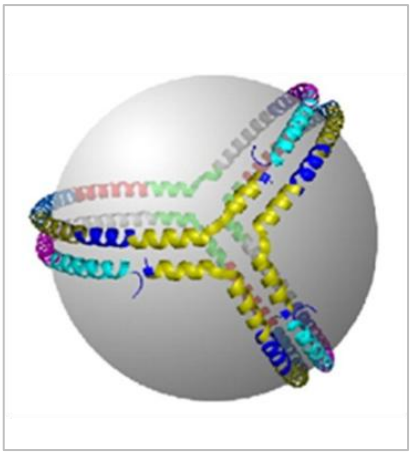

Figure 1.15 Models of apoA-I organization on spherical HDL particles (111). Trefoil organization of three apoA-I molecules on the surface of a 9.6 nm diameter spherical particle. Each putative helical domain is represented as a separate color: helix 1, teal; helix 2, purple; helix 3, dark blue; helix 4, gray; helix 5, green; helix 6, red; helix 7, light blue; helix 8, dark yellow; helix 9, navy blue; and helix 10, yellow. All helix-to-helix interactions present in the double belt between two molecules of apoA-I in a disc are also present among three apoA-I molecules in the trefoil.

question that remains is how the presence of apoA-II molecules in A-I/A-II HDL particles affects apoA-I organization. Finally, it has been found that a decrease in spherical HDL particle size is accompanied by a decrease in phospholipid content thus allowing proteins that associate with HDL to participate in protein-protein as well as protein-lipid interactions (114, 115).

In conclusion, the apoA-I amphipathic α-helices in discoidal HDL particles have relatively low stability, indicating high flexibility and dynamic unfolding and refolding in seconds (107). This highly dynamic state of apoA-I allows for stabilization of discoidal HDL particles of different sizes. With regard to the spherical conformation the flexible apoA-I molecule adapts to the surface of spherical HDL particles by bending and forming a stabilizing trefoil scaffold structure. The above characteristics of apoA-I enable the formation of nascent HDL particles ranging in size and composition. Given the great heterogeneity of the HDL particles, understanding the structural parameters of HDL particle formation will provide us with valuable insights on the arising interactions and functions involving these macromolecules.

1.4.3 Structure-function relationship in apoA-I

In the context of its versatile role HDL exerts multiple functions that contribute to cholesterol homeostasis, maintenance of endothelial integrity and modulation of immune responses, and protect from a variety of human diseases. Several of these functions either require the participation of apoA-I or are attributed to this apolipoprotein's interactions with other factors. As outlined in the previous section the functionality of apoA-I is modulated by its physical state, which allows for binding of various amounts of lipids resulting in the formation of HDL particles that differ in size and shape. Current understanding on the contribution of the structural domains of apoA-I in its functions is described below.

Interactions of apoA-I with ABCA1

ABCA1 is expressed abundantly in the liver, macrophages, brain as well as other tissues (116, 117). It is localized only on the basolateral surface of hepatocytes but in other cells it can also be found on endocytic vesicles complexed to apoA-I (118, 119). In macrophages ABCA1/apoA-I complexes are internalized, interact with intracellular lipid pools, and apoA-I is re-secreted as a lipidated particle (120, 121). Furthermore, a similar pathway that leads to transcytosis of apoA-I has been described in endothelial cells (122, 123). In other words, it appears that ABCA1 possesses a dual function, as a receptor for apoA-I and as a lipid transporter.

HDL assembly is initiated by the ABCA1-mediated transfer of cellular phospholipids and cholesterol to the extracellular lipid-free or minimally lipidated apoA-I (124). The initial lipidation of apoA-I through the action of ABCA1 mainly takes place in the liver, whereas ABCA1 interactions with apoA-I in the peripheral tissues serve to enrich the initial particle with cholesterol and increase its stability (125, 126). Structure-function analysis of apoA-I interactions with ABCA1 as presented by both *in vivo* and *in vitro* studies has led to certain conclusions. A series of animal and cell culture experiments with apoA-I mutants (13, 127, 128) have established that the C-terminal segment (220-231) of apoA-I (Fig. 1.12) is required for ABCA1-

mediated cholesterol and phospholipid efflux since deletion of this region resulted in defective lipid efflux and poor interaction with ABCA1 (129, 130). In line with this, studies have shown that although the central helices of apoA-I have the capacity to efficiently cross-link to ABCA1, promote lipid efflux and form discoidal HDL particles, these properties are diminished in the absence of the C-terminal segment of apoA-I (94, 129). Furthermore, mice expressing C-terminal mutants of apoA-I were able to form only preβ- and small size HDL particles due to non-productive interactions between ABCA1 and apoA-I (130, 131). By contrast, deletion of the N-terminal segment of apoA-I did not affect the protein's ability to efficiently cross-link to ABCA1 and promote ABCA1-dependent lipid efflux (129). Cross-linking between apoA-I and ABCA1 and cholesterol efflux was also affected by mutations in ABCA1 that are found in patients with Tangier disease resulting in the formation of only preβ- and small size HDL particles in the plasma (Fig. 1.16) (18, 132, 133). Overall, a concept that emerges from the existing data is that formation of a productive ABCA1/apoA-I complex requires not only interactions between ABCA1 and apoA-I but efficient ABCA1-mediated lipidation of apoA-I as well (134, 135).

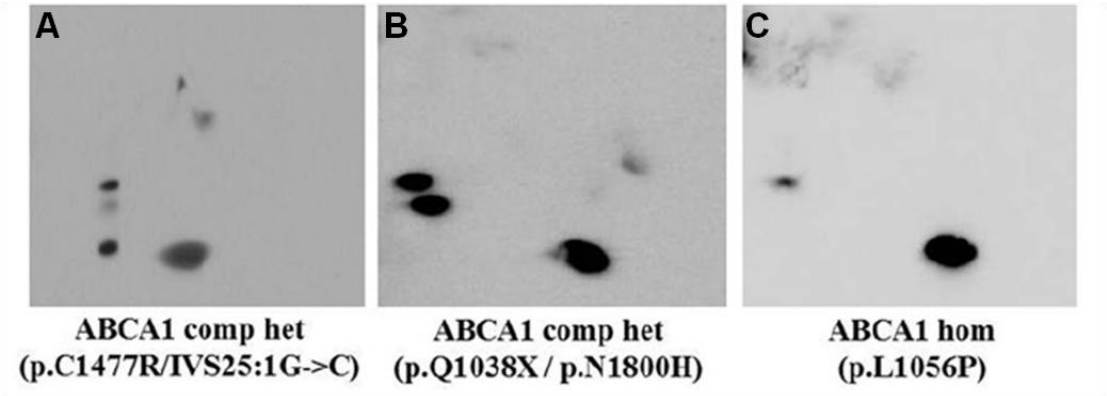

Figure 1.16 Two-dimensional gel electrophoresis of plasma obtained from homozygotes or compound heterozygotes ABCA1-deficient human subjects with Tangier disease as indicated. Adapted from (18).

Interactions of apoA-I with LCAT

Initial lipidation of apoA-I is followed by the remodeling of HDL particles, a process that involves the esterification of cholesterol by the enzyme LCAT. LCAT is synthesized and secreted primarily by the liver and to a lesser extent by the brain and the testis (136, 137). This plasma enzyme catalyzes the transfer of the 2-acyl group of lecithin or phosphatidylethanolamine to the free hydroxyl residue of cholesterol to form cholesteryl ester (138), using apoA-I as an activator (46). It has been proposed that residues R130 and K133 play an important role in the activation mechanism of LCAT by apoA-I. Specifically, these residues are implicated in the formation of an amphipathic presentation tunnel which allows migration of the hydrophobic acyl chains of phospholipids and the amphipathic unesterified cholesterol from the bilayer to the active site of LCAT (139). Ultimately, the esterification of free cholesterol of HDL *in vivo* converts the discoidal to mature spherical HDL particles (140, 141).

Studies on the apoA-I region that is responsible for the interaction with LCAT have identified the 143–164 segment (Fig. 1.12) as the LCAT activator domain of apoA-I (142, 143). However, adenovirus-mediated gene transfer studies of specific apoA-I mutants in apoA-I-deficient mice have suggested that the hydrophobic residues of the C-terminus of apoA-I may also critically participate in the *in vivo* activation of LCAT (127). Other studies using apoA-I mutants with deletions of residues1-65 have demonstrated a significant role of the N-terminal segment of apoA-I in LCAT activation (144).

Mutations in LCAT are associated with two phenotypes in humans; the familial LCAT deficiency (FLD) and the fish eye disease (FED) both of which are characterized by the inability of mutant LCAT to esterify cholesterol on HDL and/or LDL (145). In addition, complete LCAT deficiency in either patients or mice has been shown to result in the formation of only preβ- and small size α-HDL subpopulations in the plasma (Fig. 1.17) (18). A similar perturbation in the distribution of HDL subpopulations has been observed in plasma samples of LCAT heterozygotes and has been associated with increased capacity to promote ABCA1-mediated but decreased capacity to promote ABCG1- and SR-BI-mediated cholesterol efflux from macrophages (146). Finally, several natural variants of apoA-I that are associated with low

plasma HDL levels due to defective LCAT activation have been identified. This topic is discussed in detail in a later section.

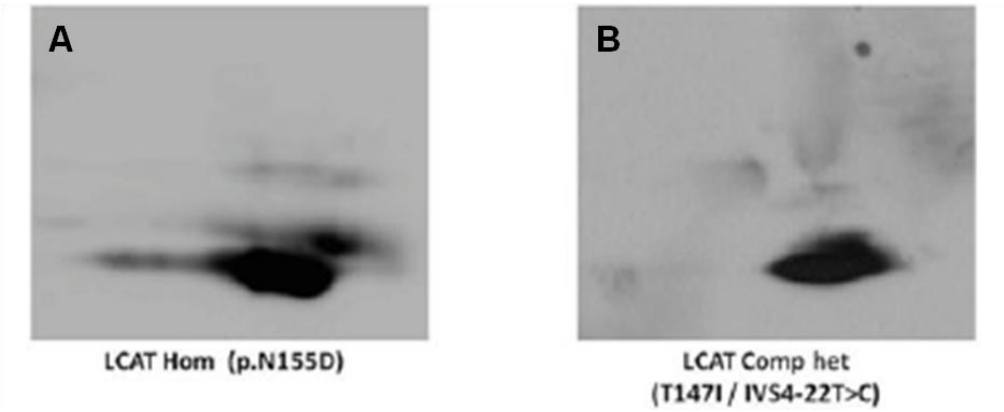

Figure 1.17 Two-dimensional gel electrophoresis from plasma obtained from one homozygote (**A**) and one compound heterozygote (**B**) for LCAT deficiency. Adapted from (18).

Interactions of apoA-I with ABCG1

Further remodeling of the spherical HDL particles is achieved through interactions with the ABCG1 transporter (Fig. 1.18). ABCG1 is expressed in the spleen, thymus, lung, and brain (147-149) and is localized on plasma membrane, the Golgi, and recycling endosomes (150-153). This transporter has been shown to mediate cholesterol efflux from different cell types such as macrophages (154), adipocytes (155) and human placental endothelial cells (156) to HDL particles but not to lipid-free apoA-I (151). Studies in ABCG1 deficient mice have also confirmed that this transporter plays a critical role in the efflux of cellular cholesterol to HDL (157).

Studies using site specific mutagenesis of ABCG1 have revealed that the ATP-binding domain in ABCG1 is essential for both lipid transport activity and protein trafficking (151). Moreover, although previous studies have indicated that there is little or no specificity of ABCG1 for the acceptor of cholesterol (42, 158) recent evidence indicates that the carboxyl-terminal domain 185-243 of apoA-I is essential for efficient ABCG1-mediated lipid efflux (159). Regarding the mechanism by which ABCG1 promotes sterol

efflux to extracellular acceptors, it has been proposed that ABCG1 transports sterols across the bilayer of endosomes before their fusion with the plasma membrane and leads to their redistribution to the outer leaflet of the plasma membrane which facilitates subsequent efflux to HDL or other acceptors (151, 153). However, several observations favor the hypothesis of transient localization of ABCG1 in the plasma membrane which allows its interaction with lipoprotein acceptors (129, 159).

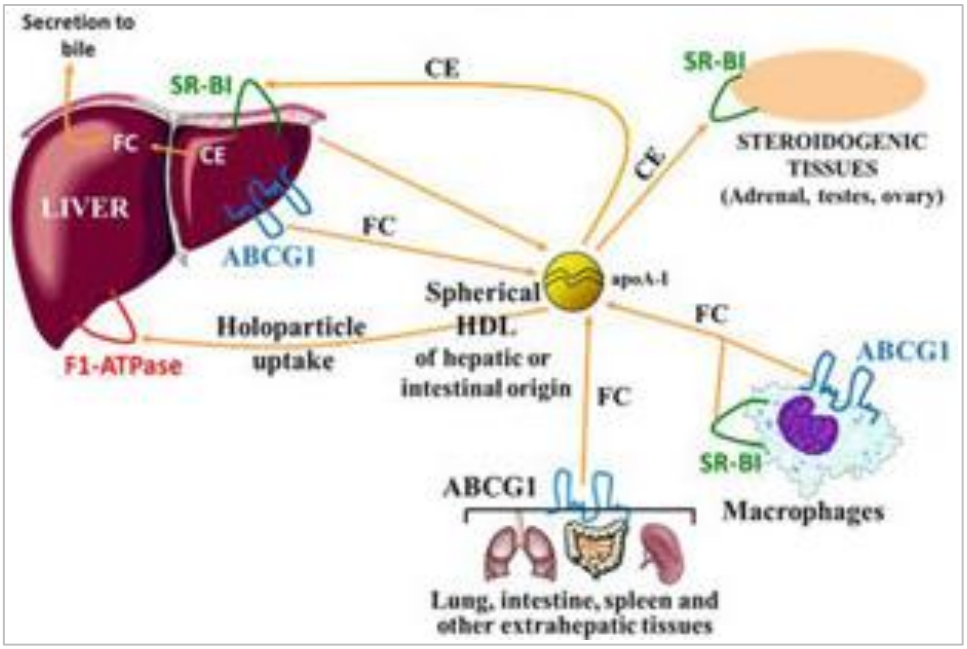

Figure 1.18 Schematic representation of the pathway of HDL remodeling by the action of the ABCG1 transporter and the SR-BI receptor. Adapted from (17).

Interactions of apoA-I with SR-BI

SR-BI is a membrane glycoprotein mainly expressed in the liver, steroidogenic tissues and endothelial cells (160). Expression of SR-BI in the liver has been proven critical for the control of plasma HDL cholesterol levels (161, 162) while its expression in steroidogenic tissues is important for synthesis of steroid hormones (163, 164). SR-BI consists of a large extracellular domain, two transmembrane domains, and two cytoplasmic N-

and C-terminal domains (164). This receptor can bind a variety of ligands (VLDL, LDL, modified lipoproteins) including lipid-bound apoA-I (23, 165, 166). Direct binding of SR-BI to apoA-I triggers selective uptake of cholesteryl ester, triglycerides and phospholipids from HDL (167-170) and promotes bidirectional movement of unesterified cholesterol (171, 172). Furthermore, SR-BI-mediated HDL holoparticle endocytosis has been reported in some types of cells (173, 174). Although the mechanism of SR-BI-mediated selective uptake of cholesteryl esters of HDL by the liver remains unclear, it has been established that it requires the function of the liver-specific protein PDZK1. Interaction of PDZK1 with the C-terminal region of SR-BI has been shown to regulate the localization and stability of SR-BI (175). A proposed model suggests that upon HDL binding to hepatic SR-BI, cholesteryl esters enter into a channel that is generated by SR-BI and move down their concentration gradient into the cell membrane. This mechanism eliminates the need for uptake and degradation of the whole HDL particle.

The physiological importance of SR-BI interactions with lipid-bound apoA-I has emerged from numerous *in vitro* and *in vivo* studies using SR-BI transgenic and SR-BI-deficient mouse models. It appears that the SR-BI/apoA-I interaction controls the structure, composition, and concentration of plasma HDL (23, 176, 177). Efforts to elucidate the molecular interaction of SR-BI with HDL have resulted in the generation of SR-BI mutants with impaired ability to bind HDL (172, 178). On the other hand, cholesterol efflux studies using reconstituted HDL (rHDL) containing mutated apoA-I have demonstrated that mutations in certain residues on helices 4 and 6 (residues 102/103 and 160/162, respectively) of apoA-I (Fig. 1.12) significantly reduced its cholesterol efflux capacity (179). These findings were confirmed by adenovirus-mediated gene transfer studies in apoA-I deficient mice (141). So far, the overall evidence suggests that efficient SR-BI-mediated cholesterol efflux may not only require direct binding of the lipoprotein to the receptor, but also the formation of a ‘‘productive complex’’. However, knowledge on the apoA-I interaction with SR-BI remains limited.

1.5 Naturally occurring mutations in apoA-I

Various naturally occurring mutations in apoA-I have been identified in humans, most of which are caused by single amino acid substitutions (Figure 1.19). To date, over fifty natural variants of apoA-I have been described (180). Roughly half of them are associated with low plasma HDL levels while the rest are known to cause no alterations in HDL (13, 181). Mutations associated with low concentrations of HDL are divided into two main groups: those which exhibit reduced capacity to activate LCAT and those associated with hereditary amyloidosis. The mutations which are found in amyloid deposits are mainly located at the N-terminus of the protein as well as in helix 7 (181, 182). These mutations cause the formation of amyloid fibrils that contain a ~10 kDa N-terminal apoA-I peptide as the major component (183). The mutations that result in poor activation of LCAT are predominantly localized in or at the vicinity of helix 6 of apoA-I (86, 108), and some of them predispose to atherosclerosis (184-187). An interesting case is the apoA-I(R173C)$_{Milano}$ mutation which has been shown to confer atheroprotection despite the low HDL levels (188, 189).

Despite the association of some of the human apoA-I mutations with predisposition to atherosclerosis, for the majority of the cases there is surprisingly little or no information on the functionality of the mutant protein. For two of these mutations, apoA-I(L141R)$_{Pisa}$ and (L159R)$_{FIN}$, studies in humans and animal models have shown that they affect HDL biogenesis and lead to low HDL-cholesterol levels as well as aberrant HDL phenotypes (185, 186, 190-192). Furthermore, they have been associated with premature CHD (185) or increased risk for developing atherosclerosis (186). However, the impact of these mutations on HDL functionality and the mechanisms underlying atherosclerosis predisposition remain unclear. The above two natural apoA-I mutants were examined in the present study and are described in detail below.

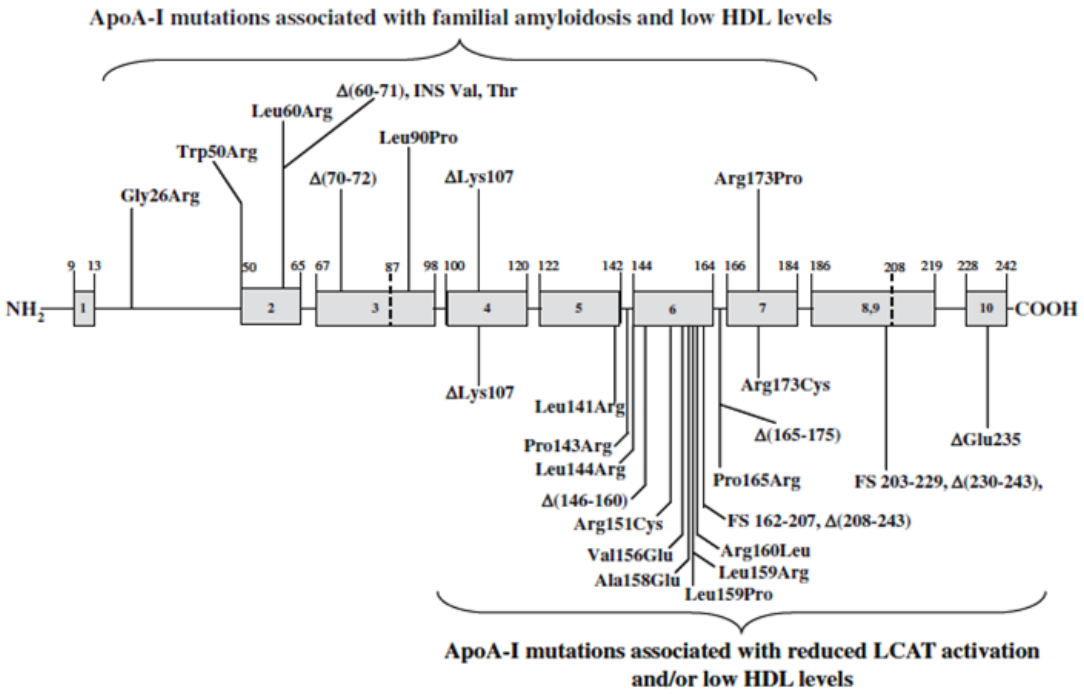

Figure 1.19 Naturally occurring apoA-I mutations that produce pathological phenotypes. The shaded boxes represent the α-helices of the molecule as determined by its sequence (13).

The apoA-I(Leu141Arg)$_{Pisa}$ mutation

In apoA-I(L141R)$_{Pisa}$ the thymidine to guanosine conversion in the apoA-I gene results in the substitution of the hydrophobic leucine residue by the positively charged arginine at position 141 of the encoded protein, which is located on helix 5 (Fig. 1.12). It has been shown that this single-amino acid substitution does not significantly alter the number of α-helical residues in the lipid-free protein and thus does not change the protein conformation. However, this mutation leads to reduced stability of the protein suggesting that Leu141 may be involved in a small number of tertiary interactions, such as leucine zipper-like structures that may be affected by the mutation. This effect could be due to new electrostatic interactions created by Arg141 in the mutant protein, which may affect both the tertiary conformation and the stability of apoA-I and may relate to the altered function of this mutant (193).

Compound heterozygotes (hemizygotes) for a null allele and the Leu141Arg missense mutation in the apoA-I gene are presented with

complete HDL deficiency, elevated LDL cholesterol concentration and reduced total apoA-I levels but relatively increased concentration of proapoA-I in the plasma (185). The increased plasma concentration of the precursor of apoA-I could suggest enhanced catabolism of the variant protein which would contribute to HDL deficiency. Moreover, hemizygotes for apoA-I(L141R)$_{Pisa}$ develop massive corneal opacities, arterial hypertension and premature coronary heart disease which implies a correlation between this structural variant of apoA-I and the risk for premature atherosclerosis. On the other hand, heterozygotes for either the null allele or the apoA-I(L141R)$_{Pisa}$ variant develop hypoalphalipoproteinemia with half-normal levels of HDL compared to unaffected subjects (185).

Subsequent studies in four hemizygotes for this mutation have revealed that the ability of their plasmas to esterify cholesterol in either endogenous or exogenous lipoproteins as well as promote cholesterol efflux was significantly reduced (191). In line with this, analysis of the distribution of HDL subclasses in plasmas of these subjects has demonstrated the presence of preβ1-HDL and low concentrations of small size α-migrating particles corresponding to α4-HDL. Interestingly, preβ-HDL particles consisted of both the wild type and the mutated isoform of apoA-I at approximately equal amounts, while the mutated isoform was absent in larger α-migrating HDL particles (191). In other words, apoA-I(L141R)$_{Pisa}$ was found to interfere with the formation of lipid-rich α-HDL but not with that of lipid-poor preβ-HDL.

With regard to the mechanism underlying the abnormal HDL phenotype observed in carriers of this mutation, a direct effect could involve inability of apoA-I(L141R)$_{Pisa}$ to undergo the necessary conformational changes to form spherical HDL particles. An indirect mechanism involving reduced LCAT activation by the variant protein, either as a primary cause or as a secondary effect due to a reduction of LCAT levels and thus availability of the enzyme, has also been proposed. The latter is further supported by data showing that the functional defect caused by this apoA-I variant was corrected following treatment with LCAT (190). According to this study, simultaneous treatment of apoA-I$^{-/-}$mice with adenoviruses expressing the apoA-I(L141R)$_{Pisa}$ variant and human LCAT normalized the plasma apoA-I, HDL cholesterol levels, and the

CE/TC ratio. It also restored normal preβ- and α-HDL subpopulations and generated spherical HDL (Fig. 1.20A).

The apoA-I(Leu159Arg)$_{FIN}$ mutation

In apoA-I(L159R)$_{FIN}$ the thymidine to guanosine point mutation substitutes arginine for leucine at residue 159 in helix 6 of the mature apoA-I protein (Fig. 1.12). Serum lipid and lipoprotein analysis of carriers of the apoA-I(L159R)$_{FIN}$ mutation has indicated a significant reduction in serum HDL-cholesterol (20% of normal) and apoA-I (25% of normal) levels compared to unaffected subjects. In addition, apoA-II concentration was reduced (50% of normal), while triglyceride levels were found elevated in the serum of these carriers (192). Despite the low HDL levels heterozygotes for apoA-I(L159R)$_{FIN}$ do not show clinical signs of coronary artery disease, however they are considered to be at increased risk for developing the disease. Pedigree analysis has revealed an autosomal-dominant inheritance pattern of this phenotype.

Miettinen *et al* have studied the effect of the apoA-I(L159R)$_{FIN}$ mutation on lipoprotein profile, apoA-I kinetics, LCAT activation, and cholesterol efflux in nine carriers of this apoA-I variant (186). In addition to diminished serum HDL-cholesterol levels these patients exhibited several other lipoprotein abnormalities. Analysis by non-denaturing gradient gel electrophoresis revealed the absence of large HDL_2-type particles (9-12 nm) and the presence of only small HDL_3-type particles (7.8 -8.9 nm). *In vitro* experiments using [^{3}H]cholesterol-loaded human fibroblasts showed that the apoA-I(L159R)$_{FIN}$ mutation did not affect the protein's ability to bind phospholipids or to promote cholesterol efflux (186). However, studies with reconstituted proteoliposomes showed that the LCAT activation by mutant apoA-I was severely compromised. In fact, the capacity of apoA-I(L159R)$_{FIN}$ protein to activate LCAT was reduced to 40% of that of the wild-type apoA-I. In line with this, in a later study using adenovirus-mediated gene transfer in apoA-I$^{-/-}$ mice it was shown that the apoA-I(L159R)$_{FIN}$ mutant had diminished capacity to activate LCAT *in vitro* leading to the generation of aberrant HDL phenotypes

(190). These aberrant phenotypes were corrected by overexpression of the mutant apoA-I form along with human LCAT (Fig. 1.20) (190). Furthermore, a recent study showed that overexpression of human apoA-I(L159R) in an apoA-I/LDL receptor double deficient (apoA-I/LDLr DKO) background was associated with the formation of large CE-enriched apoE-HDL particles and increased atherosclerosis compared to apoA-I/LDLr DKO mice which lack any apoA-I (194).

Further studies on apoA-I kinetics suggested accelerated catabolism of the mutant protein which could account for the dramatic reduction of serum HDL and apoA-I levels. These results have been later confirmed by combined *in vivo*, *ex vivo*, and *in vitro* approaches (195). In more detail, adenovirus-mediated overexpression of apoA-I(L159R)$_{FIN}$ in both wild-type mice and in apoA-I$^{-/-}$ mice expressing human apoA-I led to decreased serum HDL-cholesterol and apoA-I levels. The low apoA-I levels were attributed to protein

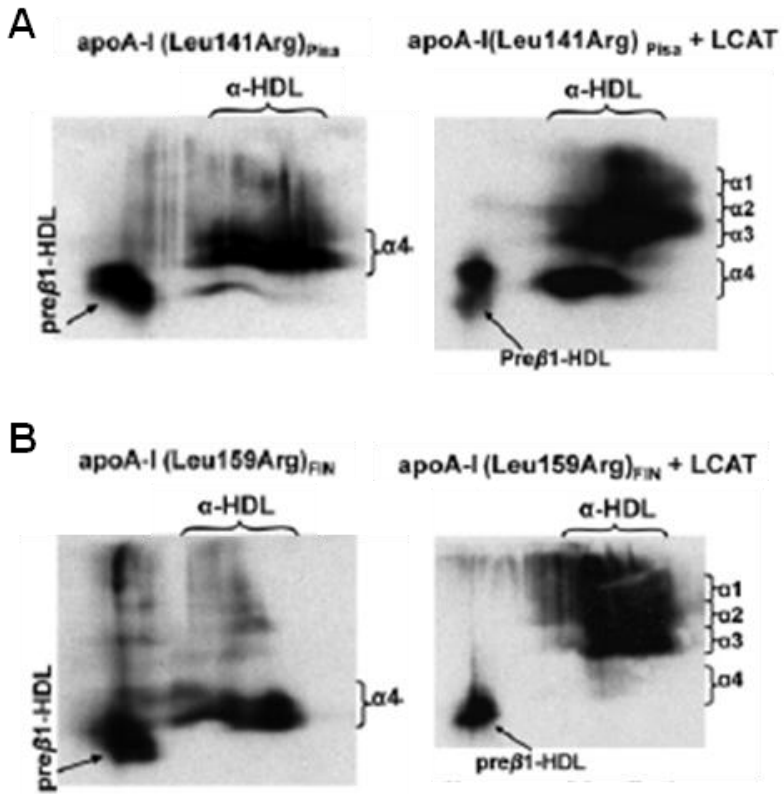

Figure 1.20 Analysis of plasma HDL subpopulations of apoA-I$^{-/-}$ mice infected with adenoviruses expressing either apoA-I(Leu141Arg)$_{Pisa}$ or apoA-I(Leu159Arg)$_{FIN}$ before and after treatment the human LCAT. Modified from (190).

degradation in the plasma. In another experimental setup mimicking the heterozygous state in carriers, co-expression of wild-type human apoA-I with apoA-I(L159R) in primary apoA-I-deficient hepatocytes resulted in decreased secretion of the protein. Based on the above data by McManus *et al,* the increased proteolytic degradation along with the impaired secretion of the mutant protein have been suggested as the mechanisms underlying the dominant negative hypoalphalipoproteinemia in carriers of the apoA-I(L159R)$_{FIN}$ mutation (195).

1.6 The role of HDL in atheroprotection

Atherosclerosis is a chronic inflammatory disease of the blood vessels (9). It is initiated by the accumulation of atherogenic lipoproteins, such as LDL, in the arterial wall as a result of their high levels in the plasma. LDL particles that are trapped in the intima undergo oxidative modifications either by the action of myeloperoxidase and lipoxygenase or by reactive oxygen species. The oxidized (ox-LDL) then triggers a series of events leading to atherosclerosis. Along with certain pro-inflammatory cytokines (TNF-α, IL1β) ox-LDL stimulates the expression of adhesion molecules (VCAM-1, ICAM-1, E-selectin) in the endothelial cells which bind blood monocytes. The modified LDL also induces the expression of chemotactic protein-1 (MCP-1) by endothelial cells, smooth muscle cells, and monocytes which attract monocytes, dendritic cells and T cells into the intima. Monocytes differentiate into macrophages which take up ox-LDL. Subsequent accumulation of excessive cholesterol transforms these macrophages to foam cells that are characteristic of the initial atherosclerotic lesion, called the fatty streak. Macrophages and activated endothelial cells promote the migration of smooth muscle cells into the intima where they proliferate and produce matrix components which are incorporated in the lesion. Over time, a more complex lesion develops where apoptotic as well as necrotic cells, cell debris and cholesterol crystals form the necrotic core of the lesion. This structure is covered by the fibrous cap which is formed by smooth muscle cells along with

matrix components. Finally, plaque growth can cause stenosis which contributes to ischemia in the surrounding tissue.

Several epidemiological studies have supported the protective role of HDL against atherosclerosis development (196). Although a solid inverse and independent relationship between HDL-cholesterol and the risk for cardiovascular disease (197) has been established, it has been postulated that HDL-cholesterol levels may not be an appropriate indicator of the impact of HDL on cardiovascular risk (198, 199). In fact, chemical composition, distribution of HDL subpopulations and functionality of HDL particles are now considered as important factors for determining the atheroprotective capacity of this lipoprotein fraction.

In addition to its effects on cholesterol homeostasis, HDL possesses several atheroprotective properties. These include anti-oxidative, anti-inflammatory, anti-infective, anti-thrombotic and anti-apoptotic properties as well as effects on endothelial cell function (200). The pleiotropic effects of HDL are discussed in the following sections.

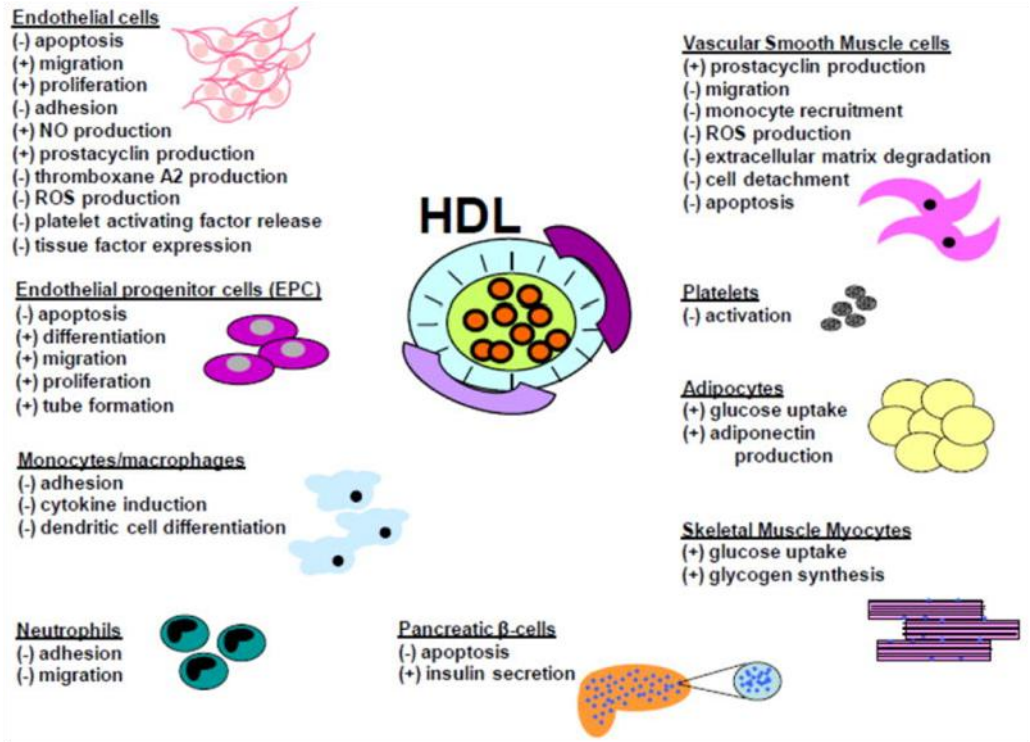

Figure 1.21 Pleiotropic atheroprotective effects of HDL on various cell types. Adapted from (201).

1.6.1 Reverse cholesterol transport in macrophages

Although cholesterol in macrophage foam cells represents only a very small fraction of total cholesterol content, macrophage-specific reverse cholesterol transport remains crucial in maintaining normal macrophage cholesterol homeostasis with significant effects in atherosclerosis development. In fact, macrophage cholesterol efflux capacity has been postulated as a more appropriate predictor for cardiovascular disease than HDL-cholesterol levels (202). This pathway involves the removal of excess cholesterol from lipid-laden macrophage foam cells in the atherosclerotic plaque by HDL and its transport to the liver for excretion in the bile (Fig. 1.22). The ability of apoA-I and HDL to promote this process has been suggested to inhibit the progression or even promote the regression of atherosclerosis (203).

To date, various pathways of cellular cholesterol removal by HDL have been described. According to one pathway which is considered rather inefficient, cholesterol can be transferred from cells to HDL by passive diffusion which follows a cholesterol concentration gradient between the plasma membrane and HDL (204). The other pathways are dependent on receptor-specific interactions. Lipid-free or lipid-poor apoA-I can mediate cholesterol efflux via the ABCA1 transporter resulting in gradual lipidation of apoA-I and generation of nascent HDL particles (205). Current understanding on the molecular interactions between apoA-I and ABCA1 remains limited. The generated mature HDL particles can then serve as cholesterol acceptors for ABCG1 (21) or SR-BI (171). Although the mechanism of ABCG1-mediated cholesterol efflux to HDL is unclear, it appears that direct binding of HDL to the cells is not required. On the other hand, direct binding of HDL to the SR-BI receptor is necessary for induction of cholesterol efflux (178). SR-BI facilitates the bidirectional movement of free cholesterol between the cells and HDL, which, similarly to aqueous diffusion, is determined by the cholesterol concentration gradient. Following efflux, HDL delivers the excess cholesterol from cells back to the liver by the action of hepatic SR-BI (160), by the combined functions of CETP and LDLr (206) or by HDL holoparticle

endocytosis (207). Ultimately, cholesterol is excreted from the liver into the bile either directly or after conversion into bile acids (208).

The important role of macrophage RCT in atheroprotection is supported by numerous evidence from *in vivo* studies. Transplantation experiments using bone marrow from ABCA1$^{-/-}$ mice in wild-type mice revealed an increase in atherosclerosis (209) while transplantation with bone marrow from ABCA1 transgenic mice resulted in reduction of atherosclerotic lesion development (210). Moreover, transplantation of bone marrow from ABCA1/ABCG1 double knockout mice into LDLr$^{-/-}$ mice led to greater atherosclerosis development than when bone marrow from either single knockout mouse model was used (211). Finally, consistent with the atheroprotective role of apoA-I, studies using an *in vivo* RCT model have shown that apoA-I overexpression promotes macrophage RCT while apoA-I deficiency impairs this process (212, 213).

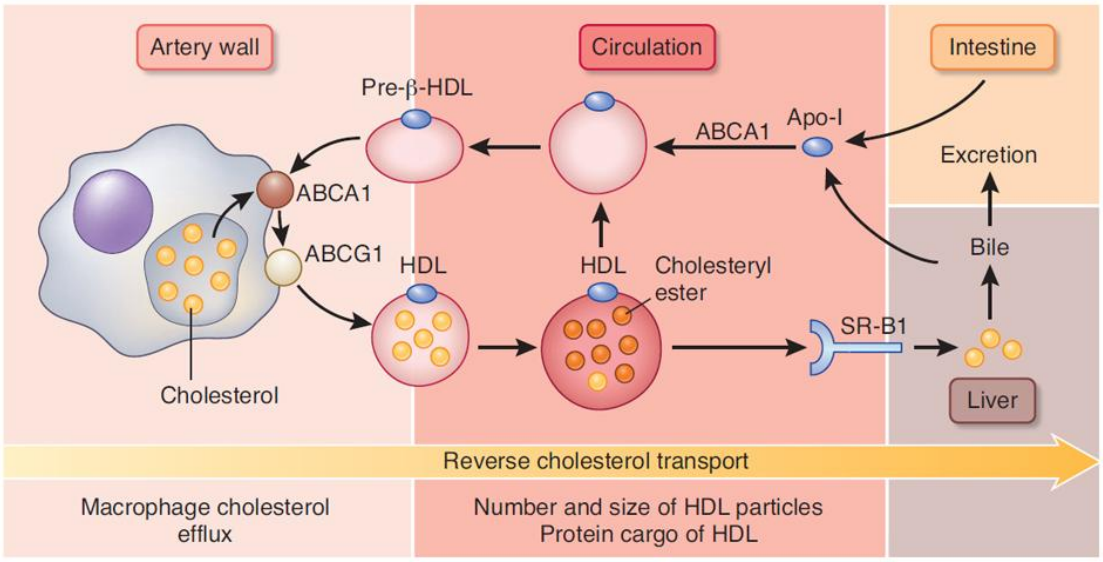

Figure 1.22 Overview of macrophage reverse cholesterol transport by HDL. Adapted from (214).

1.6.2 Effects of HDL on endothelial cells

Abnormal function of endothelial cells of blood vessels is an important hallmark of the early stages of atherosclerosis development. HDL exerts several direct protective effects on the vascular endothelium including inhibition of cell apoptosis, stimulation of endothelial cell proliferation and migration as well as induction of vasodilation (Fig. 1.23).

A series of studies have established the role of HDL as an endothelium-dependent vasodilator. HDL has been shown to induce endothelium-derived vasorelaxation in aortic segments *ex vivo* in a dose-dependent manner (215). In humans administration of rHDL has resulted in normalized endothelial vasodilator function in hypercholesterolemic men (216), while heterozygotes for loss-of-function mutations in ABCA1 with low HDL-cholesterol levels displayed impaired endothelium-dependent vasodilation, which was restored by a single infusion of apoA-I/phosphatidylcholine disks (217). The vasoprotective effect of HDL is mediated through interactions of HDL with SR-BI or the lysophospholipid receptor S1P3 in endothelial cells which trigger signaling mechanisms that involve activation of endothelial nitric oxide synthase (eNOS) and release of nitric oxide (NO) (215, 218-221). In more detail, binding of HDL to SR-BI and S1P3 leads to parallel PI3K-stimulated activation of Akt and MAP kinase signaling. Akt in turn phosphorylates eNOS at Ser-1177 which induces NO production and ultimately endothelium-dependent vasorelaxation. In addition to eNOS activation, modulation of Akt and MAPK signaling by HDL has been shown to delay the degradation of eNOS mRNA in endothelial cells, thereby upregulating eNOS protein levels (222). Finally, the ABCG1-mediated cholesterol efflux capacity of HDL has been reported to facilitate the stimulatory effect of HDL on eNOS activity (223). According to this study, increased cholesterol loading of endothelial cells in ABCA1 deficient mice enhanced the inhibitory interaction of eNOS with caveolin-1 and resulted in reduction of endothelium-dependent vasorelaxation. This effect was reversed by HDL in an ABCG1-dependent fashion.

Another beneficial effect of HDL on the vasculature entails the inhibition of endothelial cell apoptosis. The anti-apoptotic activity of HDL is supported

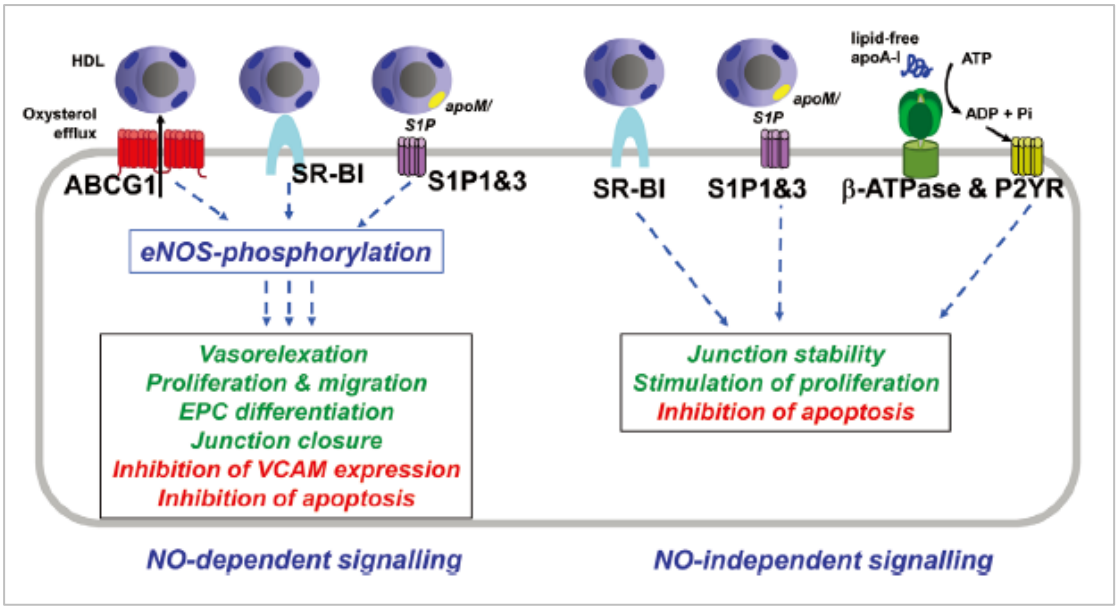

Figure 1.23 Molecules and receptors mediating the various endothelial functions of HDL. Adapted from (200).

by several *in vitro* studies. HDL treatment of endothelial cells markedly suppressed apoptosis in response to pro-atherogenic signals such as oxidized LDL (224-226), TNFα (227, 228), and growth factor deprivation (224, 227). Although the underlying mechanism has not been fully elucidated, it has been suggested that regulation of endothelial cell survival by HDL is achieved by interfering with critical steps of the apoptotic pathways. Specifically, it has been demonstrated that HDL maintains mitochondrial integrity thus preventing the release of cytochrome c and of apoptosis-inducing factor into the cytoplasm (225, 229). In addition, in the presence of HDL endothelial expression of the pro-apoptotic effector protein Bid is suppressed, whereas expression of the anti-apoptotic protein Bcl-xL is enhanced (227). The anti-apoptotic capacity of HDL in endothelial cells has been attributed to apoA-I (230) as well as to HDL-associated lysophospholipids (224, 229), and involves the induction of PI3K/Akt/eNOS signaling pathway (227, 229).

Disruption of vascular endothelium integrity is a critical event leading to atherosclerotic plaque formation. *In vitro* studies have indicated that interaction of S1P, carried by apoM-containing HDL, with S1P1 receptors on endothelial cells leads to the activation of Akt and eNOS, which in turn

promotes endothelial barrier integrity (231, 232). The significant role of HDL-associated S1P in endothelial barrier protection has also been demonstrated *in vivo*. Another mechanism that contributes to HDL's beneficial effect on endothelial function, involves acceleration of re-endothelialization following vascular injury. Hepatic expression of human apoA-I was able to rescue the impaired carotid artery re-endothelialization following perivascular electric injury in apoA-I$^{-/-}$ mice (233). Moreover, HDL has been shown to stimulate endothelial cell migration during repair through Rac-mediated formation of actin-based lamellipodia in an SR-BI-dependent manner (Fig. 1.24) (233). Activation of the re-endothelialization process by HDL and SR-BI requires the action of adaptor protein molecule PDZK1 (234). However, other studies have suggested that HDL-induced endothelial cell migration is mediated by stimulation of Akt/eNOS phosphorylation through S1P/S1P1 interactions (235). Finally, endothelial progenitor cells (EPCs) are thought to participate in vascular repair and several studies have confirmed the ability of HDL to activate the PI3K/Akt/eNOS pathway in EPCs resulting in enhanced proliferation, migration, and survival of these cells (236-238). The potential relevance for humans is supported by the positive correlation between HDL-cholesterol levels and number of circulating EPCs in patients with coronary artery disease (236).

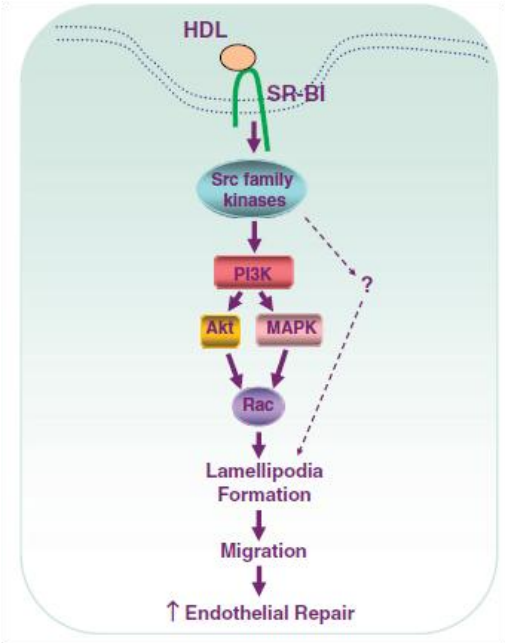

Figure 1.24 HDL signaling through SR-BI promotes endothelial cell repair. HDL binding to SR-BI sequentially activates Src family kinases, PI3K, Akt and MAPK. These events lead to increased Rac activity and lamellipodia formation which ultimately enhances endothelial cell migration (solid arrows). Alternative SR-BI-dependent and Src family kinase-dependent processes may also mediate initial lamellipodia formation (dashed arrows). Adapted from (239).

1.6.3 Anti-thrombotic properties of HDL

Platelet aggregation and thrombus formation directly contribute to the pathogenesis and complications of cardiovascular disease. An inverse correlation between HDL cholesterol levels and the risk of venous thrombosis has been suggested (240-242). In line with this, numerous studies have supported a potent inhibitory role for HDL on platelet activation and aggregation.

In humans, infusion of rHDL in subjects with type 2 diabetes significantly attenuated platelet aggregation by reducing the cholesterol content of the platelet membranes (243). Infusion of rHDL in volunteers that received low levels of endotoxin limited its pro-thrombotic and pro-coagulant effect (484). In animal studies, infusion of apoA-I Milano in a rat model of acute arterial thrombosis significantly delayed the time of thrombus formation and decreased the weight of the thrombus (244).

Recently, it was shown that transplantation of ABCG4$^{-/-}$ bone marrow in LDLr$^{-/-}$ mice enhanced thrombosis and atherosclerosis while infusion of rHDL in LDLr$^{-/-}$ mice in a mouse model of myeloproliferative neoplasm decreased the platelet count in an ABCG4-dependent fashion (245). *In vitro,* native HDL3 interfered with thrombin-induced platelet activation in an SR-BI-dependent manner (246). In support, a pro-thrombotic phenotype has been described in apoA-I$^{-/-}$, eNOS$^{-/-}$, SR-BI$^{-/-}$ mice as well as transgenic mice expressing SR-BI in the liver. The abnormal phenotype was restored by infusion of apoA-I suggesting that suppression of platelet activation is mediated by an HDL/SR-BI/eNOS signaling pathway (247). In this context, studies have shown that the HDL-induced anti-thrombotic effect in endothelial cells involves upregulation of cyclooxygenase-2 (Cox-2) and increased production of prostacyclin (PGI2) through activation of the SR-BI-mediated PI3K-Akt-eNOS signaling pathway (248). Alternatively, it has been suggested that the HDL-induced Cox-2 expression and PGI2 release in endothelial cells involves the interaction of apoA-I with ABCA1 and subsequent activation of the p38 MAPK, ERK1/2 and JAK2 signaling pathways (249). Furthermore HDL may exert its anti-coagulatory functions by inhibiting steps in the extrinsic coagulation cascade. It has been documented that HDL impairs the activity of tissue factor and

subsequent activation of factor X (250). Finally, cholesterol efflux has also been proposed as mechanism of HDL-mediated modulation of platelet function (243).

1.6.4 Anti-oxidative properties of HDL

An important step in atherogenesis is considered to involve the retention of cholesterol-rich lipoproteins, primarily LDL, in the arterial wall and their oxidative modification by the action of resident cells (251, 252). Oxidized LDL constitutes a more pro-atherogenic particle than the unmodified lipoprotein, and HDL has been found to impair oxidative changes in LDL by numerous studies. The inhibitory effect of HDL on LDL oxidation has been observed in co-cultures of endothelial cells and vascular smooth muscle cells (VSMCs) (253, 254). HDL's antioxidative activity is mainly attributed to apoA-I. Lipid removal from LDL by apoA-I renders LDL resistant to vascular cell-mediated oxidation and prevents oxidized LDL-induced monocyte adherence and chemotaxis (254). ApoA-I can also bind molecules produced by vascular cells that stimulate the formation of biologically active phospholipids in LDL (253). The oxidation of specific methionine residues in apoA-I to methionine sulfoxide forms significantly affects the ability of HDL to reduce lipid hydroperoxides (255). The oxidative modifications of apoA-I and their effect are discussed in detail in a later section.

Besides apoA-I there are two HDL-associated enzymes, paraoxonase-1 (PON-1) and platelet-activating factor acetylhydrolase (PAF-AH), that actively participate in the anti-oxidative functions of HDL. PON-1 protects against LDL oxidation *in vitro* (254, 256) by reducing oxidized phospholipids that accumulate in ox-LDL (253, 257). HDL isolated from human PON-1 transgenic mice is more potent at inhibiting LDL oxidation compared to HDL from wild-type mice (258). In support, PON-1 deficiency in mice renders their HDL incapable of preventing accumulation of lipid hydroperoxides in human LDL (259). Similarly, inactivation of HDL-associated PAF-AH abolished the protective effect of HDL against LDL modification (260) whereas adenoviral-mediated overexpression of human PAF-AH in mice resulted in reduced

circulating levels of ox-LDL (261). In contrast to these observations, high plasma levels of PAF-AH have been associated with increased cardiovascular risk (262-264). This could be attributed to the fact that the majority of plasma PAF-AH resides in LDL where it generates pro-inflammatory lysophospholipids (265). However, an opposite correlation with cardiovascular risk has been determined with PAF-AH in apoB-depleted plasma (266), thus further supporting the anti-atherogenic role of HDL-associated PAF-AH.

Finally, several studies have suggested that LCAT might also contribute to the inhibitory effects of HDL on LDL oxidation. Incubation of LDL with LCAT prevented Cu^{2+}-induced formation of lipid hydroperoxides in LDL (267). Moreover, adenovirus-mediated transfer of the human LCAT gene in mice led to significantly lower levels of auto-antibodies against oxidized LDL (268). The above effects stipulate an anti-oxidative function for LCAT.

1.6.5 Anti-inflammatory properties of HDL

An early event in the pathogenesis of atherosclerosis involves upregulation of adhesion molecules on the endothelium leading to monocyte recruitment and infiltration. This process ultimately causes vascular inflammation which is one of the main forces driving the formation of atherosclerotic plaques. A first critical determinant for monocyte migration across the vascular endothelium is the number of monocytes present in the circulation.

Recent animal studies suggest that HDL plays a key role in proliferation and mobilization of myeloid cells from the bone marrow and in myeloid differentiation through cholesterol efflux pathways. As a consequence of defective cholesterol efflux, mice deficient in both ABCA1 and ABCG1 demonstrated aberrant myeloproliferation with increased numbers of myeloid progenitor cells in bone marrow, increased myeloid progenitor cell mobilization, leukocytosis in the peripheral blood, as well as extramedullary hematopoiesis (269). A similar abnormal phenotype was observed in wild-type mice transplanted with bone marrow from $ABCA1^{-/-}ABCG1^{-/-}$ mice (270). Raising the HDL levels in these mice by overexpression of human apoA-I

efficiently reduced the number of circulating hematopoietic progenitor cells (270). Moreover, overexpression of human apoA-I in LDLr$^{-/-}$ mice transplanted with bone marrow from ABCA1$^{-/-}$ABCG1$^{-/-}$mice almost completely restored the myeloproliferative disorder (269). However, a direct effect of HDL on myeloproliferation was provided by *ex vivo* experiments showing that HDL was able to suppress the proliferation of myelopoietic stem cells (269).

Infiltration of monocytes in the arterial intima is triggered by interactions of chemokines with their corresponding receptors. Although the effect of HDL on monocytic adhesion molecules has not been extensively investigated there is some evidence supporting a regulatory role for HDL. Infusion of lipid-free apoA-I in apoE$^{-/-}$ mice that were fed a high-fat diet reduced cell expression of chemokine receptors CCR2 and CX3CR1 in atherosclerotic plaques and decreased the circulating levels of the chemokines CCL2 and CCL5 in a PPARγ-dependent manner (271). *In vitro* rHDL was able to down-regulate cell surface expression of chemokine receptors on monocytes (271, 272). Although the exact mechanism remains unknown, it has been shown that HDL suppresses chemokine expression in response to pro-inflammatory cytokines by inhibition of the NF-κB pathway (271). In addition to the effects on monocytes and endothelial cells, HDL treatment of VSMCs diminished production of the chemokine MCP-1(273). This effect was mediated by HDL binding to SR-BI and activation of signaling pathways following interactions of HDL-associated lysosphingolipids with the S1P3 receptor (273).

Once circulating monocytes are attracted by chemokines to the inflamed endothelium, the ensuing monocyte–endothelial cell interactions are mediated by several cell adhesion molecules. Monocytes bind to adhesion molecules on activated endothelial cells through monocytic cell surface receptors, such as CD11b. Treatment of stimulated human monocytes with either HDL or lipid-free apoA-I reduced the expression of CD11b (274). This inhibition of monocyte activation was associated with decreased monocyte adhesion to endothelial cells as well as monocyte migration in response to MCP-1 (274). In line with this, rHDL infusion in patients with atherosclerosis disease led to a significantly lower expression of CD11b on circulating monocytes (275). ABCA1-mediated cholesterol efflux has been determined as the mechanism responsible for monocyte deactivation by apoA-I whereas in the case of HDL

this effect occurred via an ABCA1-independent mechanism (274). *In vitro* experiments have indicated a suppressive effect of HDL on cytokine-induced adhesion molecule expression on endothelial cells (276-278). This function of HDL has also been confirmed by *in vivo* studies. Moreover, infusions of apoA-I or rHDL decreased endothelial expression of vascular cell adhesion molecule 1 (VCAM-1) and intercellular adhesion molecule 1 (ICAM-1) in a rabbit model of vascular inflammation (279, 280). Additional human studies have shown that, treatment with rHDL lowers the expression level of VCAM-1 in atherosclerotic lesions (275). HDL-mediated restriction of adhesion molecule expression on endothelial cells involves the activation of multiple receptors and signaling cascades. First, HDL-associated S1P has been shown to mediate the HDL-induced inhibition of VCAM-1 expression on endothelial cells (281). Furthermore, it has been postulated that HDL impairs VCAM-1 expression on endothelial cells via SR-BI- and S1P1-mediated activation of PI3K and eNOS (282). Another proposed mechanism involves the suppression of TNF-*α*-induced I*κ*B kinase activity in response to HDL, resulting in inhibition of nuclear translocation and transcriptional activity of NF-*κ*B (283-285). In addition, it has been demonstrated that the suppression of endothelial inflammation by HDL is dependent on the interaction of HDL with SR-BI which leads to activation of PI3K/Akt and subsequent increase in heme oxygenase-1 (HO-1) expression levels (285, 286). Finally, recent findings have revealed that the microRNA content of HDL particles may also be relevant to its anti-inflammatory capacity. According to this study, the transfer of microRNA-223 to human aortic endothelial cells by HDL resulted in significant reduction of ICAM-1 expression levels (287).

Following monocyte infiltration into the arterial intima these cells differentiate into resident macrophages of the two major subtypes that differentially produce a variety of pro- and anti-inflammatory mediators. In the sub-endothelial space, the activated macrophages become targets for HDL. The anti-inflammatory actions of HDL that follow can be extended to the role of HDL in modulating the immune response. In this context, HDL's anti-inflammatory functions are discussed in detail in the following section.

1.7 HDL and the immune system

An altered lipid and lipoprotein profile is frequently observed in pathological conditions associated with immune activation (288). Over the last three decades, a vast number of clinical and experimental evidence have pointed towards a regulatory role of HDL on general host defense activity. This is strongly supported by the ability of HDL to neutralize endotoxin toxicity and to modulate immune cell responses by regulating cholesterol content in plasma membrane lipid rafts. These activities are in accordance with the well established ability of HDL to suppress inflammatory responses during atherogenesis (289).

1.7.1 The role of HDL in innate and adaptive immunity

During infections or acute responses HDL-cholesterol levels have been shown to rapidly decrease, and HDL particles undergo changes with significant impact on their composition and function (288).

The innate immune system represents the first line of defense against infectious agents, and consists of both humoral and cell-mediated components. The humoral component is mostly represented by the complement whereas the cellular counterpart mainly involves antigen-presenting cells (APCs), such as macrophages and dendritic cells (290). As part of the humoral innate immune system HDL acts as an antimicrobial agent and assists in protecting against invading pathogens, such as parasites and bacteria (Fig. 1.25) (291, 292). Furthermore, HDL and apoA-I can modulate the APR-induced activation of the innate immune system by neutralizing major bacterial membrane components, such as LPS of Gram-negative and LTA of Gram-positive bacteria, as well as by modulating the pro-inflammatory signaling. In an early *in vivo* study, it was shown that HDL reduced LPS toxicity (293), and this effect was attributed to LPS sequestration by HDL which in turn prevented the induction of a TLR4-mediated pro-inflammatory response (294). A specific region on the N-terminal segment of apoA-I (amino acids 52–74) has been considered responsible for this scavenging effect of HDL (295). Other studies have indicated that apoA-I possesses a similar

neutralizing capacity leading to the inhibition of the LTA-induced pro-inflammatory response (296). With regard to the modulation of pro-inflammatory signaling, the ability of apoA-I and HDL to regulate cholesterol availability in lipid rafts in immune cells has been shown to considerably affect the integrity of innate immune receptor signaling. ApoA-I has been shown to deplete cholesterol from lipid rafts, thereby decreasing TLR4 functionality and LPS-induced inflammatory responses (297). In addition, it has been demonstrated that apoA-I inhibits TLR4 transport into lipid rafts thus preventing an efficient pro-inflammatory response (298, 299). Furthermore, monocytes also play a major role in innate immunity by providing non-specific protection against foreign pathogens through phagocytosis and cytokine production. By reducing CD11b expression, HDL has been shown to prevent activation, migration and adhesion of both monocytes and neutrophils thus modulating the recruitment of these cells to inflamed tissues (Fig. 1.26) (274, 300).

The adaptive immune system is activated through a process known as antigen presentation (301, 302). This is executed by specialized cells, the antigen- presenting cells (APCs) which provide a link between innate and adaptive immunity. There are several types of cells that serve to perform

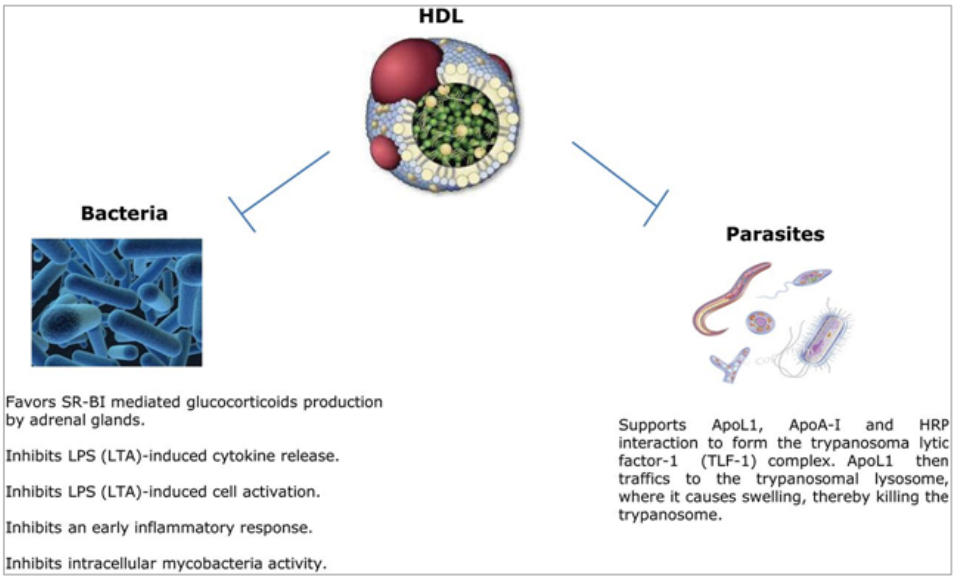

Figure 1.25 HDL and infections. HDL attenuates bacteria and parasite infection via several mechanisms. Adapted from (303).

antigen presentation, however macrophages and dendritic cells are considered as professional APCs. Based on the different cytokines produced in the microenvironment, monocytes can differentiate into two different macrophage types; the classically activated M1 macrophages, which promote inflammation and the M2 macrophages which demonstrate anti-inflammatory activity (304). M1 macrophages are induced by Th1 cytokines, express most TLRs, and secrete pro-inflammatory cytokines (IL-12, IL-6, IL-1β, TNFα) whereas M2 macrophages are induced by Th2 cytokines, and secrete IL-10 and TGFβ (304). Differentiated macrophages express a number of recognition receptors, such as TLRs, which play a key role in the macrophage-mediated mechanisms of immunity (305). Following interaction with a ligand, TLRs induce a signal transduction cascade that results in transcriptional activation of numerous genes leading to the inflammatory response (306). HDL treatment of isolated murine bone marrow macrophages shifted the macrophage phenotype into the anti-inflammatory M2 type (Fig. 1.26) (307), however this effect of HDL has not been validated in humans. Interaction of HDL-associated S1P with the S1P1 receptor in LPS-challenged macrophages resulted in inhibition of pro-inflammatory cytokine production, and promoted a shift from a M1 pro-inflammatory to the M2 anti-inflammatory phenotype (308). Furthermore, pre-incubation of macrophages with HDL was able to prevent upregulation of type I IFN response induced by LPS-mediated TLR4 activation (Fig. 1.26) (309). Recently, novel mechanistic insights into the anti-inflammatory effects of HDL in macrophages have been introduced (310). According to this study, ATF3, a transcriptional repressor of TLR-stimulated inflammation, was identified as an HDL-inducible target gene that mediated HDL's anti-inflammatory actions in macrophages (Fig. 1.26). Notably, it was shown that the protective effects of HDL on TLR responses were fully dependent on ATF3 *in vitro* and *in viv*o. Macrophages lacking ABCA1, ABCG1 or both, have been shown to exhibit an enhanced responsiveness to LPS due to the increased cholesterol content in lipid rafts which leads to a higher content of TLR4 and enhanced TLR4 signaling (311-314). On the other hand, apoA-I prevents TLR4-mediated NF-kB activation by cholesterol depletion in lipid rafts (Fig. 1.27) (299).

Dendritic cells (DCs) are professional APCs that carry antigens in the draining lymph nodes (dLNs) and promote the activation, differentiation and polarization of naïve T cells into effector Th cell subsets (315). Specifically, mature DCs present the antigen in the context of MHC and provide co-stimulatory signals that are required for efficient activation and priming of T cells. Furthermore, through secretion of pro-inflammatory cytokines, DCs direct the polarization of T cell towards the different T cell lineages. Antigen recognition in the presence of IL-12 favors the generation of Th1 cells, whereas IL-6 and IL-23 drive the generation of Th17 effector cells (316-318). Studies so far have suggested that HDL interferes with several steps of DC activation and function (Fig. 1.26). HDL has been found to significantly impair the ability of DCs to stimulate T cells and induce T cell responses (319, 320). ApoA-I has also been shown to impair DC differentiation and maturation by inducing two inhibitors of DC differentiation and function, prostaglandin E2 and IL-10 (319). Among HDL components, phospholipids have been identified as the most active in inhibiting the DC maturation (320). Lipid rafts in DCs represent microdomains of MHC-II localization and are critically involved in

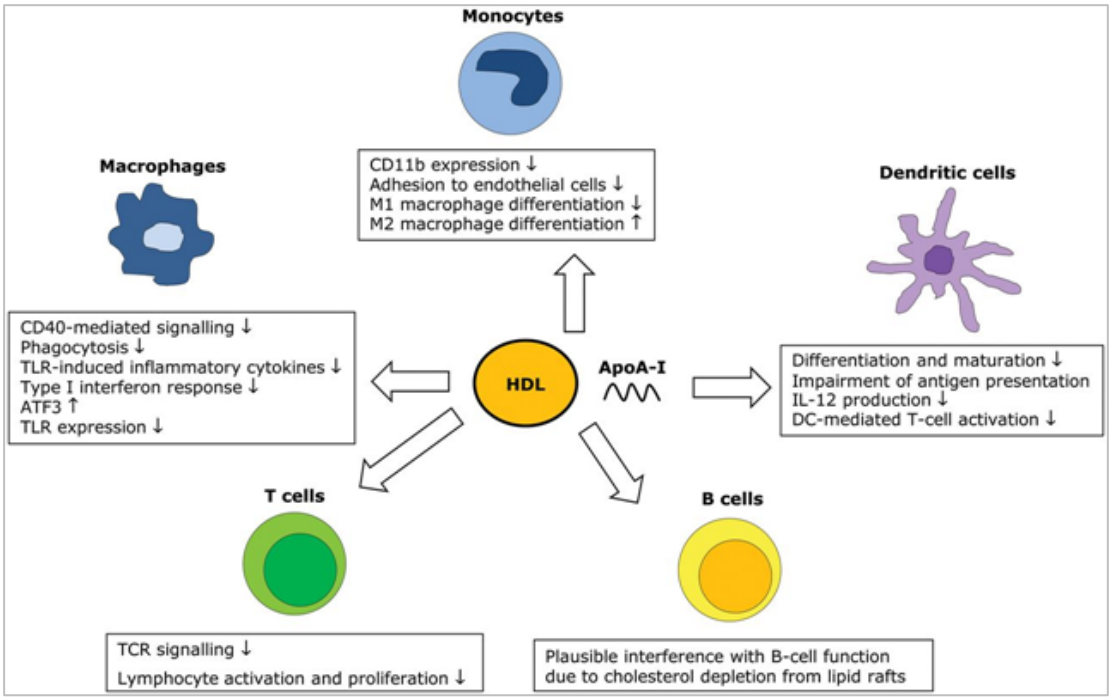

Figure 1.26 HDL- and apoA-I-mediated effects on immune cells. HDL modulates immune cells functions at different levels. Adapted from (303).

antigen presentation and T cell activation (321). Similarly to other types of immune cells, disruption of lipid rafts results in the inhibition of DC activation and function. Studies have demonstrated an inhibitory effect of both HDL and apoA-I on DC function which was associated with reduced membrane lipid raft content and decreased concentration of MHC-II (Fig. 1.27) (322). Finally, HDL-associated S1P has been shown to differentially regulate the production of some cytokines in LPS-stimulated DCs through interactions with the S1P1 receptor, by reducing the secretion of pro-inflammatory cytokines IL-12 and IL-23 and increasing IL-27 production (323).

Findings from several studies suggest that apart from innate immunity, adaptive immunity is also modulated by apoA-I and HDL. Adaptive immune response entails the activation of lymphocytes and the expansion of specific subsets in response to antigens. B lymphocytes are responsible for synthesis of immunoglobulins, while T lymphocytes orchestrate the immune response through different mechanisms. The key receptors of B and T cells (BCR and TCR, respectively) are integral membrane proteins localized within lipid rafts and their activity is modulated upon changes in the lipid raft composition and

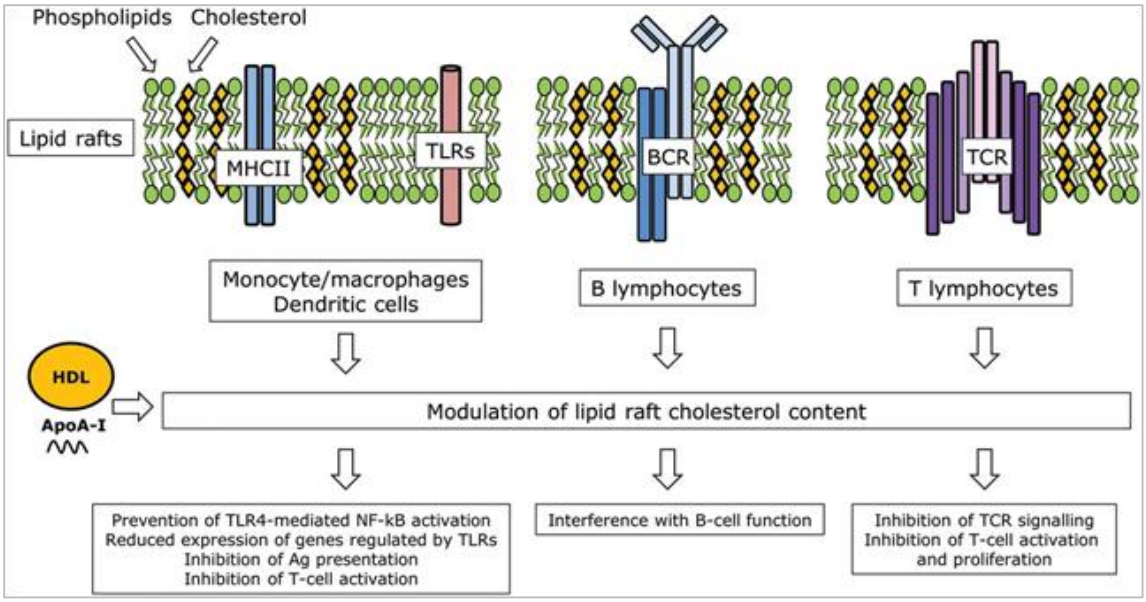

Figure 1.27 HDL interferes with lipid rafts structure in immune cells. HDL and apoA-I reduce cholesterol content in lipid rafts of several cell types, thereby modulating the function of key receptors involved in both innate and adaptive immunity. Adapted from (303).

structure (Fig. 1.27) (288, 324, 325). In other words, lipid raft integrity is crucial to both BCR- and TCR-mediated signal transduction. Although a role for HDL in modulating B cell function through cholesterol depletion and lipid raft disruption has been suggested (Fig. 1.26) (326, 327), direct evidence of HDL's effects on B cells is still lacking. With regard to T cells, $LDLr^{-/-}$ mice lacking apoA-I show characteristics of autoimmunity in response to a cholesterol-enriched diet, including enlarged cholesterol-rich lymph nodes, increased T cell activation and proliferation, production of autoantibodies, and skin inflammation (328, 329). This autoimmune phenotype could be partly reversed by administration of human apoA-I (Fig. 1.26). Moreover, perturbations in cellular cholesterol metabolism have been reported to interfere with LXR signaling. Mice deficient in LXRβ exhibit splenomegaly and lymphadenopathy while activation of LXRβ signaling results in upregulation of ABCG1 expression in T cells thereby decreasing cell proliferation (330). A regulatory role on B and T cell trafficking, as well as T cell subset differentiation has been attributed to S1P (331, 332). In support, it has been suggested that HDL-associated S1P plays a relevant role in several inflammatory disease, including atherosclerosis, RA and asthma, by modulating immune cell function (333).

Contrary to what would be expected based on the above observations, an inverse association between HDL-cholesterol and Treg count has been observed in the general population (334). Whether this correlation reflects the ability of HDL to direct the polarization of lymphocyte subsets or it emerges as bystander of the T cell status remains to be determined. Nevertheless, according to recent findings apoA-I was shown to promote the expansion of regulatory T cells in $LDLr^{-/-}$ $apoA\text{-}I^{-/-}$ mice fed an atherogenic diet, an effect that was associated with a reversal of the inflammatory and autoimmune phenotype observed in those mice (329).

1.7.2 HDL and autoimmunity: The Rheumatoid Arthritis paradigm

Autoimmune diseases are sustained by an impaired adaptive immune response, which is mainly related to a hyper-activation of T and B cells and

abnormal lipid metabolism. Chronic autoimmune-mediated inflammatory diseases such as systemic lupus erythematosus (SLE), rheumatoid arthritis (RA), and other rheumatic autoimmune disorders are associated with increased cardiovascular morbidity and mortality and patients often present with altered plasma lipid profile and compromised HDL functions (335-338). Decreased levels of HDL-C and PON1 activity have been described in SLE and RA patients (335, 336, 339). Dyslipidemia and dysfunctional HDL have also been observed in patients with T2DM and inflammatory bowel disease (IBD), a disorder characterized by sustained activation of intestinal mucosal inflammation (340-343). The abnormal HDL that is observed in these patients is associated with attenuated antioxidative activity, reduced anti-inflammatory effects, and lower capacity to promote cholesterol efflux all of which reflect a pro-inflammatory phenotype of HDL. Despite the extensive observation of altered HDL-cholesterol levels and lipoprotein composition in autoimmune disorders (344), the question remains whether HDL dysfunction occurs as a result of the altered inflammatory status or it directs the abnormal immune phenotypes.

RA is a chronic inflammatory condition manifested by leukocyte infiltration into the synovial lining leading to progressive articular cartilage destruction and bone erosion (Fig. 1.28) (345, 346). The clinical picture in RA may also involve extra-articular manifestations such as pulmonary disease which is associated with worse disease prognosis (345). The breaking of self-tolerance is a hallmark of the disease leading to the production of autoantibodies, such as rheumatoid factor and anticyclic citrullinated peptide antibodies. Anti-apoA-I autoantibodies have also been detected in the serum of RA patients (346). Besides the well-characterized effect of B lymphocytes in RA pathogenesis, T cells also play a crucial role. In fact, RA pathology is critically dependent on the presence of auto-reactive IFN-γ-producing Th1 and IL-17-releasing Th17 $CD4^+$ cell subsets, and pro-inflammatory cytokines such as TNF-α, IL-1β and IL-6 (347).

As aforementioned, RA patients are dyslipidemic with low levels of plasma HDL (348). Interestingly, although circulating levels of HDL-cholesterol are decreased, the levels of pro-inflammatory HDL (piHDL) are increased in RA patients during active disease (335). In patients with active

RA HDL has been found to be extensively modified in terms of protein content including increased amount of serum amyloid A (SAA), apoJ, fibrinogen and haptoglobin, and reduced amount of PON-1 (335, 349). Moreover, it has been reported that the cholesterol efflux capacity of HDL is impaired in RA (350, 351), while RA patients can also demonstrate defective ABCG1-mediated cholesterol efflux independent of HDL-cholesterol levels (350). Anti-rheumatic drugs have been shown to improve both HDL-cholesterol levels and HDL functionality (348). *In vivo* studies using animal models of arthritis have suggested a protective role of apoA-I and rHDL. Particularly, treatment of rats with an apoA-I mimetic peptide inhibited collagen-induced arthritis and reduced inflammatory cytokine levels (352). Moreover, administration of apoA-I or rHDL attenuated peptidoglycan-polysaccharide (PG-PS)-induced arthritis in Lewis female rats in an ABCA1-dependent manner (353).

As previously described, HDL is capable of modulating the activity of various immune cell subsets (303). Extending our understanding of the mechanisms through which HDL may regulate T cell responses *in vivo* could offer valuable insights on immune system modulation as well as unravel ways

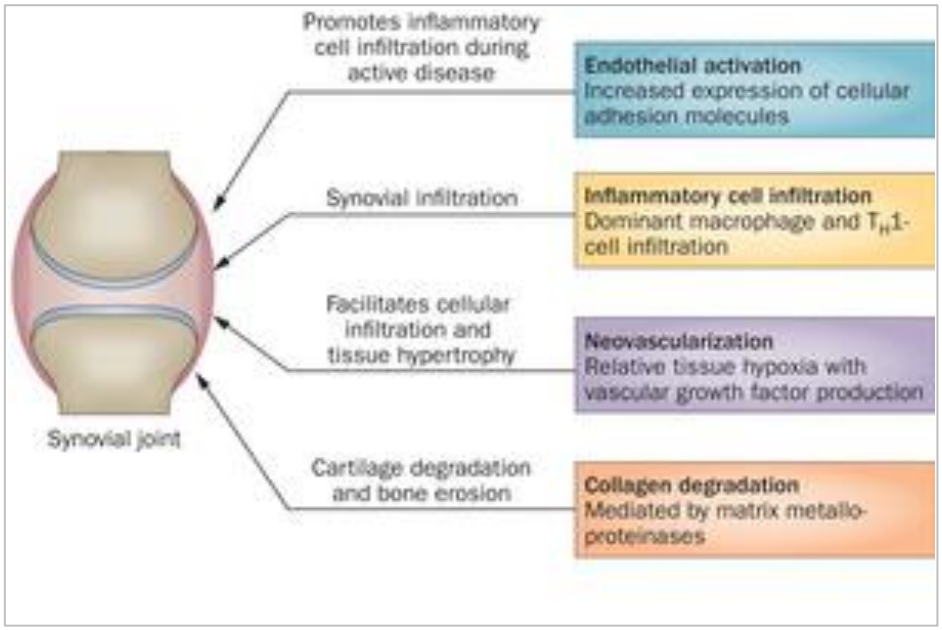

Figure 1.28 Important pathological features of the inflamed rheumatoid synovium. Adapted from (354).

to prevent an unregulated response. Finally, since Th1 and Th17 cells and pro-inflammatory cytokines orchestrate the autoimmune responses in RA, strategies exploiting HDL-mediated suppression of autoreactive Th1/Th17 responses might provide a novel approach for the treatment of this disease.

1.8 Dysfunctional HDL

It is well established that apoA-I carries out many of the HDL's protective functions, ranging from cholesterol efflux and LPS scavenging to the inhibition of several pro-oxidant, pro-inflammatory and pro-thrombotic pathways. However, acute or chronic inflammation is known to induce major alterations in both HDL levels and functionality (303). Over the years many studies have reported the loss of atheroprotective functions or even the gain of pro-atherogenic functions by HDL. Dysfunctional HDL, with reduced capacities to promote cholesterol efflux, prevent LDL oxidation and inhibit activation of antigen-presenting cells, has been isolated from patients with CAD, type 1 and type 2 diabetes mellitus (T1DM and T2DM), metabolic syndrome (MetS), chronic kidney disease (CKD), as well as autoimmune diseases (200). Moreover, in several cases the interactions of HDL with endothelial cells have been rendered defective. HDL from patients with different diseases failed to promote endothelial integrity as well as to stimulate NO production and modulate downstream activities such as vasorelaxation and expression of VCAM-1 and MCP-1 (200).

The molecular changes that underlie HDL dysfunction may relate to compositional changes of the lipoprotein's proteome, alterations of the lipid moiety and other cargo molecules, or post-translational modifications of the HDL-associated proteins. Infection and inflammation generate an acute-phase response which significantly affects the lipid and lipoprotein metabolism and leads to an abnormal lipid profile (355). In addition, during acute-phase response apoA-I in HDL is replaced by other acute-phase proteins, such as SAA protein, ceruloplasmin, and haptoglobin (356), thus transforming HDL into a pro-inflammatory molecule (357). It has also been found that SAA interferes with macrophage reverse cholesterol transport (358) and reduces

the anti-oxidative capacity of HDLs by displacing PON-1 and PAF-AH (357). Recent evidence has suggested that acute-phase response and SAA increases the retention of HDL in the arterial intima due to enhanced HDL binding to vascular proteoglycans, and renders HDL susceptible to oxidative modifications (359). Induction of specific posttranslational modifications, such as oxidation by reactive carbonyls, glycation, and chlorination, nitration or carbamylation by myeloperoxidase (MPO) can directly interfere with the functionality of apoA-I and HDL and drive the formation of pro-inflammatory particles (360).

Oxidation of apoA-I by myeloperoxidase

Current understanding on the association of HDL with disease development indicates that high HDL levels do not necessarily imply atheroprotection, and that the functionality of HDL particles is crucial. A broad range of enzymatic and oxidative modifications has been reported for both the proteins and lipids of HDL. Increased concentrations of modified HDL have been detected in patients with chronic inflammatory diseases, such as CAD, T2DM and CKD, and have been associated with abnormal function. However, it must be noted that the concentration of these modifications is markedly lower than the concentration of apoA-I or HDL particles. The oxidation of apoA-I bound to HDL by myeloperoxidase (MPO) has been identified as an important pathway for generating dysfunctional HDL particles (360, 361).

MPO is a heme protein that is expressed by neutrophil granulocytes and other myeloid cells. In human atherosclerotic lesions MPO is highly expressed in macrophages (362). This enzyme mediates the oxidative chlorination and nitration of free hydroxyl groups in tyrosine and tryptophan residues, the sulfoxidation of methionine residues via formation of hypochlorous acid (HOCl), as well as the carbamylation of free amino groups (360, 361, 363). ApoA-I and HDL have been well determined as selective targets for MPO (Fig. 1.29). According to human studies, increased concentrations of MPO (364, 365) as well as its products chlorotyrosine and nitrotyrosine in both plasma and HDL have been found in CAD patients (366) while increased

levels of carbamylated HDL have been detected in advanced atherosclerotic plaques (367, 368). Furthermore, apoA-I isolated from atherosclerotic plaques has been more strongly modified by MPO compared to plasma apoA-I indicating that either the modification occurs extravascularly or that MPO-modified apoA-I and HDL become trapped within the vascular wall (369-371). It has been shown that MPO-mediated oxidation of apoA-I and HDL severely compromises their capacity to promote ABCA1-mediated cholesterol efflux (369, 372) and to activate LCAT (373, 374). On the other hand, carbamylated HDL is characterized by reduced ability to induce SR-BI-dependent cholesterol efflux (368). A decrease in macrophage cholesterol transport has also been observed in mice following injection of MPO (358). In addition, treatment of HDL with MPO has been shown to interfere with their anti-apoptotic action as well as their ability to stimulate NO production possibly by reducing HDL binding to SR-BI (375). Importantly, in addition to the loss of protective properties related to cholesterol efflux and endothelial function, MPO-modified HDL gains pro-inflammatory activities since it has

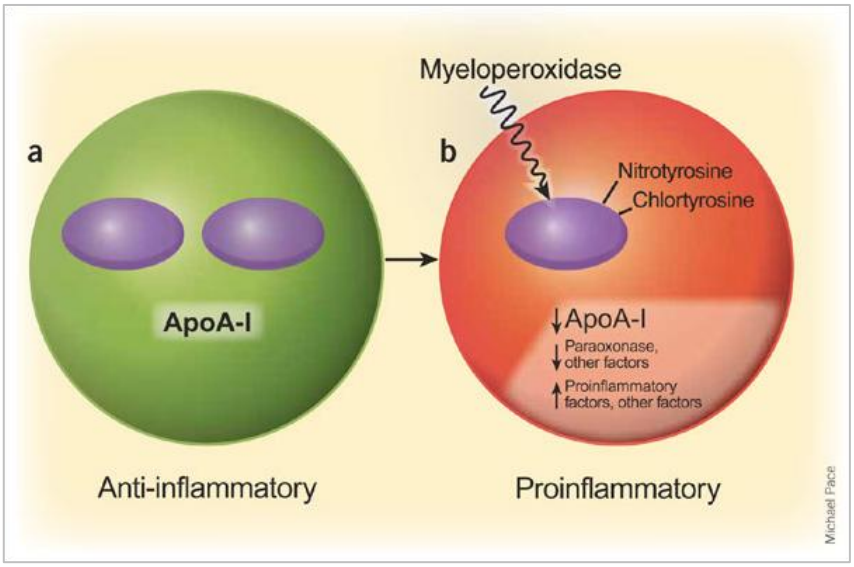

Figure 1.29 A normally anti-inflammatory HDL particle can be converted into pro-inflammatory by the action of myeloperoxidase. This enzyme, which is abundant in macrophages at atherosclerotic lesions, selectively targets apoA-I and oxidatively modifies specific amino acid residues of the protein. As a result several changes occur in the particle, including an overall reduction in the amount of apoA-I and PON-1, and an increase in pro-inflammatory factors. Adapted from (376).

been shown to induce NF-κB activation and VCAM-1 expression in endothelial cells by binding to a yet unidentified receptor (375).

There are several amino acid residues in apoA-I that can be oxidatively modified by MPO *in vitro* as well as in HDL isolated from patients. Multiple *in vitro* mutagenesis studies involving dysfunctional MPO-modified apoA-I or MPO-resistant apoA-I mutants have been performed in an effort to identify the pivotal amino acid residues modified by MPO. Although knowledge remains limited, Tyr192 and Met148 have been proposed as being critical for this process (372-374, 377). High levels of chlorinated Tyr-192 and oxidized Met-148 have been detected in subjects with CAD and this was not associated with increased plasma levels of MPO. Moreover, the modified HDL from these patients demonstrated impaired capacity to promote ABCA1-mediated cholesterol efflux (378).

Studies using tandem mass spectrometry have identified Tyr-192 as the major nitration site in apoA-I of circulating HDL, as well as the major chlorination site in apoA-I in both plasma and lesions of humans (363, 377). The chlorination of Tyr-192 has been shown to selectively impair the ability of apoA-I to promote ABCA1-dependent cholesterol efflux (366, 372, 379). Although the exact mechanism remains under investigation, it has been proposed that the lysine residue of the YxxK motif (Y = tyrosine, K = lysine, x = unreactive amino acid) in which Tyr192 lies, is responsible for the site-specific chlorination of tyrosine residues by MPO (369, 380). Zheng *et al*. have proposed a model in which direct binding of MPO to that region is required to promote site-specific chlorination of Tyr192 (366). However, an alternative model suggests that the YXXK can direct the region-specific chlorination of tyrosine residues in apoA-I independent of a direct interaction or binding of MPO to apoA-I (380). Furthermore, the resistance of Tyr115, which also resides in a YxxK motif, to chlorination has been associated with the presence of a nearby methionine residue (Met112) in an MxxY motif (369). The fact that the alkyl thiol of methionine reacts with HOCl more readily than the side chain of any other common amino acid (381), including tyrosine, further supports the hypothesis that adjacent methionine residues inhibit tyrosine chlorination, either by scavenging chlorinating intermediates or by disrupting the secondary structure of the protein (382).

An *in vitro* study has shown that MPO-mediated oxidation of Met148 impairs the ability of apoA-I to activate LCAT (374). In more detail, oxidation of Met-148 to methionine sulfoxide associated quantitatively with the loss of LCAT activity, while reversing oxidation with methionine sulfoxide reductase restored the ability of HDL to activate LCAT. This effect is further supported by the localization of Met-148 near the center of the LCAT activation domain of apoA-I. The authors propose that oxidation of Met-148 disrupts the central loop and the conformation of helix 6 in a way that leads to the relocation of these residues from the protein's hydrophobic face to its hydrophilic face. This process disturbs the LCAT activation site and diminishes apoA-I's ability to activate this enzyme.

In conclusion, the oxidative regulation of reverse cholesterol transport implicates the MPO-mediated modification of specific methionine and tyrosine residues in apoA-I which results in the inability of the oxidized protein to activate ABCA1 and LCAT, two key-steps in cholesterol efflux from macrophages. Thus, it appears that oxidation of apoA-I by MPO plays a crucial role in promoting foam cell formation and atherogenesis.

1.9 Novel insights into HDL biology and genetics: GALNT2

During the last few years there has been extensive screening for novel genes involved in HDL biology. Genome-wide association studies (GWAS) have identified several new loci that are associated with plasma lipids (383-387), however the mechanistic insights on how they affect HDL-cholesterol and/or function are remarkably lacking (388). Among the newly identified loci lie ANGPTL4, TTC39B, PPP1R3B, and GALNT2. In GWAS, variation at the GALNT2 locus has been found to be associated with plasma HDL-cholesterol as well as triglyceride levels (385-387). Viral-mediated hepatic overexpression and silencing of GALNT2 have also been shown to reduce and increase HDL-cholesterol levels in mice, respectively (387). Notably, a significant association between GALNT2 and CVD or the risk of ischaemic stroke has not been established (389, 390).

GALNT2 is located on chromosome 1 and codes for UDPN-acetyl-alpha-D-galactosamine:polypeptide N-acetylgalactosaminyltransferase-(ppGalNAc-T2) which is mainly expressed in liver, skeletal muscle and pancreas (391). This enzyme belongs to a family of ppGalNAc transferases that consists of 20 members in humans (392). ppGalNAc transferases are type II Golgi membrane proteins (393) that catalyze the transfer of GalNAc residues onto proteins thereby initiating mucin-type O-glycan synthesis on threonine and/or serine residues of protein substrates (392). Since O-linked glycosylation can act to regulate protein function, it has been hypothesized that the effect of GALNT2 on HDL-cholesterol and triglyceride levels is mediated indirectly through the glycosylation of proteins involved in lipoprotein metabolism (385). LCAT, apoC-III, the VLDL receptor and the LDL receptor are all O-glycosylated with N-acetylgalactosamine residues (394-397) and have therefore been considered as potential targets for GALNT2.

In a recent study, Holleboom *et al* identified a missense mutation in GALNT2 that resulted in impaired catalytic activity of the ppGalNAc-T2 enzyme and was associated with high HDL-cholesterol levels and improved postprandial triglyceride clearance (398). Furthermore, carriers of the mutation were characterized by attenuated glycosylation of apoC-III which is an established inhibitor of LPL. These results indicated that GALNT2 mediates its effects on HDL metabolism indirectly by affecting the catabolism of triglycerides (Fig. 1.30A). Previously, a different mechanism of GALNT2-mediated regulation of plasma lipid levels through the glycosylation of ANGTPL3, an important inhibitor of both LPL (399) and EL (400), had been suggested (Fig. 1.30B) (401). ANGPTL3 normally undergoes proprotein convertase processing for activation, and the processing site contains two potential GalNAc *O*-glycosylation sites (402). GALNT2-mediated glycosylation of ANGTPL3 at Thr226 in the proprotein convertase processing site has been shown to block activation of the protein leading to enhanced activity of LPL and EL, and changes in HDL-cholesterol and triglyceride levels.

Overall, studies so far have only indirectly associated the activity of GALNT2 with HDL-cholesterol levels through effects on triglyceride catabolism. Despite the obvious gain from GWAS in the identification of this novel lipid-modifying gene, there is a need for more comprehensive studies

that will focus on the mechanistic relations between lipid metabolism and GALNT2-mediated glycosylation.

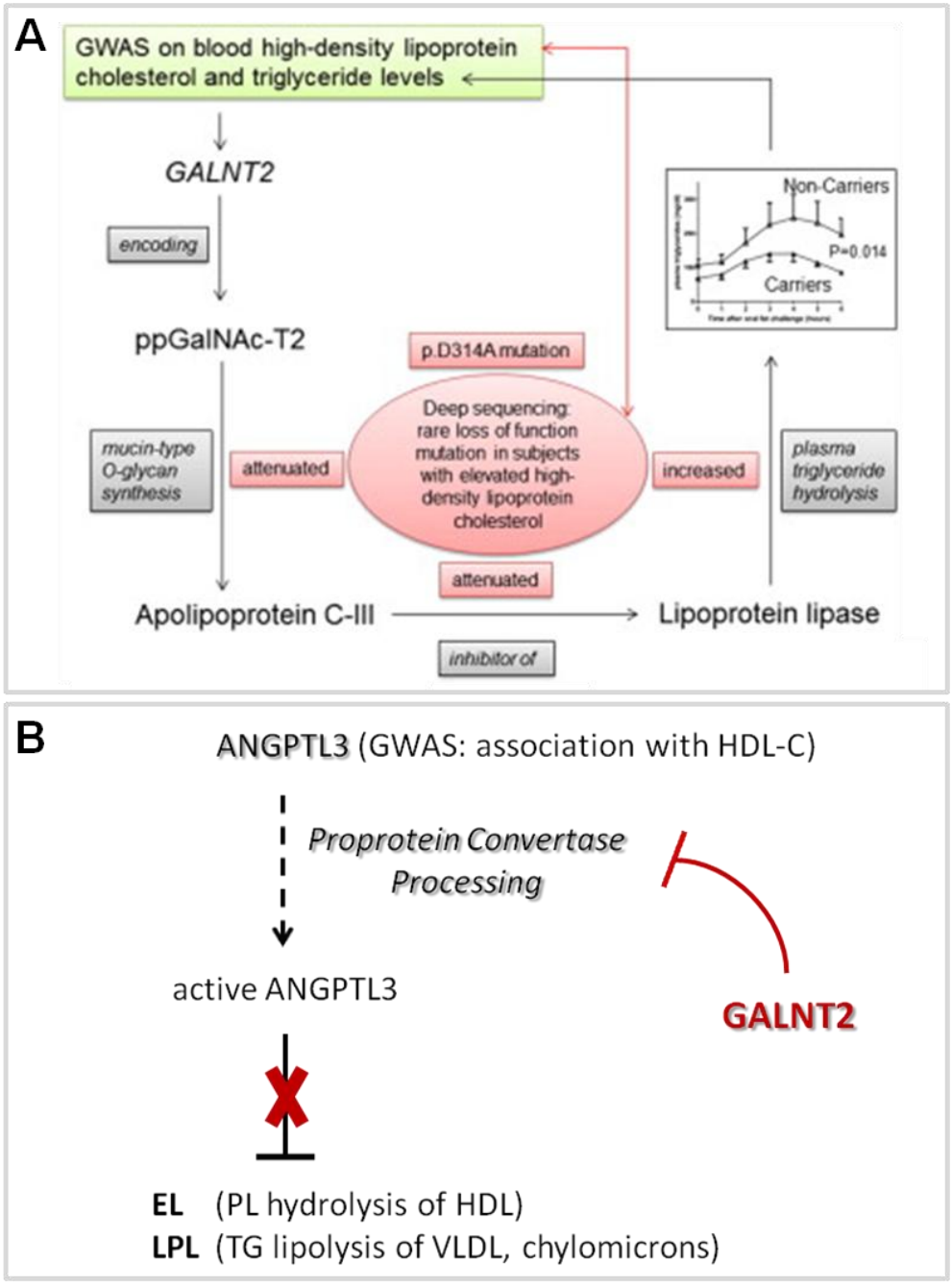

Figure 1.30 Proposed mechanisms of GALNT2-mediated regulation of plasma lipid levels through glycosylation of apoC-III (**A**) or ANGTPL3 (**B)** (see text for details). Adapted from (398).

1.10 Therapeutic targeting of apoA-I and HDL

Pharmacologic intervention for the treatment of atherosclerosis originally focused on lowering serum LDL-cholesterol concentrations as a therapeutic target. Since then, numerous studies highlighting the powerful anti-atherogenic effects of HDL have turned efforts to reduce cardiovascular morbidity and mortality, towards the elevation of apoA-I and HDL levels. In order to achieve this, several new therapeutic strategies have been developed.

One approach to modify serum HDL cholesterol includes lifestyle interventions such as physical exercise, weight loss and smoking cessation (403-406). However, the effect of such lifestyle changes on HDL levels is minor and it is often difficult to determine the mechanism that is responsible for the beneficial HDL outcomes. As mentioned previously, current therapeutic interventions that aim at restoring the abnormal plasma lipid profile, have not been designed to specifically act on HDL and therefore only have moderate effects on plasma HDL-cholesterol levels (2–30 %) (407-409). Statins are the most widely used lipid-lowering drug therapy in cardiovascular prevention, while fibrates are mainly used to reduce plasma triglycerides. Niacin is the most potent drug in increasing HDL-cholesterol levels (up to 30 %), however its use is limited by side effects such as flushing. Novel therapeutic strategies to either raise HDL-cholesterol levels or improve HDL functionality are being developed as complementary therapy to statins and fibrates for cardiovascular diseases. This approach includes CETP inhibitors, novel PPAR agonists and LXR agonists. However, until now most therapies have failed in clinical trials due to the presence of side effects or the absence of clinical benefits. To date, four CETP inhibitors have been developed in humans. Torcetrapib has been tested in phase III clinical trials and although results showed a marked increase in HDL-cholesterol and a moderate decrease in LDL-cholesterol (410) an increased risk of cardiovascular events and an excess of mortality was observed. Subsequent investigations suggested that toxicity of torcetrapib most probably was independent of CETP inhibition. Clinical trials on dalcetrapib demonstrated a considerable increase in HDL-cholesterol but failed to demonstrate a beneficial effect on

cardiovascular disease (411). At the moment two other more potent CETP inhibitors, anacetrapib and evacetrapib, with significant effects on both HDL- and LDL-cholesterol and absence of adverse effects are still in phase III clinical trials (412). Besides fibrates, which are already pharmacologically used, a dual PPAR α/γ agonist (aleglitazar) has been developed (413). Despite the initial encouraging results, phase III clinical trial of aleglitazar failed due to adverse effects on heart failure. Since then several highly selective and potent PPAR agonists have been developed (414), and are currently in various phases of clinical trials. Results so far show obvious clinical benefits and no side effects, thus these PPAR agonists appear as promising drugs for the treatment of cardiovascular risk associated with metabolic syndrome and type 2 diabetes. With regard to the LXR agonists, the beneficial effects of T0901317 and GW3965 have been extensively described in preclinical animal models of cardiovascular diseases, neurodegenerative diseases and inflammation (415-418). However, due to their lipogenic adverse effects (hepatic lipogenesis, hypertriglyceridemia and hepatosteatosis) (419) LXR ligands have not yet been tested in clinical trials. Efforts are presently focused on developing selective LXR modulators, either LXRβ-specific agonists or ligands which act selectively in specific tissues that will maintain the beneficial effects but minimize the lipid side effects. Therefore, their therapeutic value remains to be shown.

Recently, some promising results have been obtained from preclinical or clinical studies on targeting HDL metabolism and function by antisense oligonucleotides and miRNA-based therapies (420-426). Although major concerns regarding delivery, specificity, and toxicity need yet to be overcome this approach is considered to hold true therapeutic potential. In addition, several monoclonal antibodies (mAbs) have been developed and are being tested in clinical studies for the treatment of dyslipidemia and cardiovascular disease (427-430). The specificity of mAbs offers a clear benefit over conventional therapy, and initial studies have shown that these compounds are generally safe and well tolerated. However, their long-term safety and efficacy will be determined by the ongoing large clinical studies.

Despite the development of new state-of-the-art therapeutic interventions, several strategies aiming at increasing HDL-cholesterol levels

have failed to show the anticipated clinical benefit. As a result, focus has shifted toward strategies to improve HDL functionality. As the major functional component of HDL, apoA-I has been considered as an attractive target for the treatment of atherosclerosis as well as of other chronic inflammatory diseases. As a consequence, therapies designed to mimic apoA-I function are being developed, and include administration of full length apoA-I, mutated variants of apoA-I, and apoA-I mimetic peptides.

ApoA-I mimetic peptides are small amphipathic peptides of 18-36 amino acids, that were designed based on the apoA-I sequence in a way that they maintain the fundamental properties of apoA-I, such as the ability to promote cholesterol efflux and to activate LCAT. So far, a considerable number of apoA-I mimetic peptides has been examined for their therapeutic potential. Administration of the peptide 4F has been shown to reduce atherosclerosis without raising plasma levels of HDL-cholesterol (431). This orally administered peptide can also promote macrophage RCT in mice and has been suggested to enhance the anti-inflammatory functions of HDL (432). However, despite its potent anti-inflammatory and antioxidant effects *in vitro* and in experimental models, human studies have indicated otherwise (431, 432). In two trials of 4F in patients with coronary heart disease, its effect on the HDL-mediated protection provided conflicting results (433, 434). L-6F is another peptide that has been shown to possess antioxidant and anti-inflammatory properties in several mouse models (435, 436). Administration of L-6F has prevented the WTD-mediated pro-atherogenic changes in intestinal gene expression, while feeding $LDLr^{-/-}$ mice a WTD with transgenic tomatoes expressing L-6F significantly reduced the aortic lesion area (435). In addition, the peptide 5A has been found to induce cholesterol efflux specifically through ABCA1 (437, 438), while the 5A-phospholipid complex can promote both ABCA1- and ABCG1-mediated cholesterol efflux. Administration of a 5A-phospholipid complex has been shown to enhance RCT (439), and inhibit atherosclerosis development in $apoE^{-/-}$ mice. Recently, a peptide consisting of 36 amino acids, ATI-5261, has been developed. This peptide has been shown to induce ABCA1-mediated cholesterol efflux with similar efficiency as apoA-I (440). Administration of ATI-5261 in $LDLr^{-/-}$ or $apoE^{-/-}$ mice fed a WTD resulted in a significant reduction of both the aortic

lesion area and the lipid content of the plaque. Finally, ETC-642, a single helical 22-amino-acid-long amphipathic peptide complexed with phospholipids, has been shown to reduce pro-inflammatory oxLDL as well as the atherogenic small dense LDL, while shifting the HDL subpopulations toward the anti-atherogenic pre-β fraction (441). Moreover, ETC-642 has been characterized as a potent inducer of cholesterol efflux from human macrophages in *in vitro* assays and has been found to enhance RCT *in vivo* (442, 443). The anti-inflammatory effects of ETC-642 have also been demonstrated in rabbit models of acute and chronic inflammation (441-443). The efficiency of ETC-642 as an anti-atherosclerotic agent has been demonstrated since treatment with high-dose ETC-642 significantly inhibited plaque formation in hyperlipidemic rabbits (443).

In a similar context, the beneficial effects of apoA-I-based infusion therapies on atherosclerosis have been examined. HDL-VHDL infusions have been shown to inhibit plaque formation, as well as reduce the extent of pre-existing lesions in rabbits fed an atherogenic diet (444, 445). Similarly, treatment of hyperlipidemic rabbits with purified apoA-I has resulted in a significant reduction in atherosclerotic plaques. However, apoA-I infusions did not induce regression of established plaques (446). In addition, recombinant $apoAI_{Milano}$ has also been used for treatment of atherosclerosis. Carriers of the apoA-I_{Milano} mutation are characterized by reduced levels of HDL-C but this is not associated with the anticipated increased risk of CVD (188). This apoA-I variant has displayed remarkable atheroprotective activities, including enhanced ABCA1-mediated cholesterol efflux and anti-inflammatory and plaque stabilizing properties (447). Infusion of recombinant apoA-I_{Milano} has been shown to inhibit plaque progression and reduce plaque area of established lesions in various animal models (448-452). Interestingly, in a small clinical trial infusion of recombinant apoA-I_{Milano} complexed with phospholipids caused regression of atherosclerotic lesions in coronary patients (453). Furthermore, the efficacy of infusion of rHDL compounds, consisting of native apoA-I and phospholipids, on coronary atherosclerosis has been investigated. Infusion of one of these compounds, CSL-112, has resulted in an increase in both apoA-I and pre-β HDL levels, which was accompanied by enhanced ABCA1-mediated cholesterol efflux (454). A

different rHDL particle designed to mimic nascent pre-β HDL, CER-001, has also been developed. CER-001 infusions have been shown to reduce atherosclerotic plaque size and aortic macrophage and lipid content in mice (455). Finally, given that cholesterol-poor HDL particles are particularly effective in inducing RCT, an alternative strategy involving selective delipidation of HDL *ex vivo* resulting in lipid-poor apoA-I is currently under investigation (456).

Despite the overall disappointment, the clinical failure of therapeutic strategies aiming at increasing HDL-cholesterol levels has opened up a new perspective in the field of HDL-based therapies. Thus, HDL-cholesterol concentration in plasma is no longer considered to reflect the atheroprotective capacity of HDL. As a result, the focus of HDL-based therapeutic approaches has shifted towards raising the components of HDL that mediate its beneficial effects. To this end, a large number of apoA-I analogue proteins and apoA-I-based infusion therapies are currently being developed. However, the actual clinical benefit from apoA-I-based therapies needs to be addressed by well-designed clinical trials in patients.

1.11 Clinical significance

Over the past decades HDL biology and genetics have been extensively investigated, however translating basic research findings into effective treatments for cardiovascular and other inflammatory diseases remains unattainable. The inverse correlation between HDL-cholesterol levels and the risk for cardiovascular disease has been substantiated. On the other hand, efforts to establish a causal link between the two parameters have failed thus diminishing the value of HDL quantity as a biomarker. This has turned the focus of recent studies towards determining HDL particle functionality.

The heterogeneity and compositional complexity of the HDL particles is reflected in its pleiotropic effects. HDL contributes to atheroprotection by exerting numerous functions including promoting cholesterol efflux from macrophages, maintenance of endothelium integrity and vasodilation. In addition, HDL possesses anti-oxidant, anti-inflammatory, anti-thrombotic and

anti-apoptotic properties, while it also mediates anti-bacterial, anti-parasitic and anti-viral effects. Compositional changes in the proteome of HDL or modifications of its protein and lipid moieties may alter HDL functionality in a way that renders the HDL particles pro-atherogenic. Advancing our knowledge on the mechanisms leading to HDL dysfunction as well as the signaling pathways that are involved in HDL's protective activities may facilitate the development of new HDL-based therapies to prevent or treat atherosclerosis and other human chronic inflammatory diseases.

2 MATERIALS AND METHODS

2.6 Reagents

Restriction and modifying enzymes were purchased from Minotech (Heraklion, Greece) or New England Biolabs (Ipswich, MA) unless stated otherwise. Oligonucleotides were synthesized at the microchemical facility of the Institute of Molecular Biology and Biotechnology (IMBB; Heraklion, Greece) or purchased from Eurofins MWG Operon. All necessary reagents for PCR amplification were from Promega. Cell cultures were maintained in complete medium consisting of Leibovitz's L-15 (Corning Cellgro) or Dulbecco's modified Eagle medium (DMEM) (Invitrogen), supplemented with 10% fetal bovine serum (FBS) (Biochrom) and 1X of 100X antibiotic-antimycotic solution (Invitrogen). For amplification of adenoviruses cells were grown in medium supplemented with 2% heat-inactivated horse serum (HIHS; Invitrogen) and 1X antibiotic-antimycotic solution. For flow cytometric analysis, the following fluorescent-conjugated antibodies were used: anti-CD11b (M1/70) and anti-MHC class II (AF6-120.1) were purchased from BD Biosciences. Antibodies against CD3 (145-2C11), CD4 (RM4-5), CD8a (53-6.7), CD44 (IM7), CD45R/B220 (RA3-6B2), Ly-6G/Ly-6C (Gr-1) (RB6-8C5), CD11c (N418), CD40 (3/23), CD80 (16-10A1), CD86 (GL-1) were all purchased from BioLegend.

2.7 Molecular Cloning Protocols

Site-Directed Mutagenesis by Overlap Extension Using PCR

Single base substitutions in the ApoA-I gene were generated by overlapping PCR. In this technique of site-directed mutagenesis, complementary oligodeoxyribonucleotide primers are used in PCR to generate two DNA fragments having overlapping ends. These fragments are combined in a subsequent 'fusion' reaction and the resulting product is amplified further by

PCR. The pCDNA3.1-apoAIg(ΔBglII) plasmid (190) was used as template for the generation of Met148Ala and Tyr192Ala mutations in the apoA-I gene. For the amplification, a set of 5'- and 3'-flanking primers designated apoAIg F and apoAIg R was used. The first primer was designed to carry the XbaI (5'-TCTAGA-3') and BglII (5'-AGATCT-3') recognition sites, and the second primer carried the EcoRV (5'-GATATC-3') recognition site. The primers and the PCR conditions used to create apoA-I(M148A) and apoA-I(Y192A) are shown in Table 2.1.

Table 2.1 Mutagenic primers used in PCR amplifications.

Name	**Sequence**
apoAIg - Fw	5'- GCTCTAGATCTGACATAAATAGGCCCTGC -3'
apoAIg - Rev	5'- GCGGATATCCAGGCCTTGTTTGAGCC -3'
apoAI(M148A) - Fw	5'- CCACTGGGCGAGGAG**GCG**[a]CGCGACCGCGCGCG -3'
apoAI(M148A) - Rev	5'- CGCGCGCGGTCGCG**CGC**[a]CTCCTCGCCCAGTGG -3'
apoAI(Y192A) - Fw	5'- GCCAGACTGGCCGAG**GCC**[a]CACGCCAAGGCCAC -3'
apoAI(Y192A) - Rev	5'- GTGGCCTTGGCGTG**GGC**[a]CTCGGCCAGTCTGGC -3'

[a] Mutagenized residues are marked in bold and underlined.

Agarose Gel Electrophoresis

Agarose gels were set up in 1x TAE (50x TAE: 121 g Tris, 18.6 g EDTA, 28.55 mL acetic acid glacial in 500 mL dH_2O) containing 0.5 - 3% agarose, depending on the estimated size of the expected DNA fragments. The solution was boiled in a microwave oven and cooled down to approximately 50 °C. 4 µL of ethidium bromide solution (10 mg/ml) were added per 100 mL of agarose solution. λDNA digested with BstEII or 100 bp DNA ladder (Invitrogen) was used as a DNA size marker. Samples were mixed with 6x gel loading dye (0.25% bromophenol blue, 0.25% xylene cyanol FF, 30% glycerol) and run in tanks under the appropriate electrical field (50-120 V). The bands were visualized using the TFX-35M UV transilluminator (GIBCO).

Molecular Cloning Techniques

The cDNA sequences of human myeloperoxidase (MPO) and GALNT2 were amplified by PCR using the primers shown in Table 2.2 and subsequently cloned into appropriate vectors. Generally, plasmids and PCR products were digested with the appropriate restriction enzymes. The digestions were performed in the proper reaction conditions as recommended by the manufacturer. Small amounts of DNA (≤1 μg of DNA) were incubated at 37 °C for 1 h, while in large-scale digests 5-15 μg of DNA were incubated at 37 °C for 3-5 hrs. Shrimp Alkaline Phosphatase (SAP) (Roche) was used for the dephosphorylation of digested DNA fragments. The reaction assay was performed by adding 1 μL of SAP in the digestion, followed by incubation at 37 ^{o}C for 1 h and heat inactivation of the enzyme at 65 ^{o}C for 20 min. Large Fragment of DNA Polymerase I (Klenow Fragment) was used to fill in 5´-protruding ends of digested DNA fragments. The reaction was set up according to the manufacturer's recommendations and the mixture was incubated at RT for 15 min. The reaction was terminated by addition of 0.5 M EDTA pH 8.0 at a final concentration of 10 mM and heat inactivation of the enzyme at 75 ^{o}C for 20 min. PCR products, digested DNA fragments and reaction mixtures were purified with Wizard® SV Gel and PCR Clean-Up System by Promega following the manufacturer's protocol. The concentration of the purified DNA fragments was determined either by gel quantitation or by spectrophotometry. For ligation of digested DNA fragments, T4 DNA Ligase (New England Biolabs) was used and the reactions were performed in a final volume of 20 μL. The molar ratio of insert to vector was 3:1 to 5:1 molecules by using 50-100 ng of the vector DNA. The final mixture was incubated at 4 ^{o}C overnight, and the terminated ligation reaction was subsequently used for transformation of 100 μL chemically competent DH10β cells. TA cloning was performed using pGEM-T Easy vector system (Promega) according to the manufacturer's recommendations.

Table 2.2 Primers used in PCR amplifications for cloning of human MPO and GALNT2 cDNAs into appropriate vectors.

Name	Sequence
hMPO - Fw	5'-C**AAGCTT**[a]**GCGACC**ATGGGGGTTCCCTTCTTCTC-3'
hMPO - Rev	5'-**GATATC**[b]CTAGGAGGCTTCCCTCCAGGAAGCCAG-3'
hGALNT2 - Fw	5'-**GTCGAC**[c]**GCGACC**ATGCGGCGGCGCTCGCGGATGCTGCTCT-3'
hGALNT2 - Fw	5'-TGC**TCTAGA**[d]CTACTGCTGCAGGTTGAGCGTGAACTTCCAC-3'

[a,b,c,d] Sequences corresponding to HindIII, EcoRV, SalI and XbaI recognition sites, respectively, are marked in bold and underlined.
[e] Kozak consensus sequence is marked in red letters.

Cultivation of Bacteria

Escherichia coli (*E.coli*) cells were grown in and on LB medium (10 g NaCl, 5 g yeast extract, 10 g tryptone, ddH_2O up to 1L and autoclave). Depending on the resistance cassette on the transformed plasmids, appropriate antibiotics were used to a final concentration of 100 µg/mL for ampicillin, 50 µg/mL for kanamycin and 25 µg/mL for chloramphenicol. The bacterial cells in shaking cultures had a ratio of one volume growth medium to five volumes air. *E.coli* cultures were incubated at 37 °C for 16-18 h.

Transformation of *E.coli* DH10β Cells by Heat Shock

Approximately 100 µL of frozen competent cells were thawed on ice and the appropriate amount of DNA (20 µL of the ligation reaction or 20-100 ng of plasmid) was added to the cells. The cells were incubated for 30 min on ice, heat-shocked at 42 °C for 45 sec and immediately placed on ice for 2-3 min. Subsequently, 0.9 mL of LB was added and the cells were incubated at 37 °C for 1 h. If the DNA that was used for transformation derived from a ligation reaction, the cells were centrifuged at 380 x g for 5 min at RT, resuspended in 150 µL LB and the entire amount of resuspended bacteria was spread on LB plate with the appropriate antibiotic. If plasmid DNA was used for

transformation 100 µL of cells were spread on the appropriate selective plate. The plated were then incubated at 37 °C for 16-18 h.

Transformation of *E.coli* BJ5183-AD1 by Electroporation

For the generation of recombinant adenoviruses using the AdEasy system (457), PmeI-linearized pAdTrack-CMV-X vectors (where X is the gene of interest) were used to transform BJ-5183-AD1 (Agilent Technologies) bacterial cells carrying the pAdEasy-1 plasmid by electroporation according to manufacturer's instructions. For each reaction 40 µL of BJ-5183-AD1 cells were used. Electroporation was performed (200 Ω, 2.5 kV, 25 µF) in 0.2 cm Gene Pulser Cuvettes (Bio-Rad) using the Bio-Rad Gene Pulser II electroporation machine. The cells were then plated on agar plates and the recombinant clones were selected based on their resistance to kanamycin.

Plasmid Mini-Preparation by Alkaline Lysis of Bacterial Cells

Single bacterial colonies were picked from selective plates and used to inoculate 2 mL of the appropriate selective LB medium. Following 16-18 h incubation at 37 ^{o}C in a shaking incubator, the mini cultures were transferred in eppendorf tubes and centrifuged at 15,000 x g for 1 min. Plasmid extraction and purification was performed using either the QIAGEN Plasmid Mini Kit or the High Purity Plasmid Miniprep System (Origene) according to the manufacturer's instructions. Briefly, the supernatant was removed and the cell pellet was resuspended in the appropriate suspension buffer, lysed and centrifuged to pellet cell debris. The plasmid-containing supernatant was collected and plasmid DNA was precipitated, air-dried and resuspended in 30-35 µL sterile dH_2O.

Plasmid Midi- and Maxi-Preparation

Large-scale preparations of plasmids were performed according to the QIAGEN Plasmid Midi kit or the High Purity Plasmid Maxiprep System (Origene) protocol. The concentration of the purified DNA was determined by spectrophotometry.

Nucleic Acid Quantification by UV Spectrophotometry

To determine the concentration of nucleic acids the Jenway 6405 UV/VIS Spectrophotometer was used. 1 mL of ddH_2O was added in the cuvette and used to calibrate the instrument. The samples were diluted 1:200 in ddH_2O (5 μL DNA or RNA sample + 995 μL ddH_2O) and the readings were taken at wavelengths of 260 nm and 280 nm. Pure preparations of DNA and RNA have OD_{260}/OD_{280} values of 1.8 to 2.0. The concentration of each sample is calculated as indicated below:

OD_{260} * 50 ng/μL * dilution factor, for double-stranded DNA

OD_{260} * 35 ng/μL * dilution factor, for single-stranded DNA

OD_{260} * 40 ng/μL * dilution factor, for RNA

DNA Sequencing

All sequencing reactions were performed by the laboratory of L. Spanos in IMBB, FORTH.

2.8 Preparation of rHDL Containing ApoA-I

Purified apoA-I was kindly provided by Prof. Vassilis Zannis. The recombinant apoA-I was produced and purified from the culture medium of adenovirus-infected HTB-13 cells as previously described (458) by Dr. Panagiotis Fotakis. rHDL particles were prepared by the sodium cholate dialysis method (459)

using POPC/cholesterol/apoA-I/sodium cholate in a molar ratio of 100:10:1:100 as previously described (460). Briefly, the required amounts of cholesterol and POPC were dissolved in chloroform:methanol (2:1), gently mixed and dried under nitrogen. The dried lipid was dissolved in salt buffer (10 mM Tris-HCl pH 8.3, 150 mM NaCl, and 0.01% EDTA) by gentle vortexing and the suspension was incubated on ice for 1 h. Next, an appropriate amount of sodium cholate was dissolved in salt buffer, gently mixed with the lipid suspension and the solution was kept on ice for 1 h more. Finally, apoA-I was added, and the mixture was gently vortexed and incubated on ice for another 1 h. The rHDL preparation was extensively dialyzed against PBS using membranes with a molecular weight cut-off of 12,000–14,000 Daltons and the formation of apolipoprotein-lipid complexes was verified by two-dimensional gel electrophoresis (38, 461). Concentration of rHDL was based on apoA-I content and was determined by DC Protein Assay (Bio-Rad).

2.9 Cell Culture Protocols

Subculture of Cell Lines

The cell lines used in the present study were HepG2 (human hepatocellular liver carcinoma cells), 911 (human embryonic retinoblasts), HEK293T (human embryonic kidney 293T cells), HEK293 (human embryonic kidney 293 cells), EA.hy926 (human umbilical vein endothelial hybrid cell line) and J774 (murine macrophages). The stocks of the cultures are kept at -80 ^{o}C. All cell cultures were grown in T75 flasks in complete medium (DMEM / 10% FBS / 1x antibiotic-antimycotic) and maintained at 37 °C in a 5% CO_2 incubator. The medium was renewed every 48 h. As soon as a confluent monolayer had been formed in the flask, the cells were subcultured to an appropriate concentration either by scraping (J774 cells) or by using trypsin-EDTA. HTB-13 cells were grown in L-15 medium (Corning Cellgro, Cat No 10-045-CV), HepG2, 911 and HEK293T cells were grown in high glucose DMEM (Invitrogen, Cat No 41966), J774 cells were grown in high glucose DMEM with GlutaMAX supplement (Invitrogen, Cat No 31966) and EA.hy926 cells were

grown in low glucose DMEM with GlutaMAX supplement (Invitrogen, Cat No 21885). HEK293 cells used for recombinant adenovirus amplification were grown in L-15 medium.

Transient Transfection Assay

Transient transfection of cells using the $CaPO_4$ was performed in order to assess the levels of protein expression. For this purpose, p60 and p100 cell culture plates were used. One day before the transfection experiment, the appropriate number of cells (Table 2.3) was plated in the dish and incubated in complete growth medium at 37 °C overnight. After 24 h the cells had reached the desired density of 60-80% confluency. To transfect cells, the proper amount of DNA, 2M $CaCl_2$ and H_2O were added in an eppendorf tube. Salmon Sperm DNA Solution (GIBCO) was used either as control or to equilibrate the DNA amount in all samples. The DNA/ $CaCl_2$ mix was then added dropwise while vortexing to a tube containing an equal amount of 2x HBS (274 mM NaCl, 10 mM KCl, 1.5 mM $Na_2HPO_4{\cdot}H_2O$, 12 mM Dextrose, 42 mM Hepes, pH 7 ± 0.1). The mixture was incubated at RT for 15 min and added to the cells dropwise. Cells were incubated at 37 °C and the medium was renewed 7-17 h post-transfection. Cells were incubated at 37 °C for another 24 h and then harvested for protein isolation. For adenovirus amplification cells were transfected using Lipofectamine 2000 according to the manufacturer's recommendations.

Table 2.3 Setup for transfection assays using the $CaPO_4$ method.

Culture dish	Number of cells		Volume of medium	DNA	2 M $CaCl_2$	2x HBS	H_2O
	HepG2	HEK293T					
p60	10^6	500.000	3 mL	15 µg	15,5 µL	125 µL	up to 125 µL
p100	2 x 10^6	10^6	5 mL	30 µg	31 µL	250 µL	up to 250 µL

Neutrophil Isolation from Human Peripheral Blood

About 12 mL of peripheral blood were obtained from a healthy donor and collected in a vacutainer consisting of EDTA as anti-coagulant. Six mL of whole blood were mixed by inversion with 2 mL dextran (5% solution in PBS; Sigma-Aldrich) and incubated at 37 ^{o}C for 30 min. After sedimentation, the neutrophil rich supernatant at upper layer was collected and carefully layered on top of equal volume (~4.5 mL) of Histopaque-1077 (Sigma-Aldrich). The layers were centrifuged at 450 x g for 20 min at RT without brakes. The pellet was resuspended in 3 mL hemolysis buffer (155 mM NH_4Cl, 10 mM $KHCO_3$, 0.1 mM EDTA) and incubated for 5 min on ice. The tube was then filled with 1x PBS and centrifuged at 160 x g for 5 min at RT with brakes. After centrifugation, the supernatant was discarded and the white pellet consisting of granulocytes was obtained and re-suspended immediately in 1x PBS. Morphological examination and trypan blue exclusion test were performed to determine the cell count and purity of the neutrophils. RNA was extracted from the isolated cells and used for cDNA synthesis. The neutrophils' cDNA was used for amplification of the human MPO cDNA sequence by PCR and its subsequent cloning into the appropriate vector.

Generation of Mouse Bone Marrow-Derived Dendritic Cells (BMDCs)

BMDCs were generated from bone marrow progenitors, as previously described (462). Bone marrow was isolated from femurs and tibias of female mice, treated with RBC lysis buffer (155 mM NH_4Cl, 10 mM $KHCO_3$, 0.1 mM Na_2EDTA) to remove red blood cells and plated at 2.5×10^6 cells per 100 mm cell culture dish in complete medium supplemented with 20% supernatant from a murine GM-CSF secreting cell line (X63Ag8; kindly provided by B. Stockinger, National Institute of Medical Research, London, U.K.) (463). The culture medium was half-renewed on days 3, 6 and 8. On day 9, non adherent cells were collected and cultured in 24-well tissue culture plates (1×10^6 cells / 500 µL / well) in the presence of either 0.5 µg/mL Lipopolysaccharide from *Escherichia coli* O111: B4 *(*LPS) (Calbiochem) or 20 µg/mL zymosan (InvivoGen) and/or 4 µM rHDL. BMDCs were harvested as indicated for RNA,

Western blot and FACS analysis. Culture supernatants were collected at 12 h or 18 h for cytokine analysis by ELISA.

In Vitro Proliferation of dLN Cells (dLNCs)

Female mice (8-10 week old) were immunized subcutaneously at the base of the tail with 100 µg OVA (Sigma-Aldrich) emulsified in equal volume of CFA. dLNs were excised 9 days later and single cell suspensions were prepared. dLNCs were cultured in flat-bottom 96-well plates (5 x 10^5 cells/well) in the presence of OVA (15 µg/mL) and/or increasing concentrations of rHDL (1µM = 28 µg/mL) for 72 h. Cells were then pulsed with 1µCi [^{3}H]thymidine (TRK120; Amersham Biosciences) for 18 h, and the incorporated radioactivity was measured using a Beckman beta counter. Cytokine levels in culture supernatants were determined by ELISA and cells were analyzed by flow cytometry after 48 h of stimulation.

Cocultures

BMDCs from WT mice were plated in 24-well tissue culture plates (1 × 10^6 cells / 500 µL / well), stimulated with 0.25 µg/mL LPS and pulsed with 20 µg/mL OVA in the presence or absence of 4 µM rHDL for 12 h. Stimulated BMDCs were collected and washed to remove excess LPS, OVA and rHDL. Next, cells were co-cultured with dLNCs (5 x 10^4 BMDCs with 4 x 10^5 dLNCs / 200 µL / well) isolated from OVA-immunized mice (9d post immunization) as described above, in the presence or absence of 15 µg/mL OVA . Culture supernatants were harvested 48 h later.

Isolation of thioglycollate-elicited peritoneal macrophages

To isolate thioglycollate-elicited peritoneal macrophages, mice were injected intraperitoneally (i.p.) with 1 mL thioglycollate medium (Lab M, Lancashire, UK). Four days later, mice were sacrificed and their peritoneal cavities were

washed with 10 mL of ice-cold PBS. Cells were collected by centrifugation at 500 x g for 10 min at room temperature and cultured in complete medium in 6-well plates at a density of 2 x 10^6 cells/mL/well. 16 h later cells were washed twice with PBS to remove non-adherent cells and adherent macrophages were collected for further analysis

Endothelial Cell Assays

For signaling assays, cells were plated in 6-well plates at a density of 2.5 x 10^5 cells/mL/well. When the cells reached ~80% confluency the medium was replaced with starvation medium (DMEM/antibiotics) and 4 h later cells were incubated with serum HDL (40 µg/mL final concentration based on apoA-I content) for 20 min. Following treatment, cells were collected, lysed and subjected to western blot analysis for pAkt, Akt, peNOS, eNOS and actin expression, as described below. For migration assays, cells were plated in 24-well plates at a density of 6 x 10^4 cells/0.5 mL/well. When the cells reached near confluency the medium was replaced with starvation medium (DMEM/antibiotics) and 24h later cell monolayers were scratched using a pipette tip. The medium was changed immediately after wounding and cells were incubated with serum HDL (40 µg/mL final concentration based on apoA-I content) for 12 h and then fixed. Cell migration into the wounded area was assessed by measuring the scratch area at t=0 h and t= 12 h. Results are calculated as % of the initial scratch area and expressed as % of untreated cells (control). Images were acquired using a 5x objective of an Axio Vert.A1 microscope coupled with an AxioCam ICM1 camera (Carl Zeiss MicroImaging GmbH, Oberkochen, Germany). Scratch area (µm^2) measurements were performed using the AxioVision software (Carl Zeiss MicroImaging GmbH, Oberkochen, Germany) and images were processed with Adobe Photoshop 7.0 (Adobe Systems, San Jose, CA). For endothelial cell assays pooled serum HDL samples from 2-5 mice of the same genotype were used.

ABCA1-Dependent Cholesterol Efflux Assay

ABCA1-dependent efflux of [^{14}C]-cholesterol (American Radiolabeled Chemicals, St.Louis, MO) was measured using J774 mouse macrophages, in which the expression of ABCA1 was induced by a 3',5'-cyclic adenosine monophosphate (cAMP) analogue, using serum HDL from transgenic mice carrying WT and mutant apoA-I forms as cholesterol acceptors. J774 cells were plated in 48-well plates at a density of 2.5 x 10^4 cells/0.2 mL/well and 48 h later cells were labeled with 0.2 mL of labeling medium ([^{14}C]-cholesterol dissolved in ethanol and dispersed into DMEM supplemented with 0.2% (w/v) BSA at a concentration of 0.25 μCi/mL) for 24 h. Cells were next treated with 0.3 mM cpt-cAMP (Sigma-Aldrich, St.Louis, MI) in DMEM/0.2% BSA for 24 h and then incubated for 4 h with either equal concentration (28 μg/mL final concentration based on apoA-I content) or equal volume (2 or 5 μL/well) of serum HDL diluted in DMEM/0.2% BSA in a final volume of 0.2 mL. At the end of the incubation, the medium was collected and clarified by centrifugation for 5 min and the cells were lysed in 0.2 mL lysis buffer [1x PBS/1% (v/v) Triton X-100] by shaking for 30 min at RT. The radioactivity in 0.1 mL of supernatant and 0.1 mL of cell lysate was determined by liquid scintillation counting. [^{14}C]-cholesterol efflux was expressed as the percentage of the radioactivity released in the medium relative to the total radioactivity in cells and medium. Basal efflux to BSA (in the absence of acceptors) has been subtracted from the data shown. For cholesterol efflux assays using equal concentration of HDL pooled serum HDL samples from 2-5 mice of the same genotype were used.

2.10 Expression Analyses

mRNA Expression Analysis

Total RNA was prepared from cells or tissues using TRIzol reagent according to the manufacturer's protocol (Invitrogen). Isolated RNA (1 μg) was reverse-transcribed using SuperScript II Reverse Transcriptase using random primers (both from Invitrogen). The cDNAs produced were used for PCR amplification

with the appropriate pair of primers (Table 2.4). For standard PCR, the expression of the target gene was normalized to the expression of the housekeeping gene. Quantification of the results was performed by measuring the intensity of the bands using the NIH ImageJ software (Bethesda, MD). Quantitative PCR (qPCR) was performed on a StepOnePlus Real-Time PCR system (Applied Biosystems) using either SYBR Green or TaqMan assays. For expression analysis by SYBR Green assay, the KAPA SYBR FAST qPCR Master Mix (Kapa Biosystems) was used. Primers for qPCR were designed using Lasergene PrimerSelect software (DNASTAR) (Table 2.4). Melting curve analysis was performed to ensure primer specificity. For expression analysis of the human apoA-I transgene, qPCR was performed using the TaqMan Universal Master Mix II with UNG (Applied Biosystems) with the appropriate TaqMan probe/primer sets. The mouse actin b (Mm00607939_s1-VIC labeled) probe/primer set was pre-optimized and purchased from Applied Biosystems. The human apoA-I probe/primer set was custom-designed (Table 2.4) and purchased from Eurofins MWG Operon. The reactions were setup in final volume 15 µL using 15 ng cDNA as template, 1x TaqMan Universal Master Mix II and 1x probe/primer mix. The 10x human apoA-I probe/primer mix was prepared by mixing 7.5 µL forward primer (100 pmol/µL), 7.5 µL reverse primer (100 pmol/µL) and 2.5 µL probe (100 pmol/µL) in final volume 100 µL. The thermal cycling program was optimized for human apoA-I expression analysis and was used as follows: 50 ^{o}C for 2 min, 95 ^{o}C for 10 min, 40 cycles at 95 ^{o}C for 15 sec followed by 1 min at 62 ^{o}C. In all cases, the expression of the target genes was normalized to the expression of the housekeeping gene and the normalized Ct values were calibrated against the control condition/sample in each case. The relative gene expression levels were determined using the relative standard curve method and the comparative Ct method (ΔΔCt method) as described in Applied Biosystems Guide.

Table 2.4 Primers used in standard and quantitative RT-PCR.

Primer pairs used in Standard RT-PCR		
Specificity	**Name**	**Sequence**
mouse/ human	*GAPDH*	**Fw:** 5'-ACCACAGTCCATGCCATCAC-3' **Rev:** 5'-TCCACCACCCTGTTGCTGTA-3'
human	*APOA-I*	**Fw:** 5'-GCGTGACCTCCACCTTCAGCAA-3' **Rev:** 5'-TGAGCGTGCTCAGATGCTCGGTG-3'
Primer pairs used in qPCR (SYBR Green assay)		
Specificity	**Name**	**Sequence**
mouse	*Hprt*	**Fw:** 5'-CGAAGTGTTGGATACAGGCC-3' **Rev:** 5'-GGCAACATCAACAGGACTCC-3'
mouse	*Gapdh*	**Fw:** 5'-TGTTCCTACCCCCAATGTGT-3' **Rev:** 5'-CCTGCTTCACCACCTTCTTG-3'
mouse	*Myd88*	**Fw:** 5'-CCACCCTTGATGACCCCCTA-3' **Rev:** 5'-TGCGGCGACACCTTTTCTC-3'
mouse	*Trif*	**Fw:** 5'-TCTACCAGCTCAAGACCCCT-3' **Rev:** 5'-GTCAGCCTGTCCCTTTCCAA-3'
mouse	*Atf3*	**Fw:** 5'-GAGCTGAGATTCGCCATCCA-3′ **Rev:** 5'-CCGCCTCCTTTTCCTCTCAT-3′
mouse	*Abca1*	**Fw:** 5'-GGGCTGGATACGAAAAACAA-3′ **Rev:** 5'-GGGTGGTTGAAAGCAGTGAT-3′
Primer pairs used in qPCR (TaqMan assays)		
Specificity	**Name**	**Sequence**
human	*APOA-I*	**Fw:** 5'-GGGAAAACAGCTAAACCTAAAG-3' **Rev:** 5'-TCCAGGTTATCCCAGAACTC-3' **Probe:** 5'-CCTTGACAACTGGGACAGCGTG- 3' **Reporter dye:** 5'- FAM **Quencher:** 3'- BHQ1

Protein Isolation from Cells and Tissues

Protein extracts were obtained from cells or tissues using different lysis protocols. Tissues, thioglycollate-elicited macrophages and bone marrow-derived DCs were lysed on ice for 30 min in RIPA lysis buffer (50 mM Tris-HCl pH 8.0, 150 mM NaCl, 1% Triton X-100, 0.1% SDS and 0.5% sodium

deoxycholate) supplemented with cOmplete protease inhibitor cocktail (Roche), 5 mM NaF, 1 mM Na_3VO_4 and centrifuged at 13,000 x g for 30 min at 4 ^oC. EA.hy926 cells were washed with ice-cold PBS, scraped, collected by centrifugation at 2,500 x g for 5 min at 4^oC and resuspended in CoIP lysis buffer (20 mM Tris-HCl pH 7.5, 150 mM NaCl, 10% glycerol and 1% Triton X-100) supplemented with cOmplete protease inhibitor cocktail (Roche), 50 mM NaF, 1 mM Na_3VO_4. Cell lysates were rotated at 4^oC for 30 min and centrifuged at 13,000 x g for 5 min at 4^oC. In all protocols after the final centrifugation the supernatant was collected as total cell lysate, and protein concentration was determined by DC Protein Assay (Bio-Rad).

SDS-PAGE

For analysis by SDS-PAGE protein samples were mixed 3:1 with 4 x Sample buffer (5 mL Tris-Cl 1M pH 6.8, 1.6 mL β-mercaptoethanol, 4 mL glycerol, 1.6 g SDS, 8 mg bromophenol blue, dH_2O up to 20 mL), denatured at 100 °C for 10 min (3 min for ABCA1 expression analysis) and loaded on 8.5-12.5% SDS polyacrylamide gel (Table 2.5). The BenchMark Prestained Protein Ladder (Invitrogen) was used as a size marker. Electrophoresis was performed in 1x TGS buffer (1L 10x TGS: 30.3 g Tris, 144.2 g Glycine, 10 g SDS), at 120-140 V using Mini-PROTEAN Tetra Cell System (Bio-Rad). For visualization of the protein bands, gels were either stained with Coomassie Brilliant Blue R-250 or used for immunoblotting as described below.

Table 2.5 Buffers used for the preparation of SDS polyacrylamide gels.

Separating Buffer		**Stacking Buffer**	
Tris	18.165 g (1.5 M)	Tris	6.05 g (0.5 M)
SDS	0.4 g (0.4% w/v)	SDS	0.4 g (0.4% w/v)
pH	8.8	pH	6.8
V_{final}	100 mL	V_{final}	100 mL

Stacking Gel		Separating Gel			
			8.5%	10.5%	12.5%
dH_2O	3.6 mL	dH_2O	4.6 mL	3.9 mL	3.2 mL
30% acrylamide	900 µL	30% acrylamide	2.8 mL	3.5 mL	4.2 mL
stacking buffer	1.5 mL	separating buffer	2.5 mL		
10% APS	60 µL	10% APS	160 µL		
TEMED	6 µL	TEMED	8 µL		
V_{final}	6 mL	V_{final}	10 mL		

Western Blot Analysis

Following SDS-PAGE proteins were transferred to nitrocellulose membranes (GE Healthcare Life Sciences). The transfer was performed using Mini-PROTEAN Tetra Cell System (Bio-Rad) by electroblotting in 1 L transfer buffer (100 mL 10x TGS, 200 mL methanol and 700 mL dH_2O) at 400 mA for ~1.5 h. Membranes were then blocked in 5% non-fat milk in TBS-Tween 20 (TBS-T) for 1 h. Incubation with primary antibodies was performed as shown in Table 2.6. Incubation with HRP-conjugated secondary antibodies (anti-goat, Sigma-Aldrich Cat No A4174; anti-rabbit and anti-mouse, Jackson ImmunoResearch Laboratories Cat No 111-035-045 and 315-035-003, respectively) diluted 1:10,000 in 5% non-fat milk in TBS-T was performed at RT for 1 h. Signals were detected by enhanced chemiluminescence (Thermo Scientific) and proteins were visualized on a ChemiDoc XRS+ imaging system (Bio-Rad) and band intensities were quantified using the Image Lab Software (Bio-Rad). Alternatively, membranes were exposed on film (Fujifilm). Actin levels were used for normalization.

Table 2.6 Antibodies used for analysis of protein expression by western blot.

Antibody	Dilution	Incubation
anti-actin Merck Millipore; Cat No MAB1501	1:5,000 in TBS-T	overnight at 4 ^{o}C
anti-pStat3 (Tyr705) Cell Signaling; Cat No 9131	1:1,000 in 5% BSA in TBS-T	overnight at 4 ^{o}C
anti-STAT3 BD Biosciences; Cat No 610190	1:1,000 in 5% non-fat milk in TBS-T	overnight at 4 ^{o}C
anti-pAkt (Ser473) Cell Signaling; Cat No 4060	1:3,000 in 5% BSA in TBS-T	overnight at 4 ^{o}C
anti-Akt Cell Signaling; Cat No 4691	1:5,000 in 5% BSA in TBS-T	overnight at 4 ^{o}C
anti-peNOS (Ser1177) Cell Signaling; Cat No 9570	1:6,000 in 5% BSA in TBS-T	overnight at 4 ^{o}C
anti-eNOS Cell Signaling; Cat No 8586	1:2,000 in 5% BSA in TBS-T	overnight at 4 ^{o}C
anti-neutrophil myeloperoxidase Sigma-Aldrich; Cat No N5787	1:2,000 in 5% non-fat milk in TBS-T	overnight at 4 ^{o}C
anti-GALNT2 GeneTex Inc.; Cat No GTX104070	1:1,500 in 5% non-fat milk in TBS-T	overnight at 4 ^{o}C
anti-human apoA-I Millipore (Chemicon); Cat No AB740	1:4,000 in 5% non-fat milk in TBS-T	1 h at 37 ^{o}C
anti-mouse apoA-I Meridian Life Science; Cat No K23500R	1:2,000 in 5% non-fat milk in TBS-T	overnight at 4 ^{o}C
anti-ABCA1 Novus Biologicals; Cat No NB400-105	1:500 in 5% non-fat milk in TBS-T	overnight at 4 ^{o}C
anti-GFP Minotech, IMBB-FORTH	1:20,000 in 5% non-fat milk in TBS-T	overnight at 4 ^{o}C

Immunofluorescence

Cells were seeded onto poly-L-lysine (Sigma-Aldrich) coated coverslips in 24-well tissue culture plates (1 x 10^6 cells / well). 24 h later cells were stimulated with 0.5 μg/mL LPS and treated with 4 μM rHDL for 2 h. Cells were washed once with PBS, fixed with 4% paraformaldehyde (Sigma-Aldrich) for 5 min, washed three times with PBS, permeabilized with PBS - Triton X100 0.5% for 5 min, washed three times with TBS-T and blocked in 5% BSA in TBS-T for 1 h. Cells were incubated for 1 h with primary antibody, anti-p65 (sc-109, Santa

Cruz Biotechnology) 1:150 diluted in TBS-T. Secondary antibody Alexa Fluor 555 Goat Anti-Rabbit IgG (Molecular Probes) was added for 1 h at 1:1,000 dilution in TBS. DNA was stained with 1 µg/mL DAPI for 5 min, cells were washed and coverslips were mounted on Mowiol 4-88 (Sigma-Aldrich). Three washes with TBS-T were performed in-between all stainings. All incubations and washes were performed at RT. Images were acquired using a confocal laser scanning microscope (TCS SP8, Leica Microsystems) and a HC PL APO CS2 40x/1.30 oil objective using identical settings within each experiment. Images were obtained using the LAS AF v3.3 software (Leica Microsystems) and processed with Adobe Photoshop 7.0 (Adobe Systems). A total of 100 cells from four different fields from each slide were analyzed for fluorescence intensity of nucleus and cytoplasm using the NIH ImageJ software.

ELISA

Cytokine levels in culture supernatants were measured by ELISA kits following the manufacturer's recommendations. Mouse IL-17, IFN-γ, IL-12 p70, IL-8, IL-6 and TNF-α were purchased from R&D Systems. Mouse IL-23, IL-2 were obtained from eBioscience, and IL-10 from BioLegend.

Flow Cytometry

Cells were stained by incubation with fluorescent-conjugated antibodies for 20 min at 4 ^{o}C in PBS/5% FBS. Intracellular Foxp3 staining was performed using the Alexa Fluor® 488 anti-mouse Foxp3 antibody (BioLegend) and the Foxp3 / Transcription Factor Staining Buffer Set (eBioscience), according to the manufacturer's protocol. Cells were acquired on a FACSCalibur (BD Biosciences) and data were analyzed using the FlowJo software (Tree Star).

2.11 Generation and Analysis of Recombinant Adenoviruses

Generation of Recombinant Adenoviral Plasmids by Homologous Recombination in *E. coli*

For the generation of adenoviral recombinants, appropriate restriction sites were introduced at both ends of the gene of interest (GOI) by PCR amplification. A consensus Kozak signal sequence was also included to ensure efficient transgene expression. The GOI was then subcloned into the pAdTrack-CMV shuttle vector and the presence and correct orientation of the GOI was confirmed by restriction analysis. Transgene expression in the shuttle vector was confirmed by transient transfection assay. *PmeI* was used to linearize the shuttle vector and the linear DNA was purified by gel extraction using the Wizard SV Gel and PCR Clean-Up System. The purified linearized shuttle vector was used to transform BJ5183-AD1 *E.coli* cells that carry the pAdEasy-1 adenoviral backbone plasmid. The correct recombinant clones were selected following *PacI* digestion based on the presence of a large fragment (+30 kb) and a smaller fragment of 3.0 or 4.5 kb, depending on the sites of the homologous recombination. The correct recombinants were then used to retransform competent DH10β *E.coli* cells that are not prone to recombination for large-scale amplification.

Transfection of Adenoviral Genome into 911 Cells

The selected recombinants for each GOI (~15 μg) were linearized by *PacI* digestion and 5 μg of linear DNA were used to transfect 911 packaging cells using Lipofectamine 2000 reagent (Invitrogen) according to the manufacturer's instructions. The transfected cells were maintained at 37 ^{o}C in a 5% CO_2 incubator. 48 h later transfection efficiency and virus production was confirmed by monitoring GFP expression with fluorescence microscopy. 10-14 days post-transfection the viral particles that were formed caused lysis of the cells and the cell lysate was used for infection of a confluent T175 flask of 911 cells. Two to three days after the new infection the cells were lysed and the new lysate was used for the infection of HEK293 cells in a larger scale.

The infections were performed in DMEM supplemented with 2% HIHS and 1x antibiotic-antimycotic.

Large Scale Amplification in HEK293 Cells and Purification of Recombinant Adenoviruses

For large scale amplification of recombinant adenoviruses, HEK293 cells were plated in T175 triple flasks. When cells reached confluency, the collected lysate from the T175 flask was used to infect cells. The infections were performed in L-15 medium supplemented with 2% HIHS and 1x antibiotic-antimycotic. Two to five days after the infection and before lysis occurs, the cells that carry large amounts of recombinant viral particles were harvested by centrifugation at 1,000 rpm for 10 min at 4 ^{o}C. The medium was discarded and the pellet was resuspended in 2 ml of medium (L-15, 2% HIHS, 1x antibiotic-antimycotic) and stored at -80 ^{o}C. The cell suspension was frozen (-80 ^{o}C) and thawed in a 37 ^{o}C water bath three times to lyse cells and release the viral particles. The suspension was centrifuged at 3,000 rpm for 10 min at 4 ^{o}C to pellet cell debris. The supernatant that contained the viral particles was subsequently centrifuged in a $CsCl_2$ gradient twice in order to isolate the viral particles. For the first centrifugation 2 mL of CsCl I (0.619 g/mL in TE pH 8.0) were transferred in a centrifuge tube, overlaid with 5 mL of CsCl II (0.277 g/mL in TE pH 8.0) and 3-4 mL of the viral particles were placed on top. The gradient was centrifuged at 30,000 rpm for 90 min at 4 ^{o}C in a Beckman L8-M Ultracentrifuge using a SW41 rotor. The viral particles were concentrated in a region between the two dilutions. This region was collected using 18g syringe and transferred in a quick-seal tube (Beckman) containing 12 mL of CsCl III (0.450 g/mL in TE pH 8.0). The gradient was centrifuged at 55,000 rpm at 4 ^{o}C for 16-20 h using a 70 Ti rotor. The viral particles were concentrated in a small ~2 mm zone. This zone was collected and extensively dialyzed against sucrose buffer (10 mM Tris, 2 mM $MgCl_2$, 5% sucrose, pH 8.0) in a Slide-A-Lyzer® molecular weight cut-off 10,000 dialysis cassette (Pierce). The viral dilution was aliquoted (50 µL) in 1.5 mL tubes and stored at -80 ^{o}C.

Titration of Recombinant Adenoviruses by Plaque Assay

911 cells were cultured in 6-well plates (1.5 x 10^6 cells/well), grown to confluency and infected with serial dilutions of the virus. The produced adenovirus was sequentially diluted 10^4 to 10^7 times in L-15 medium supplemented with 2% HIHS and 1x antibiotic-antimycotic, and then used to infect 911 cells. Following 30 min of incubation with the adenovirus, the virus-containing medium was removed and the cells were overlayed with agarose solution (1.5% agarose in 40 mM Hepes pH 7.4) diluted in equal volume of medium mixture (1x MEM, 4% HIHS, and 25 mM $MgCl_2$). The cells were incubated at 37 ^oC for 10 to 12 days. The plaques formed characteristic gray regions which were visible to the naked eye, but were also observed under a fluorescence microscope based on the expression of green fluorescence protein (GFP). The number of plaques formed by each dilution was counted, and the titer of the virus was determined in pfu/µL.

Protein Expression by Recombinant Adenoviruses

To determine the expression of the various genes of interest carried by the recombinant adenoviruses, HepG2 cells were cultured in 6-well plates (5 x 10^5 cells/well) in DMEM supplemented with 10% FBS and 1x antibiotic-antimycotic. When cells reached ~80% confluency, the medium was replaced with DMEM supplemented with 2% HIHS and 1x antibiotic-antimycotic and 2 h later the cells were infected with the adenovirus at 10, 20 and 40 multiplicity of infection (MOI). The MOI is defined as the number of viral particles per cell and is calculated as virus titer/number of cells. The cells were incubated with the adenovirus for 3 h, then the medium was replaced with DMEM supplemented with 10% FBS and 1x antibiotic-antimycotic and the cells were incubated for 24 h at 37 ^oC. In the case of apoA-I adenoviruses the medium was replaced with serum-free medium. The cells were examined for GFP expression under a fluorescence microscope and the cells were collected for protein extraction using the CoIP lysis protocol as described above. To confirm the presence of secreted proteins such as apoA-I the medium was also collected. Concentrated medium (40 µL) and 30 µg of cell extract was

analyzed by western blot to determine the expression/secretion of the protein of interest.

2.12 Animal Study Protocols

Generation of Transgenic Mice Expressing Human ApoA-I Under the Mouse Transthyretin (TTR) Promoter

A pBluescript SK plasmid containing the TTR1 exV3 hepatocyte-specific expression cassette (kindly provided by Dr. Theodoros Kosteas; IMBB-FORTH, Heraklion, Greece) was digested with StuI and treated with SAP (Roche). The pCDNA3.1-apoA-Ig(ΔBglII), pAdTrackCMV-apoA-I(L141R) and pAdTrackCMV-apoA-I(L159R) constructs(190) were digested with BglII-EcoRV. The isolated 2.2 kb fragments containing either the WT or the mutant human apoA-I genomic sequences were treated with the Klenow fragment of DNA polymerase I and subcloned downstream of the TTR1 promoter into the dephosphorylated StuI site of the TTR1 exV3 cassette (464). The TTR1-apoA-I transgenes were excised from the corresponding vectors by digestion with BamHI-SalI, separated on a 1% low-melting agarose gel and purified with β-agarase I. The transgene fragments were further purified using the Geneclean Turbo kit (MP Biomedicals) and diluted to a concentration of 3 ng/μL in EmbryoMAX injection buffer (Merck Millipore). Generation of transgenic mice was performed as previously described (465). To identify transgenic founders, genomic DNA was isolated from tail biopsies with standard methods as described below and analyzed by Southern blot and PCR amplification (Table 2.7). PCR reactions for detection of the transgene (human apoA-I) were performed for 33 cycles under the following conditions: 94 °C for 30 sec, 60 °C for 1 min and 72 °C for 1 min. For Southern blot analysis, DNAs were digested with EcoRI, separated in 0.8% agarose gel and then transferred to a Hybond-N^+ membrane (GE Healthcare Life Sciences) by capillary diffusion. The blots were probed with the 2.2 kb fragment of WT human apoA-I obtained following HindIII digestion of the pBluescript-TTR1-apoA-Ig(ΔBglII) vector. The probe was [α-^{32}P]dGTP-labeled using the Nick

Translation System (Invitrogen) and purified using G-50 Sephadex columns (Roche). The membrane was first incubated in prehybridization solution (5xSSPE, 5x Denhardt's solution, 0.5% SDS) containing 20 μg/mL of heat-denatured salmon sperm DNA for 1 h at 65 ^{o}C and then hybridized with the radiolabeled probe overnight at 65 ^{o}C. After a wash with 1xSSPE/0.1% SDS for 15 min and 0.1xSSPE/0.1% SDS for 5 min at 65 °C, the nylon membrane was sealed and transferred to an exposure cassette with an intensifying screen. The membrane was exposed either for 3 h at RT and then scanned on a Phosphorimager, or overnight at -80 °C on film. Transgenic mice were generated and bred at the specific pathogen free Transgenic Mouse Facility of the Biomedical Research Foundation of the Academy of Athens and maintained on a standard chow diet.

Genomic DNA Extraction from Mouse Tails

A small tail piece (<0.5 cm) was cut and incubated in 0.5 mL tail buffer (50 mM Tris pH 8.0, 100 mM EDTA, 100 mM NaCl, 1% SDS) with 5-10 μL Proteinase K (10 mg/mL stock solution; Sigma-Aldrich) at 55 ^{o}C overnight. The tails were vortexed and 0.5 mL of phenol/chloroform/isoamyl alcohol (25:24:1; AppliChem) was added. The mix was thoroughly vortexed and centrifuged at 15,000 x g for 20 min at RT. The upper phase was transferred into a new eppendorf tube containing 0.5 mL chloroform and thoroughly vortexed. The new mix was centrifuged at 15,000 x g for 20 min at RT and the upper phase was transferred into a new eppendorf tube containing 0.28 mL isopropanol and mixed by inversion. DNA was precipitated by centrifugation at 15,000 x g for 15 min at RT and the supernatant was discarded. The DNA pellet was washed with 0.5 mL of 70% ethanol and centrifuged at 15,000 x g for 15 min at RT. The supernatant was discarded and the DNA was allowed to air-dry inside a hood for 10 min. The DNA pellet was resuspended in 0.1 mL UltraPure DNase/RNase-free dH_2O (Invitrogen) and incubated at 4 ^{o}C overnight before use. For genotyping 15 ng gDNA was used in each PCR reaction. gDNAs from mouse tails were stored at 4 ^{o}C.

Mice and Diet

Wild-type C57BL/6 and apoA-I$^{-/-}$ (ApoA1^{tm1Unc}) mice on a C57BL/6 background (Jackson Laboratories) were obtained from the specific pathogen-free animal facility of the Institute of Molecular Biology and Biotechnology (IMBB; Heraklion, Greece). Femurs and tibias were obtained from ABCA1$^{-/-}$ (466), ABCG1$^{-/-}$ (Deltagen Inc) and SR-BI$^{-/-}$ mice (467). Human apoA-I transgenic founders (50% C57BL/6; 50% CBA) were backcrossed with apoA-I$^{-/-}$ mice for six additional generations to obtain human apoA-I transgenic mice on an apoA-I deficient C57BL/6 background. Genotyping of the progenies was performed by PCR. Detection of the human apoA-I transgene was performed as described above, while the mouse apoA-I gene was analyzed as indicated in the Jackson Laboratory genotyping protocols database (Table 2.7). Mice received a regular chow diet (Mucedola) until the beginning of the atherosclerosis study, when mice at 8 to 10 weeks of age were fed a HFD containing 15% wt/wt cocoa butter, 1% v/wt corn oil, 1% wt/wt cholesterol and 0.5% cholic acid (468) (AB Diets) for 14 weeks to induce hypercholesterolemia and atherosclerosis. Mice were housed in the specific pathogen free animal facility of IMBB on a 12 h light/dark cycle. All experimental protocols were in accordance with institutional guidelines and were approved by the Greek Federal Veterinary Office.

Table 2.7 Primers used for genotyping of human apoA-I transgenic mice.

Specificity	Name	Sequence
human	*APOA-I*	**Fw:** 5'-AGTTTGAAGGCTCCGCCTTGGGAAA-3'
		Rev: 5'-CACTTCTTCTGGAAGTCGTCCAGGTA-3'
mouse	*apoA-I*	**common:** 5'-GTTCATCTTGCTGCCATACG-3'
		wt: 5'-TCTGGTCTTCCTGACAGGTAGG-3'
		mutant: 5'-CCTTCTATCGCCTTCTTGACG-3'

Induction of Arthritis and Clinical Assessment

Mice were immunized subcutaneously at the base of the tail with 100 µg methylated BSA (mBSA) (Sigma-Aldrich) in 50 µL PBS emulsified with equal volume of CFA (Sigma-Aldrich). On day 21 post immunization, mice were injected intra-articularly (i.a.) with 50 µg mBSA in 20 µL PBS into the left knee joint. The swelling of the joint was evaluated by daily measurement (day 21-30) of the knee diameter (mm) using a digital vernier caliper (Cocraft). Nine days post i.a injection (day 30) mice were euthanized and blood and tissues were collected.

Histological Grading of Tissue Inflammation

Tissues were fixed in 3.7% formaldehyde for 24 h and legs were decalcified in Schaefer solution for 2-3 days. Tissues were embedded in paraffin, cut into 4 µm thick sections and stained with haematoxylin-eosin (H&E). Specimens were blindly evaluated by two pathologists. Histological grade of arthritis was determined according to the intensity of inflammatory cells, the degree of synovial reaction and pannus formation associated with articular cartilage erosion, as follows: 0= normal knee joint, 1=normal synovium or mild synovial reaction with scarce inflammatory cells, 2= moderate synovial reaction and moderate density of inflammatory cells, 3= severe synovial hyperplasia and dense population of inflammatory cells, 4= pannus formation associated with articular cartilage erosion. The extent of skin inflammation was evaluated by scoring samples separately for the following parameters: severity of inflammation, extent of epidermal changes, and size of abscesses (Table 2.8). A total histological score was assessed by summing the scores for each parameter. The range of possible score was 0-9. Histopathology images were captured using a Nikon Eclipse E-400 microscope and Nikon Digital sight, DS-SM, photographic system. Images were auto-corrected in Windows Photo Manager.

Table 2.8 Histological scoring system of the skin.

Score / Parameter evaluated	0	1	2	3
acute inflammation	none (normal)	mild	moderate	severe
epidermal changes	none (normal)	mild (acanthosis)	moderate (acanthosis, hyperkeratosis)	severe (acanthosis, hyperkeratosis, ulcerations)
abscess formation	none (normal)	microabscess	small abscess	large abscess

Histological Analysis of the Aortic Root

To assess atherosclerosis development, human apoA-I transgenic and apoA-$I^{-/-}$ mice were euthanized after 14 weeks of HFD feeding. The arterial tree was perfused *in situ* with 1x PBS for 15-20 min via a cannula in the left ventricle. The heart and aorta were excised and stored in zinc formalin (Zinc Formalin Fixative; Sigma-Aldrich). Serial sections (10 µm) of the aortic root were cut using a Leica CM3050S cryostat and stained with oil red O/hematoxylin (Sigma-Aldrich). Sections on separate slides were stained with Masson's trichrome stain (Sigma-Aldrich) to visualize collagen deposition. Images of the atherosclerotic lesion areas in the aortic root were acquired using a Leica image analysis system, consisting of Leica DMRE microscope coupled to Leica DC500 camera and Leica Qwin Imaging software (Leica Ltd). Mean lesion area (in μm^2) was calculated from 4-9 consecutive oil red-O stained sections, starting at the appearance of the tricuspid valves. All quantifications were performed blinded by computer-aided morphometric analysis using the Leica image analysis system.

2.13 Lipid and Lipoprotein Analyses

HDL Preparation from Mouse Serum

Blood was drawn from mice either by cardiac puncture or tail bleeding following a 4 h fast. Blood was allowed to clot for 30 min at RT and then centrifuged at 1,000 x g for 20 min at 4 ^{o}C. Serum was collected and an aliquot was used for HDL preparation using the dextran-Mg^{2+} method. Briefly, equal volumes of dextran sulfate (MP biomedicals) and $MgCl_2$ stock solutions were mixed to produce the precipitation solution consisting of 10 g/L dextran sulfate and 0.5 M $MgCl_2$. Serum samples were mixed thoroughly with precipitation solution at a volume ratio of 10:1 and incubated for 10 min at RT. The mixture was centrifuged for 40 min at 14,000 x g at 4 ^{o}C and the HDL-containing supernatant was collected for determination of cholesterol levels and functionality assays.

LDL Isolation from Human Serum

Blood was collected from healthy volunteers and serum was isolated by centrifugation at 1,500 x g for 10 min. LDL was isolated from human serum as previously described (469). Briefly, the serum was mixed with the appropriate amount of KBr according to the following equation *1 x (1.063-1)/1-(0.298 x 1.063) = g KBr / mL of serum.* The adjusted sample was centrifuged at 40,000 rpm for 27 h and 8 min at 4 ^{o}C in a Beckman XL-90 Ultracentrifuge using a 70 Ti rotor. The upper layer (containing LDL, IDL, VLDL) was carefully collected, mixed with the appropriate volume of 1x PBS according to the following equation $V_{PBS} = V_{upper\ phase}\ x\ (1.063\text{-}1.019)\ /\ (1.019 - 1)$ and centrifuged at 40,000 rpm for 27 h and 8 min at 4 ^{o}C using the above rotor. The supernatant was carefully discarded and the LDL was resuspended in ~1 mL of solution left at the bottom of the tube. The LDL pellet was incubated at 4 ^{o}C for 2 h until it was completely resuspended and then extensively dialyzed against 1x PBS at 4 ^{o}C using membranes with a molecular weight cut-off of 12,000–

14,000 Daltons. The LDL preparation was stored at 4 ^{o}C and was used within 2 weeks.

Lipid Analyses and ApoA-I Levels

The concentration of total cholesterol, HDL-cholesterol, free cholesterol, phospholipids and triglycerides in the serum was determined using Infinity cholesterol (Thermo Scientific, Waltham, MA), Free Cholesterol E, Labassay Phospholipid and Labassay Triglyceride reagents (Wako Chemicals Inc.), respectively, according to the manufacturer's instructions. The concentration of cholesteryl esters was determined by subtracting the concentration of free cholesterol from the concentration of total cholesterol. The levels of human apoA-I in the serum were determined by ELISA (Mabtech) following the manufacturer's recommendations. Lipoprotein profiles were determined by fractionation of 200 µL of pooled serum samples from two mice of the same genotype by fast protein liquid chromatography (FPLC) gel filtration using a Superose 6 10/300 GL column (GE Healthcare) on a Pharmacia FPLC system. A total of 40 fractions of 0.5 mL volume each were collected for further analyses. The concentration of lipids in the FPLC fractions was determined as described above.

Serum Fractionation by Density Gradient Ultracentrifugation and Electron Microscopy (EM) Analysis

Serum was fractionated by KBr density gradient ultracentrifugation and the fractions were analyzed by SDS-PAGE as described previously (141). Briefly, 240 µL of mouse serum were diluted with 1x PBS to a total volume of 0.4 mL and adjusted to a density of 1.23 g/mL with KBr. The adjusted sample was successively overlayed with 0.8 mL of a KBr solution with a *d* of 1.21 g/mL, 2 mL of a KBr solution with a *d* of 1.063 g/mL, 0.4 mL of a KBr solution with a *d* of 1.019 g/mL, and 0.4 mL of 1x PBS. The mixture was centrifuged for 22 h in a SW60 rotor at 28,500 rpm. Following ultracentrifugation, 0.4 mL fractions were collected from the top and the refractive index of the fractions was

measured using an Abbe refractometer model RMT (EXACTA+OPTECH GmbH). The fractions were then dialyzed against dH_2O and 100 µL aliquots from each fraction were analyzed on 12.5% SDS-PAGE. The protein bands were visualized by staining the gels with Coomassie Brilliant Blue R 250 (Merck). In brief, the gels were stained with Coomassie Brilliant Blue [2.5 g Coomassie Brilliant Blue R in 45 % methanol and 10% acetic acid] for 20 min and then destained in destaining solution [50% methanol, 8.5% acetic acid] overnight while shaking. The gels were rehydrated in dH_2O overnight and dried in a Hoefer SE 1160 gel dryer under vacuum at 80 ^{o}C for 1 h. For EM analysis, fractions 6-8 that float in the HDL region were applied on carbon-coated grids, stained with sodium phosphotungstate, visualized using a Phillips CM-12 electron microscope (Philips Electron Optics) and photographed as previously described (470). These procedures were performed by Dr. Donald Gantz at the Department of Biophysics of Boston University. The photomicrographs were taken at x75,000 magnification and enlarged three times.

Non-Denaturing Two-Dimensional (2D) Gel Electrophoresis

Serum HDL subpopulations were analyzed by 2D gel electrophoresis as previously described (471) with some modifications. Briefly, in the first dimension, 0.7-2 µL of serum sample was separated by electrophoresis at 4 °C on a 0.75% agarose gel using 25 mM Tris-tricine buffer, pH 8.6 / 3 mM calcium lactate / 0.05% sodium azide as running buffer until the bromophenol blue marker had migrated 5.5 cm. Agarose gel strips containing the separated lipoproteins were then transferred to a 4-20% polyacrylamide gradient gel (Bio-Rad). Separation in the second dimension was performed at 100 V for 2–3 h at 4 °C. The separated proteins were transferred onto nitrocellulose membranes and apoA-I was detected by immunoblotting using anti-human apoA-I (Merck Millipore) and anti-goat (Sigma-Aldrich) as described above.

Paraoxonase-1 (PON-1) Activity

PON-1 activity was determined in HDL preparations from mouse serum using paraoxon as substrate (472). Briefly, 5 µL of HDL were added in 245 µL of buffer (100 mM Tris–HCl, pH 8.0 and 2 mM $CaCl_2$) containing 1.1 mM paraoxon-ethyl (Sigma-Aldrich) and the absorbance at 405 nm was measured every 40 sec for 20 min at RT in a microplate spectrophotometer. The rate of p-nitrophenol formed by the hydrolysis of paraoxon was determined by monitoring the increase in absorbance. PON-1 activity was expressed as units per liter (U/L) of HDL with 1 U defined as the activity that catalyzes the formation of 1 µmoL p-nitrophenol per min.

Dichlorofluorescein (DCF) Assay

The antioxidant properties of HDL were tested in the presence or absence of LDL as previously described (473) with some modifications. First, LDL was isolated from normal human serum by ultracentrifugation as described above, exposed to normal atmospheric conditions by gentle mixing at RT for 16 h to generate mildly oxidized LDL and stored at 4 °C under nitrogen. The same stock LDL solution was used for the analysis of all samples. 2',7'-Dichlorodihydrofluorescein diacetate (H_2DCFDA; Invitrogen) was dissolved in fresh methanol at 2 mg/mL and incubated at RT for 20 min in the dark. This results in the generation of 2',7'-dichlorofluorescin (DCFH). Upon interaction with lipid peroxidation products the non-fluorescent DCFH is oxidized to the highly fluorescent 2',7'-dichlorofluorescein (DCF). Normal HDL does not promote the oxidation of DCFH and the subsequent release of DCF. Also, normal HDL can prevent the oxidation of DCFH that is induced by oxidized LDL. In this assay, serum HDL from transgenic mice (final concentration 0.025 µg cholesterol/mL) was incubated in the presence or absence of oxidized LDL (final concentration 100 µg cholesterol/mL) in a black 96-well plate in a final volume of 100 µL. The plate was incubated on a rotator at 37 °C for 1 h in the dark. Next, 10 µL of DCFH solution (0.2 mg/mL diluted in 1x PBS) was added to each well, mixed, and incubated for an additional 2 h at

37 °C with rotation in the dark. Fluorescence was measured in a microplate reader (excitation/emission: 465 / 535 nm).

Platelet-Activating Factor Acetylhydrolase (PAF-AH) Activity

PAF-AH activity in HDL was measured by the trichloroacetic acid (TCA) precipitation procedure using [^{3}H]-PAF (100 μM final concentration, specific activity 20,000 cpm/nmol) as a substrate(472). 1-O-hexadecyl-2-[^{3}H-acetyl]-sn-glycero-3-phosphocholine (0.1 mCi/mL, specific activity 27 Ci/mmol) was purchased from PerkinElmer and unlabeled PAF (1-O-hexadecyl-2-acetyl-sn-glycero-3-phosphocholine) was from Sigma-Aldrich. Briefly, 30 μL of HDL diluted 1:12 (v/v) in HEPES buffer, pH 7.4 were mixed with HEPES in a final volume of 54 μL and used as the source of the enzyme. Incubations with [^{3}H]-PAF were performed for 10 min at 37^{o}C and 75 μL of the mixture were subsequently incubated with equal volumes of TCA for 30 min on ice and centrifuged at 6,000 x g for 10 min at 4^{o}C. The radioactivity in 75 μL of the supernatant was determined by liquid scintillation counting. PAF-AH activity was expressed as nmoles PAF degraded per min per mL of HDL.

2.14 Statistical Analysis

Data are expressed as mean ± SEM unless stated otherwise. Statistical significance was determined using two-tailed Student's t test or one-way analysis of variance and the Tukey's post-hoc test to evaluate differences between three or more groups. The χ^2 test was used for categorical variables. For all results, $p<0.05$ was considered statistically significant (*$p<0.05$, **$p<0.01$, ***$p<0.001$). Analysis was performed using GraphPad Prism software (GraphPad Software Inc., La Jolla, CA).

3 RESULTS AND DISCUSSION

CHAPTER I:

The Role of HDL in the Development of Autoimmune Responses

Aberrant levels and function of the potent anti-inflammatory HDL and accelerated atherosclerosis have been reported in patients with autoimmune inflammatory diseases. Although recent evidence suggests a role of HDL in modulating both innate and adaptive immune responses, whether HDL affects the development of an autoimmune response remains elusive. The objective of this study was to investigate the anti-inflammatory mechanisms of HDL and delineate its role in autoimmunity. For this purpose we used a mouse model of antigen-induced arthritis (AIA) and studied the effects of HDL on the development of adaptive T cell responses.

ApoA-I$^{-/-}$ mice develop increased severity of antigen-induced arthritis

To determine whether there is a role for HDL in induction and perpetuation of the autoimmune response we investigated the development of AIA in apoA-I$^{-/-}$ mice that are characterized by very low serum HDL-c levels (~15-20% of wild-type; Fig. 3.1) (474). AIA is induced upon intra-articular injection of mBSA

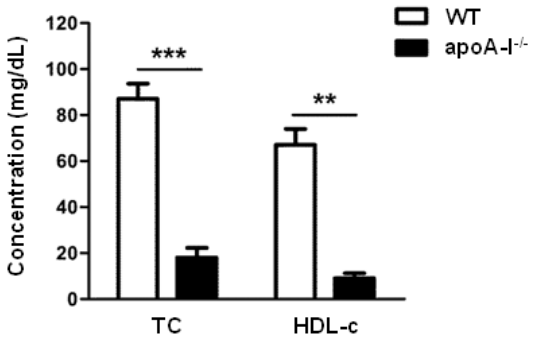

Figure 3.1 ApoA-I$^{-/-}$ mice demonstrate very low levels of circulating HDL. Total and HDL cholesterol levels in the serum of naïve wild-type and apoA-I$^{-/-}$ mice.

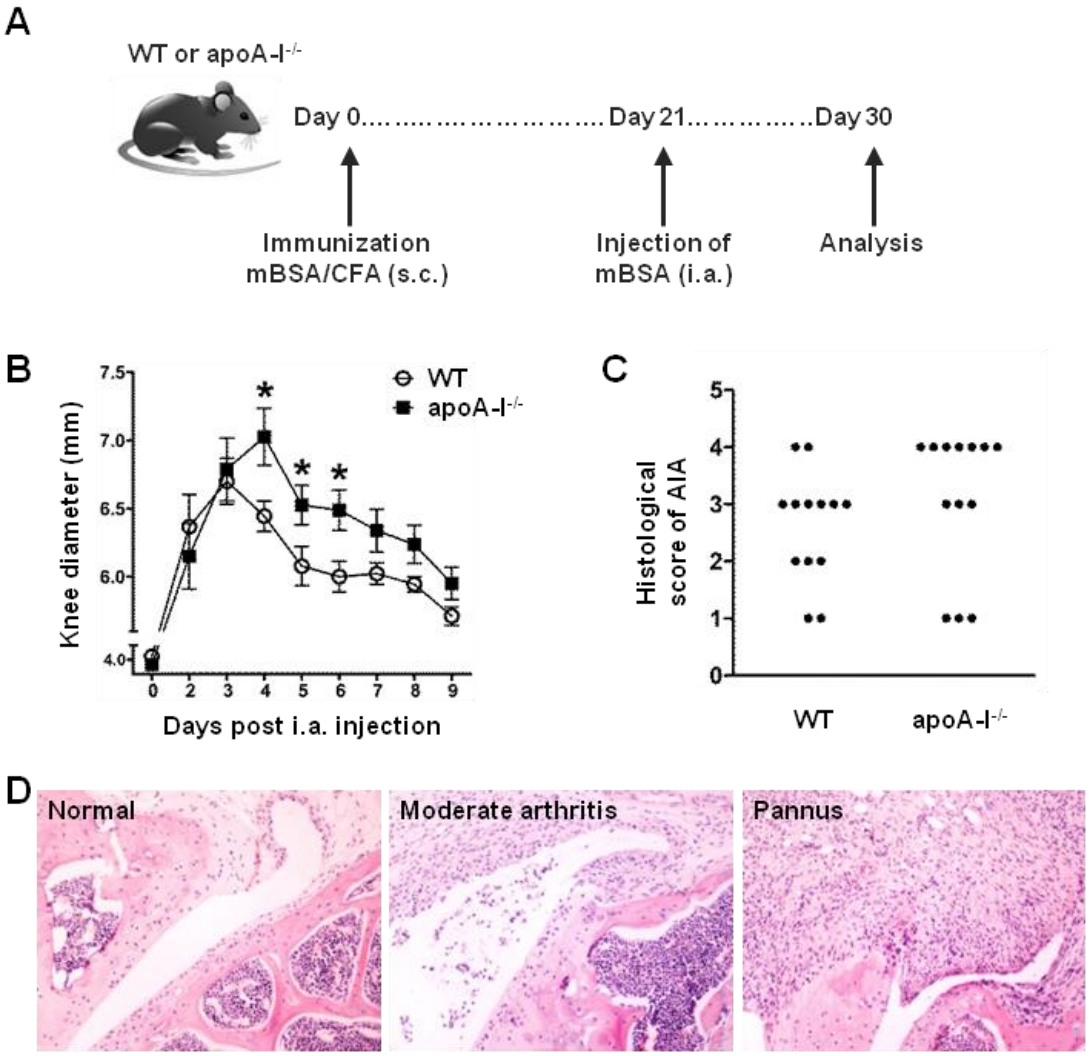

Figure 3.2 ApoA-I$^{-/-}$ mice demonstrate an aggravated AIA phenotype. (**A**) WT and apoA-I$^{-/-}$ mice (n=13/group) were immunized subcutaneously (s.c.) with mBSA/CFA and arthritis was induced upon intra-articular (i.a.) injection of mBSA 21 days later. (**B**) Evaluation of arthritis by measurement of knee joint swelling daily after i.a. injection (n=8-9/group) (day 4: *p=0.0233, day 5: *p=0.0455, day 6: *p=0.0182). Results are expressed as mean ± SEM. (**C**) Histological scores for AIA in WT and apoA-I$^{-/-}$ mice. The histopathologies of injected knee joints were scored as described in *Methods*; *p=0.0393 for pannus vs non-pannus. (**D**) Representative H&E stained sections of inflamed joints from WT (moderate arthritis) and apoA-I$^{-/-}$ mice (pannus) as well as non-injected knee joint (normal) are shown (original magnification x200). In all panels, the data are from two independent experiments.

in mBSA-sensitized animals (Fig. 3.2A) and serves as a model for RA (475, 476). Interestingly, apoA-I$^{-/-}$ mice developed increased severity of AIA compared to WT animals as indicated by the measurements of knee swelling (Fig. 3.2B). This result correlated well with the histological examination of

injected knee joints of apoA-I$^{-/-}$ mice which developed extensive pannus formation (grade 4) contrary to WT mice which exhibited moderate to severe inflammation (grade 2-3) (*p=0.0393 for pannus vs non-pannus; Fig. 3.2C and 3.2D). A striking observation was the extensive inflammatory reaction in the skin of apoA-I$^{-/-}$ mice three weeks after immunization as opposed to WT mice (Fig. 3.3A), that was characterized by significant epidermis alterations at the site of the injection including ulceration, dense inflammation in the dermis with abundant neutrophil infiltration and formation of large abscesses (Fig. 3.3B and 3.3C). In contrast, WT mice showed moderate inflammatory reaction in the dermis, and occasional small neutrophil aggregates (Fig. 3.3B and 3.3C). Collectively, these findings indicate that decreased levels of circulating HDL are associated with exacerbation of inflammatory arthritis and severe inflammatory reactions in the skin.

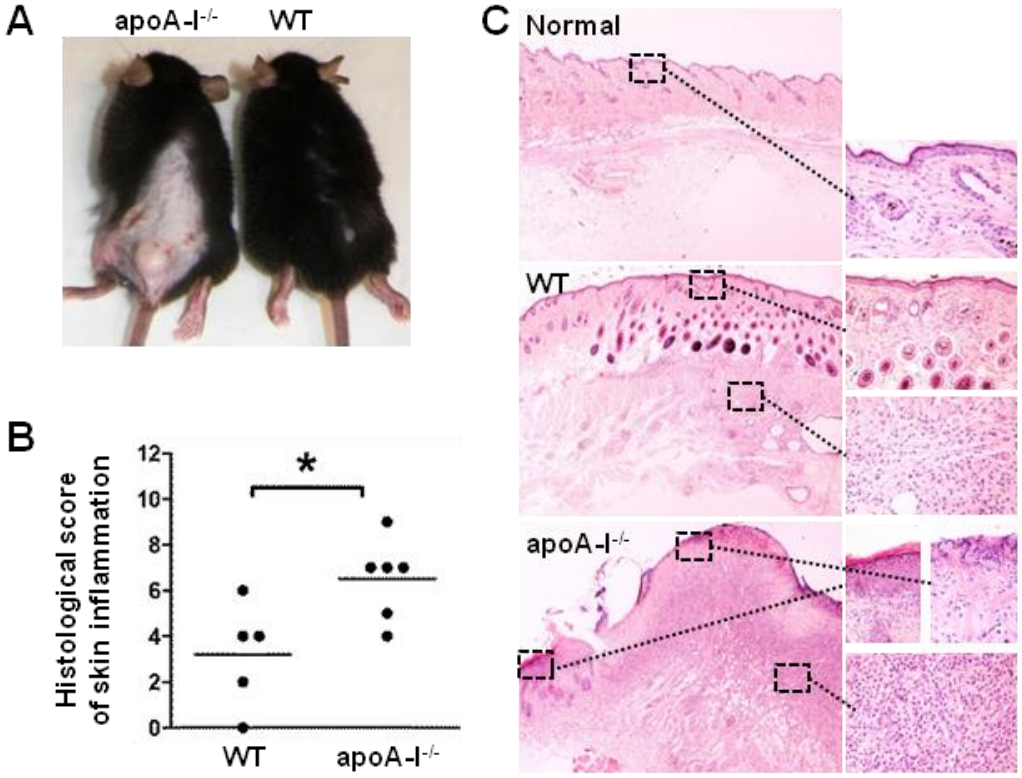

Figure 3.3 ApoA-I$^{-/-}$ mice demonstrate extensive skin inflammation during AIA. (**A**) Photos of skin lesions in apoA-I$^{-/-}$ mice 21 days after mBSA immunization. (**B**) Histological grading of skin inflammation developed in WT and apoA-I$^{-/-}$ mice (*p=0.0239). (**C**) Representative H&E stained sections of control and inflamed skin (original magnification: left side x20, right side x400). In all panels, the data are from two independent experiments.

HDL's anti-inflammatory functions are compromised in arthritic WT mice

Under chronic inflammatory conditions, such as in the case of rheumatoid arthritis, HDL's protein and lipid composition is considerably altered in a way that renders these, normally protective, particles pro-inflammatory (288, 335). In fact, it has been demonstrated that despite the decrease in normal HDL-c levels, pro-inflammatory HDL (piHDL) levels are increased in patients with autoimmune disorders (336, 477). Thus, we next examined whether HDL-c levels were affected by the inflammatory response and if HDL functionality was altered during AIA development. According to our results total and HDL cholesterol levels of both mBSA-immunized (day 21) and arthritic (day 30 i.a.) mice showed no significant differences as compared to naïve WT mice (Fig. 3.4A). To assess the functional properties of HDL, we measured HDL-associated PON-1 activity at different time points during disease development. Our results indicated that there is a biphasic response of the immunized mice in terms of HDL activity: an early up-regulation of HDL functionality (day 10) which could be accounted for by an early attempt to attenuate the inflammation followed by a gradual decline in HDL functionality as the inflammation resolves (day 21 and day 30; Fig. 3.4B). Importantly, our data showed that upon the intra-articular antigenic challenge HDL functionality significantly decreased to even lower levels (day 21 vs day 30 i.a.; Fig. 3.4B). Although mice are still capable of responding to the intra-articular mBSA challenge by increasing PON-1 activity (day 30 vs day 30 i.a.), this potential is markedly compromised compared to day 10 (Fig. 3.4B). Collectively, our results signify that although the HDL-c levels remained unaffected, the anti-inflammatory/anti-oxidant properties of circulating HDL were attenuated in an inflammatory environment.

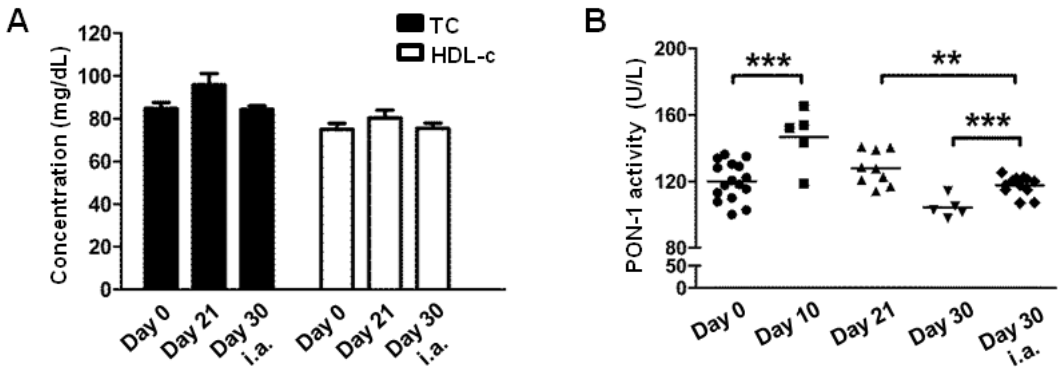

Figure 3.4 HDL functionality is altered during AIA in WT mice. (**A**) Total (TC) and HDL-cholesterol (HDL-c) levels in serum of naïve mice (day 0), mBSA-immunized (day 21) and arthritic mice (day 30 i.a.). (**B**) Characterization of HDL antioxidant/anti-inflammatory properties by assessment of HDL-associated PON-1 activity (**p=0.0084, ***p=0.0007). Results are expressed as mean ± SEM; data are combined of two independent experiments; n=5-16/group.

ApoA-I$^{-/-}$ mice exhibit exacerbated OVA-specific Th1 and Th17 immune responses

Development and progression of arthritis depends on the generation of autoreactive Th1 and Th17 cells (478, 479). To monitor the induction of T cell responses in apoA-I$^{-/-}$ mice we first examined whether T cell lymphopoiesis was affected. Analysis of CD4^{+} and CD8^{+} T cell subsets in thymus and peripheral lymphoid organs revealed no differences between naïve apoA-I$^{-/-}$ and WT mice indicating that loss of apoA-I did not cause alterations in T cell development and homeostasis (Fig. 3.5A). In addition, the frequency of peripheral CD4^{+}Foxp3^{+} T regulatory cells (Tregs) was similar in apoA-I$^{-/-}$ and WT mice (Fig. 3.5B). We next assessed whether decreased HDL levels could affect the induction of antigen-specific Th1 and Th17 responses. Interestingly, dLNs of apoA-I$^{-/-}$ mice showed increased cellularity 9 days after the antigenic challenge compared to WT mice (53.54 ± 2.556 versus 42.13 ± 2.020 x 10^{6} cells; Fig. 3.6). Detailed analysis of the dLNs for the different cells subsets revealed a significant increase of CD11c^{+} DCs in apoA-I$^{-/-}$, 3.5 and 9 days after the antigenic challenge, compared to WT mice, and to a lesser extent of CD4^{+} T cells (Fig. 3.7A and 3.7B). Of note, no significant differences were observed in the frequencies of B220^{+} B cells and CD11b^{+} macrophages

whereas $CD8^+$ T cells were slightly decreased in dLNs of apoA-$I^{-/-}$ mice (Fig. 3.7C – 3.7E). Moreover, the absolute numbers of $CD4^+Foxp3^+$ Tregs were significantly increased in immunized apoA-$I^{-/-}$ mice (Fig. 3.7F). Although both

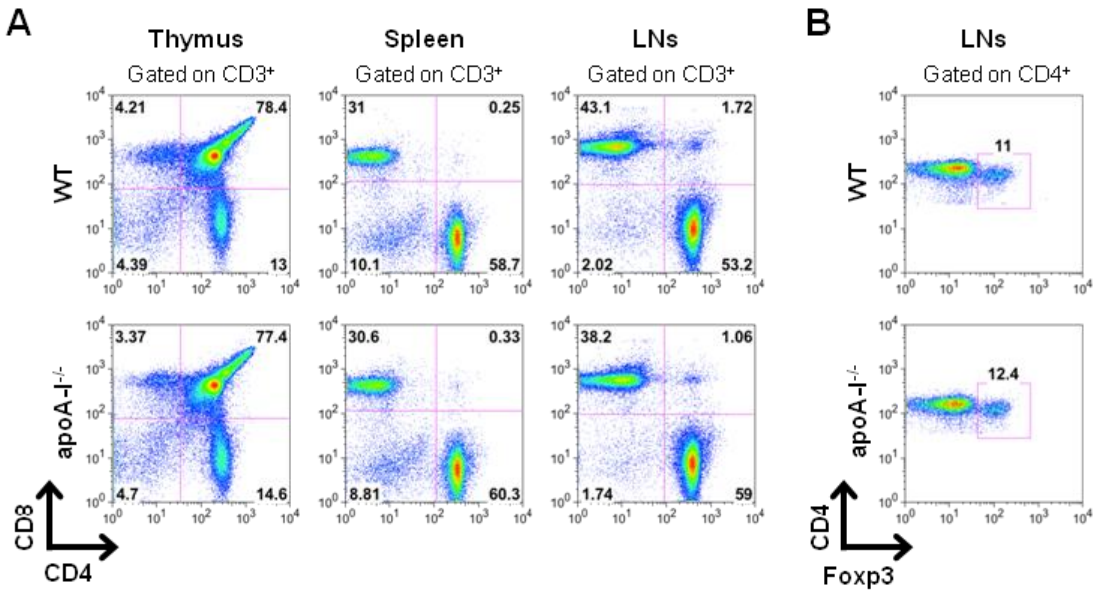

Figure 3.5 T cell development and homeostasis is not affected in apoA-$I^{-/-}$ mice. (**A** and **B**) Flow cytometric analysis of thymocytes, slpenocytes and lymph node cells from naïve WT and apoA-$I^{-/-}$ mice (n=3/group) are shown. Gates were set as indicated. Data are representative of two independent experiments.

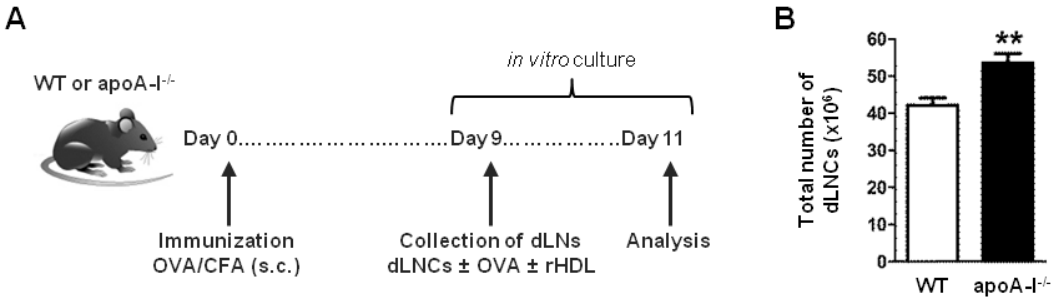

Figure 3.6 Immunized apoA-$I^{-/-}$ mice demonstrate increased dLN cellularity. (**A**) Outline of the immunization experimental setup. Mice were immunized subcutaneously (s.c.) with OVA/CFA and 9 days later dLNCs were isolated and cultured *in vitro*. Cells were treated as indicated for 48 h. (**B**) LN cellularity in WT and apoA-$I^{-/-}$ mice (n=12-13/group) 9 days after OVA immunization (**p=0.0018). Results are expressed as mean ± SEM; data are combined of five independent experiments.

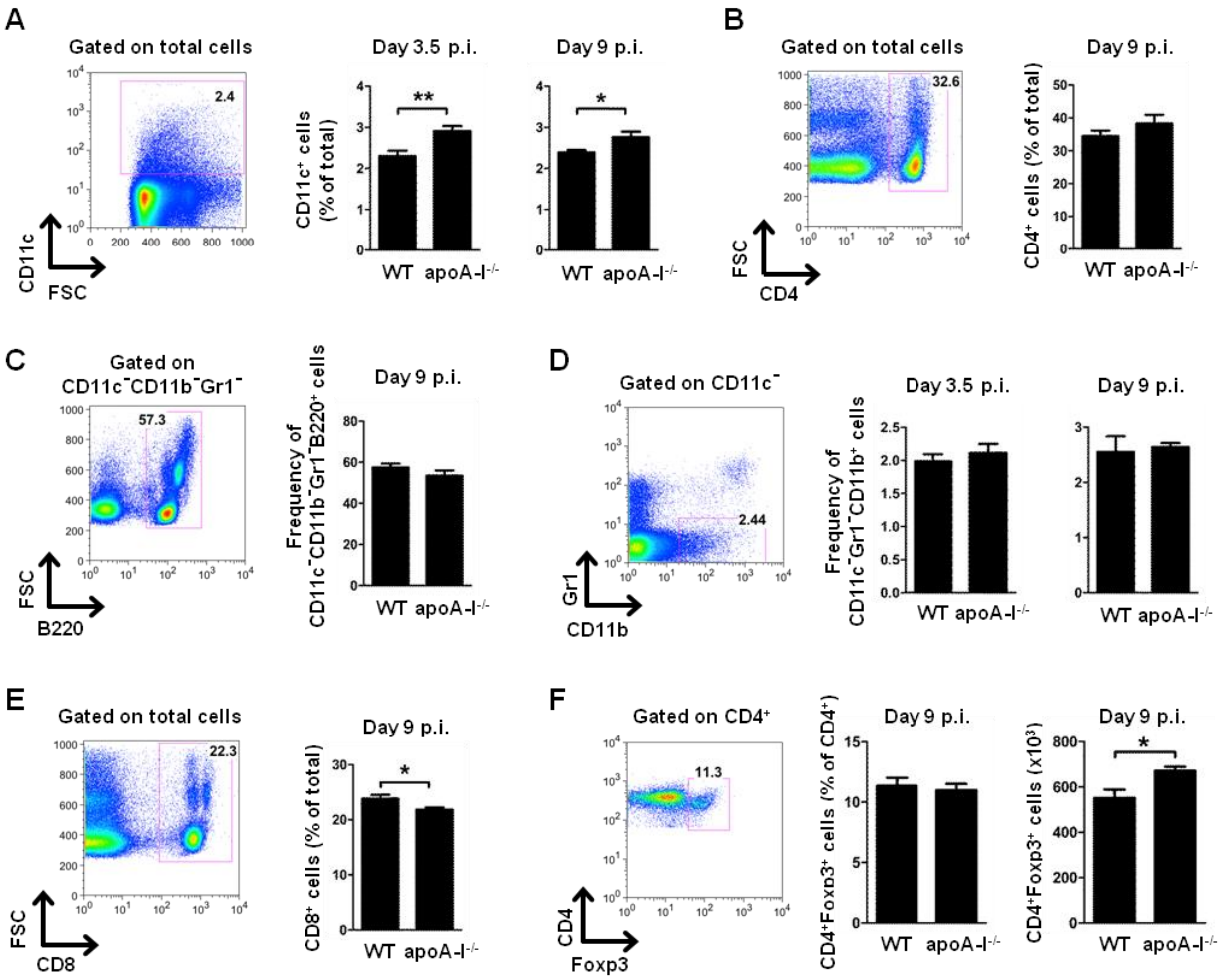

Figure 3.7 Flow cytometric analyses for major cell subsets in the dLNs of immunized apoA-I$^{-/-}$ mice. dLNCs from WT and apoA-I$^{-/-}$ mice (n=4-6/group) were collected 3.5 and 9 days post OVA immunization (p.i.). Gating strategy and frequencies or absolute numbers of CD11c^{+} DCs (**A**), CD4^{+} T cells (**B**), B220^{+} B cells (**C**), CD11b^{+} macrophages (**D**), CD8^{+} T cells (**E**) and Foxp3^{+} Tregs (**F**) are shown. Numbers on the gates denote frequencies. Results are expressed as mean ± SEM.

groups of mice exhibited similar frequencies of activated CD3^{+}CD4^{+}CD44^{+} T cells after *in vitro* re-stimulation with OVA (Fig. 3.8A), dLNCs from apoA-I$^{-/-}$ mice exhibited increased proliferation as indicated by IL-2 levels (181.3 ± 14.1 versus 74.7 ± 7.9; Fig. 3.8B). This finding was accompanied by markedly increased production of both IL-17 (773.1 ± 105.9 versus 292.5 ± 85.8; Fig. 3.8C) and IFN-γ (708.9 ± 114.8 versus 172.4 ± 40.0; Fig. 3.8D) in apoA-I$^{-/-}$ OVA-stimulated dLNC supernatants whereas IL-10 was undetectable (data not shown). Taken together, these data demonstrate that apoA-I deficiency

promotes T cell proliferation and enhances antigen-specific Th1 and Th17 immune responses.

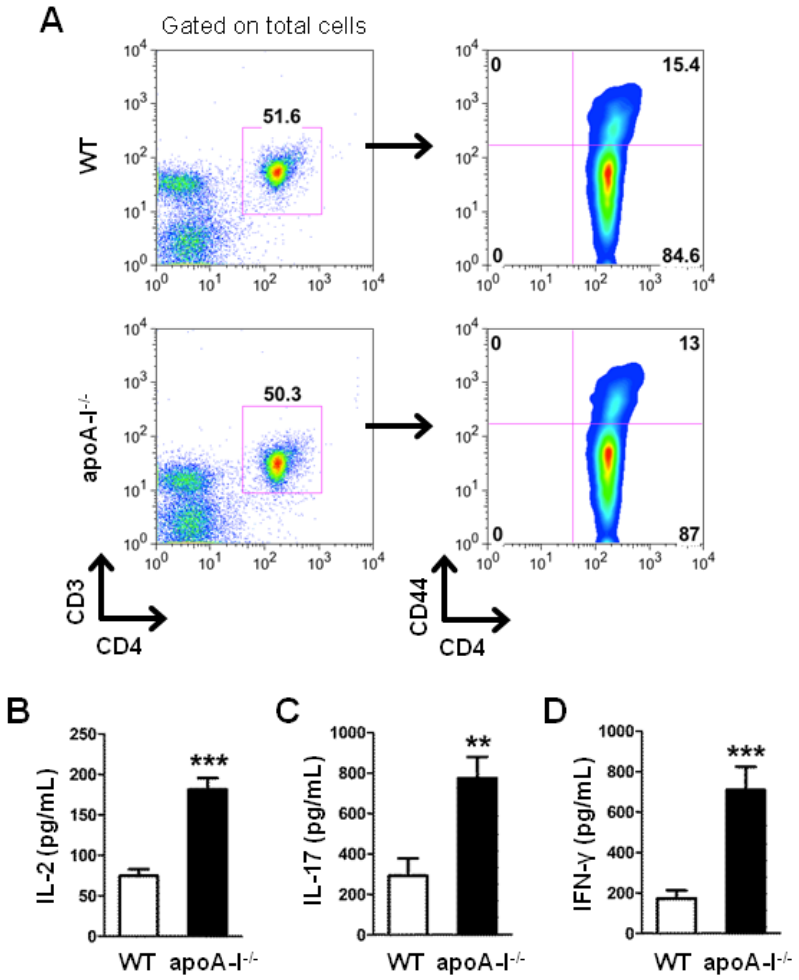

Figure 3.8 OVA-specific Th1 and Th17 immune responses are enhanced in apoA-I$^{-/-}$ mice. (**A**) Flow cytometric analysis of OVA-primed dLNCs from WT and apoA-I$^{-/-}$ mice (n=6/group) after *in vitro* re-stimulation with 15 µg/mL OVA for 48 h. Gates were set as indicated. Data are representative of three independent experiments. (**B-D**) Levels of IL-2 (***p<0.0001), IL-17 (**p=0.0055) and IFN-γ (***p=0.0008) in culture supernatants of OVA-primed dLNCs are shown (n=6-7/group). Results are expressed as mean ± SEM; data are combined of at least four independent experiments.

rHDL inhibits antigen-specific Th1 and Th17 immune responses *in vitro*.

Next, we examined whether HDL could directly affect the induction of Th1 and Th17 immune responses. To address this, we performed *in vitro* re-stimulation assays of dLNCs from OVA-immunized WT animals in the

presence of titrating amounts of rHDL. Treatment with rHDL led to impaired proliferation of OVA-specific T cells as a response to the antigenic stimulus (Fig. 3.9A). In support, IL-2 secretion was decreased in culture supernatants of rHDL-treated dLNCs (Fig. 3.9B). Furthermore, decreased proliferation of dLNCs in the presence of rHDL was accompanied by a dose-dependent decrease in secretion of IL-17 (Fig. 3.9C) and IFN-γ (Fig. 3.9D). Overall, these results provide direct evidence for a potent role of rHDL in the suppression of Th1 and Th17 immune responses *in vitro*.

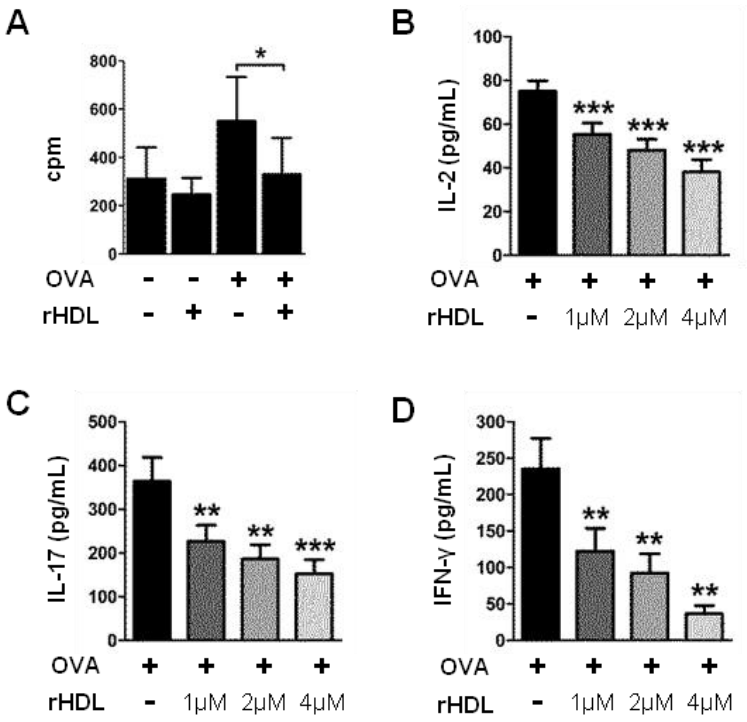

Figure 3.9 OVA-specific Th1 and Th17 immune responses are suppressed by rHDL. (**A**) OVA-primed dLNCs from WT mice (n=3/group) were re-stimulated with OVA (15 μg/mL) *in vitro* in the presence of rHDL (1 μM) for 72 h and then pulsed with 1 μCi [^{3}H]thymidine for 18 h. The incorporated radioactivity was measured. Results are expressed as mean ± SEM. (**B-D)**, dLNCs from OVA-immunized WT mice (n=6-8/group) were cultured with increasing concentrations of rHDL in the presence of OVA (15 μg/mL). Levels of IL-2 (***p≤0.0004), IL-17 (**p=0.001, ***p=0.0006) and IFN-γ (**p≤0.0081) were determined in culture supernatants 48 h later. Results are expressed as mean ± SEM; data are combined of at least three independent experiments.

rHDL downregulates co-stimulatory molecule expression and suppresses pro-inflammatory cytokine production in stimulated BMDCs

T cell activation, polarization and proliferation *in vivo* require antigen presentation by professional APCs. DCs serve as the best candidate that upon maturation provide the necessary co-stimulatory molecules and secrete pro-inflammatory cytokines to instruct T cell responses (315, 480). We asked whether the suppressive effect of rHDL on T cell responses is mediated through modulation of DC function. To this end, we first examined the maturation status of DCs in dLNs and spleen of immunized apoA-I$^{-/-}$ and WT mice. Our findings demonstrated an increase of MHC class II and CD40 expression in CD11c^{+} DCs from apoA-I$^{-/-}$ compared to WT mice and a more prominent increase in the expression of the co-stimulatory molecule CD86 in both dLNs and spleen (Fig. 3.10). On the other hand, no differences were

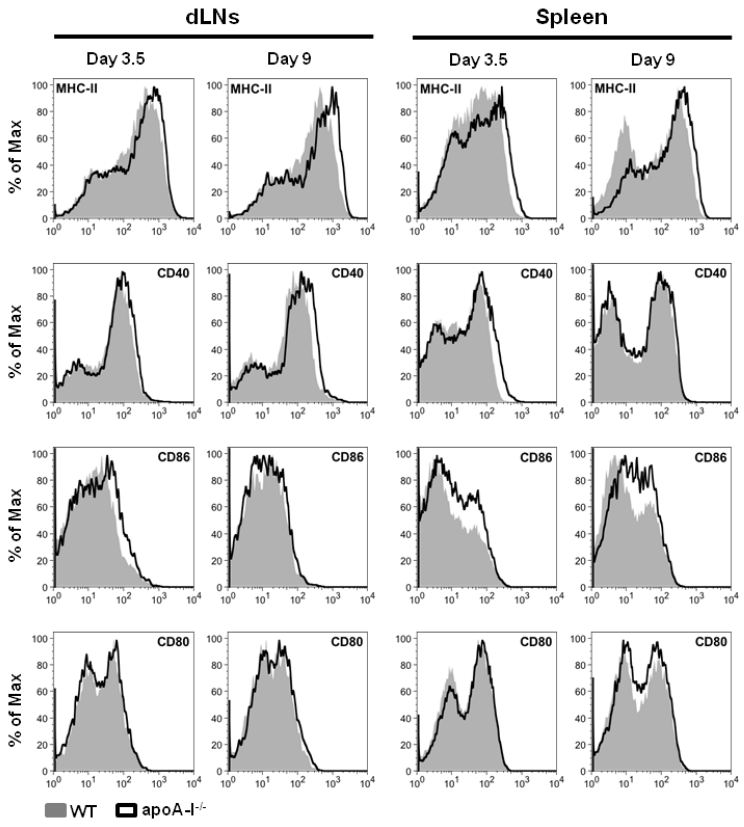

Figure 3.10 The expression of DC maturation markers is increased in immunized apoA-I$^{-/-}$ mice. dLNCs and slpenocytes from WT and apoA-I$^{-/-}$ mice (n=4-8/group) were collected 3.5 and 9 days post OVA immunization. Expression levels of MHC-II, CD40, CD86 and CD80 were evaluated by flow cytometry. Representative FACS histograms are shown. Gates were set on CD11c^{+} cells.

observed in the expression levels of CD80 (Fig. 3.10). To examine a direct role of HDL on DC maturation, we generated BMDCs from WT mice and treated them with rHDL during LPS stimulation. As shown in Fig. 3.11A, treatment with rHDL led to downregulation of MHC class II (MHC-II) and CD40, CD86 and CD80. To determine whether this effect was specific to the TLR4-mediated response in DCs, we stimulated BMDCs from WT mice with zymosan, a TLR2 ligand, and treated them with rHDL. Although expression of MHC-II was not altered, a significant down-regulation of CD40, CD86 and CD80 expression was observed in rHDL-treated zymosan-activated BMDCs compared to zymosan alone (Fig. 3.11B). These results indicate that rHDL's

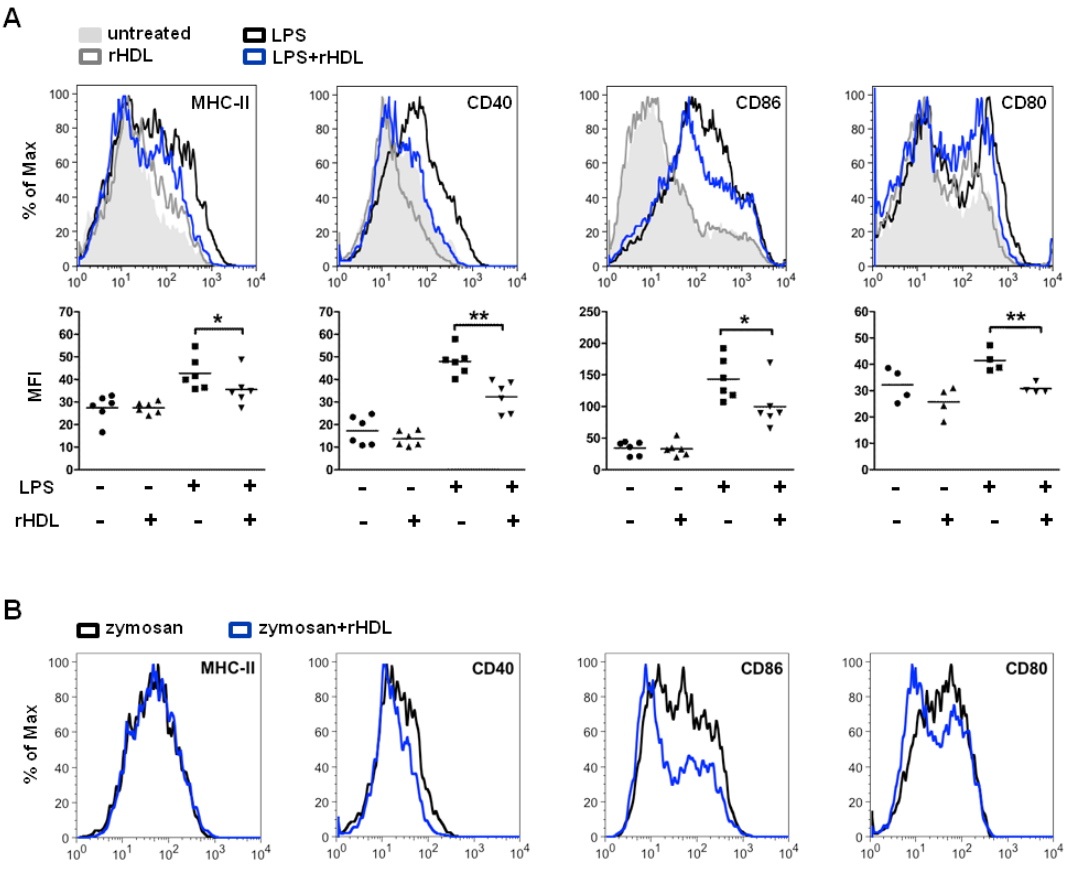

Figure 3.11 rHDL prevents activation and maturation of BMDCs. BMDCs from WT mice (n=2-6) were stimulated with LPS (0.5 µg/mL) or zymosan (20 µg/mL) and treated with 4 µM rHDL for 18 h. (**A**) Expression levels of MHC-II (*p=0.026), CD40 (**p=0.0076), CD86 (*p=0.0226) and CD80 (**p=0.0047) were evaluated by flow cytometry. Representative FACS histograms are shown. Gates were set on $CD11c^+$ cells. Dot plots represent the averages of the geometric mean fluorescence intensity (MFI) of at least two independent experiments. . (**B**) Expression levels of MHC-II, CD40, CD86 and CD80 were evaluated by flow cytometry. Representative FACS histograms are shown. Gates were set on $CD11c^+$ cells.

suppressive effect on DC maturation is not limited to TLR4-induced immune responses. Furthermore, secretion of pro-inflammatory cytokines IL-6, IL-12, IL-23, chemokine IL-8 and the anti-inflammatory cytokine IL-10 were reduced in rHDL-treated LPS-stimulated BMDCs, whereas TNF-α production was unaffected by rHDL treatment (Fig. 3.12). Of note, rHDL suppressed the secretion of IL-6, IL-8 and TNF-α in immature DCs indicating that the anti-inflammatory properties of rHDL could be independent of LPS. Collectively, these data demonstrate an inhibitory effect of rHDL on activation and maturation of and cytokine secretion by DCs *in vitro*.

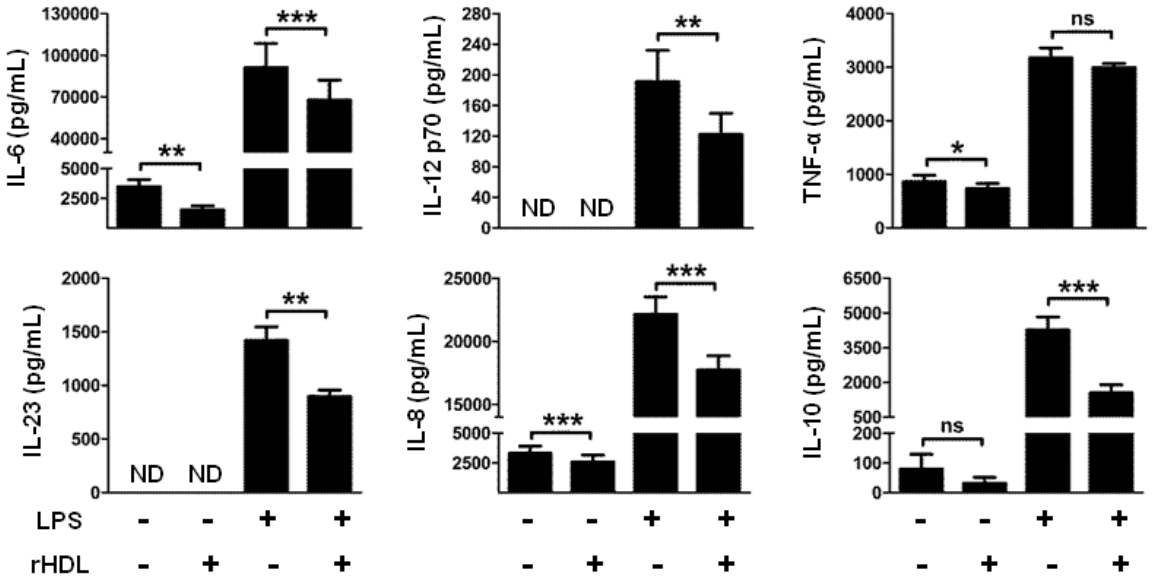

Figure 3.12 rHDL prevents pro-inflammatory cytokine secretion from stimulated BMDCs. BMDCs from WT mice (n=2-6) were stimulated with LPS (0.5 µg/mL) and treated with 4 µM rHDL for 18 h. Levels of IL-6, IL-23, IL-12 p70, IL-8, IL-10 and TNF-α in culture supernatants were measured by ELISA. Results are expressed as mean ± SEM; data are combined of three independent experiments; *p=0.0229, **p≤0.0038, ***p≤0.0008; ns;not significantly different. ND; not detectable.

rHDL treatment of mature BMDCs suppresses antigen-specific T cell proliferation

To assess the functional importance of our findings, we performed co-culture experiments with rHDL-treated OVA-pulsed BMDCs and OVA-primed dLNCs as shown in Fig. 3.13A. To this end, WT BMDCs were activated with

LPS and pulsed with OVA in the presence or absence of rHDL for 12 h. BMDCs were then co-cultured with dLNCs isolated from OVA-immunized WT syngeneic mice. 48 h later culture supernatants were collected and IL-2 production was assessed. Interestingly, rHDL-treated OVA-pulsed BMDCs significantly reduced IL-2 production by OVA-primed LNCs as compared to OVA-pulsed BMDCs (Fig. 3.13B). These findings provide evidence for the impaired capacity of rHDL-treated DCs to promote T cell proliferation.

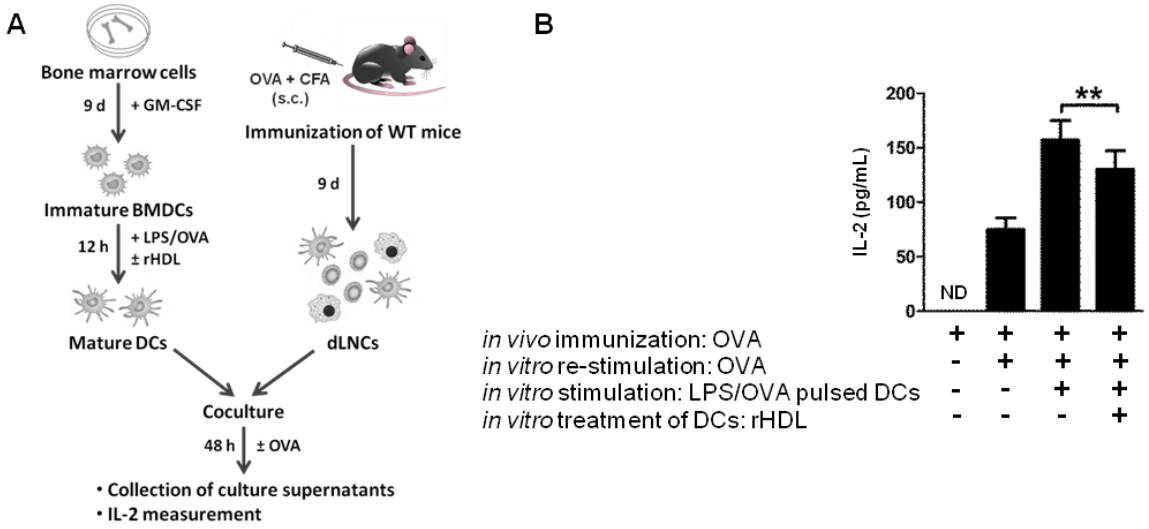

Figure 3.13 rHDL-treated DCs suppress antigen-specific T cell proliferation *in vitro*. (**A**) Outline of the co-culture experimental setup. LPS-stimulated OVA-pulsed BMDCs from WT mice (n=5/experiment) were treated with rHDL for 12 h and co-cultured with OVA-primed dLNCs. Cells were re-stimulated with OVA and 48 h later (**B**) IL-2 secretion in culture supernatants was assessed by ELISA. Results are expressed as mean ± SEM; data are combined of two independent experiments (**p=0.005).

rHDL prevents activation of the MyD88-dependent pathway in stimulated BMDCs

LPS binding to TLR4 leads to NF-κB nuclear translocation and induction of inflammatory cytokine gene transcription (481). To gain insights into the molecular events leading to HDL-mediated suppression of DC function, we examined whether rHDL suppressed LPS-induced pro-inflammatory cytokine secretion by interfering with the NF-κB pathway. To this end, we performed

immunofluorescence studies to assess nuclear translocation of the p65 subunit of NF-κB in LPS-stimulated BMDCs. Our findings showed a marked increase in nuclear p65 compared to unstimulated cells, whereas LPS-induced translocation of p65 to the nucleus was impaired after rHDL treatment (Fig. 3.14A and 3.14B). In TLR4 signaling, activation of NF-κB is initiated by interactions with either MyD88 or TIR-domain-containing adapter-inducing interferon-β (TRIF) adaptor protein (481). In order to determine whether these two pathways were disrupted by rHDL, we assessed mRNA levels in LPS-stimulated BMDCs. We found that, rHDL decreased *Myd88* mRNA levels in LPS-stimulated BMDCs after 18h of treatment (Fig. 3.15A). In contrast, relative to LPS-stimulated BMDCs' levels, rHDL treatment did not affect *Trif* expression neither at an early nor at a later time point (Fig. 3.15B). These data suggest a role for rHDL in modulating inflammatory responses through interference with the MyD88-dependent TLR4 signaling pathway.

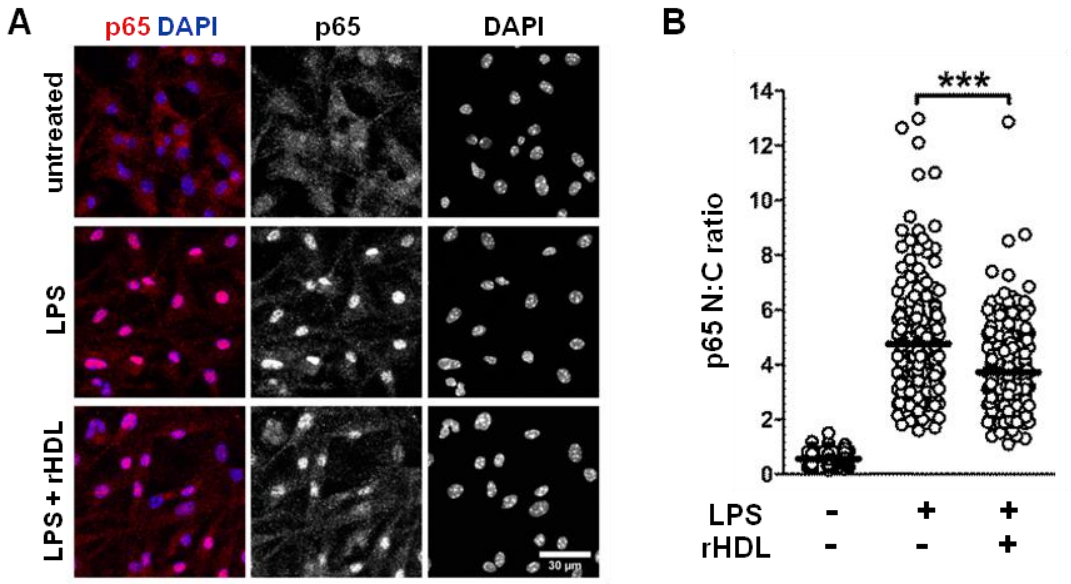

Figure 3.14 rHDL suppresses BMDC function by inhibiting NF-kB activation. WT BMDCs were stimulated with LPS (0.5 µg/mL) and treated with 4 µM rHDL for the indicated time periods. (**A**) Confocal immunofluorescence microscopy for p65 (red) translocation into the nucleus (DAPI stained, blue) in BMDCs stimulated with LPS for 2 h. Maximum projections of image stacks are shown; representative of two independent experiments. (**B**) Quantification of p65 cell distribution by determining nuclear:cytoplasmic (N:C) ratios of signal intensity at single cell level. Data are combined of two independent experiments; ***p<0.0001.

Recently, activating transcription factor 3 (ATF3), a transcriptional regulator that provide negative feedback on TLR-induced inflammation, was identified as a critical mediator of HDL's anti-inflammatory effects in macrophages (310). Thus, we assessed *Atf3* mRNA levels in rHDL-treated BMDC's. Indeed, after 4 h of treatment with rHDL, LPS-stimulated BMDCs demonstrated increased expression of *Atf3* compared to non-treated cells (Fig. 3.15C), whereas expression was decreased at 18h (Fig. 3.15C). This finding suggests that an HDL-inducible ATF3-dependent mechanism may operate in DCs, acting as a restrainer of the TLR-stimulated response by preventing excessive pro-inflammatory cytokine production.

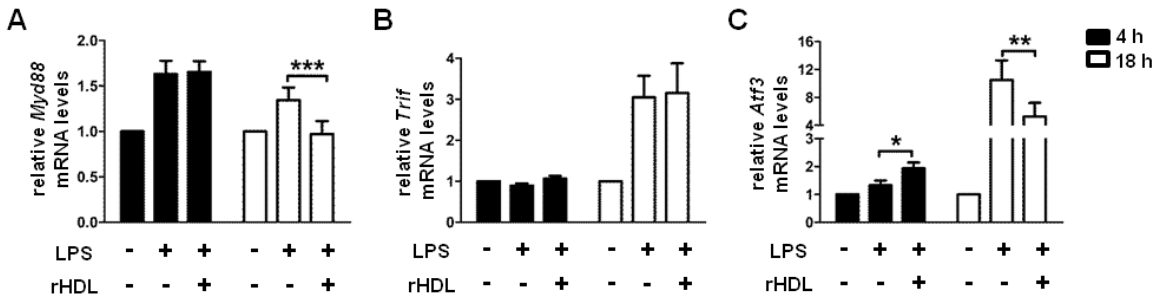

Figure 3.15 rHDL inhibits activation of BMDCs by interfering with the TLR4 pathway. WT BMDCs were stimulated with LPS (0.5 µg/mL) and treated with 4 µM rHDL for the indicated time periods. (**A-C**) Relative mRNA levels of *Myd88* (***p=0.0004), *Trif* and *Atf3* (*p=0.0177, **p=0.0016) after treatment of WT BMDCs (n=6-8) with rHDL for 4h and 18h. Results are expressed as mean ± SEM; data are combined of at least three independent experiments.

The anti-inflammatory effects of rHDL on stimulated BMDCs are mediated through ABCA1 and SR-BI

It is well established that HDL exerts its pleiotropic functions through interactions with SR-BI, ABCA1 and ABCG1 transporters (482, 483). To investigate the contribution of each transporter in rHDL's anti-inflammatory effects on DCs, we assessed cytokine secretion in LPS-stimulated ABCG1$^{-/-}$, ABCA1$^{-/-}$ and SR-BI$^{-/-}$ BMDCs in the presence or absence of rHDL. Deficiency in any of these transporters in BMDCs did not affect their ability to upregulate maturation markers and efficiently secrete pro-inflammatory cytokines upon

LPS stimulation (Fig. 3.16 and 3.17). Interestingly, rHDL suppressed the levels of IL-12, IL-8 or IL-23 in ABCG1$^{-/-}$ BMDCs as efficiently as in BMDCs from WT mice and to an even greater extent the secretion of IL-6, indicating that this transporter is not involved in rHDL's inhibitory effect on DC activation (Fig. 3.17 and 3.18A). In contrast, rHDL was unable to efficiently impair pro-inflammatory cytokine secretion in ABCA1$^{-/-}$ and SR-BI$^{-/-}$ BMDCs suggesting that rHDL-mediated modulation of DC function is ABCA1- and SR-BI-dependent (Fig. 3.17 and 3.18A). Notably, the decrease in IL-10 levels that was observed upon rHDL treatment of LPS-stimulated WT BMDCs (34.5 ± 1.6 %) was retained independent of ABCG1, ABCA1 or SR-BI deficiency (ABCG1$^{-/-}$: 30.5 ± 1.2 %; ABCA1$^{-/-}$: 38.0 ± 1.4 %; SR-BI$^{-/-}$: 35.9 ± 2.6 %; Fig. 3.18A). This result suggests either that the ABCG1 transporter does not contribute to rHDL's inhibitory actions or that in the case of IL-10 there is a redundancy in the functions of the three transporters.

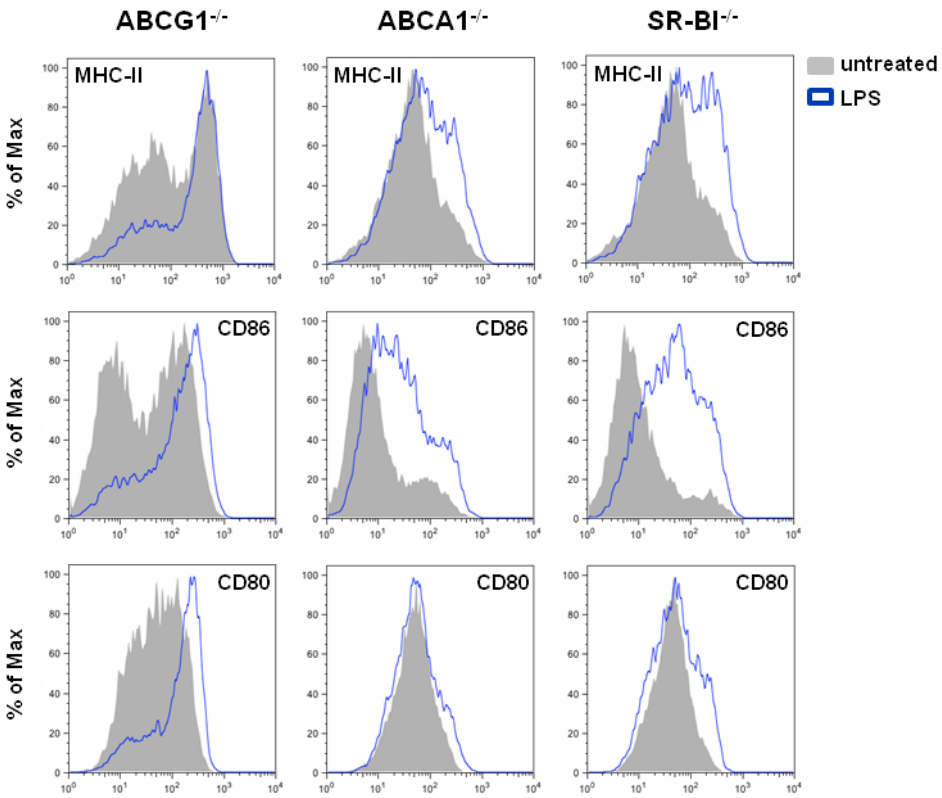

Figure 3.16 BMDCs maturation is independent of ABCG1, ABCA1 or SR-BI deficiency. BMDCs from ABCG1$^{-/-}$, ABCA1$^{-/-}$ and SR-BI$^{-/-}$ mice (n=4-6/group) were stimulated with LPS (0.5 µg/mL) for 12 h. Expression levels of MHC-II, CD86 and CD80 were evaluated by flow cytometry. Representative FACS histograms are shown. Gates were set on CD11c^{+} cells.

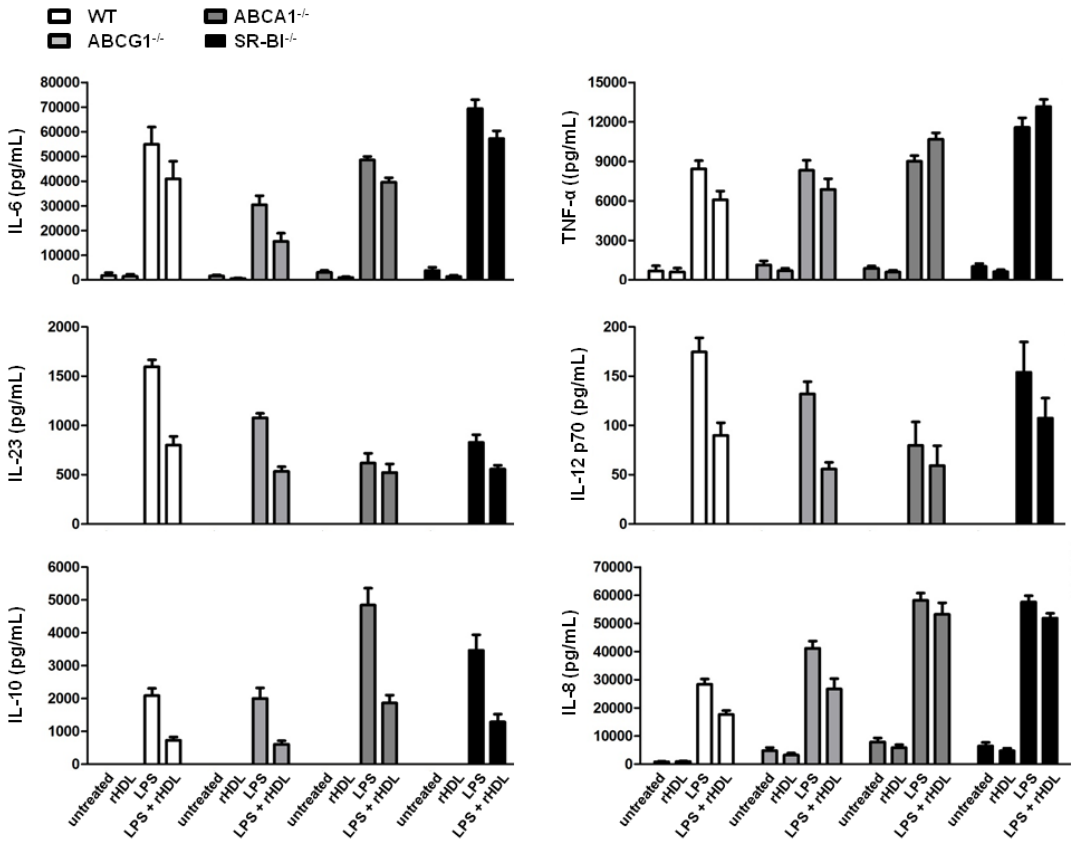

Figure 3.17 BMDCs activation is independent of ABCG1, ABCA1 or SR-BI deficiency. BMDCs from WT, ABCG1$^{-/-}$, ABCA1$^{-/-}$ and SR-BI$^{-/-}$ mice (n=4-6/group) were stimulated with LPS (0.5 µg/mL) and treated with 4 µM rHDL for 12 h. Levels of IL-6, IL-12 p70, TNF-α, IL-23, IL-8 and IL-10 in culture supernatants of stimulated BMDCs are shown. Results are expressed as mean ± SEM; data are combined of at least two independent experiments.

Further support for these findings was obtained upon assessment of rHDL's effects on signaling events downstream of the NF-κB pathway in BMDCs from WT mice or mice deficient for any of the above transporters. Upon LPS stimulation STAT3 signaling, as indicated by increased STAT3 phosphorylation, was efficiently induced in BMDCs from all groups as compared with non-stimulated cells (WT: 6.0 ± 0.8 fold; ABCG1$^{-/-}$: 4.3 ± 0.5 fold; ABCA1$^{-/-}$: 4.2 ± 0.5 fold; SR-BI$^{-/-}$: 3.9 ± 0.5 fold; Fig. 3.18B and 3.18C) and treatment with rHDL was able to diminish STAT3 activation in WT (4.5 ± 0.7 fold; *p=0.0283) and ABCG1$^{-/-}$ BMDCs (2.5 ± 0.2 fold; *p=0.0127). However, rHDL-treated ABCA1$^{-/-}$ and SR-BI$^{-/-}$ BMDCs demonstrated similar levels of LPS-induced STAT3 phosphorylation (ABCA1$^{-/-}$: 3.9 ± 0.7 fold; SR-BI$^{-/-}$: 4.2 ± 0.7 fold; Fig. 3.18B and 3.18C) as compared with cells treated with

LPS alone. Overall, our data provide evidence for an important role of ABCA1 and SR-BI but not ABCG1 in the HDL-mediated anti-inflammatory function on DCs.

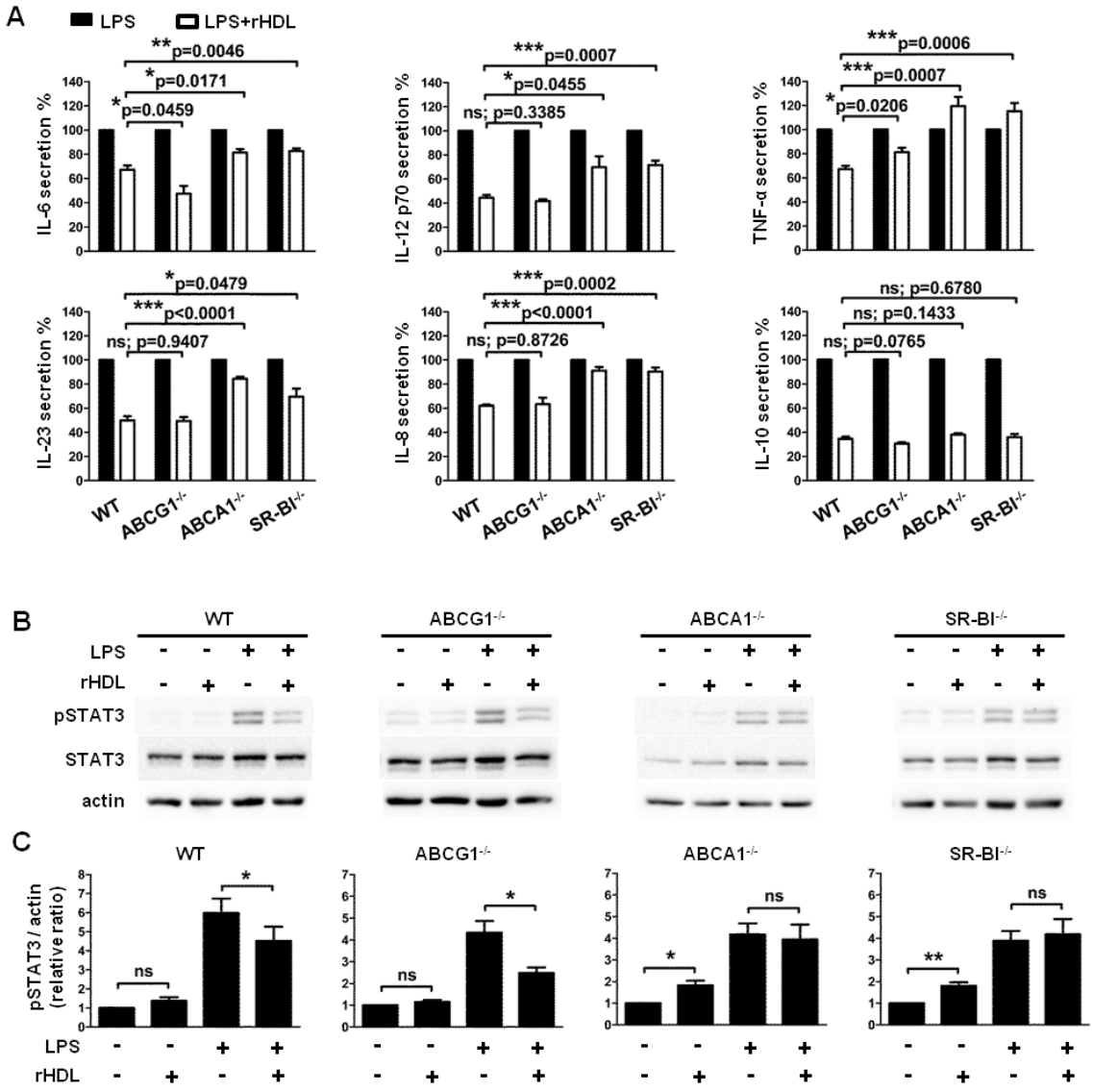

Figure 3.18 The suppressive effect of rHDL on BMDCs activation is dependent on ABCA1 and SR-BI. BMDCs from WT, ABCG1$^{-/-}$, ABCA1$^{-/-}$ and SR-BI$^{-/-}$ mice (n=4-6/group) were stimulated with LPS (0.5 µg/mL) and treated with 4 µM rHDL for 12 h. (**A**) Levels of IL-6, IL-12 p70, TNF-α, IL-23, IL-8 and IL-10 in culture supernatants of stimulated BMDCs. Percentages of cytokine secretion are shown for LPS-stimulated BMDCs after treatment with rHDL, normalized against untreated LPS-stimulated BMDCs of the same genotype. (**B**) Representative western blot images of pSTAT3, total STAT3 and actin are shown for each genotype. (**C**) Levels of pSTAT3 and actin were quantified by densitometry and the pSTAT3/actin ratio was calculated. In panels **A** and **C** results are expressed as mean ± SEM; data are combined of at least two independent experiments. *p<0.05, **p<0.01, ***p<0.001; ns; not significantly different.

Chapter I - Discussion

HDL constitutes a heterogeneous population of particles that is characterized by great complexity in terms of structure and functionality (484). Although it has been best recognized for its inverse correlation with cardiovascular events (485, 486), numerous *in vivo* and *in vitro* studies have revealed novel roles of HDL in cholesterol metabolism, endothelial integrity and inflammation (487, 488). HDL interacts with a variety of cells and exerts its anti-oxidant, anti-inflammatory, anti-thrombotic and anti-apoptotic activities, but also promotes cholesterol efflux, endothelial cell migration and offers protection from bacterial or viral infections (489-491). However, under certain conditions HDL can become functionally defective. HDL's protective functions are compromised in patients with coronary heart disease (492), diabetes (493) and other chronic inflammatory conditions such as Crohn's disease, chronic kidney disease and rheumatoid arthritis (335, 340, 477, 494).

Rheumatoid arthritis is an autoimmune disease that causes destruction of the joints and is associated with increased cardiovascular morbidity and mortality (495). The majority of RA patients are dyslipidemic (348). Specifically, levels of total HDL are decreased whereas those of pro-inflammatory HDL are increased in patients with rheumatoid arthritis whereas anti-rheumatic drugs improve HDL levels and functionality (335, 496-498).

Although numerous studies have reported the anti-inflammatory properties of HDL, the mechanisms involved in HDL-mediated suppression of autoimmune inflammatory responses are not well understood. Our results demonstrate that HDL suppresses the activation, maturation of and cytokine secretion by DCs resulting in the establishment of a "semi-mature phenotype" of these cells. To this end, treatment of BMDCs with rHDL resulted in reduced expression of MHC-II and co-stimulatory molecules that are required for efficient antigen-presentation and activation of T lymphocytes. This is in line with previous reports revealing a role of HDL and apoA-I on human DC differentiation and function (319, 320). Antigen loading to MHC-II is mediated either through the classical or via the autophagy pathway (499, 500). Recent data suggest that HDL inhibits autophagy induced by oxidized low-density lipoproteins (oxLDL) in endothelial cells (501). Whether HDL could suppress

the induction of autophagy in DCs and delivery of antigens to MHC loading compartments remains to be shown.

The functional importance of the anti-inflammatory effects of HDL on DCs is demonstrated by the decreased ability of rHDL-treated BMDCs to promote T cell proliferation *in vitro*. DCs with a "semi-mature phenotype" have the ability to down-regulate immune responses and to ameliorate autoimmunity upon adoptive transfer *in vivo* (502, 503). In particular, it was shown that TNF-α-treated DCs are tolerogenic and suppress experimental autoimmune thyroiditis through induction of $CD4^+CD25^+$ Tregs *in vivo* and *in vitro* (503). Since Tregs, play a prominent role in the re-establishment but also maintenance of self-tolerance it remains to be examined whether rHDL-treated BMDCs possess the ability to induce and/or expand Tregs *in vivo*. Interestingly, absolute numbers of $CD4^+Foxp3^+$ Tregs in the dLNs of immunized apoA-$I^{-/-}$ were elevated compared to WT mice. However, the suppressive potential of $Foxp3^+$ Tregs in an inflammatory environment is currently under debate (504, 505).

According to our data, absence of apoA-I in mice resulted in exacerbated inflammation in the knee joints during AIA and caused extensive inflammatory reactions in the skin. These findings are in line with previous studies demonstrating that lack of apoA-I in low-density lipoprotein receptor (LDLR) deficient mice fed with high-fat diet was associated with skin lesion development due to enlarged skin dLNs that contained expanded populations of cholesterol-enriched lymphocytes including T cells, B cells and DCs (328). Moreover, when fed an atherogenic diet these double knockout mice exhibited increased T cell activation, proliferation and production of autoantibodies in the plasma. Importantly, this autoimmune phenotype was restored after treatment of mice with either lipid-free apoA-I or adenovirus-mediated gene transfer of apoA-I (328, 329).

HDL metabolism entails the successive interactions of apoA-I with the ABCA1, ABCG1 and SR-BI receptors (13). Numerous studies have implicated each of these transporters in HDL's anti-atherogenic actions involving mechanisms such as cholesterol efflux and activation of HDL-induced signaling pathways (482, 483, 506, 507).The capacity of HDL to bind LPS and neutralize its inflammatory activity has been demonstrated in multiple *in vitro*

and *in vivo* studies (294, 295). Although this possibility cannot be excluded, the data presented in this study using BMDCs from ABCA1, ABCG1 or SR-BI deficient mice do not support such a mechanism of action for rHDL. In our experiments, rHDL did not efficiently suppress LPS-induced secretion of IL-6, IL-12 or IL-23 in mice lacking ABCA1 or SR-BI, indicating that a specific interaction between rHDL and these transporters, rather than sequestration of LPS by rHDL, is responsible for its anti-inflammatory functions on BMDCs.

LPS stimulation of DCs activates NF-κB, via either the MyD88- or the TRIF-dependent pathway, which is then recruited to the nucleus to induce inflammatory cytokine gene transcription (481). Our data demonstrate that rHDL's anti-inflammatory effects on LPS-stimulated BMDCs are mediated through interference with the MyD88/NF-κB pathway. Although the inhibitory actions of apoA-I and HDL on TLR signaling have been previously reported (353, 508), a mechanism by which HDL selectively impedes the MyD88-dependent signaling in DCs has not yet been established. Based on our findings we speculate that interaction of apoA-I on HDL with cell surface lipid transporters such as ABCA1 or SR-BI, leads to changes in downstream signaling events that in turn compromise NF-κB activation and transcriptional upregulation of *Myd88* by LPS. This could be mediated via two alternative, but not necessarily mutually exclusive pathways. One mechanism could involve depletion of lipid rafts from plasma membranes as a result of cholesterol efflux initiated by apoA-I/ABCA1 or apoA-I/SR-BI interactions. Lipid rafts are dynamic structures that have been critically implicated in a variety of cellular processes including signal transduction, endocytosis, vesicular transport, and immunoregulation (509). Treatment of APCs with either HDL or apoA-I has been associated with cholesterol depletion and lipid raft disruption leading to suppressed T cell activation and down-regulation of pro-inflammatory cytokine secretion (322, 510) . The second mechanism could involve activation of ABCA1- or SR-BI-induced signaling that results in inhibition of the TLR-induced response. According to previous studies, interaction of HDL or apoA-I with SR-BI present on endothelial cells activates downstream signaling cascades stimulating a variety of protective cellular responses (511). In addition, apoA-I binding to ABCA1 activates the JAK2/STAT3 pathway in macrophages leading to suppression of LPS-induced inflammatory cytokine

production through the action of the mRNA-destabilizing protein, tristetraprolin (512). To date no signaling events have been reported as a result of interactions between apoA-I or HDL and ABCG1, a transporter known to greatly contribute to the cholesterol efflux process in macrophages. Notably, in our study the inhibitory properties of rHDL on BMDCs were found to be independent of ABCG1. These data argue against the hypothesis that the anti-inflammatory effects of rHDL on BMDCs are due to cholesterol depletion leading to lipid raft remodeling and favor a model which implicates transporter-specific downstream signaling events.

In a recent study ATF3, a transcriptional repressor of TLR-stimulated inflammation, was identified as an HDL-inducible target gene that mediated HDL's anti-inflammatory actions in macrophages (310). It was shown that the protective effects of HDL on TLR responses were fully dependent on ATF3 *in vitro* and *in viv*o. We show here that treatment of LPS-stimulated BMDCs with rHDL caused an upregulation in *Atf3* expression. These data support the notion that an ATF3-dependent mechanism may also be activated by HDL in DCs to constrain the inflammatory response.

In summary, our findings provide evidence for a novel role of HDL in shaping the autoimmune responses both *in vivo* and *in vitro*. HDL suppresses adaptive T cell responses by modulating the pro-inflammatory function of DCs, in an ABCA1- and SR-BI-dependent fashion. The results presented here shed light on the mechanism underlying the anti-inflammatory properties of HDL that could aid the development of new therapeutic approaches for autoimmune and other inflammatory diseases.

CHAPTER II:

The Role of ApoA-I(L141R)$_{Pisa}$ and ApoA-I(L159R)$_{FIN}$ in HDL Biogenesis and the Development of Atherosclerosis *In Vivo*

Mutations in human apoA-I are associated with low levels of HDL cholesterol and pathological conditions such as premature atherosclerosis and amyloidosis. In this study we functionally characterized two natural human apoA-I mutations, (L141R)$_{Pisa}$ and (L159R)$_{FIN}$, *in vivo*. For this purpose we generated transgenic mice expressing either wild-type or mutant human apoA-I in a mouse apoA-I$^{-/-}$ background and analyzed for abnormalities in their lipid and lipoprotein profiles. In addition, HDL structure and functionality, and the predisposition to atherosclerosis following a 14-week high-fat diet was assessed.

Generation of transgenic mice carrying WT or mutant forms of human apoA-I

We generated transgenic mice expressing either WT human apoA-I or each of the two mutant forms of human apoA-I [apoA-I(L141R)$_{Pisa}$ and apoA-I(L159R)$_{FIN}$]. In our constructs, the human apoA-I gene was linked to the mouse transthyretin 1 (TTR1) liver-specific promoter (Fig. 3.19A). The founder animals for each line were identified by Southern blot (Fig. 3.19B). Selected founders (F0, hapoA-I^{Tg} mapoA-I$^{+/+}$; Fig. 3.19C) were crossed with apoA-I$^{-/-}$ mice to generate mice that express human but not mouse apoA-I (F1, hapoA-I^{Tg} mapoA-I$^{+/-}$; F2, hapoA-I^{Tg} mapoA-I$^{-/-}$; Fig. 3.19C), and these mice [designated as WT apoA-I, apoA-I(L141R) and apoA-I(L159R)] were used for further studies. The expression of human apoA-I mRNA in the liver of these mice was examined by quantitative RT-PCR and was determined at 1.1-fold and 0.3-fold respectively for apoA-I(L141R) and apoA-I(L159R) compared to WT apoA-I mice (Fig. 3.20A and 3.20B). In addition, lower levels of apoA-I mRNA were detected in other tissues such as the brain and the adipose (Fig. 3.20C). Western blot analysis using an antibody specific for human apoA-I

confirmed the presence of human apoA-I in the liver (Fig. 3.20D) and the serum of mice of all three transgenic lines (Fig. 3.20E). Consistent with the lower mRNA levels of human apoA-I in the liver of apoA-I(L159R) transgenic mice, hepatic apoA-I levels in these mice were found decreased (0.6 fold) compared to both WT apoA-I and apoA-I(L141R) (Fig. 3.20D). Serum apoA-I levels in apoA-I(L141R) and apoA-I(L159R) mice were significantly lower compared to WT apoA-I mice (26.6 ± 4.0 and 18.1 ± 1.8 versus 302.0 ± 16.8 mg/dL, respectively; Fig. 3.20E) as determined by ELISA.

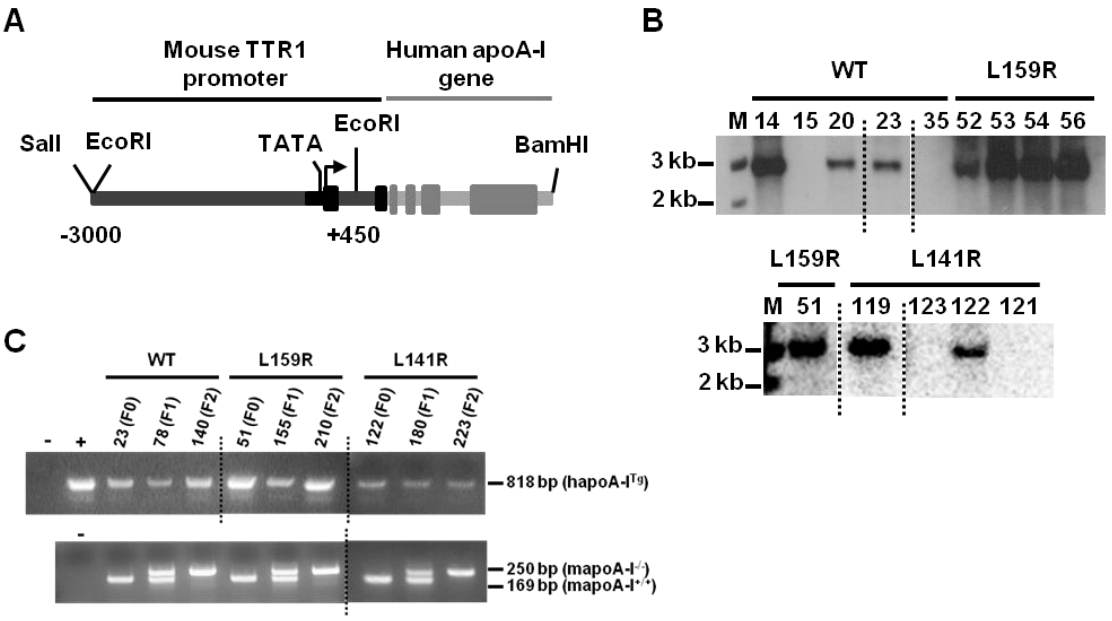

Figure 3.19 Generation of transgenic mice expressing WT or mutant forms of human apoA-I. (**A**) Schematic representation of the construct used for the generation of the human apoA-I transgenic mice. (**B**) Southern blot analysis to identify the transgenic founder animals for each line. Images were either acquired after exposure on film (upper blot) or scanned on Phosphorimager (lower blot). M, DNA size marker. (**C**) PCR amplification to analyze the expression of the human apoA-I transgene and of the endogenous gene for each line. (-); negative control, (+); positive control. (**B-C**) Numbers on top designate different mouse lines. Dashed lines mark the different segments of the same image that were joined together.

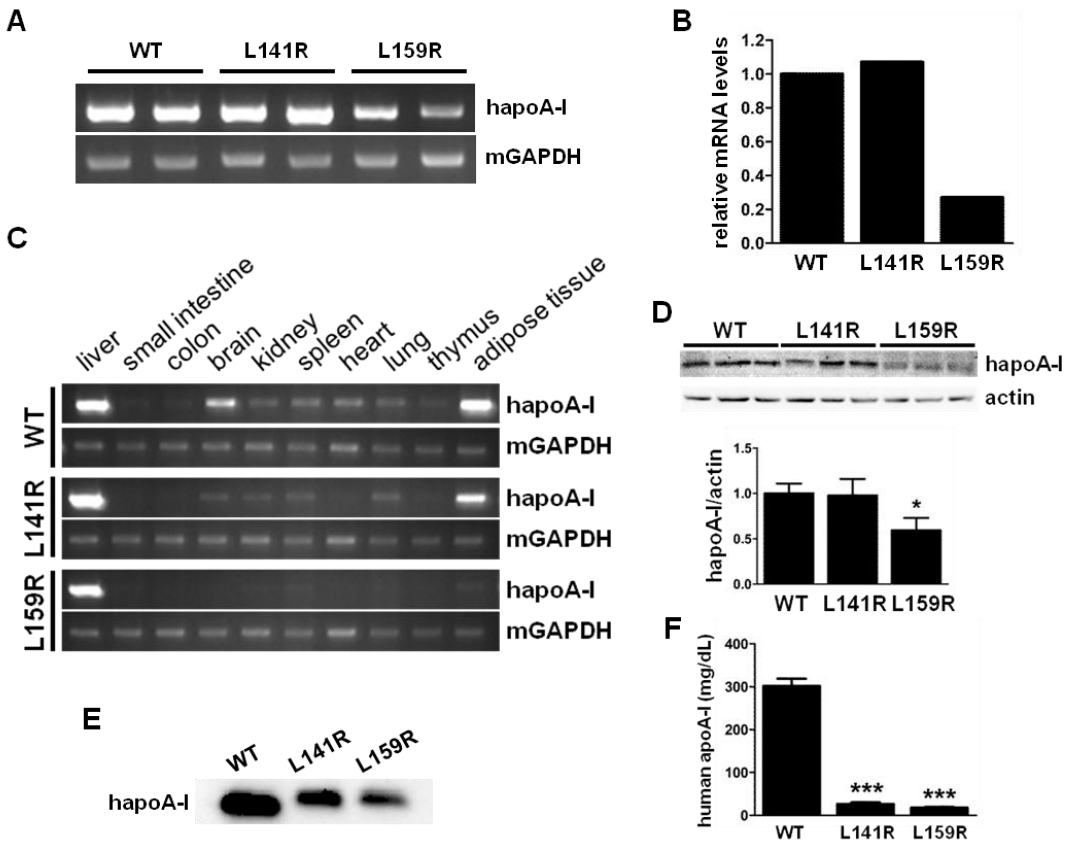

Figure 3.20 Expression analysis of transgenic mice carrying WT or mutant forms of human apoA-I. (**A**) RT-PCR analysis to determine the hepatic apoA-I mRNA levels of transgenic mice. Representative images are shown of n=4-5/group. (**B**) Human apoA-I mRNA levels in the livers of transgenic mice as determined by quantitative RT-PCR (n=5-9/group). (**C**) RT-PCR analysis of apoA-I mRNA levels in various tissues of transgenic mice. Human apoA-I levels in the liver (**D**) and the serum (**E**) of the transgenic animals as determined by Western blot analysis (n=4-5/group). (**F**) Human apoA-I levels in the serum of transgenic mice as determined by ELISA (n=10/group). Data represent mean ± SEM. ****P*<0.0001 vs WT apoA-I.

ApoA-I(L141R) and apoA-I(L159R) transgenic mice exhibit very low levels of serum total and esterified cholesterol

To determine the lipid profiles of the human apoA-I transgenic mice, we measured the levels of cholesterol, phospholipids and triglycerides in the serum. Mice expressing the apoA-I(L141R) and apoA-I(L159R) mutants had greatly reduced total cholesterol levels (~20%) and decreased cholesteryl ester to total cholesterol (CE/TC) ratio (~60%) compared to mice expressing WT apoA-I (Table 3.1). Serum phospholipid levels of mice expressing either mutant were also decreased (~40%) compared to mice expressing WT apoA-

I, whereas the triglyceride levels were within the normal range in all mice. However, apoA-I(L159R) mice had slightly elevated triglyceride levels compared to WT apoA-I mice (Table 3.1). FPLC analysis of the serum showed that the HDL-cholesterol peak of the mice expressing the apoA-I mutants was greatly diminished compared to mice expressing WT apoA-I (Fig. 3.21).

Table 3.1. Serum lipid levels in human apoA-I transgenic and apoA-I$^{-/-}$ mice before and after 14 weeks of high-fat diet (HFD) feeding.

Diet	Genotype	TC	HDL-c	FC	CE	CE/TC	TG	PL
Chow								
	WT apoA-I	68 ± 3	44 ± 3	16 ± 1	52 ± 2	0.77 ± 0.01	37 ± 3	167 ± 9
	apoA-I(L141R)	14 ± 1*	3 ± 0.3*	7 ± 1*	7 ± 1*	0.47 ± 0.03*	42 ± 4	69 ± 4*
	apoA-I(L159R)	15 ± 2*	3 ± 0.3*	7 ± 1*	8 ± 1*	0.48 ± 0.04*	54 ± 8†	69 ± 5*
	apoA-I$^{-/-}$	19 ± 1*	8 ± 0.4*	6 ± 1*	13 ± 1*	0.69 ± 0.01*	29 ± 2†	70 ± 3*
HFD								
	WT apoA-I	110 ± 5§	23 ± 1§	26 ± 2§	84 ± 3§	0.77 ± 0.01	16 ± 2§	109 ± 5§
	apoA-I(L141R)	107 ± 8§	7 ± 0.8*§	31 ± 3§	77 ± 6§	0.71 ± 0.01*§	22 ± 1‡§	103 ± 8§
	apoA-I(L159R)	105 ± 7§	5 ± 0.6$^{*\#}$	26 ± 2§	78 ± 5§	0.75 ± 0.01§	25 ± 2$^{*\|\|}$	78 ± 6*
	apoA-I$^{-/-}$	85 ± 4*§	22 ± 1§	21 ± 1‡§	64 ± 3*§	0.76 ± 0.01§	18 ± 1§	101 ± 5§

Total cholesterol (TC), HDL-cholesterol (HDL-c), free cholesterol (FC), cholesteryl esters (CE), triglyceride (TG) and phospholipid (PL) levels in the serum of human apoA-I transgenic and apoA-I$^{-/-}$ mice were determined before (chow diet) and after a 14-week HFD (n=13-23/group). Data represent mean ± SEM; Values are given in mg/dL.

*P<0.001 vs WT apoA-I of the same diet group
$^{\dagger}P$<0.05 vs WT apoA-I of the same diet group
$^{\ddagger}P$<0.01 vs WT apoA-I of the same diet group
$^{\S}P$<0.001 vs same genotype of the chow diet group
$^{\|}P$<0.01 vs same genotype of the chow diet group
$^{\#}P$<0.05 vs same genotype of the chow diet group

ApoA-I(L141R) and apoA-I(L159R) transgenic mice form fewer and smaller HDL particles

To assess the apolipoprotein distribution among the lipoprotein subclasses, the serum of human apoA-I transgenic mice was fractionated by density gradient ultracentrifugation and the resulting fractions were analyzed by SDS-

PAGE. In WT apoA-I mice, apoA-I was predominantly distributed in the HDL2 (*d*>1.084 g/mL) and HDL3 regions (Fig. 3.22A). A similar distribution of apoA-I was found in mice expressing either of the two apoA-I mutants. However, both mutants were characterized by very low apoA-I levels and increased levels of mouse apoE in the HDL2 region (Fig. 3.22A). Electron microscopy analysis of HDL fractions 6-8 showed that WT apoA-I mice formed spherical HDL particles (9.0 ± 1.9 nm; Fig. 3.22B), while apoA-I(L141R) and apoA-I(L159R) mice formed very few small-sized particles (6.3 ± 1.1 and 5.0 ± 0.8 nm, respectively; Fig. 3.22B). To further characterize HDL subpopulations, serum was analyzed by two-dimensional gel electrophoresis. WT apoA-I mice formed α-HDL particles (α1-α4), whereas mice expressing either of the apoA-I mutants formed pre-β2- and α3-, α4-HDL subpopulations (Fig. 3.22C).

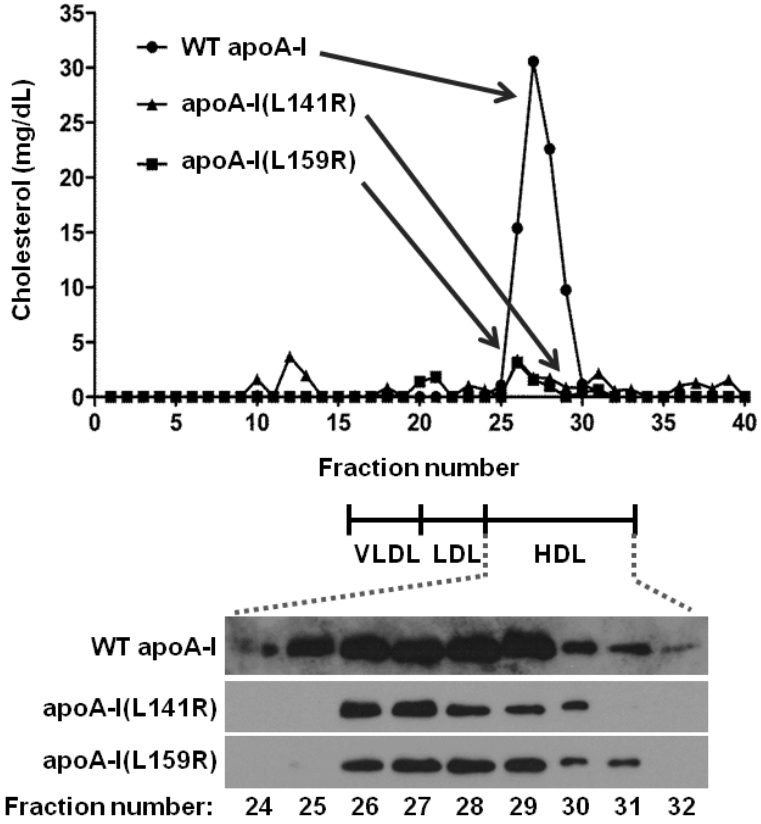

Figure 3.21 Cholesterol distribution in different lipoprotein subclasses in human apoA-I transgenic mice on chow diet. Pooled serum samples (n=2/group/pool) were subjected to gel filtration and cholesterol levels in each fraction were determined. Fractions corresponding to HDL were analyzed by SDS-PAGE and blotted against anti-human apoA-I antibody. Data are representative of two independent experiments.

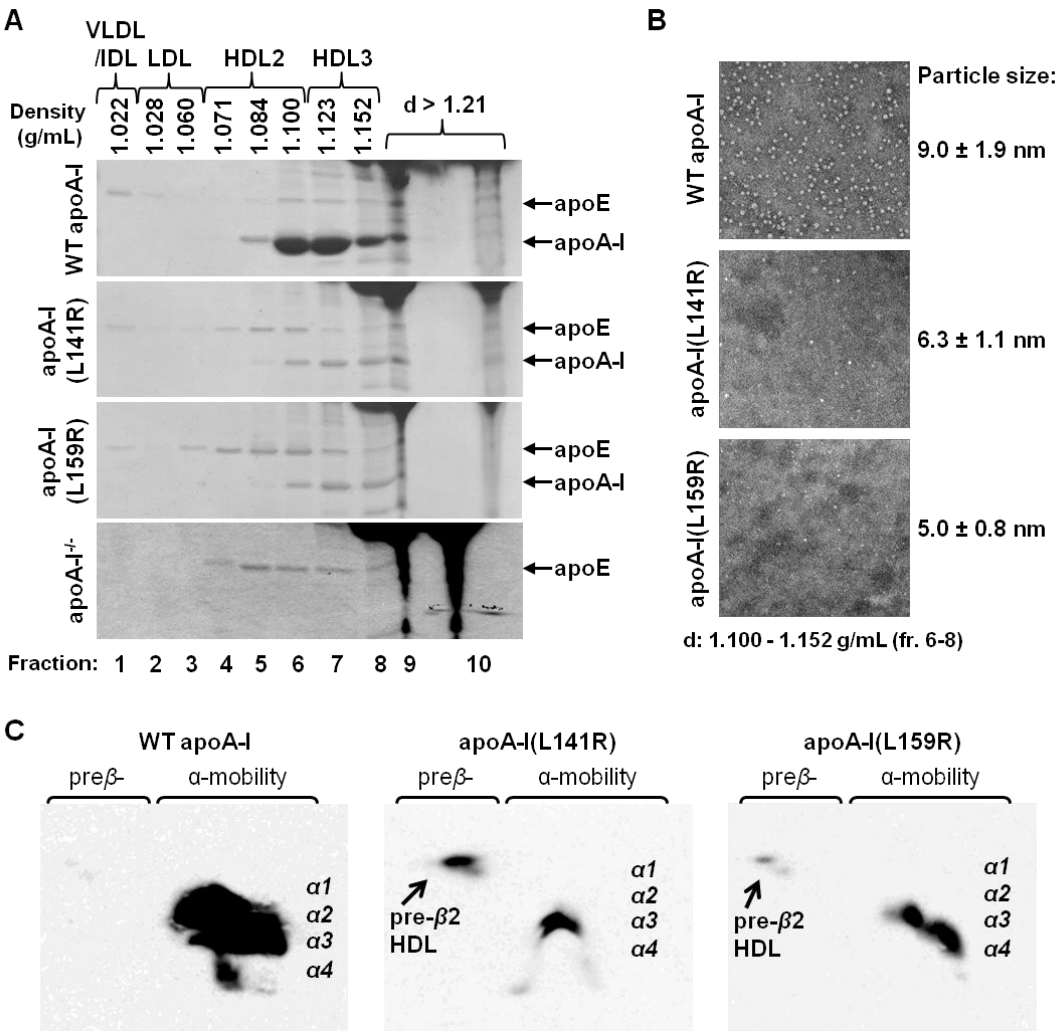

Figure 3.22 Apolipoprotein distribution and characterization of apoA-I-containing HDL subpopulations in the serum of human apoA-I transgenic mice on chow diet. (**A**) Density gradient ultracentrifugation and SDS-PAGE analysis of the serum of human apoA-I transgenic and apoA-I$^{-/-}$ mice (n=3/group). (**B**) Electron microscopy analysis of HDL fractions 6-8 obtained by density gradient ultracentrifugation shown in panel A. The photomicrographs were taken at x75,000 magnification and enlarged three times. (**C**) The serum of human apoA-I transgenic mice (n=4/group) was analyzed by two-dimensional gel electrophoresis and western blotting using anti-human apoA-I antibody. For all analyses, representative images are shown.

HDL from apoA-I(L141R) and apoA-I(L159R) transgenic mice is associated with reduced anti-oxidant capacity

Following the structural characterization of the HDL particles, we performed a series of *in vitro* assays to determine whether the HDL formed in the transgenic mice expressing the apoA-I mutants retained its anti-oxidant

properties. First, we examined the ability of HDL to protect against LDL oxidation by performing the DCF assay (Fig. 3.23A). HDL from apoA-I(L141R) or apoA-I(L159R) mice incubated either alone or in the presence of oxidized LDL produced a markedly stronger fluorescence signal compared to the signal produced by HDL from WT apoA-I mice (Fig. 3.23A) indicating that HDL carrying these apoA-I mutants has a reduced anti-oxidant capacity. Furthermore, in the case of the apoA-I mutants the level of the fluorescence signal was similar to the signal produced following incubation of oxidized LDL with HDL isolated from apoA-I$^{-/-}$ mice (Fig. 3.23A). Next, we assessed the

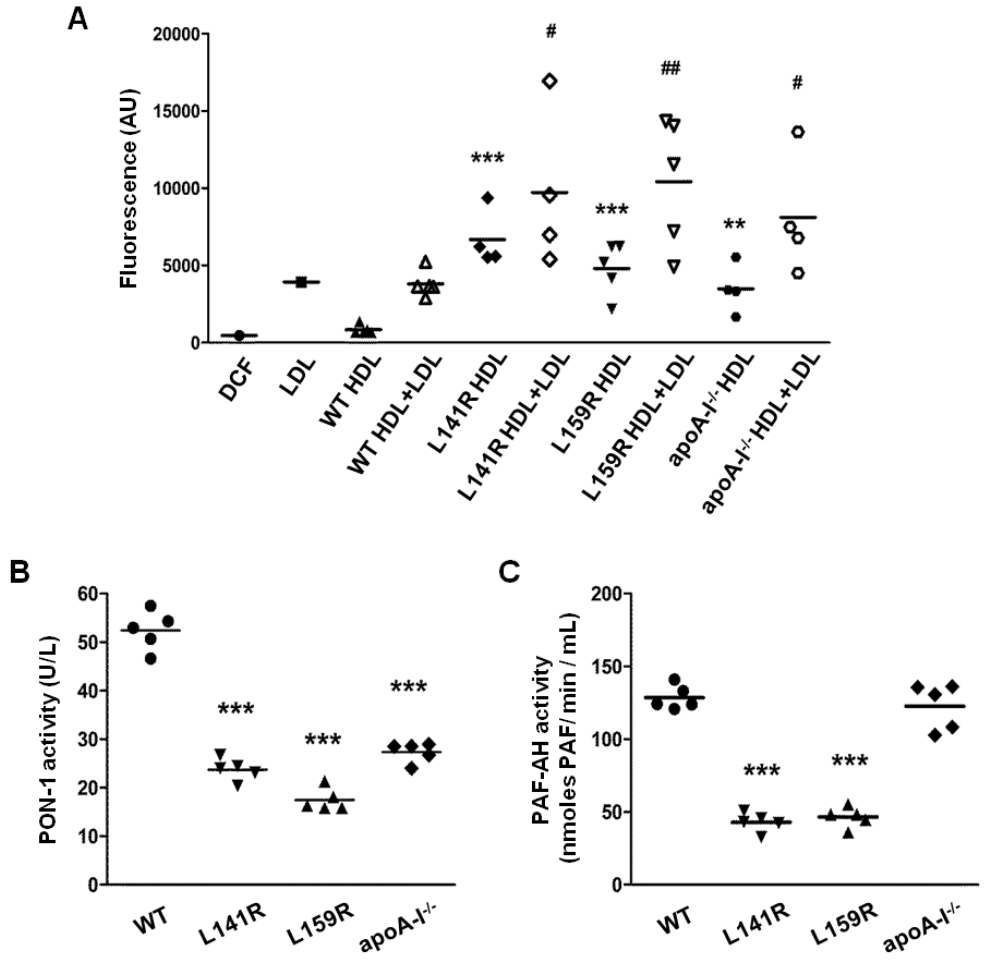

Figure 3.23 Characterization of the anti-oxidant properties of HDL isolated from human apoA-I transgenic and apoA-I$^{-/-}$ mice. (**A**) Anti-oxidant properties of HDL analyzed by the DCF assay. The fluorescence intensity resulting from oxidation of DCFH by HDL in the presence or absence of oxidized LDL was measured. ***P*=0.0077,****P*≤0.0009 vs WT HDL; $^{\#}$*P*≤0.0457, $^{\#\#}$*P*=0.0087 vs WT HDL+LDL. AU, arbitrary units. HDL-associated PON-1 (**B**) and PAF-AH (**C**) activity in the serum of human apoA-I transgenic and apoA-I$^{-/-}$ mice. ****P*<0.0001 vs WT apoA-I.

activity of two HDL-associated enzymes, PON-1 and PAF-AH which are known to contribute to HDL's anti-oxidant and atheroprotective functions (257, 260, 513). The HDL-associated PON-1 and PAF-AH activities were found greatly reduced in the serum of both apoA-I(L141R) and apoA-I(L159R) mice compared to WT apoA-I mice (Fig. 3.23B and 3.23C). These data suggest that the anti-oxidant functions of HDL are compromised in the transgenic mice expressing the human apoA-I mutant forms.

HDL from apoA-I(L141R) and apoA-I(L159R) mice exhibits enhanced capacity to promote ABCA1-dependent cholesterol efflux

To further investigate the effect of apoA-I(L141R) and apoA-I(L159R) mutations on HDL functionality *in vivo*, we examined the ability of HDL to promote ABCA1-mediated cholesterol efflux. For this purpose, J774 mouse macrophages were stimulated with a cAMP analog and treated with HDL either at equal apoA-I concentration (Fig. 3.24A) or at equal volume (Fig. 3.24B). This analysis showed that in both cases HDL containing the mutant apoA-I forms had enhanced ability to promote cholesterol efflux upon cAMP-mediated induction of ABCA1 expression compared to HDL containing WT apoA-I (-cAMP vs +cAMP; Fig. 3.24). Moreover, similarly to previous studies (514, 515), HDL from mice expressing the WT apoA-I showed similar capacity to promote cholesterol efflux in the absence or presence of the cAMP analog (Fig. 3.24) due to the very low concentration of pre-β HDL in these mice. However, when treated with equal HDL volume the percentage of cholesterol efflux induced by HDL isolated from WT apoA-I mice in J774 cells was significantly higher compared to HDL isolated from all other groups of mice (+cAMP groups; Fig. 3.24B).

To assess the properties of macrophages in human apoA-I transgenic mice as well as in apoA-I$^{-/-}$ mice independently of the circulating HDL particles, we isolated thioglycollate-elicited peritoneal macrophages and determined ABCA1 expression levels in these cells. According to our results no statistically significant differences were observed in either mRNA or protein levels of ABCA1 among the different groups of mice (Fig. 3.25).

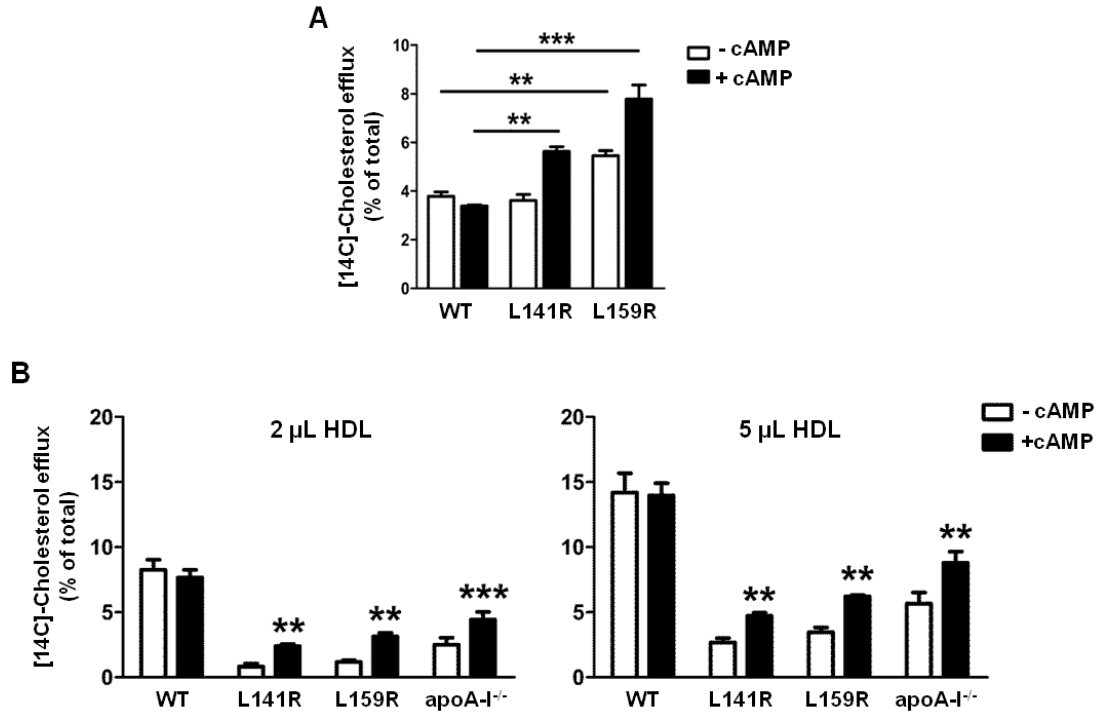

Figure 3.24 Cholesterol efflux capacity of HDL isolated from human apoA-I transgenic mice. J774 mouse macrophages were incubated in the presence or absence of cAMP using equal concentration (28 µg/mL based on apoA-I content) (**A**) or equal volume (2 or 5 µL/well) (**B**) of serum HDL as cholesterol acceptor. Data represent mean ± SEM; ***P*<0.01, ****P*<0.001. Results are representative of two independent experiments. N=6 pooled HDL samples/group for (**A**) and n=5 individual HDL samples/group for (**B**). cAMP, 3′,5′-cyclic adenosine monophosphate.

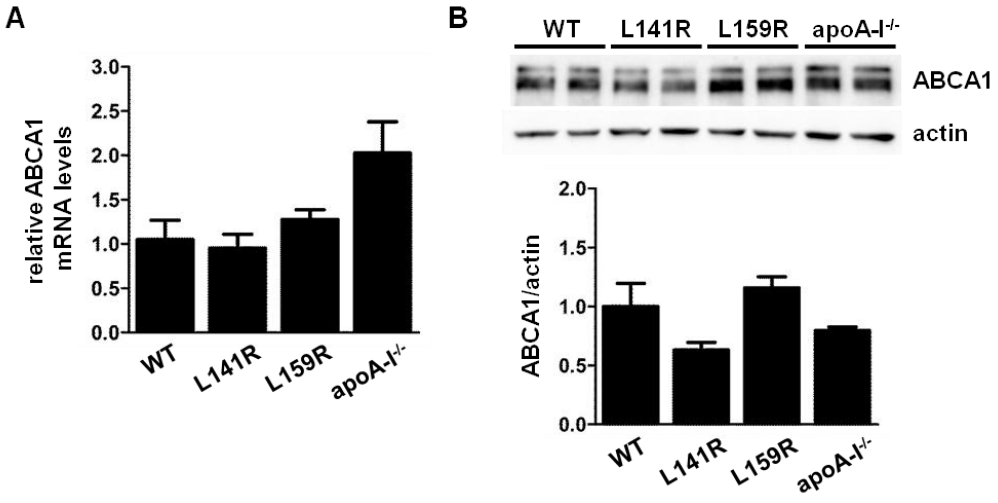

Figure 3.25 Expression analysis of ABCA1 in macrophages from human apoA-I transgenic and apoA-I$^{-/-}$ mice. Thioglycollate-elicited macrophages were isolated from mice (n=3/group) and ABCA1 expression levels were determined by quantitative RT-PCR (**A**) and by western blot analysis (**B**). Data represent mean ± SEM.

HDL from apoA-I(L141R) and apoA-I(L159R) mice promotes endothelial cell migration

The processes of endothelial cell proliferation and migration underlie both neovascularization and maintenance of intimal layer integrity (516) which are crucial for normal homeostasis of the arterial wall and cardiovascular protection. One of HDL's anti-atherogenic mechanisms of action includes inhibiting apoptosis and promoting endothelial cell proliferation and migration. To study the effects of the two apoA-I mutations on endothelial cell function we next investigated the ability of HDL isolated from WT apoA-I or apoA-I(L141R) and apoA-I(L159R) mice to promote endothelial cell migration. Interestingly, endothelial cells treated with HDL carrying the apoA-I mutants (used at equal concentration with HDL containing WT apoA-I) demonstrated increased migration (scratch area 48.0 ± 6.6 and 51.2 ± 7.1 % of control, respectively; Fig. 3.26A) compared to HDL carrying WT apoA-I (scratch area 74.4 ± 3.0 % of control, respectively; Fig. 3.26A).

HDL is known to exert its anti-atherogenic effects on endothelial cells through interactions with S1P3 or SR-BI receptor (215, 218). HDL binding to endothelial SR-BI activates PI3K/Akt which leads to phosphorylation of eNOS at serine residue 1177 and stimulation of nitric oxide production (219). To examine whether the two natural apoA-I mutations had an effect on these processes we stimulated EA.hy926 endothelial cells with HDL isolated from mice expressing either the WT or the mutant apoA-I forms and assessed Akt and eNOS activation. As indicated by the phosphorylation levels, HDL isolated from apoA-I(L141R) or apoA-I(L159R) mice induced the activation of Akt (1.4 ± 0.1 and 1.2 ± 0.2, respectively; Fig. 3.26B) and eNOS (2.2 ± 0.2 and 1.6 ± 0.2, respectively; Fig. 3.26B) to a similar extent as HDL isolated from WT apoA-I mice (Akt: 1.3 ± 0.1, eNOS: 2.4 ± 0.3; Fig. 3.26B). These data suggest improved functionality of HDL particles carrying either apoA-I mutant as demonstrated by their enhanced ability to stimulate endothelial cell migration through an eNOS and Akt-independent mechanism.

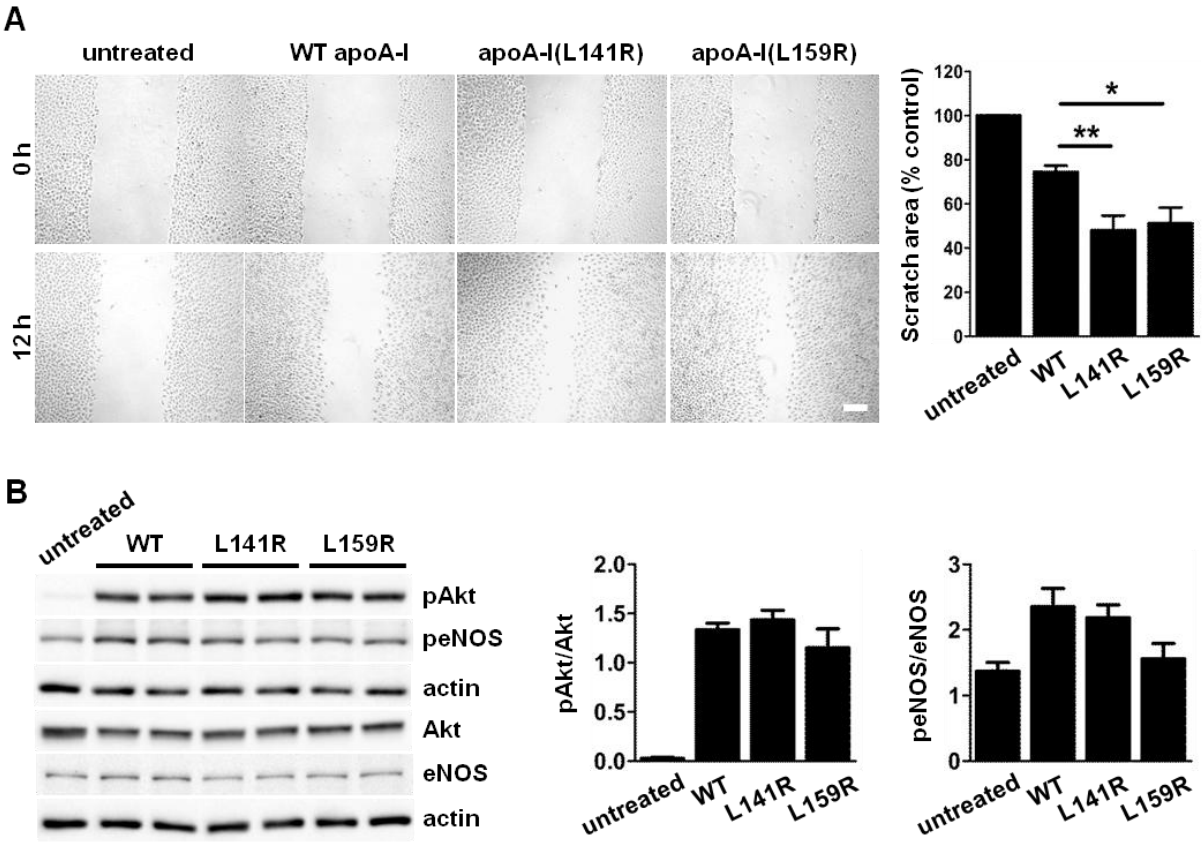

Figure 3.26 Effect of HDL isolated from human apoA-I transgenic mice on endothelial cells. (**A**) HDL-induced endothelial cell migration. EA.hy926 cells were scratched and treated with serum HDL (40 µg/mL based on apoA-I content). Migration was evaluated by measuring the scratched area before (t=0 h) and at the end of the incubation with HDL (t=12 h). Scale bar: 200 µm; **P*=0.0110, ***P*=0.0046. (**B**) HDL-mediated activation of Akt and eNOS in endothelial cells. EA.hy926 cells were treated with serum HDL (40 µg/mL based on apoA-I content) for 20 min and the phosphorylation of Akt and eNOS were evaluated by western blotting. (**A** and **B**) Data represent mean ± SEM; data are combined from two independent experiments (n=5-6 pooled HDL samples/group).

ApoA-I(L141R) and apoA-I(L159R) transgenic mice develop increased atherosclerosis

To study the impact of the apoA-I mutations on atherosclerosis development, mice were fed a high-fat diet (HFD) for 14 weeks and the aortic roots were analyzed for lipid accumulation and collagen deposition (Fig. 3.27). Serum lipids were also determined before (chow diet) and at the end of the HFD (Table 3.1). After 14 weeks of HFD, serum total cholesterol was

Figure 3.27 Outline of diet-induced atherosclerosis study in transgenic mice expressing either WT or mutant forms of human apoA-I.

increased approximately 2-fold in WT apoA-I mice and approximately 7-fold in apoA-I(L141R) and apoA-I(L159R) mice. In agreement with previous studies (468, 517) HDL-cholesterol levels in WT apoA-I mice were decreased by ~50% after the HFD feeding (Table 3.1). In mice expressing either apoA-I mutant, although HFD feeding resulted in a slight increase in the HDL-cholesterol content (Table 3.1), the percentage of HDL-cholesterol relative to total cholesterol was decreased (Fig. 3.28). Interestingly, in apoA-I$^{-/-}$ mice the HDL-cholesterol levels were increased by the HFD to levels that were similar to the WT apoA-I mice (Table 3.1). In addition, CE levels in both apoA-I mutant mice were significantly elevated resulting in a CE/TC ratio similar to the ratio observed in WT apoA-I mice (Table 3.1). Serum phospholipid levels were moderately decreased in WT apoA-I mice fed a HFD (Table 3.1). In contrast, phospholipid levels in apoA-I(L141R) and apoA-I$^{-/-}$ mice were elevated while in apoA-I(L159R) phospholipid levels remained unaffected by the HFD. Serum triglyceride levels were reduced in all four genotypes (Table 3.1).

Analysis of the HDL subpopulations showed that similar to chow-fed mice, after HFD feeding WT apoA-I mice formed large α1-α4 HDL particles whereas mice expressing either apoA-I mutant formed smaller α3 and α4 HDL particles (Fig. 3.29A). Fractionation of the serum isolated from human apoA-I transgenic mice fed a HFD by density gradient ultracentrifugation showed that there were no differences in the distribution of apoA-I among the different groups (Fig. 3.29B). This pattern was similar to the distribution of apoA-I that was observed in mice fed a chow diet (Fig. 3.22A). Following HFD feeding

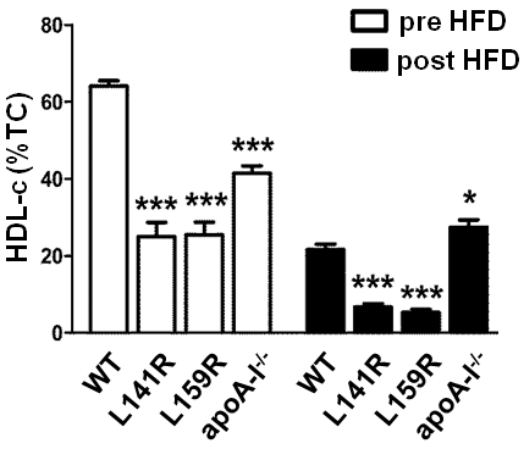

Figure 3.28 Effect of high-fat diet feeding in the cholesterol profile of human apoA-I transgenic mice. HDL-cholesterol content in the serum of human apoA-I transgenic and apoA-I$^{-/-}$ mice (n=15-24 samples/group) before and after high-fat diet feeding. *P=0.023, ***P<0.0001 vs WT apoA-I of the same diet group.

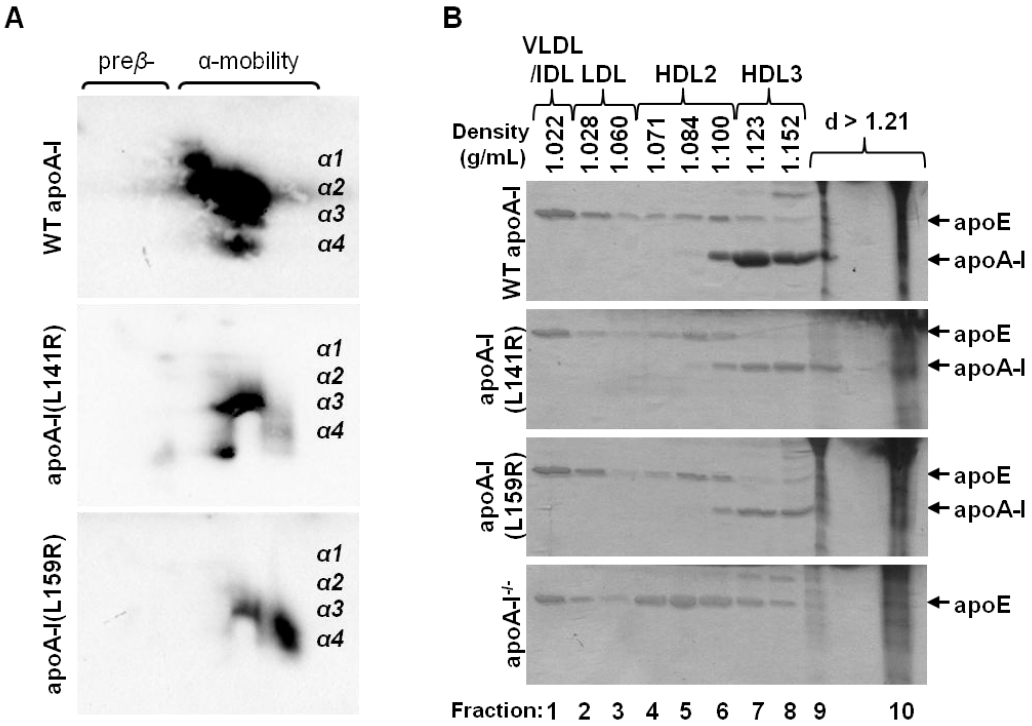

Figure 3.29 Apolipoprotein distribution and characterization of apoA-I-containing HDL subpopulations in the serum of human apoA-I transgenic mice following a 14-week high-fat diet. (**A**) The serum of human apoA-I transgenic mice (n=3 pooled samples/group) was analyzed by two-dimensional gel electrophoresis and western blotting using anti-human apoA-I antibody. Representative images of three independent experiments are shown. (**B**) Density gradient ultracentrifugation and SDS-PAGE analysis of the serum of human apoA-I transgenic and apoA-I$^{-/-}$ mice (n=3 pooled samples/group) following high-fat diet feeding. Representative images of three independent experiments are shown.

apoA-I$^{-/-}$ mice demonstrated a marked increase in apoE levels which was distributed in all HDL but also in the VLDL/IDL/LDL fractions (Fig. 3.29B) and was consistent with the increased HDL-cholesterol levels observed in these mice (Table 3.1). Furthermore, in line with the increased total cholesterol content of all mice fed a HFD (Table 3.1), the apoE levels in the VLDL/IDL fraction were significantly elevated (Fig. 3.29B). Finally, after HFD feeding the HDL-associated PON-1 activity in WT apoA-I mice was significantly reduced to levels that were similar to the PON-1 activity levels of HDL isolated from either mice expressing the apoA-I mutants or apoA-I$^{-/-}$ mice (Fig. 3.30).

At the end of the HFD feeding period, atherosclerotic lesion development was assessed in the aortic roots. In WT apoA-I mice lesions were either absent or very small (10090 ± 1140 μm^2; Fig. 3.31). Transgenic mice expressing either apoA-I mutant developed significantly larger collagen-rich lesions (L141R: 31680 ± 4696, L159R: 27390 ± 5394 μm^2; Fig. 3.31).

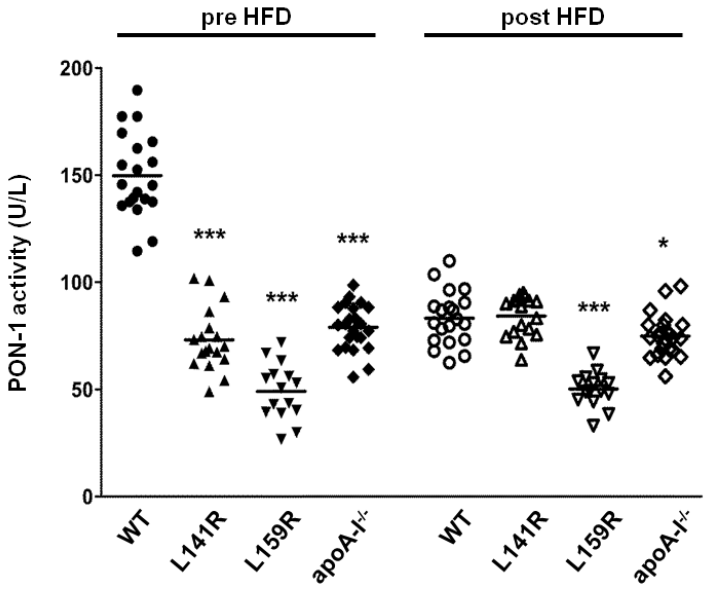

Figure 3.30 Characterization of anti-oxidant properties of HDL in the serum of human apoA-I transgenic mice following a 14-week high-fat diet. HDL-associated PON-1 activity in the serum of human apoA-I transgenic and apoA-I$^{-/-}$ mice (n=15-24 samples/group) before and after high-fat diet feeding. *P=0.0166, ***P<0.0001 vs WT apoA-I of the same diet group.

Importantly, both apoA-I(L141R) and apoA-I(L159R) transgenic mice developed more extensive atherosclerotic lesions compared to apoA-I$^{-/-}$ mice (11180 ± 1798 μm^2; Fig. 3.31) suggesting that the presence of few HDL particles containing either apoA-I mutant promotes atherosclerosis to a greater extent than total absence of HDL.

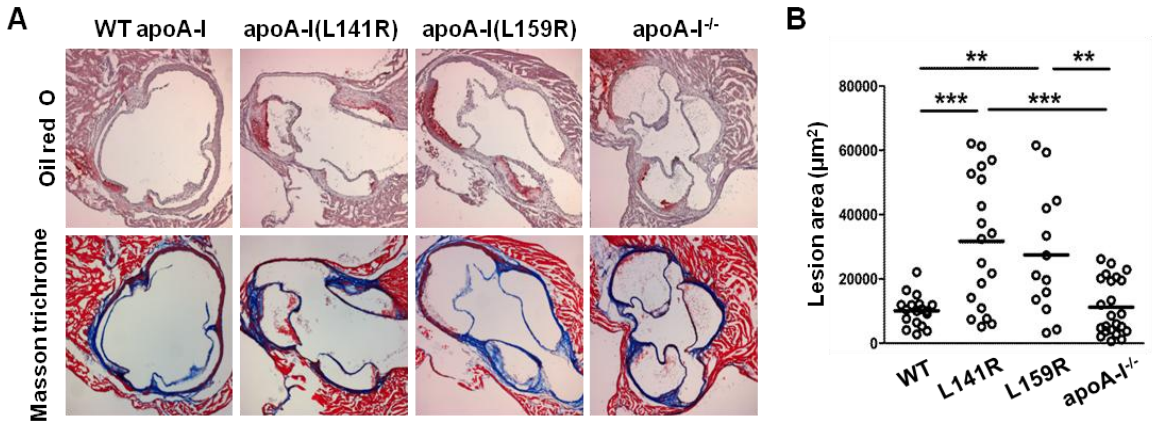

Figure 3.31 Diet-induced atherosclerosis in transgenic mice expressing either WT or mutant forms of human apoA-I. (**A**) Atherosclerotic lesion development in the aortic root of human apoA-I transgenic and apoA-I$^{-/-}$ mice following a 14-week high-fat diet. Representative images for oil red O (lipids) and Masson trichrome (collagen) staining are shown (original magnification x50). (**B**) Quantification of lesion area in oil red O/hematoxylin-stained sections of the aortic root at the level of the tricuspid valves. ***P*<0.01, ****P*<0.001.

Chapter II - Discussion

The importance of apoA-I for HDL biogenesis, functions and protection from atherosclerosis and coronary heart disease is supported by several pieces of evidence (17, 486, 518). To date, several naturally occurring mutations in the human apoA-I gene that predispose to atherosclerosis have been described but the association of these mutations with apoA-I functionality remains obscure for the majority of the cases (181, 184-187). For two of these mutations that are localized in the vicinity of helix 6 of apoA-I, apoA-I(L141R)$_{Pisa}$ and (L159R)$_{FIN}$, studies in humans and animal models have shown that they affect HDL biogenesis and lead to low HDL-cholesterol levels as well as aberrant HDL phenotypes(185, 186, 190-192). Hemizygous male carriers of apoA-I(L141R)$_{Pisa}$ presented with premature CHD (185) while some heterozygous carriers of the apoA-I(L159R)$_{FIN}$ mutation showed increased risk for developing atherosclerosis (186). However, the impact of these mutations on HDL functionality and the mechanisms underlying atherosclerosis predisposition remain unclear. The long-term expression of the two human apoA-I mutants in transgenic mice lacking endogenous apoA-I allowed us to study how these mutations affect previously identified functions of HDL and to examine whether they could induce atherosclerosis in the absence of other genetic defects.

In this study, all three apoA-I transgenes were efficiently expressed in the livers of the transgenic mice. At the protein level, a significantly lower amount of apoA-I was detected in the serum of both apoA-I mutant mice (<10% of WT apoA-I) which is consistent with earlier animal and human studies (185, 190, 192). This could be attributed to either impaired secretion, protein instability or accelerated catabolism of the formed HDL particles. We have previously shown using adenovirus-mediated gene transfer in apoA-I$^{-/-}$ mice that the low HDL levels observed, were due to fast catabolism of the nascent HDL particles formed before they reach maturation (190). Studies in cell cultures examining the secretion of these mutant apoA-I forms have led to controversial results. In a previous study we have shown that the two mutations do not affect the secretion of apoA-I from HTB13 cells (190) whereas other studies have suggested defective secretion and increased

susceptibility to proteolytic degradation of the apoA-I(L159R) mutant (195). However, proteolysis of the apoA-I(L159R) mutant was not detected in human carriers (186) or in the transgenic mice that we created. In addition to low apoA-I levels, apoA-I(L141R) and apoA-I(L159R) mice were characterized by greatly reduced serum HDL-cholesterol levels and a decreased CE/TC ratio compared to WT apoA-I mice. Combined with previous studies (190, 191, 195), these data support the impaired LCAT activation by these two apoA-I mutants *in vivo*.

HDL exerts various biological actions which could potentially interfere with several processes that lead to atherosclerosis development. Thus, HDL stimulates cholesterol efflux, promotes endothelial integrity, suppresses pro-inflammatory cytokine secretion from macrophages and inhibits lipoprotein oxidation (201, 487, 519-521). Our studies showed that HDL particles containing either apoA-I(L141R) or apoA-I(L159R) had reduced anti-oxidative potential and decreased PON-1 and PAF-AH activities. The impaired functionality of these HDL particles could contribute to the increased atherosclerotic plaque formation observed in the atherosclerosis studies presented here and in humans (185, 186). Interestingly however, HDL particles containing either mutant apoA-I form demonstrated enhanced ability to promote cholesterol efflux via ABCA1 compared to HDL containing WT apoA-I, when studied at either equal volume or equal apoA-I concentration. In line with our findings, carriers of LCAT mutations have shown similarly enhanced capacity of ABCA1-mediated cholesterol efflux which was attributed to an increased content of preβ-HDL particles in the serum of these subjects (146). It was recently shown that the concentration of pre-β1 HDL correlates significantly with the ABCA1-mediated cholesterol efflux (514) and that small size rHDL particles (<8 nm in diameter) are more efficient in promoting ABCA1-mediated cholesterol efflux from macrophages than larger rHDL particles (41, 42). These studies further support our results of enhanced ABCA1-dependent efflux by small size HDL particles (~5-6 nm) isolated from apoA-I(L141R) or apoA-I(L159R) mice contrary to larger HDL particles (~9 nm) isolated from WT apoA-I mice. However, although HDL containing either apoA-I mutant exhibits increased ABCA1-dependent cholesterol efflux capacity, the markedly low amounts of circulating HDL particles in the apoA-

I(L141R) and apoA-I(L159R) mice may lead to insufficient cholesterol removal from peripheral tissues and therefore may contribute to atherosclerosis development.

The same concern arises regarding the effect of these two apoA-I mutations on endothelial cell migration. Disruption of the intimal layer is known to introduce a greater risk for vascular disease (522, 523) and although endothelial cell removal aggravates vascular lesion severity (524), enhanced reendothelialization attenuates lesion formation (525). According to our results HDL particles carrying either apoA-I mutant demonstrated enhanced ability to stimulate endothelial cell migration compared to HDL particles carrying WT apoA-I, when studied at equal apoA-I concentration. However, the low concentration of circulating HDL in the apoA-I(L141R) and apoA-I(L159R) mice could signify that the improved function of these particles may not be translated into atheroprotective capacity.

Previous studies have revealed that multiple signaling events occur in endothelial cells in response to HDL leading to maintenance of endothelium integrity and paracrine functions. HDL promotes endothelial cell migration by binding to SR-BI and sequentially activating Src family kinases, PI3K, Akt kinase and MAPK. Activation of these signaling pathways lead to increased lamellipodia formation and enhanced endothelial cell migration (233). On the other hand, HDL promotes the NO production by upregulating eNOS expression and by stimulating eNOS as a result of the same SR-BI-mediated kinase cascade activation (219). According to our results HDL particles containing either apoA-I(L141R) or apoA-I(L159R) demonstrated enhanced ability to promote endothelial cell migration but activated both Akt and eNOS to a similar extent as HDL particles carrying WT apoA-I suggesting that the enhanced cellular response to HDL carrying the apoA-I mutants leading to endothelial cell migration is independent of these pathways. In support of our data, previous studies have shown that HDL-induced migration is independent of NO and therefore eNOS activation. In fact, despite involving the activation of common upstream signaling events, it has been shown that NO production and migration of endothelial cells are independently promoted by HDL (233). Moreover, the increased capacity of HDL from apoA-I(L141R) or apoA-I(L159R) mice to promote endothelial cell migration could be mediated via

activation of either MAPK or alternative SR-BI- and Src family kinase-dependent processes (233).

Our atherosclerosis study clearly established that the transgenic mice expressing apoA-I(L141R) or apoA-I(L159R) develop significantly larger collagen-rich lesions compared to both WT apoA-I transgenic and apoA-I$^{-/-}$ mice. This suggests that total absence of apoA-I does not predispose to atherosclerosis whereas the presence of few small HDL particles containing either apoA-I mutant favors atherosclerosis development. Of note, apoA-I$^{-/-}$ mice contain apoE-enriched HDL particles and the presence of these particles could, at least in part, compensate for the absence of apoA-I in HDL. In support of this hypothesis, we showed that after 14 weeks of HFD, HDL-cholesterol levels in apoA-I$^{-/-}$ mice were greatly increased and this was associated with elevated apoE levels in the HDL fractions. In contrast, the HDL-cholesterol levels in mice expressing the two apoA-I mutants remained low after the HFD feeding whereas the apolipoprotein distribution in the HDL region remained the same. This difference in the HDL-cholesterol and apoE levels in the apoA-I$^{-/-}$ mice could account for the observed atheroprotection in these mice Consistent with our findings, a recent study using a different mouse model showed that overexpression of human apoA-I(L159R) in an apoA-I/LDL receptor double deficient (apoA-I/LDLr DKO) background was associated with the formation of large CE-enriched apoE-HDL particles and increased atherosclerosis compared to apoA-I/LDLr DKO mice which lack any apoA-I(194).

This is the first study in which the effect of two natural human apoA-I mutations, apoA-I(L141R)$_{Pisa}$ and apoA-I(L159R)$_{FIN,}$ on HDL structure, function and atheroprotection are studied in mice in the absence of any other genetic defect. Our findings indicate a strong impact of these apoA-I mutations, found in patients with severe hypoalphalipoproteinemia, on HDL biogenesis, structure and functionality which could account for the predisposition to atherosclerosis that is observed in some of the human carriers of these mutations. Overall, our study increases the understanding of the molecular mechanisms that lead to atherogenesis in patients with aberrant HDL metabolism as well as on the critical association between HDL particle structure and functionality.

CHAPTER III:

The Role of Myeloperoxidase in Generating Dysfunctional HDL Particles *In Vivo*

HDL possesses a potent atheroprotective role that is at least in part attributed to its anti-inflammatory, anti-oxidant, anti-apoptotic and anti-thrombotic properties. Despite previous notion, accumulating evidence reveals that HDL functionality rather than HDL levels constitutes a major determinant for atheroprotection (526, 527). As was discussed in the Introduction, HDL can become pro-atherogenic as a result of oxidative modification of apoA-I by the enzyme myeloperoxidase, a mechanism that renders HDL particles dysfunctional. Specifically, it has been shown that chlorination of Tyr-192 combined with oxidation of Met-148 residues of apoA-I impair its ability to promote ABCA1-mediated cholesterol efflux, while other studies have suggested that oxidation of Met-148 inhibits LCAT activation and subsequent maturation of HDL particles (372, 374, 528). In this chapter we intended to study the mechanisms of MPO-dependent oxidation of specific residues of apoA-I (Tyr-192, Met-148) that lead to the generation of dysfunctional HDL particles. To this end, we generated recombinant adenoviruses that express wild-type (apoA-I WT) or mutant forms of human apoA-I [apoA-I(Met148Ala) and apoA-I(Tyr192Ala)] as well as the human myeloperoxidase with the purpose of using them for adenovirus-mediated gene transfer in apoA-I$^{-/-}$ mice.

Generation of recombinant adenoviruses expressing mutant forms of human apoA-I and human myeloperoxidase

The aforementioned single base substitutions in the human apoA-I gene were generated by site-directed mutagenesis using the overlapping PCR method and the pcDNA3.1-apoA-Ig(ΔBglII) plasmid was used as template in the initial PCR reactions. (Fig. 3.32). The human myeloperoxidase cDNA was cloned from neutrophils isolated from human peripheral blood as described in the “Materials and Methods” section (Fig. 3.33 and 3.34). The cloned

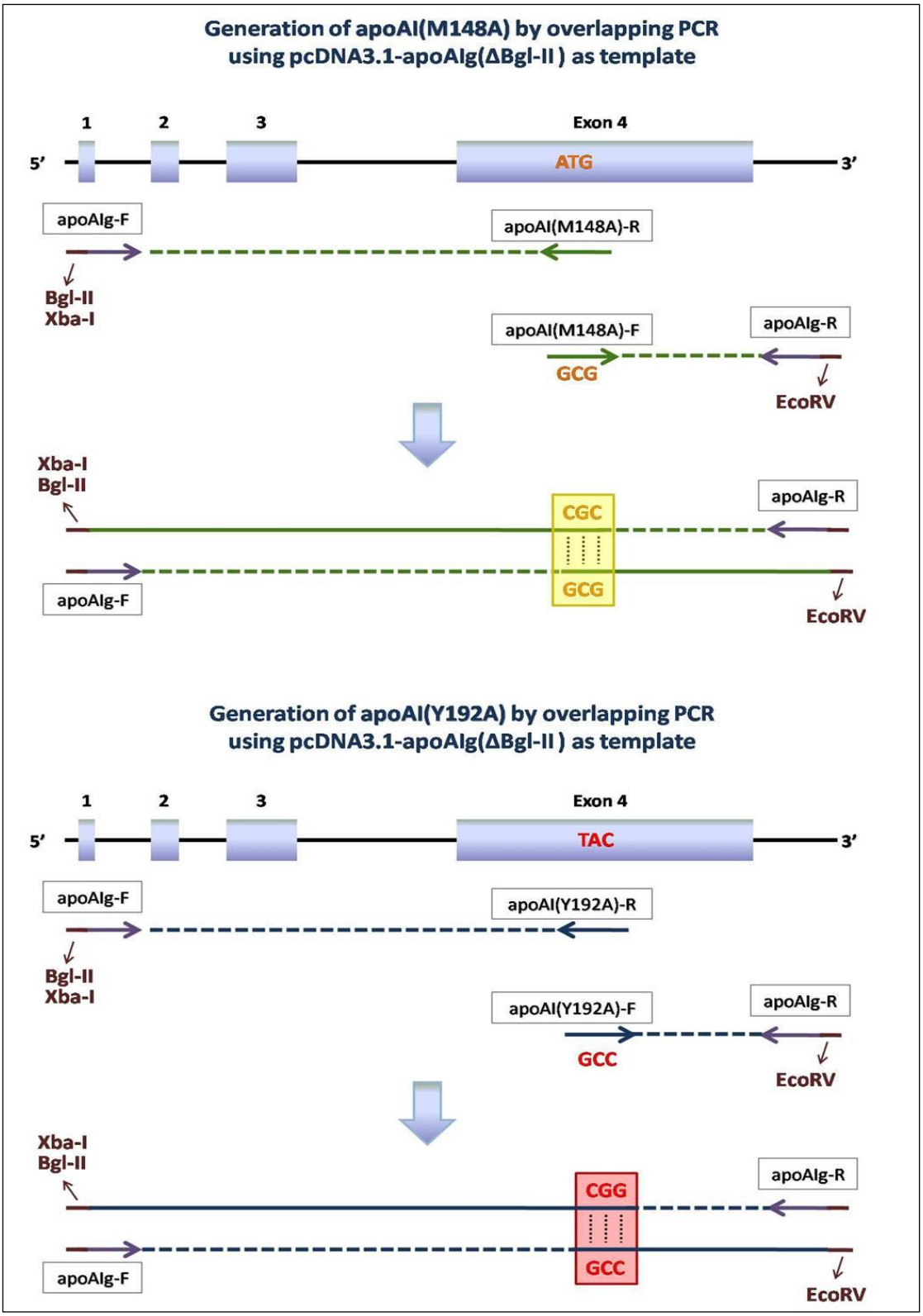

Figure 3.32 Schematic representation of the overlapping PCR methodology for the generation of apoA-I(M148A) and apoA-I(Y192A). The nucleotide substitutions created in each case are shown. The flanking primers were designed in a way that the final mutated PCR products would carry the XbaI (5'-TCTAGA-3') and BglII (5'-AGATCT-3') recognition sites at the 5'- terminus, and the EcoRV (5'-GATATC-3') recognition site at the 3'- terminus.

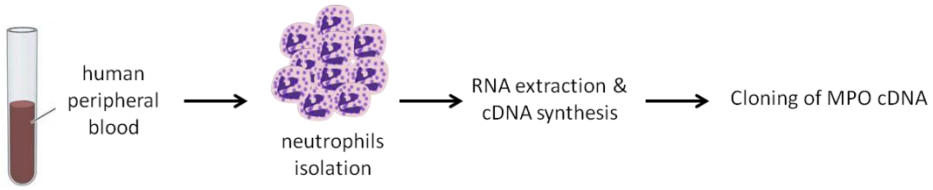

Figure 3.33 Outline of the methodology used to clone the human myeloperoxidase cDNA. Neutrophils were isolated from human peripheral blood and RNA was extracted from these cells. Finally, RT-PCR was used to clone human MPO cDNA.

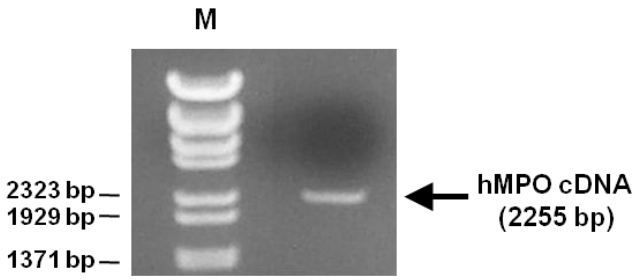

Figure 3.34 Cloning of human myeloperoxidase cDNA. The human MPO cDNA sequence was cloned from neutrophils by RT-PCR, then digested with appropriate restriction enzymes and purified. The purified product is shown following agarose gel electrophoresis. M; λ/BstEII DNA ladder.

sequence was then subcloned into the pGEM-T Easy vector. The mutated apoA-I genomic sequence and the MPO cDNA were subsequently cloned into the shuttle vector pAdTrack-CMV and the expression of the corresponding proteins was confirmed by transient transfection assay in HEK293T cells and western blot analysis (Fig. 3.35). Recombinant viruses were subsequently generated using the Ad-Easy system (Fig. 3.36) (457, 529). Briefly, the pAdTrack-CMV vectors containing the desired genomic or cDNA sequences were linearized with PmeI and used to transform by electroporation BJ-5183-AD1 cells. Within these cells the pAdTrack-CMV vectors are recombined with the pAdEasy-1 shuttle vector to form the adenoviral plasmid which is resident in these bacteria. The recombinant adenoviral DNAs were isolated and digested with PacI to screen for positive clones that produce a 3 or 4.5 kb

insert (data not shown). The PacI-linearized plasmids obtained from positive clones were used for production and large scale amplification of recombinant adenoviruses. Following purification with CsCl gradient, the titers of the adenoviruses were estimated by performing the plaque assay as described in the "Materials and Methods" section. The titers of Ad-apoA-I(M148A), Ad-apoA-I(Y192A) and Ad-MPO were estimated at 1.25 x 10^6 pfu/μL, 3.15 x 10^6 pfu/μL and 1.3 x 10^7 pfu/μL, respectively. To evaluate the expression of the various transgenes, HepG2 cells were infected with the adenoviruses and protein production and secretion was assessed in culture medium and cell extract by immunoblotting. Both apoA-I mutants were detected in the culture medium of infected HepG2 cells, suggesting that the M148A and Y192A mutations in the apoA-I gene do not impair secretion of the protein (Fig. 3.37). Finally, according to our results the infected cells efficiently produced all three recombinant adenoviruses generated for the purposes of this study (Fig. 3.37).

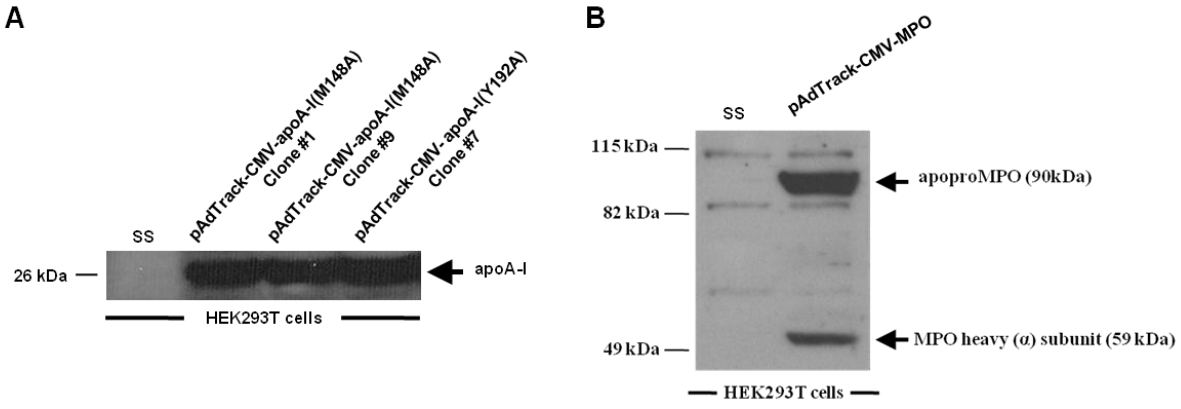

Figure 3.35 Expression analysis of the pAdTrack-CMV constructs. (**A**) Transfection of HEK293T cells with the indicated pAdTrack-CMV-apoA-I constructs carrying the M148A and Y192A mutations and immunoblotting of the protein extracts. (**B**) Western blot analysis of the protein extracts obtained from HEK293T cells transfected with pAdTrack-CMV-MPO. SS; salmon sperm DNA.

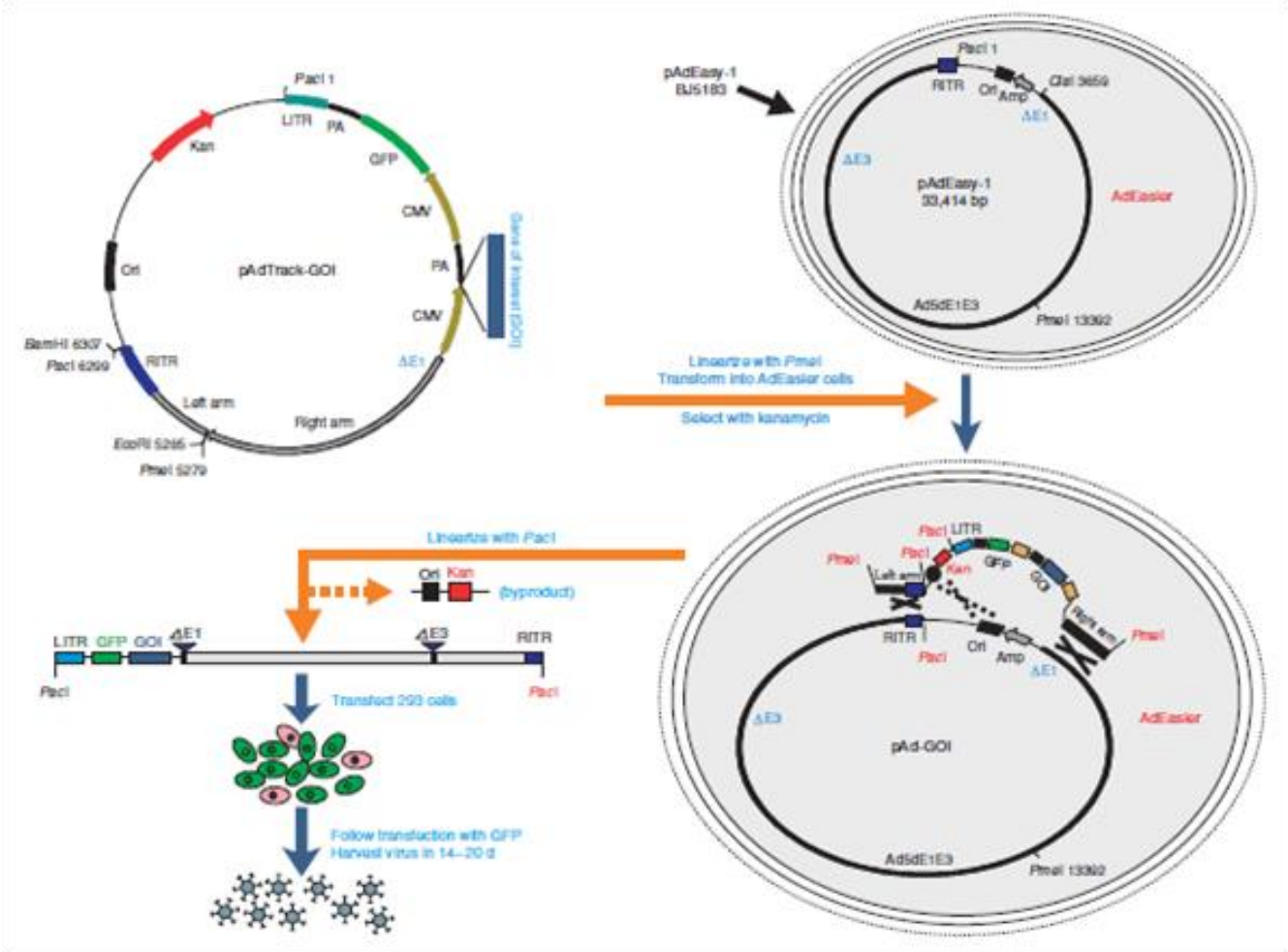

Figure 3.36 Schematic representation of the AdEasy technology (457). The gene of interest (GOI) is first cloned into a shuttle vector (pAdTrack-CMV). The resultant plasmid is linearized by digestion with restriction endonuclease PmeI and subsequently transformed into competent BJ5183 cells that contain the adenoviral backbone plasmid pAdEasy-1. The confirmed recombinant adenovirus plasmids are digested with PacI to liberate both inverted terminal repeats (ITRs) and transfected into 911 cells. The “left arm” and “right arm” represent the regions mediating homologous recombination between the shuttle vector and the adenoviral backbone vector. Alternative homologous recombination between two Ori sites is shown with dotted lines. PA: polyadenylation site, LITR: left-hand ITR and packaging signal, RITR: right-hand ITR.

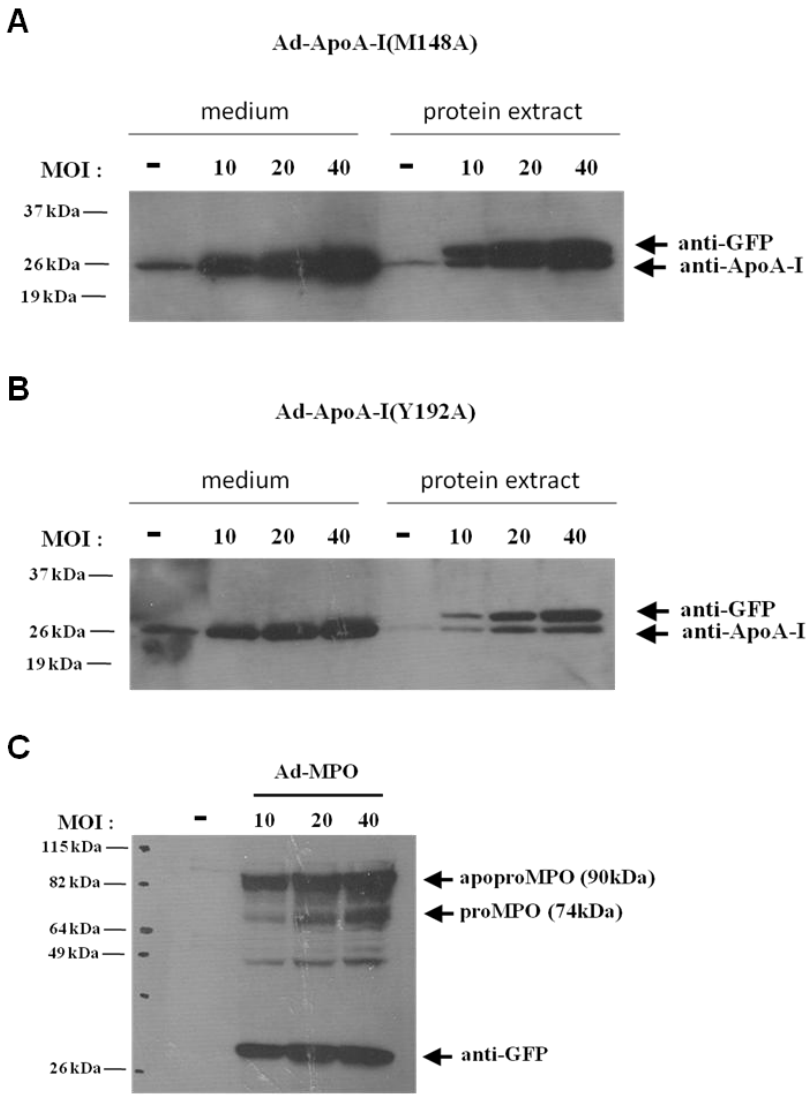

Figure 3.37 Expression analysis of mutant apoA-I and MPO recombinant adenoviruses. Western blot analysis of culture medium and/or total cell extract from HepG2 cells infected with adenoviruses expressing the mutant apoA-I forms (**A** and **B**) and MPO (**C**) at 10, 20 and 40 multiplicity of infection (MOI).

Chapter III – Future Directions

Although a causative role has not been established yet, a strong correlation between low HDL levels and the risk for coronary artery disease has long been ascertained (196, 488). The cardioprotective functions of HDL are exerted through several mechanisms which include cholesterol efflux from peripheral macrophages, inhibition of LDL oxidation, induction of nitric oxide production and maintenance of endothelial integrity among others (201, 489, 520, 521). However, under inflammatory conditions it has been shown that HDL can be rendered dysfunctional and promote inflammation. To date, the mechanisms responsible for reversing HDL's normally anti-inflammatory function to pro-inflammatory remain elusive, but previous studies have suggested that reactive intermediates generated by the enzyme myeloperoxidase (MPO) can convert HDL into dysfunctional forms in humans. In fact, MPO-dependent oxidation of specific residues of apoA-I has been detected in human serum of CVD patients and in human aortic lesions (369, 372). Moreover, it has been shown that MPO-dependent modification of specific tyrosine and methionine residues of apoA-I, including Met148 and Tyr192, inhibits HDL's ability to promote ABCA1-mediated cholesterol efflux from cells (374, 379).

In the present study recombinant adenoviruses expressing apoA-I(M148A), apoA-I(Y192) or MPO have been generated, amplified and purified for use in both *in vitro* and *in vivo* studies. *In vitro*, the purified apoA-I mutant proteins will be studied for their ability to activate LCAT and promote ABCA1-dependent cholesterol efflux. *In vivo*, the adenoviruses expressing wild-type (generated, amplified and purified by Dr. Panagiotis Fotakis) or mutant forms of apoA-I will be used either separately or in combination with the adenovirus expressing MPO to infect apoA-I$^{-/-}$ mice. Following adenovirus-mediated gene transfer the hepatic apoA-I mRNA levels will be assessed and serum lipid and apoA-I levels will be measured. Co-infection experiments with adenoviruses expressing either apoA-I mutant and MPO will enable the investigation of the *in vivo* effect of MPO on lipids concentration, HDL structure (size, shape, apolipoprotein content) and functions (cholesterol efflux, anti-oxidant and anti-inflammatory properties). Mutating the above residues of apoA-I is expected

to prevent MPO-mediated modifications of apoA-I, thus allowing HDL to retain its ability to interact with other key-proteins of the HDL pathway as well as its atheroprotective properties.

In conclusion, this study has provided the tools for further investigation of the aforementioned mechanisms resulting in MPO-mediated impediment of normal apoA-I and HDL function. Since MPO-dependent oxidation of HDL has been shown to convert the cardioprotective HDL into a dysfunctional form, this research will advance our knowledge on the mechanisms underlying the biogenesis of atherogenic HDL, and may lead to potential therapeutic approaches for preventing vascular disease in humans.

CHAPTER IV:

The Role of GALNT2 in HDL Biogenesis and Functions *In Vivo*

Several genome-wide association studies (GWAS) have identified a number of new genomic loci, including the GALNT2 gene, which are associated with low levels of HDL cholesterol (384-387). GALNT2 is a member of a family of GalNAc-transferases which participates in O-glycosylation of proteins by catalyzing the transfer an N-acetyl galactosamine to the hydroxyl group of a serine/threonine residue. Since O-glycosylation possesses a regulatory role in protein function it is possible that GALNT2 affects lipid concentration by modifying several of the proteins that participate in the HDL pathway. The aim of this study was to unravel the role of GALNT2 in HDL metabolism *in vivo*. For this purpose we generated recombinant adenovirus that express human GALNT2 with the purpose of using them for adenovirus-mediated gene transfer in apoA-I$^{-/-}$ mice.

Generation of recombinant adenoviruses expressing human GALNT2

The human GALNT2 cDNA was cloned from HepG2 cells as described in the "Materials and Methods" section (Fig. 3.38 and 3.39). The GALNT2 cDNA sequence was then subcloned into the shuttle vector pAdTrack-CMV and the expression of the protein was confirmed by transient transfection assay in

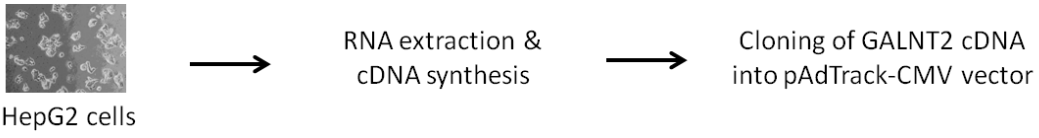

Figure 3.38 Outline of the methodology used to clone the human GALNT2 cDNA. RNA was extracted from HepG2 cells and RT-PCR was performed to clone the human GALNT2 cDNA into the pAdTrack-CMV-GALNT2 vector.

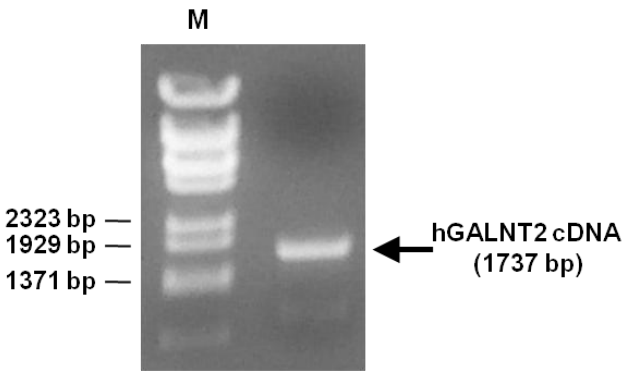

Figure 3.39 Cloning of human GALNT2 cDNA. The human GALNT2 cDNA sequence was cloned from HepG2 cells by RT-PCR, then digested with appropriate restriction enzymes and purified. The purified product is shown following agarose gel electrophoresis. M; λ/BstEII DNA ladder.

HEK293T cells and western blot analysis (Fig. 3.40). The pAdTrack-CMV-GALNT2 construct was subsequently used to produce the recombinant adenovirus Ad-GALNT2 according to the Ad-Easy protocol (Fig. 3.36) (457, 529). Briefly, the PmeI-linearized pAdTrack-CMV-GALNT2 construct was used to transform BJ-5183-AD1 cells. Following recombination of the pAdTrack-CMV vector with the pAdEasy-1 shuttle vector within the cells, the resulting adenoviral plasmid was digested with PacI to detect positive clones that produce a 3 or 4.5 kb insert (data not shown). Selected positive clones were linearized with PacI and used for production and large scale amplification of recombinant adenoviruses. Following purification with CsCl gradient, the titers of the adenovirus was assessed by the plaque assay as described in the “Materials and Methods” section. The titer of Ad-GALNT2 was measured at 1 x 10^7 pfu/µL. Finally, to determine the expression of the transgene, HepG2 cells were infected with the adenovirus and protein production was assessed in total cell extracts by western blot analysis. The results showed that the infected cells efficiently produced the GALNT2 protein (Fig. 3.41).

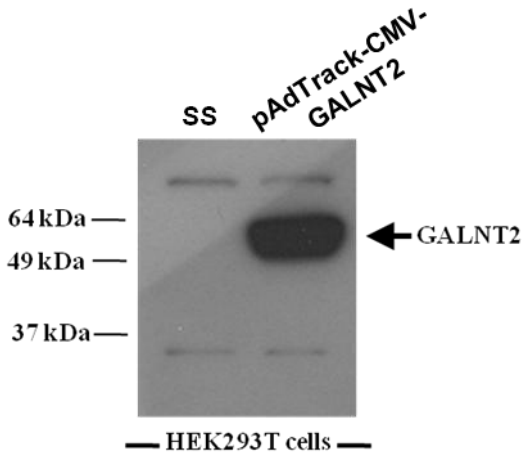

Figure 3.40 Expression analysis of the pAdTrack-CMV-GALNT2 construct. Transfection of HEK293T cells with pAdTrack-CMV-GALNT2 and western blot analysis of the protein extracts. SS; salmon sperm DNA.

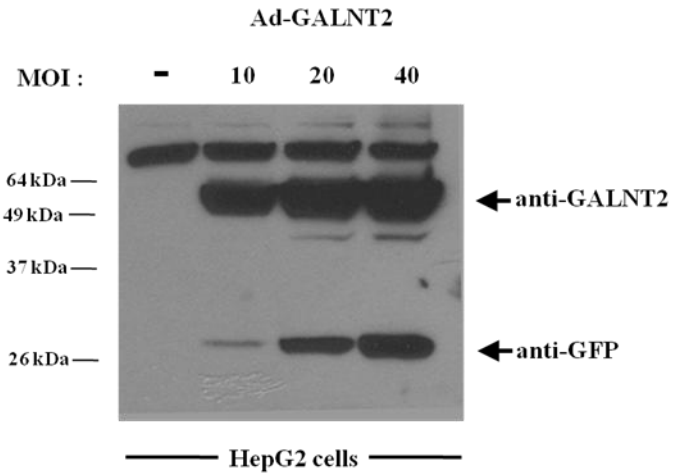

Figure 3.41 Expression analysis of GALNT2 recombinant adenovirus. Western blot analysis of total cell extract from HepG2 cells infected with adenovirus carrying the GALNT2 cDNA at 10, 20 and 40 multiplicity of infection (MOI).

Chapter IV – Future Directions

Multiple GWAS studies have identified N-acetylgalactosaminyltransferase 2 (GALNT2) as a candidate gene for low HDL and high triglyceride levels in the blood (383-387). *In vivo* studies of liver-specific overexpression or knockdown of endogenous GALNT2 have confirmed this enzyme as a biological regulator of HDL levels. GALNT2 is an enzyme that is involved in the initiation of O-linked glycosylation and the transfer of N-acetylgalactosamine to serine or threonine residues on proteins (391). Since this process has a regulatory role that determines activation or inactivation of many proteins, efforts have been focused on identifying proteins involved in lipid metabolism as possible targets of GALNT2. So far studies have revealed that activation of ANGPTL3, an important inhibitor of lipoprotein lipase and endothelial lipase, is modulated by GALNT2-mediated *O*-glycosylation (401). Glycosylation of apoC-III, an established inhibitor of endothelial lipase, by GALNT2 has also been reported (398). Although some progress has been made, the knowledge on the pathways of lipid metabolism that are affected by GALNT2 still remains limited.

In the present study a recombinant adenovirus carrying the human GALNT2 cDNA sequence has been generated, amplified and purified for use in *in vivo* studies. Adenovirus-mediated gene transfer will be performed in a transgenic mouse line that was generated previously by our team which expresses the human apoA-I gene under the control of its proximal promoter and enhancer in an apoA-I deficient background and thus synthesizes human HDL (48, 530). Following infection, a series of analyses will be performed in order to determine serum lipids concentration, enzyme activities (LPL, LCAT) as well as HDL levels and structure (particle size, shape and apolipoprotein content). Moreover, HDL functions including cholesterol efflux, maintenance of endothelial cell integrity, anti-oxidant and anti-inflammatory properties will be assessed. Liver-specific overexpression of GALNT2 in human apoA-I transgenic mice is expected to modify the lipid and lipoprotein profile in these animal models but the extent and the direction of this effect are to be shown. Moreover, phenotypic abnormalities concerning either HDL structure and

metabolism or the induction of some form of dyslipidemia remain to be investigated.

In conclusion, this study has provided the tools for assessment of the *in vivo* effects of enzymatic glycosylation of any of a number of proteins involved in HDL cholesterol and triglyceride metabolism. The above experiments will allow in-depth investigation of the role of this newly identified gene in HDL biogenesis, structure and functionality as well as its overall effect on lipid metabolism and vascular disease. Finally, this research will assist in developing a broader biological understanding of lipoprotein metabolism and identifying potential new therapeutic opportunities.

4 REFERENCES

1. Saher, G., and S. K. Stumpf. 2015. Cholesterol in myelin biogenesis and hypomyelinating disorders. *Biochim Biophys Acta*.
2. Chiang, J. Y. 2009. Bile acids: regulation of synthesis. *J Lipid Res* 50:1955-1966.
3. Payne, A. H., and D. B. Hales. 2004. Overview of steroidogenic enzymes in the pathway from cholesterol to active steroid hormones. *Endocr Rev* 25:947-970.
4. Rendell, M. 2004. Advances in diabetes for the millennium: diabetes and cholesterol. *MedGenMed* 6:5.
5. Saini, H. K., A. S. Arneja, and N. S. Dhalla. 2004. Role of cholesterol in cardiovascular dysfunction. *Can J Cardiol* 20:333-346.
6. Shobab, L. A., G. Y. Hsiung, and H. H. Feldman. 2005. Cholesterol in Alzheimer's disease. *Lancet Neurol* 4:841-852.
7. Brown, A. J. 2007. Cholesterol, statins and cancer. *Clin Exp Pharmacol Physiol* 34:135-141.
8. Gotto, A. M., Jr., H. J. Pownall, and R. J. Havel. 1986. Introduction to the plasma lipoproteins. *Methods Enzymol* 128:3-41.
9. **Zannis, V. I., Kypreos, K. E., Chroni, A., Kardassis, D., and Zanni, E. E.** 2004. **Lipoproteins and atherogenesis** In ***Molecular Mechanisms of Atherosclerosis***. J. Loscalzo, ed. Taylor & Francis, Abingdon, UK. 154-244.
10. Hussain, M. M., R. K. Kancha, Z. Zhou, J. Luchoomun, H. Zu, and A. Bakillah. 1996. Chylomicron assembly and catabolism: role of apolipoproteins and receptors. *Biochim Biophys Acta* 1300:151-170.
11. Shelness, G. S., and J. A. Sellers. 2001. Very-low-density lipoprotein assembly and secretion. *Curr Opin Lipidol* 12:151-157.
12. Willnow, T. E. 1997. Mechanisms of hepatic chylomicron remnant clearance. *Diabet Med* 14 Suppl 3:S75-80.
13. Zannis, V. I., A. Chroni, and M. Krieger. 2006. Role of apoA-I, ABCA1, LCAT, and SR-BI in the biogenesis of HDL. *Journal of molecular medicine* 84:276-294.
14. Barter, P. a. R., K. A. 2007. HDL and atherosclerosis. In *High-Density Lipoproteins: From basic biology to clinical aspects*. C. J. Fielding, ed. Wiley-Vch Verlag GmbH & Co, Weinheim. 491-505.
15. Hegele, R. A. 2009. Plasma lipoproteins: genetic influences and clinical implications. *Nat Rev Genet* 10:109-121.
16. Zannis, V. I., F. S. Cole, C. L. Jackson, D. M. Kurnit, and S. K. Karathanasis. 1985. Distribution of apolipoprotein A-I, C-II, C-III, and E mRNA in fetal human tissues. Time-dependent induction of apolipoprotein E mRNA by cultures of human monocyte-macrophages. *Biochemistry* 24:4450-4455.
17. Zannis, V. I., P. Fotakis, G. Koukos, D. Kardassis, C. Ehnholm, M. Jauhiainen, and A. Chroni. 2015. HDL Biogenesis, Remodeling, and Catabolism. *Handb Exp Pharmacol* 224:53-111.
18. Daniil, G., A. A. Phedonos, A. G. Holleboom, M. M. Motazacker, L. Argyri, J. A. Kuivenhoven, and A. Chroni. 2011. Characterization of antioxidant/anti-inflammatory properties and apoA-I-containing subpopulations of HDL from family subjects with monogenic low HDL disorders. *Clin Chim Acta* 412:1213-1220.
19. Duka, A., P. Fotakis, D. Georgiadou, A. Kateifides, K. Tzavlaki, L. von Eckardstein, E. Stratikos, D. Kardassis, and V. I. Zannis. 2013. ApoA-IV promotes the biogenesis of apoA-IV-containing HDL particles with the participation of ABCA1 and LCAT. *J Lipid Res* 54:107-115.

20. Kypreos, K. E., and V. I. Zannis. 2007. Pathway of biogenesis of apolipoprotein E-containing HDL in vivo with the participation of ABCA1 and LCAT. *Biochem J* 403:359-367.
21. Wang, N., D. Lan, W. Chen, F. Matsuura, and A. R. Tall. 2004. ATP-binding cassette transporters G1 and G4 mediate cellular cholesterol efflux to high-density lipoproteins. *Proc Natl Acad Sci U S A* 101:9774-9779.
22. Lusa, S., M. Jauhiainen, J. Metso, P. Somerharju, and C. Ehnholm. 1996. The mechanism of human plasma phospholipid transfer protein-induced enlargement of high-density lipoprotein particles: evidence for particle fusion. *Biochem J* 313 (Pt 1):275-282.
23. Krieger, M. 2001. Scavenger receptor class B type I is a multiligand HDL receptor that influences diverse physiologic systems. *The Journal of clinical investigation* 108:793-797.
24. Barter, P. J., H. B. Brewer, Jr., M. J. Chapman, C. H. Hennekens, D. J. Rader, and A. R. Tall. 2003. Cholesteryl ester transfer protein: a novel target for raising HDL and inhibiting atherosclerosis. *Arterioscler Thromb Vasc Biol* 23:160-167.
25. Breckenridge, W. C., J. A. Little, P. Alaupovic, C. S. Wang, A. Kuksis, G. Kakis, F. Lindgren, and G. Gardiner. 1982. Lipoprotein abnormalities associated with a familial deficiency of hepatic lipase. *Atherosclerosis* 45:161-179.
26. Kersten, S. 2014. Physiological regulation of lipoprotein lipase. *Biochim Biophys Acta* 1841:919-933.
27. Ishida, T., S. Choi, R. K. Kundu, K. Hirata, E. M. Rubin, A. D. Cooper, and T. Quertermous. 2003. Endothelial lipase is a major determinant of HDL level. *The Journal of clinical investigation* 111:347-355.
28. Rye, K. A., M. A. Clay, and P. J. Barter. 1999. Remodelling of high density lipoproteins by plasma factors. *Atherosclerosis* 145:227-238.
29. Rye, K. A., C. A. Bursill, G. Lambert, F. Tabet, and P. J. Barter. 2009. The metabolism and anti-atherogenic properties of HDL. *J Lipid Res* 50 Suppl:S195-200.
30. Blanche, P. J., E. L. Gong, T. M. Forte, and A. V. Nichols. 1981. Characterization of human high-density lipoproteins by gradient gel electrophoresis. *Biochim Biophys Acta* 665:408-419.
31. Cheung, M. C., and J. J. Albers. 1984. Characterization of lipoprotein particles isolated by immunoaffinity chromatography. Particles containing A-I and A-II and particles containing A-I but no A-II. *J Biol Chem* 259:12201-12209.
32. Cheung, M. C., and J. J. Albers. 1982. Distribution of high density lipoprotein particles with different apoprotein composition: particles with A-I and A-II and particles with A-I but no A-II. *J Lipid Res* 23:747-753.
33. Warden, C. H., C. C. Hedrick, J. H. Qiao, L. W. Castellani, and A. J. Lusis. 1993. Atherosclerosis in transgenic mice overexpressing apolipoprotein A-II. *Science* 261:469-472.
34. Amouyel, P., D. Isorez, J. M. Bard, M. Goldman, P. Lebel, G. Zylberberg, and J. C. Fruchart. 1993. Parental history of early myocardial infarction is associated with decreased levels of lipoparticle AI in adolescents. *Arterioscler Thromb* 13:1640-1644.
35. Tailleux, A., M. Bouly, G. Luc, G. Castro, J. M. Caillaud, N. Hennuyer, P. Poulain, J. C. Fruchart, N. Duverger, and C. Fievet. 2000. Decreased susceptibility to diet-induced atherosclerosis in human apolipoprotein A-II transgenic mice. *Arterioscler Thromb Vasc Biol* 20:2453-2458.
36. Castro, G. R., and C. J. Fielding. 1988. Early incorporation of cell-derived cholesterol into pre-beta-migrating high-density lipoprotein. *Biochemistry* 27:25-29.
37. Huang, Y., A. von Eckardstein, S. Wu, N. Maeda, and G. Assmann. 1994. A plasma lipoprotein containing only apolipoprotein E and with gamma mobility on

electrophoresis releases cholesterol from cells. *Proc Natl Acad Sci U S A* 91:1834-1838.

38. Asztalos, B. F., C. H. Sloop, L. Wong, and P. S. Roheim. 1993. Two-dimensional electrophoresis of plasma lipoproteins: recognition of new apo A-I-containing subpopulations. *Biochim Biophys Acta* 1169:291-300.
39. Fielding, C. J. 2007. *High-Density Lipoproteins: From Basic Biology to Clinical Aspects*. Wiley-VCH Verlag GmbH & Co. KGaA Weinheim.
40. Oram, J. F., and A. M. Vaughan. 2006. ATP-Binding cassette cholesterol transporters and cardiovascular disease. *Circulation research* 99:1031-1043.
41. Du, X., M. J. Kim, L. Hou, W. Le Goff, M. J. Chapman, M. van Eck, L. K. Curtiss, J. Burnett, S. P. Cartland, C. M. Quinn, M. Kockx, A. Kontush, K. A. Rye, L. Kritharides, and W. Jessup. 2015. HDL Particle Size is a Critical Determinant of ABCA1-Mediated Macrophage Cellular Cholesterol Export. *Circulation research*.
42. Favari, E., L. Calabresi, M. P. Adorni, W. Jessup, S. Simonelli, G. Franceschini, and F. Bernini. 2009. Small discoidal pre-beta1 HDL particles are efficient acceptors of cell cholesterol via ABCA1 and ABCG1. *Biochemistry* 48:11067-11074.
43. Asztalos, B. F., D. Collins, K. V. Horvath, H. E. Bloomfield, S. J. Robins, and E. J. Schaefer. 2008. Relation of gemfibrozil treatment and high-density lipoprotein subpopulation profile with cardiovascular events in the Veterans Affairs High-Density Lipoprotein Intervention Trial. *Metabolism* 57:77-83.
44. Asztalos, B. F., P. S. Roheim, R. L. Milani, M. Lefevre, J. R. McNamara, K. V. Horvath, and E. J. Schaefer. 2000. Distribution of ApoA-I-containing HDL subpopulations in patients with coronary heart disease. *Arterioscler Thromb Vasc Biol* 20:2670-2676.
45. Asztalos, B. F., and E. J. Schaefer. 2003. High-density lipoprotein subpopulations in pathologic conditions. *Am J Cardiol* 91:12E-17E.
46. Fielding, C. J., V. G. Shore, and P. E. Fielding. 1972. A protein cofactor of lecithin:cholesterol acyltransferase. *Biochem Biophys Res Commun* 46:1493-1498.
47. Schaefer, E. J., W. H. Heaton, M. G. Wetzel, and H. B. Brewer, Jr. 1982. Plasma apolipoprotein A-1 absence associated with a marked reduction of high density lipoproteins and premature coronary artery disease. *Arteriosclerosis* 2:16-26.
48. Kan, H. Y., S. Georgopoulos, and V. Zannis. 2000. A hormone response element in the human apolipoprotein CIII (ApoCIII) enhancer is essential for intestinal expression of the ApoA-I and ApoCIII genes and contributes to the hepatic expression of the two linked genes in transgenic mice. *J Biol Chem* 275:30423-30431.
49. Rubin, E. M., R. M. Krauss, E. A. Spangler, J. G. Verstuyft, and S. M. Clift. 1991. Inhibition of early atherogenesis in transgenic mice by human apolipoprotein AI. *Nature* 353:265-267.
50. Paszty, C., N. Maeda, J. Verstuyft, and E. M. Rubin. 1994. Apolipoprotein AI transgene corrects apolipoprotein E deficiency-induced atherosclerosis in mice. *The Journal of clinical investigation* 94:899-903.
51. Belalcazar, L. M., A. Merched, B. Carr, K. Oka, K. H. Chen, L. Pastore, A. Beaudet, and L. Chan. 2003. Long-term stable expression of human apolipoprotein A-I mediated by helper-dependent adenovirus gene transfer inhibits atherosclerosis progression and remodels atherosclerotic plaques in a mouse model of familial hypercholesterolemia. *Circulation* 107:2726-2732.
52. Valenta, D. T., J. J. Bulgrien, C. L. Banka, and L. K. Curtiss. 2006. Overexpression of human ApoAI transgene provides long-term atheroprotection in LDL receptor-deficient mice. *Atherosclerosis* 189:255-263.
53. Breslow, J. L., D. Ross, J. McPherson, H. Williams, D. Kurnit, A. L. Nussbaum, S. K. Karathanasis, and V. I. Zannis. 1982. Isolation and characterization of cDNA clones for human apolipoprotein A-I. *Proc Natl Acad Sci U S A* 79:6861-6865.

54. Karathanasis, S. K., V. I. Zannis, and J. L. Breslow. 1983. Isolation and characterization of the human apolipoprotein A-I gene. *Proc Natl Acad Sci U S A* 80:6147-6151.
55. Bruns, G. A., S. K. Karathanasis, and J. L. Breslow. 1984. Human apolipoprotein A-I--C-III gene complex is located on chromosome 11. *Arteriosclerosis* 4:97-102.
56. Cheung, P., F. T. Kao, M. L. Law, C. Jones, T. T. Puck, and L. Chan. 1984. Localization of the structural gene for human apolipoprotein A-I on the long arm of human chromosome 11. *Proc Natl Acad Sci U S A* 81:508-511.
57. Karathanasis, S. K. 1985. Apolipoprotein multigene family: tandem organization of human apolipoprotein AI, CIII, and AIV genes. *Proc Natl Acad Sci U S A* 82:6374-6378.
58. Karathanasis, S. K., J. McPherson, V. I. Zannis, and J. L. Breslow. 1983. Linkage of human apolipoproteins A-I and C-III genes. *Nature* 304:371-373.
59. Zannis, V. I., H. Y. Kan, A. Kritis, E. Zanni, and D. Kardassis. 2001. Transcriptional regulation of the human apolipoprotein genes. *Front Biosci* 6:D456-504.
60. Zannis, V. I., H. Y. Kan, A. Kritis, E. E. Zanni, and D. Kardassis. 2001. Transcriptional regulatory mechanisms of the human apolipoprotein genes in vitro and in vivo. *Curr Opin Lipidol* 12:181-207.
61. Haas, M. J., and A. D. Mooradian. 2010. Therapeutic interventions to enhance apolipoprotein A-I-mediated cardioprotection. *Drugs* 70:805-821.
62. Papazafiri, P., K. Ogami, D. P. Ramji, A. Nicosia, P. Monaci, C. Cladaras, and V. I. Zannis. 1991. Promoter elements and factors involved in hepatic transcription of the human ApoA-I gene positive and negative regulators bind to overlapping sites. *J Biol Chem* 266:5790-5797.
63. Widom, R. L., J. A. Ladias, S. Kouidou, and S. K. Karathanasis. 1991. Synergistic interactions between transcription factors control expression of the apolipoprotein AI gene in liver cells. *Mol Cell Biol* 11:677-687.
64. Tzameli, I., and V. I. Zannis. 1996. Binding specificity and modulation of the ApoA-I promoter activity by homo- and heterodimers of nuclear receptors. *J Biol Chem* 271:8402-8415.
65. Delerive, P., C. M. Galardi, J. E. Bisi, E. Nicodeme, and B. Goodwin. 2004. Identification of liver receptor homolog-1 as a novel regulator of apolipoprotein AI gene transcription. *Mol Endocrinol* 18:2378-2387.
66. Ladias, J. A., and S. K. Karathanasis. 1991. Regulation of the apolipoprotein AI gene by ARP-1, a novel member of the steroid receptor superfamily. *Science* 251:561-565.
67. Ge, R., M. Rhee, S. Malik, and S. K. Karathanasis. 1994. Transcriptional repression of apolipoprotein AI gene expression by orphan receptor ARP-1. *J Biol Chem* 269:13185-13192.
68. Rottman, J. N., R. L. Widom, B. Nadal-Ginard, V. Mahdavi, and S. K. Karathanasis. 1991. A retinoic acid-responsive element in the apolipoprotein AI gene distinguishes between two different retinoic acid response pathways. *Mol Cell Biol* 11:3814-3820.
69. Vu-Dac, N., K. Schoonjans, B. Laine, J. C. Fruchart, J. Auwerx, and B. Staels. 1994. Negative regulation of the human apolipoprotein A-I promoter by fibrates can be attenuated by the interaction of the peroxisome proliferator-activated receptor with its response element. *J Biol Chem* 269:31012-31018.
70. Li, J., G. Ning, and S. A. Duncan. 2000. Mammalian hepatocyte differentiation requires the transcription factor HNF-4alpha. *Genes Dev* 14:464-474.
71. Staels, B., J. Dallongeville, J. Auwerx, K. Schoonjans, E. Leitersdorf, and J. C. Fruchart. 1998. Mechanism of action of fibrates on lipid and lipoprotein metabolism. *Circulation* 98:2088-2093.
72. Huuskonen, J., M. Vishnu, P. Chau, P. E. Fielding, and C. J. Fielding. 2006. Liver X receptor inhibits the synthesis and secretion of apolipoprotein A1 by human liver-derived cells. *Biochemistry* 45:15068-15074.

73. Walsh, A., Y. Ito, and J. L. Breslow. 1989. High levels of human apolipoprotein A-I in transgenic mice result in increased plasma levels of small high density lipoprotein (HDL) particles comparable to human HDL3. *J Biol Chem* 264:6488-6494.
74. Hu, Y., X. Ren, H. Wang, Y. Ma, L. Wang, Y. Shen, K. Oka, Z. Zhang, and Y. Zhang. 2010. Liver-specific expression of an exogenous gene controlled by human apolipoprotein A-I promoter. *Int J Pharm* 398:161-164.
75. Kardassis, D., I. Tzameli, M. Hadzopoulou-Cladaras, I. Talianidis, and V. Zannis. 1997. Distal apolipoprotein C-III regulatory elements F to J act as a general modular enhancer for proximal promoters that contain hormone response elements. Synergism between hepatic nuclear factor-4 molecules bound to the proximal promoter and distal enhancer sites. *Arterioscler Thromb Vasc Biol* 17:222-232.
76. Talianidis, I., A. Tambakaki, J. Toursounova, and V. I. Zannis. 1995. Complex interactions between SP1 bound to multiple distal regulatory sites and HNF-4 bound to the proximal promoter lead to transcriptional activation of liver-specific human APOCIII gene. *Biochemistry* 34:10298-10309.
77. Lavrentiadou, S. N., M. Hadzopoulou-Cladaras, D. Kardassis, and V. I. Zannis. 1999. Binding specificity and modulation of the human ApoCIII promoter activity by heterodimers of ligand-dependent nuclear receptors. *Biochemistry* 38:964-975.
78. Kardassis, D., A. Gafencu, V. I. Zannis, and A. Davalos. 2015. Regulation of HDL genes: transcriptional, posttranscriptional, and posttranslational. *Handb Exp Pharmacol* 224:113-179.
79. Kardassis, D., E. Falvey, P. Tsantili, M. Hadzopoulou-Cladaras, and V. Zannis. 2002. Direct physical interactions between HNF-4 and Sp1 mediate synergistic transactivation of the apolipoprotein CIII promoter. *Biochemistry* 41:1217-1228.
80. Zannis, V. I., D. M. Kurnit, and J. L. Breslow. 1982. Hepatic apo-A-I and apo-E and intestinal apo-A-I are synthesized in precursor isoprotein forms by organ cultures of human fetal tissues. *J Biol Chem* 257:536-544.
81. Zannis, V. I., S. K. Karathanasis, H. T. Keutmann, G. Goldberger, and J. L. Breslow. 1983. Intracellular and extracellular processing of human apolipoprotein A-I: secreted apolipoprotein A-I isoprotein 2 is a propeptide. *Proc Natl Acad Sci U S A* 80:2574-2578.
82. Law, S. W., and H. B. Brewer, Jr. 1984. Nucleotide sequence and the encoded amino acids of human apolipoprotein A-I mRNA. *Proc Natl Acad Sci U S A* 81:66-70.
83. Chau, P., P. E. Fielding, and C. J. Fielding. 2007. Bone morphogenetic protein-1 (BMP-1) cleaves human proapolipoprotein A1 and regulates its activation for lipid binding. *Biochemistry* 46:8445-8450.
84. Nolte, R. T., and D. Atkinson. 1992. Conformational analysis of apolipoprotein A-I and E-3 based on primary sequence and circular dichroism. *Biophys J* 63:1221-1239.
85. Brouillette, C. G., and G. M. Anantharamaiah. 1995. Structural models of human apolipoprotein A-I. *Biochim Biophys Acta* 1256:103-129.
86. Borhani, D. W., J. A. Engler, and C. G. Brouillette. 1999. Crystallization of truncated human apolipoprotein A-I in a novel conformation. *Acta Crystallogr D Biol Crystallogr* 55:1578-1583.
87. Borhani, D. W., D. P. Rogers, J. A. Engler, and C. G. Brouillette. 1997. Crystal structure of truncated human apolipoprotein A-I suggests a lipid-bound conformation. *Proc Natl Acad Sci U S A* 94:12291-12296.
88. Palgunachari, M. N., V. K. Mishra, S. Lund-Katz, M. C. Phillips, S. O. Adeyeye, S. Alluri, G. M. Anantharamaiah, and J. P. Segrest. 1996. Only the two end helixes of eight tandem amphipathic helical domains of human apo A-I have significant lipid affinity. Implications for HDL assembly. *Arterioscler Thromb Vasc Biol* 16:328-338.

89. Tanaka, M., P. Dhanasekaran, D. Nguyen, S. Ohta, S. Lund-Katz, M. C. Phillips, and H. Saito. 2006. Contributions of the N- and C-terminal helical segments to the lipid-free structure and lipid interaction of apolipoprotein A-I. *Biochemistry* 45:10351-10358.
90. Tanaka, M., T. Tanaka, S. Ohta, T. Kawakami, H. Konno, K. Akaji, S. Aimoto, and H. Saito. 2009. Evaluation of lipid-binding properties of the N-terminal helical segments in human apolipoprotein A-I using fragment peptides. *J Pept Sci* 15:36-42.
91. Davidson, W. S., K. Arnvig-McGuire, A. Kennedy, J. Kosman, T. L. Hazlett, and A. Jonas. 1999. Structural organization of the N-terminal domain of apolipoprotein A-I: studies of tryptophan mutants. *Biochemistry* 38:14387-14395.
92. Brouillette, C. G., W. J. Dong, Z. W. Yang, M. J. Ray, Protasevich, II, H. C. Cheung, and J. A. Engler. 2005. Forster resonance energy transfer measurements are consistent with a helical bundle model for lipid-free apolipoprotein A-I. *Biochemistry* 44:16413-16425.
93. Silva, R. A., G. M. Hilliard, J. Fang, S. Macha, and W. S. Davidson. 2005. A three-dimensional molecular model of lipid-free apolipoprotein A-I determined by cross-linking/mass spectrometry and sequence threading. *Biochemistry* 44:2759-2769.
94. Beckstead, J. A., B. L. Block, J. K. Bielicki, C. M. Kay, M. N. Oda, and R. O. Ryan. 2005. Combined N- and C-terminal truncation of human apolipoprotein A-I yields a folded, functional central domain. *Biochemistry* 44:4591-4599.
95. Pollard, R. D., B. Fulp, M. P. Samuel, M. G. Sorci-Thomas, and M. J. Thomas. 2013. The conformation of lipid-free human apolipoprotein A-I in solution. *Biochemistry* 52:9470-9481.
96. Gorshkova, I. N., T. Liu, H. Y. Kan, A. Chroni, V. I. Zannis, and D. Atkinson. 2006. Structure and stability of apolipoprotein a-I in solution and in discoidal high-density lipoprotein probed by double charge ablation and deletion mutation. *Biochemistry* 45:1242-1254.
97. Guha, M., X. Gao, S. Jayaraman, and O. Gursky. 2008. Correlation of structural stability with functional remodeling of high-density lipoproteins: the importance of being disordered. *Biochemistry* 47:11393-11397.
98. Koyama, M., M. Tanaka, P. Dhanasekaran, S. Lund-Katz, M. C. Phillips, and H. Saito. 2009. Interaction between the N- and C-terminal domains modulates the stability and lipid binding of apolipoprotein A-I. *Biochemistry* 48:2529-2537.
99. Phillips, M. C. 2013. New insights into the determination of HDL structure by apolipoproteins: Thematic review series: high density lipoprotein structure, function, and metabolism. *J Lipid Res* 54:2034-2048.
100. Tanaka, M., M. Koyama, P. Dhanasekaran, D. Nguyen, M. Nickel, S. Lund-Katz, H. Saito, and M. C. Phillips. 2008. Influence of tertiary structure domain properties on the functionality of apolipoprotein A-I. *Biochemistry* 47:2172-2180.
101. Thomas, M. J., S. Bhat, and M. G. Sorci-Thomas. 2006. The use of chemical cross-linking and mass spectrometry to elucidate the tertiary conformation of lipid-bound apolipoprotein A-I. *Curr Opin Lipidol* 17:214-220.
102. Davidson, W. S., and R. A. Silva. 2005. Apolipoprotein structural organization in high density lipoproteins: belts, bundles, hinges and hairpins. *Curr Opin Lipidol* 16:295-300.
103. Tricerri, M. A., A. K. Behling Agree, S. A. Sanchez, J. Bronski, and A. Jonas. 2001. Arrangement of apolipoprotein A-I in reconstituted high-density lipoprotein disks: an alternative model based on fluorescence resonance energy transfer experiments. *Biochemistry* 40:5065-5074.
104. Panagotopulos, S. E., E. M. Horace, J. N. Maiorano, and W. S. Davidson. 2001. Apolipoprotein A-I adopts a belt-like orientation in reconstituted high density lipoproteins. *J Biol Chem* 276:42965-42970.

105. Koppaka, V., L. Silvestro, J. A. Engler, C. G. Brouillette, and P. H. Axelsen. 1999. The structure of human lipoprotein A-I. Evidence for the "belt" model. *J Biol Chem* 274:14541-14544.
106. Segrest, J. P., M. K. Jones, A. E. Klon, C. J. Sheldahl, M. Hellinger, H. De Loof, and S. C. Harvey. 1999. A detailed molecular belt model for apolipoprotein A-I in discoidal high density lipoprotein. *J Biol Chem* 274:31755-31758.
107. Sevugan Chetty, P., L. Mayne, Z. Y. Kan, S. Lund-Katz, S. W. Englander, and M. C. Phillips. 2012. Apolipoprotein A-I helical structure and stability in discoidal high-density lipoprotein (HDL) particles by hydrogen exchange and mass spectrometry. *Proc Natl Acad Sci U S A* 109:11687-11692.
108. Mei, X., and D. Atkinson. 2011. Crystal structure of C-terminal truncated apolipoprotein A-I reveals the assembly of high density lipoprotein (HDL) by dimerization. *J Biol Chem* 286:38570-38582.
109. Li, L., J. Chen, V. K. Mishra, J. A. Kurtz, D. Cao, A. E. Klon, S. C. Harvey, G. M. Anantharamaiah, and J. P. Segrest. 2004. Double belt structure of discoidal high density lipoproteins: molecular basis for size heterogeneity. *J Mol Biol* 343:1293-1311.
110. Silva, R. A., L. A. Schneeweis, S. C. Krishnan, X. Zhang, P. H. Axelsen, and W. S. Davidson. 2007. The structure of apolipoprotein A-II in discoidal high density lipoproteins. *J Biol Chem* 282:9713-9721.
111. Silva, R. A., R. Huang, J. Morris, J. Fang, E. O. Gracheva, G. Ren, A. Kontush, W. G. Jerome, K. A. Rye, and W. S. Davidson. 2008. Structure of apolipoprotein A-I in spherical high density lipoproteins of different sizes. *Proc Natl Acad Sci U S A* 105:12176-12181.
112. Gursky, O. 2013. Crystal structure of Delta(185-243)ApoA-I suggests a mechanistic framework for the protein adaptation to the changing lipid load in good cholesterol: from flatland to sphereland via double belt, belt buckle, double hairpin and trefoil/tetrafoil. *J Mol Biol* 425:1-16.
113. Wu, Z., V. Gogonea, X. Lee, R. P. May, V. Pipich, M. A. Wagner, A. Undurti, T. C. Tallant, C. Baleanu-Gogonea, F. Charlton, A. Ioffe, J. A. DiDonato, K. A. Rye, and S. L. Hazen. 2011. The low resolution structure of ApoA1 in spherical high density lipoprotein revealed by small angle neutron scattering. *J Biol Chem* 286:12495-12508.
114. Huang, R., R. A. Silva, W. G. Jerome, A. Kontush, M. J. Chapman, L. K. Curtiss, T. J. Hodges, and W. S. Davidson. 2011. Apolipoprotein A-I structural organization in high-density lipoproteins isolated from human plasma. *Nat Struct Mol Biol* 18:416-422.
115. Lund-Katz, S., D. Nguyen, P. Dhanasekaran, M. Kono, M. Nickel, H. Saito, and M. C. Phillips. 2010. Surface plasmon resonance analysis of the mechanism of binding of apoA-I to high density lipoprotein particles. *J Lipid Res* 51:606-617.
116. Langmann, T., J. Klucken, M. Reil, G. Liebisch, M. F. Luciani, G. Chimini, W. E. Kaminski, and G. Schmitz. 1999. Molecular cloning of the human ATP-binding cassette transporter 1 (hABC1): evidence for sterol-dependent regulation in macrophages. *Biochem Biophys Res Commun* 257:29-33.
117. Kielar, D., W. Dietmaier, T. Langmann, C. Aslanidis, M. Probst, M. Naruszewicz, and G. Schmitz. 2001. Rapid quantification of human ABCA1 mRNA in various cell types and tissues by real-time reverse transcription-PCR. *Clin Chem* 47:2089-2097.
118. Neufeld, E. B., A. T. Remaley, S. J. Demosky, J. A. Stonik, A. M. Cooney, M. Comly, N. K. Dwyer, M. Zhang, J. Blanchette-Mackie, S. Santamarina-Fojo, and H. B. Brewer, Jr. 2001. Cellular localization and trafficking of the human ABCA1 transporter. *J Biol Chem* 276:27584-27590.

119. Neufeld, E. B., S. J. Demosky, Jr., J. A. Stonik, C. Combs, A. T. Remaley, N. Duverger, S. Santamarina-Fojo, and H. B. Brewer, Jr. 2002. The ABCA1 transporter functions on the basolateral surface of hepatocytes. *Biochem Biophys Res Commun* 297:974-979.
120. Takahashi, Y., and J. D. Smith. 1999. Cholesterol efflux to apolipoprotein AI involves endocytosis and resecretion in a calcium-dependent pathway. *Proc Natl Acad Sci U S A* 96:11358-11363.
121. Lorenzi, I., A. von Eckardstein, C. Cavelier, S. Radosavljevic, and L. Rohrer. 2008. Apolipoprotein A-I but not high-density lipoproteins are internalised by RAW macrophages: roles of ATP-binding cassette transporter A1 and scavenger receptor BI. *Journal of molecular medicine* 86:171-183.
122. Ohnsorg, P. M., L. Rohrer, D. Perisa, A. Kateifides, A. Chroni, D. Kardassis, V. I. Zannis, and A. von Eckardstein. 2011. Carboxyl terminus of apolipoprotein A-I (ApoA-I) is necessary for the transport of lipid-free ApoA-I but not prelipidated ApoA-I particles through aortic endothelial cells. *J Biol Chem* 286:7744-7754.
123. Cavelier, C., L. Rohrer, and A. von Eckardstein. 2006. ATP-Binding cassette transporter A1 modulates apolipoprotein A-I transcytosis through aortic endothelial cells. *Circulation research* 99:1060-1066.
124. Remaley, A. T., J. A. Stonik, S. J. Demosky, E. B. Neufeld, A. V. Bocharov, T. G. Vishnyakova, T. L. Eggerman, A. P. Patterson, N. J. Duverger, S. Santamarina-Fojo, and H. B. Brewer, Jr. 2001. Apolipoprotein specificity for lipid efflux by the human ABCAI transporter. *Biochem Biophys Res Commun* 280:818-823.
125. Singaraja, R. R., M. Van Eck, N. Bissada, F. Zimetti, H. L. Collins, R. B. Hildebrand, A. Hayden, L. R. Brunham, M. H. Kang, J. C. Fruchart, T. J. Van Berkel, J. S. Parks, B. Staels, G. H. Rothblat, C. Fievet, and M. R. Hayden. 2006. Both hepatic and extrahepatic ABCA1 have discrete and essential functions in the maintenance of plasma high-density lipoprotein cholesterol levels in vivo. *Circulation* 114:1301-1309.
126. Timmins, J. M., J. Y. Lee, E. Boudyguina, K. D. Kluckman, L. R. Brunham, A. Mulya, A. K. Gebre, J. M. Coutinho, P. L. Colvin, T. L. Smith, M. R. Hayden, N. Maeda, and J. S. Parks. 2005. Targeted inactivation of hepatic Abca1 causes profound hypoalphalipoproteinemia and kidney hypercatabolism of apoA-I. *J Clin Invest* 115:1333-1342.
127. Reardon, C. A., H. Y. Kan, V. Cabana, L. Blachowicz, J. R. Lukens, Q. Wu, K. Liadaki, G. S. Getz, and V. I. Zannis. 2001. In vivo studies of HDL assembly and metabolism using adenovirus-mediated transfer of ApoA-I mutants in ApoA-I-deficient mice. *Biochemistry* 40:13670-13680.
128. Zannis, V. I., A. Chroni, K. E. Kypreos, H. Y. Kan, T. B. Cesar, E. E. Zanni, and D. Kardassis. 2004. Probing the pathways of chylomicron and HDL metabolism using adenovirus-mediated gene transfer. *Curr Opin Lipidol* 15:151-166.
129. Chroni, A., T. Liu, I. Gorshkova, H. Y. Kan, Y. Uehara, A. Von Eckardstein, and V. I. Zannis. 2003. The central helices of ApoA-I can promote ATP-binding cassette transporter A1 (ABCA1)-mediated lipid efflux. Amino acid residues 220-231 of the wild-type ApoA-I are required for lipid efflux in vitro and high density lipoprotein formation in vivo. *J Biol Chem* 278:6719-6730.
130. Chroni, A., G. Koukos, A. Duka, and V. I. Zannis. 2007. The carboxy-terminal region of apoA-I is required for the ABCA1-dependent formation of alpha-HDL but not prebeta-HDL particles in vivo. *Biochemistry* 46:5697-5708.
131. Fotakis, P., A. K. Kateifides, C. Gkolfinopoulou, D. Georgiadou, M. Beck, K. Grundler, A. Chroni, E. Stratikos, D. Kardassis, and V. I. Zannis. 2013. Role of the hydrophobic and charged residues in the 218-226 region of apoA-I in the biogenesis of HDL. *J Lipid Res* 54:3281-3292.

132. Bodzioch, M., E. Orso, J. Klucken, T. Langmann, A. Bottcher, W. Diederich, W. Drobnik, S. Barlage, C. Buchler, M. Porsch-Ozcurumez, W. E. Kaminski, H. W. Hahmann, K. Oette, G. Rothe, C. Aslanidis, K. J. Lackner, and G. Schmitz. 1999. The gene encoding ATP-binding cassette transporter 1 is mutated in Tangier disease. *Nat Genet* 22:347-351.
133. Fitzgerald, M. L., A. L. Morris, J. S. Rhee, L. P. Andersson, A. J. Mendez, and M. W. Freeman. 2002. Naturally occurring mutations in the largest extracellular loops of ABCA1 can disrupt its direct interaction with apolipoprotein A-I. *J Biol Chem* 277:33178-33187.
134. Chroni, A., T. Liu, M. L. Fitzgerald, M. W. Freeman, and V. I. Zannis. 2004. Cross-linking and lipid efflux properties of apoA-I mutants suggest direct association between apoA-I helices and ABCA1. *Biochemistry* 43:2126-2139.
135. Fitzgerald, M. L., A. L. Morris, A. Chroni, A. J. Mendez, V. I. Zannis, and M. W. Freeman. 2004. ABCA1 and amphipathic apolipoproteins form high-affinity molecular complexes required for cholesterol efflux. *J Lipid Res* 45:287-294.
136. Warden, C. H., C. A. Langner, J. I. Gordon, B. A. Taylor, J. W. McLean, and A. J. Lusis. 1989. Tissue-specific expression, developmental regulation, and chromosomal mapping of the lecithin: cholesterol acyltransferase gene. Evidence for expression in brain and testes as well as liver. *J Biol Chem* 264:21573-21581.
137. Simon, J. B., and J. L. Boyer. 1970. Production of lecithin: cholesterol acyltransferase by the isolated perfused rat liver. *Biochim Biophys Acta* 218:549-551.
138. Jonas, A., N. L. Zorich, K. E. Kezdy, and W. E. Trick. 1987. Reaction of discoidal complexes of apolipoprotein A-I and various phosphatidylcholines with lecithin cholesterol acyltransferase. Interfacial effects. *J Biol Chem* 262:3969-3974.
139. Jones, M. K., A. Catte, L. Li, and J. P. Segrest. 2009. Dynamics of activation of lecithin:cholesterol acyltransferase by apolipoprotein A-I. *Biochemistry* 48:11196-11210.
140. Jonas, A. 2000. Lecithin cholesterol acyltransferase. *Biochim Biophys Acta* 1529:245-256.
141. Chroni, A., A. Duka, H. Y. Kan, T. Liu, and V. I. Zannis. 2005. Point mutations in apolipoprotein A-I mimic the phenotype observed in patients with classical lecithin:cholesterol acyltransferase deficiency. *Biochemistry* 44:14353-14366.
142. McManus, D. C., B. R. Scott, P. G. Frank, V. Franklin, J. R. Schultz, and Y. L. Marcel. 2000. Distinct central amphipathic alpha-helices in apolipoprotein A-I contribute to the in vivo maturation of high density lipoprotein by either activating lecithin-cholesterol acyltransferase or binding lipids. *J Biol Chem* 275:5043-5051.
143. Sorci-Thomas, M. G., L. Curtiss, J. S. Parks, M. J. Thomas, M. W. Kearns, and M. Landrum. 1998. The hydrophobic face orientation of apolipoprotein A-I amphipathic helix domain 143-164 regulates lecithin:cholesterol acyltransferase activation. *J Biol Chem* 273:11776-11782.
144. Scott, B. R., D. C. McManus, V. Franklin, A. G. McKenzie, T. Neville, D. L. Sparks, and Y. L. Marcel. 2001. The N-terminal globular domain and the first class A amphipathic helix of apolipoprotein A-I are important for lecithin:cholesterol acyltransferase activation and the maturation of high density lipoprotein in vivo. *J Biol Chem* 276:48716-48724.
145. Santamarina-Fojo S, H. J., Assmann G, Brewer HB Jr. 2001. Lecithin cholesterol acyltransferase deficiency and fish eye disease. In *The metabolic and molecular bases of inherited disease.* B. A. Scriver CR, Sly WS, Valle D, ed. McGraw-Hill, New York, NY. 2817–2834.
146. Calabresi, L., E. Favari, E. Moleri, M. P. Adorni, M. Pedrelli, S. Costa, W. Jessup, I. C. Gelissen, P. T. Kovanen, F. Bernini, and G. Franceschini. 2009. Functional LCAT is not

required for macrophage cholesterol efflux to human serum. *Atherosclerosis* 204:141-146.

147. Savary, S., F. Denizot, M. Luciani, M. Mattei, and G. Chimini. 1996. Molecular cloning of a mammalian ABC transporter homologous to Drosophila white gene. *Mamm Genome* 7:673-676.
148. Croop, J. M., G. E. Tiller, J. A. Fletcher, M. L. Lux, E. Raab, D. Goldenson, D. Son, S. Arciniegas, and R. L. Wu. 1997. Isolation and characterization of a mammalian homolog of the Drosophila white gene. *Gene* 185:77-85.
149. Nakamura, K., M. A. Kennedy, A. Baldan, D. D. Bojanic, K. Lyons, and P. A. Edwards. 2004. Expression and regulation of multiple murine ATP-binding cassette transporter G1 mRNAs/isoforms that stimulate cellular cholesterol efflux to high density lipoprotein. *J Biol Chem* 279:45980-45989.
150. Wang, N., M. Ranalletta, F. Matsuura, F. Peng, and A. R. Tall. 2006. LXR-induced redistribution of ABCG1 to plasma membrane in macrophages enhances cholesterol mass efflux to HDL. *Arterioscler Thromb Vasc Biol* 26:1310-1316.
151. Vaughan, A. M., and J. F. Oram. 2005. ABCG1 redistributes cell cholesterol to domains removable by high density lipoprotein but not by lipid-depleted apolipoproteins. *J Biol Chem* 280:30150-30157.
152. Sturek, J. M., J. D. Castle, A. P. Trace, L. C. Page, A. M. Castle, C. Evans-Molina, J. S. Parks, R. G. Mirmira, and C. C. Hedrick. 2010. An intracellular role for ABCG1-mediated cholesterol transport in the regulated secretory pathway of mouse pancreatic beta cells. *The Journal of clinical investigation* 120:2575-2589.
153. Tarling, E. J., and P. A. Edwards. 2011. ATP binding cassette transporter G1 (ABCG1) is an intracellular sterol transporter. *Proc Natl Acad Sci U S A* 108:19719-19724.
154. Wang, X., H. L. Collins, M. Ranalletta, I. V. Fuki, J. T. Billheimer, G. H. Rothblat, A. R. Tall, and D. J. Rader. 2007. Macrophage ABCA1 and ABCG1, but not SR-BI, promote macrophage reverse cholesterol transport in vivo. *The Journal of clinical investigation* 117:2216-2224.
155. Zhang, Y., F. C. McGillicuddy, C. C. Hinkle, S. O'Neill, J. M. Glick, G. H. Rothblat, and M. P. Reilly. 2010. Adipocyte modulation of high-density lipoprotein cholesterol. *Circulation* 121:1347-1355.
156. Stefulj, J., U. Panzenboeck, T. Becker, B. Hirschmugl, C. Schweinzer, I. Lang, G. Marsche, A. Sadjak, U. Lang, G. Desoye, and C. Wadsack. 2009. Human endothelial cells of the placental barrier efficiently deliver cholesterol to the fetal circulation via ABCA1 and ABCG1. *Circulation research* 104:600-608.
157. Kennedy, M. A., G. C. Barrera, K. Nakamura, A. Baldan, P. Tarr, M. C. Fishbein, J. Frank, O. L. Francone, and P. A. Edwards. 2005. ABCG1 has a critical role in mediating cholesterol efflux to HDL and preventing cellular lipid accumulation. *Cell metabolism* 1:121-131.
158. Sankaranarayanan, S., J. F. Oram, B. F. Asztalos, A. M. Vaughan, S. Lund-Katz, M. P. Adorni, M. C. Phillips, and G. H. Rothblat. 2009. Effects of acceptor composition and mechanism of ABCG1-mediated cellular free cholesterol efflux. *J Lipid Res* 50:275-284.
159. Daniil, G., V. I. Zannis, and A. Chroni. 2013. Effect of apoA-I Mutations in the Capacity of Reconstituted HDL to Promote ABCG1-Mediated Cholesterol Efflux. *PLoS One* 8:e67993.
160. Acton, S., A. Rigotti, K. T. Landschulz, S. Xu, H. H. Hobbs, and M. Krieger. 1996. Identification of scavenger receptor SR-BI as a high density lipoprotein receptor. *Science* 271:518-520.

161. Leiva, A., H. Verdejo, M. L. Benitez, A. Martinez, D. Busso, and A. Rigotti. 2011. Mechanisms regulating hepatic SR-BI expression and their impact on HDL metabolism. *Atherosclerosis* 217:299-307.
162. Zhang, Y., A. M. Ahmed, T. L. Tran, J. Lin, N. McFarlane, D. R. Boreham, S. A. Igdoura, R. Truant, and B. L. Trigatti. 2007. The inhibition of endocytosis affects HDL-lipid uptake mediated by the human scavenger receptor class B type I. *Mol Membr Biol* 24:442-454.
163. Landschulz, K. T., R. K. Pathak, A. Rigotti, M. Krieger, and H. H. Hobbs. 1996. Regulation of scavenger receptor, class B, type I, a high density lipoprotein receptor, in liver and steroidogenic tissues of the rat. *The Journal of clinical investigation* 98:984-995.
164. Krieger, M. 1999. Charting the fate of the "good cholesterol": identification and characterization of the high-density lipoprotein receptor SR-BI. *Annu Rev Biochem* 68:523-558.
165. Liadaki, K. N., T. Liu, S. Xu, B. Y. Ishida, P. N. Duchateaux, J. P. Krieger, J. Kane, M. Krieger, and V. I. Zannis. 2000. Binding of high density lipoprotein (HDL) and discoidal reconstituted HDL to the HDL receptor scavenger receptor class B type I. Effect of lipid association and APOA-I mutations on receptor binding. *J Biol Chem* 275:21262-21271.
166. Chroni, A., T. J. Nieland, K. E. Kypreos, M. Krieger, and V. I. Zannis. 2005. SR-BI mediates cholesterol efflux via its interactions with lipid-bound ApoE. Structural mutations in SR-BI diminish cholesterol efflux. *Biochemistry* 44:13132-13143.
167. Thuahnai, S. T., S. Lund-Katz, D. L. Williams, and M. C. Phillips. 2001. Scavenger receptor class B, type I-mediated uptake of various lipids into cells. Influence of the nature of the donor particle interaction with the receptor. *J Biol Chem* 276:43801-43808.
168. Greene, D. J., J. W. Skeggs, and R. E. Morton. 2001. Elevated triglyceride content diminishes the capacity of high density lipoprotein to deliver cholesteryl esters via the scavenger receptor class B type I (SR-BI). *J Biol Chem* 276:4804-4811.
169. Stangl, H., M. Hyatt, and H. H. Hobbs. 1999. Transport of lipids from high and low density lipoproteins via scavenger receptor-BI. *J Biol Chem* 274:32692-32698.
170. Urban, S., S. Zieseniss, M. Werder, H. Hauser, R. Budzinski, and B. Engelmann. 2000. Scavenger receptor BI transfers major lipoprotein-associated phospholipids into the cells. *J Biol Chem* 275:33409-33415.
171. Ji, Y., B. Jian, N. Wang, Y. Sun, M. L. Moya, M. C. Phillips, G. H. Rothblat, J. B. Swaney, and A. R. Tall. 1997. Scavenger receptor BI promotes high density lipoprotein-mediated cellular cholesterol efflux. *J Biol Chem* 272:20982-20985.
172. Gu, X., R. Lawrence, and M. Krieger. 2000. Dissociation of the high density lipoprotein and low density lipoprotein binding activities of murine scavenger receptor class B type I (mSR-BI) using retrovirus library-based activity dissection. *J Biol Chem* 275:9120-9130.
173. Ahras, M., T. Naing, and R. McPherson. 2008. Scavenger receptor class B type I localizes to a late endosomal compartment. *J Lipid Res* 49:1569-1576.
174. Pagler, T. A., S. Rhode, A. Neuhofer, H. Laggner, W. Strobl, C. Hinterndorfer, I. Volf, M. Pavelka, E. R. Eckhardt, D. R. van der Westhuyzen, G. J. Schutz, and H. Stangl. 2006. SR-BI-mediated high density lipoprotein (HDL) endocytosis leads to HDL resecretion facilitating cholesterol efflux. *J Biol Chem* 281:11193-11204.
175. Fenske, S. A., A. Yesilaltay, R. Pal, K. Daniels, C. Barker, V. Quinones, A. Rigotti, M. Krieger, and O. Kocher. 2009. Normal hepatic cell surface localization of the high density lipoprotein receptor, scavenger receptor class B, type I, depends on all four PDZ domains of PDZK1. *J Biol Chem* 284:5797-5806.

176. Ueda, Y., L. Royer, E. Gong, J. Zhang, P. N. Cooper, O. Francone, and E. M. Rubin. 1999. Lower plasma levels and accelerated clearance of high density lipoprotein (HDL) and non-HDL cholesterol in scavenger receptor class B type I transgenic mice. *J Biol Chem* 274:7165-7171.
177. Webb, N. R., M. C. de Beer, J. Yu, M. S. Kindy, A. Daugherty, D. R. van der Westhuyzen, and F. C. de Beer. 2002. Overexpression of SR-BI by adenoviral vector promotes clearance of apoA-I, but not apoB, in human apoB transgenic mice. *J Lipid Res* 43:1421-1428.
178. Gu, X., K. Kozarsky, and M. Krieger. 2000. Scavenger receptor class B, type I-mediated [3H]cholesterol efflux to high and low density lipoproteins is dependent on lipoprotein binding to the receptor. *J Biol Chem* 275:29993-30001.
179. Liu, T., M. Krieger, H. Y. Kan, and V. I. Zannis. 2002. The effects of mutations in helices 4 and 6 of ApoA-I on scavenger receptor class B type I (SR-BI)-mediated cholesterol efflux suggest that formation of a productive complex between reconstituted high density lipoprotein and SR-BI is required for efficient lipid transport. *J Biol Chem* 277:21576-21584.
180. Johnson, W. J., M. C. Phillips, and G. H. Rothblat. 1997. Lipoproteins and cellular cholesterol homeostasis. *Subcell Biochem* 28:235-276.
181. Sorci-Thomas, M. G., and M. J. Thomas. 2002. The effects of altered apolipoprotein A-I structure on plasma HDL concentration. *Trends Cardiovasc Med* 12:121-128.
182. Zannis, V. I., D. Kardassis, and E. E. Zanni. 1993. Genetic mutations affecting human lipoproteins, their receptors, and their enzymes. *Adv Hum Genet* 21:145-319.
183. Obici, L., G. Franceschini, L. Calabresi, S. Giorgetti, M. Stoppini, G. Merlini, and V. Bellotti. 2006. Structure, function and amyloidogenic propensity of apolipoprotein A-I. *Amyloid* 13:191-205.
184. Hovingh, G. K., A. Brownlie, R. J. Bisoendial, M. P. Dube, J. H. Levels, W. Petersen, R. P. Dullaart, E. S. Stroes, A. H. Zwinderman, E. de Groot, M. R. Hayden, J. A. Kuivenhoven, and J. J. Kastelein. 2004. A novel apoA-I mutation (L178P) leads to endothelial dysfunction, increased arterial wall thickness, and premature coronary artery disease. *J Am Coll Cardiol* 44:1429-1435.
185. Miccoli, R., A. Bertolotto, R. Navalesi, L. Odoguardi, A. Boni, J. Wessling, H. Funke, H. Wiebusch, A. Eckardstein, and G. Assmann. 1996. Compound heterozygosity for a structural apolipoprotein A-I variant, apo A-I(L141R)Pisa, and an apolipoprotein A-I null allele in patients with absence of HDL cholesterol, corneal opacifications, and coronary heart disease. *Circulation* 94:1622-1628.
186. Miettinen, H. E., M. Jauhiainen, H. Gylling, S. Ehnholm, A. Palomaki, T. A. Miettinen, and K. Kontula. 1997. Apolipoprotein A-IFIN (Leu159-->Arg) mutation affects lecithin cholesterol acyltransferase activation and subclass distribution of HDL but not cholesterol efflux from fibroblasts. *Arterioscler Thromb Vasc Biol* 17:3021-3032.
187. Miller, M., D. Aiello, H. Pritchard, G. Friel, and K. Zeller. 1998. Apolipoprotein A-I(Zavalla) (Leu159-->Pro): HDL cholesterol deficiency in a kindred associated with premature coronary artery disease. *Arterioscler Thromb Vasc Biol* 18:1242-1247.
188. Franceschini, G., C. R. Sirtori, A. Capurso, 2nd, K. H. Weisgraber, and R. W. Mahley. 1980. A-IMilano apoprotein. Decreased high density lipoprotein cholesterol levels with significant lipoprotein modifications and without clinical atherosclerosis in an Italian family. *The Journal of clinical investigation* 66:892-900.
189. Gomaraschi, M., D. Baldassarre, M. Amato, S. Eligini, P. Conca, C. R. Sirtori, G. Franceschini, and L. Calabresi. 2007. Normal vascular function despite low levels of high-density lipoprotein cholesterol in carriers of the apolipoprotein A-I(Milano) mutant. *Circulation* 116:2165-2172.

190. Koukos, G., A. Chroni, A. Duka, D. Kardassis, and V. I. Zannis. 2007. LCAT can rescue the abnormal phenotype produced by the natural ApoA-I mutations (Leu141Arg)Pisa and (Leu159Arg)FIN. *Biochemistry* 46:10713-10721.
191. Miccoli, R., Y. Zhu, U. Daum, J. Wessling, Y. Huang, R. Navalesi, G. Assmann, and A. von Eckardstein. 1997. A natural apolipoprotein A-I variant, apoA-I (L141R)Pisa, interferes with the formation of alpha-high density lipoproteins (HDL) but not with the formation of pre beta 1-HDL and influences efflux of cholesterol into plasma. *J Lipid Res* 38:1242-1253.
192. Miettinen, H. E., H. Gylling, T. A. Miettinen, J. Viikari, L. Paulin, and K. Kontula. 1997. Apolipoprotein A-IFin. Dominantly inherited hypoalphalipoproteinemia due to a single base substitution in the apolipoprotein A-I gene. *Arterioscler Thromb Vasc Biol* 17:83-90.
193. Gorshkova, I. N., T. Liu, V. I. Zannis, and D. Atkinson. 2002. Lipid-free structure and stability of apolipoprotein A-I: probing the central region by mutation. *Biochemistry* 41:10529-10539.
194. Sorci-Thomas, M. G., M. Zabalawi, M. S. Bharadwaj, A. J. Wilhelm, J. S. Owen, B. F. Asztalos, S. Bhat, and M. J. Thomas. 2012. Dysfunctional HDL containing L159R ApoA-I leads to exacerbation of atherosclerosis in hyperlipidemic mice. *Biochim Biophys Acta* 1821:502-512.
195. McManus, D. C., B. R. Scott, V. Franklin, D. L. Sparks, and Y. L. Marcel. 2001. Proteolytic degradation and impaired secretion of an apolipoprotein A-I mutant associated with dominantly inherited hypoalphalipoproteinemia. *J Biol Chem* 276:21292-21302.
196. Gordon, D. J., J. L. Probstfield, R. J. Garrison, J. D. Neaton, W. P. Castelli, J. D. Knoke, D. R. Jacobs, Jr., S. Bangdiwala, and H. A. Tyroler. 1989. High-density lipoprotein cholesterol and cardiovascular disease. Four prospective American studies. *Circulation* 79:8-15.
197. Toth, P. P., P. J. Barter, R. S. Rosenson, W. E. Boden, M. J. Chapman, M. Cuchel, R. B. D'Agostino, Sr., M. H. Davidson, W. S. Davidson, J. W. Heinecke, R. H. Karas, A. Kontush, R. M. Krauss, M. Miller, and D. J. Rader. 2013. High-density lipoproteins: a consensus statement from the National Lipid Association. *J Clin Lipidol* 7:484-525.
198. Sirtori, C. R., L. Calabresi, G. Franceschini, D. Baldassarre, M. Amato, J. Johansson, M. Salvetti, C. Monteduro, R. Zulli, M. L. Muiesan, and E. Agabiti-Rosei. 2001. Cardiovascular status of carriers of the apolipoprotein A-I(Milano) mutant: the Limone sul Garda study. *Circulation* 103:1949-1954.
199. van Capelleveen, J. C., A. E. Bochem, M. M. Motazacker, G. K. Hovingh, and J. J. Kastelein. 2013. Genetics of HDL-C: a causal link to atherosclerosis? *Curr Atheroscler Rep* 15:326.
200. Annema, W., and A. von Eckardstein. 2013. High-density lipoproteins. Multifunctional but vulnerable protections from atherosclerosis. *Circ J* 77:2432-2448.
201. Mineo, C., and P. W. Shaul. 2012. Novel biological functions of high-density lipoprotein cholesterol. *Circulation research* 111:1079-1090.
202. Khera, A. V., M. Cuchel, M. de la Llera-Moya, A. Rodrigues, M. F. Burke, K. Jafri, B. C. French, J. A. Phillips, M. L. Mucksavage, R. L. Wilensky, E. R. Mohler, G. H. Rothblat, and D. J. Rader. 2011. Cholesterol efflux capacity, high-density lipoprotein function, and atherosclerosis. *The New England journal of medicine* 364:127-135.
203. Cuchel, M., and D. J. Rader. 2006. Macrophage reverse cholesterol transport: key to the regression of atherosclerosis? *Circulation* 113:2548-2555.

204. Yancey, P. G., A. E. Bortnick, G. Kellner-Weibel, M. de la Llera-Moya, M. C. Phillips, and G. H. Rothblat. 2003. Importance of different pathways of cellular cholesterol efflux. *Arterioscler Thromb Vasc Biol* 23:712-719.
205. Wang, N., and A. R. Tall. 2003. Regulation and mechanisms of ATP-binding cassette transporter A1-mediated cellular cholesterol efflux. *Arterioscler Thromb Vasc Biol* 23:1178-1184.
206. Rader, D. J. 2003. Regulation of reverse cholesterol transport and clinical implications. *Am J Cardiol* 92:42J-49J.
207. Malaval, C., M. Laffargue, R. Barbaras, C. Rolland, C. Peres, E. Champagne, B. Perret, F. Terce, X. Collet, and L. O. Martinez. 2009. RhoA/ROCK I signalling downstream of the P2Y13 ADP-receptor controls HDL endocytosis in human hepatocytes. *Cell Signal* 21:120-127.
208. Nijstad, N., T. Gautier, F. Briand, D. J. Rader, and U. J. Tietge. 2011. Biliary sterol secretion is required for functional in vivo reverse cholesterol transport in mice. *Gastroenterology* 140:1043-1051.
209. van Eck, M., I. S. Bos, W. E. Kaminski, E. Orso, G. Rothe, J. Twisk, A. Bottcher, E. S. Van Amersfoort, T. A. Christiansen-Weber, W. P. Fung-Leung, T. J. Van Berkel, and G. Schmitz. 2002. Leukocyte ABCA1 controls susceptibility to atherosclerosis and macrophage recruitment into tissues. *Proc Natl Acad Sci U S A* 99:6298-6303.
210. Van Eck, M., R. R. Singaraja, D. Ye, R. B. Hildebrand, E. R. James, M. R. Hayden, and T. J. Van Berkel. 2006. Macrophage ATP-binding cassette transporter A1 overexpression inhibits atherosclerotic lesion progression in low-density lipoprotein receptor knockout mice. *Arterioscler Thromb Vasc Biol* 26:929-934.
211. Yvan-Charvet, L., M. Ranalletta, N. Wang, S. Han, N. Terasaka, R. Li, C. Welch, and A. R. Tall. 2007. Combined deficiency of ABCA1 and ABCG1 promotes foam cell accumulation and accelerates atherosclerosis in mice. *The Journal of clinical investigation* 117:3900-3908.
212. Moore, R. E., M. Navab, J. S. Millar, F. Zimetti, S. Hama, G. H. Rothblat, and D. J. Rader. 2005. Increased atherosclerosis in mice lacking apolipoprotein A-I attributable to both impaired reverse cholesterol transport and increased inflammation. *Circulation research* 97:763-771.
213. Zhang, Y., I. Zanotti, M. P. Reilly, J. M. Glick, G. H. Rothblat, and D. J. Rader. 2003. Overexpression of apolipoprotein A-I promotes reverse transport of cholesterol from macrophages to feces in vivo. *Circulation* 108:661-663.
214. Heinecke, J. W. 2012. The not-so-simple HDL story: A new era for quantifying HDL and cardiovascular risk? *Nat Med* 18:1346-1347.
215. Nofer, J. R., M. van der Giet, M. Tolle, I. Wolinska, K. von Wnuck Lipinski, H. A. Baba, U. J. Tietge, A. Godecke, I. Ishii, B. Kleuser, M. Schafers, M. Fobker, W. Zidek, G. Assmann, J. Chun, and B. Levkau. 2004. HDL induces NO-dependent vasorelaxation via the lysophospholipid receptor S1P3. *The Journal of clinical investigation* 113:569-581.
216. Spieker, L. E., I. Sudano, D. Hurlimann, P. G. Lerch, M. G. Lang, C. Binggeli, R. Corti, F. Ruschitzka, T. F. Luscher, and G. Noll. 2002. High-density lipoprotein restores endothelial function in hypercholesterolemic men. *Circulation* 105:1399-1402.
217. Bisoendial, R. J., G. K. Hovingh, J. H. Levels, P. G. Lerch, I. Andresen, M. R. Hayden, J. J. Kastelein, and E. S. Stroes. 2003. Restoration of endothelial function by increasing high-density lipoprotein in subjects with isolated low high-density lipoprotein. *Circulation* 107:2944-2948.
218. Yuhanna, I. S., Y. Zhu, B. E. Cox, L. D. Hahner, S. Osborne-Lawrence, P. Lu, Y. L. Marcel, R. G. Anderson, M. E. Mendelsohn, H. H. Hobbs, and P. W. Shaul. 2001. High-

density lipoprotein binding to scavenger receptor-BI activates endothelial nitric oxide synthase. *Nat Med* 7:853-857.

219. Mineo, C., I. S. Yuhanna, M. J. Quon, and P. W. Shaul. 2003. High density lipoprotein-induced endothelial nitric-oxide synthase activation is mediated by Akt and MAP kinases. *J Biol Chem* 278:9142-9149.
220. Li, X. A., W. B. Titlow, B. A. Jackson, N. Giltiay, M. Nikolova-Karakashian, A. Uittenbogaard, and E. J. Smart. 2002. High density lipoprotein binding to scavenger receptor, Class B, type I activates endothelial nitric-oxide synthase in a ceramide-dependent manner. *J Biol Chem* 277:11058-11063.
221. Gong, M., M. Wilson, T. Kelly, W. Su, J. Dressman, J. Kincer, S. V. Matveev, L. Guo, T. Guerin, X. A. Li, W. Zhu, A. Uittenbogaard, and E. J. Smart. 2003. HDL-associated estradiol stimulates endothelial NO synthase and vasodilation in an SR-BI-dependent manner. *The Journal of clinical investigation* 111:1579-1587.
222. Ramet, M. E., M. Ramet, Q. Lu, M. Nickerson, M. J. Savolainen, A. Malzone, and R. H. Karas. 2003. High-density lipoprotein increases the abundance of eNOS protein in human vascular endothelial cells by increasing its half-life. *J Am Coll Cardiol* 41:2288-2297.
223. Terasaka, N., M. Westerterp, J. Koetsveld, C. Fernandez-Hernando, L. Yvan-Charvet, N. Wang, W. C. Sessa, and A. R. Tall. 2010. ATP-binding cassette transporter G1 and high-density lipoprotein promote endothelial NO synthesis through a decrease in the interaction of caveolin-1 and endothelial NO synthase. *Arterioscler Thromb Vasc Biol* 30:2219-2225.
224. Kimura, T., K. Sato, A. Kuwabara, H. Tomura, M. Ishiwara, I. Kobayashi, M. Ui, and F. Okajima. 2001. Sphingosine 1-phosphate may be a major component of plasma lipoproteins responsible for the cytoprotective actions in human umbilical vein endothelial cells. *J Biol Chem* 276:31780-31785.
225. de Souza, J. A., C. Vindis, A. Negre-Salvayre, K. A. Rye, M. Couturier, P. Therond, S. Chantepie, R. Salvayre, M. J. Chapman, and A. Kontush. 2010. Small, dense HDL 3 particles attenuate apoptosis in endothelial cells: pivotal role of apolipoprotein A-I. *J Cell Mol Med* 14:608-620.
226. Suc, I., I. Escargueil-Blanc, M. Troly, R. Salvayre, and A. Negre-Salvayre. 1997. HDL and ApoA prevent cell death of endothelial cells induced by oxidized LDL. *Arterioscler Thromb Vasc Biol* 17:2158-2166.
227. Riwanto, M., L. Rohrer, B. Roschitzki, C. Besler, P. Mocharla, M. Mueller, D. Perisa, K. Heinrich, L. Altwegg, A. von Eckardstein, T. F. Luscher, and U. Landmesser. 2013. Altered activation of endothelial anti- and proapoptotic pathways by high-density lipoprotein from patients with coronary artery disease: role of high-density lipoprotein-proteome remodeling. *Circulation* 127:891-904.
228. Sugano, M., K. Tsuchida, and N. Makino. 2000. High-density lipoproteins protect endothelial cells from tumor necrosis factor-alpha-induced apoptosis. *Biochem Biophys Res Commun* 272:872-876.
229. Nofer, J. R., B. Levkau, I. Wolinska, R. Junker, M. Fobker, A. von Eckardstein, U. Seedorf, and G. Assmann. 2001. Suppression of endothelial cell apoptosis by high density lipoproteins (HDL) and HDL-associated lysosphingolipids. *J Biol Chem* 276:34480-34485.
230. Radojkovic, C., A. Genoux, V. Pons, G. Combes, H. de Jonge, E. Champagne, C. Rolland, B. Perret, X. Collet, F. Terce, and L. O. Martinez. 2009. Stimulation of cell surface F1-ATPase activity by apolipoprotein A-I inhibits endothelial cell apoptosis and promotes proliferation. *Arterioscler Thromb Vasc Biol* 29:1125-1130.
231. Argraves, K. M., P. J. Gazzolo, E. M. Groh, B. A. Wilkerson, B. S. Matsuura, W. O. Twal, S. M. Hammad, and W. S. Argraves. 2008. High density lipoprotein-associated

sphingosine 1-phosphate promotes endothelial barrier function. *J Biol Chem* 283:25074-25081.

232. Wilkerson, B. A., G. D. Grass, S. B. Wing, W. S. Argraves, and K. M. Argraves. 2012. Sphingosine 1-phosphate (S1P) carrier-dependent regulation of endothelial barrier: high density lipoprotein (HDL)-S1P prolongs endothelial barrier enhancement as compared with albumin-S1P via effects on levels, trafficking, and signaling of S1P1. *J Biol Chem* 287:44645-44653.
233. Seetharam, D., C. Mineo, A. K. Gormley, L. L. Gibson, W. Vongpatanasin, K. L. Chambliss, L. D. Hahner, M. L. Cummings, R. L. Kitchens, Y. L. Marcel, D. J. Rader, and P. W. Shaul. 2006. High-density lipoprotein promotes endothelial cell migration and reendothelialization via scavenger receptor-B type I. *Circulation research* 98:63-72.
234. Zhu, W., S. Saddar, D. Seetharam, K. L. Chambliss, C. Longoria, D. L. Silver, I. S. Yuhanna, P. W. Shaul, and C. Mineo. 2008. The scavenger receptor class B type I adaptor protein PDZK1 maintains endothelial monolayer integrity. *Circulation research* 102:480-487.
235. Tatematsu, S., S. A. Francis, P. Natarajan, D. J. Rader, A. Saghatelian, J. D. Brown, T. Michel, and J. Plutzky. 2013. Endothelial lipase is a critical determinant of high-density lipoprotein-stimulated sphingosine 1-phosphate-dependent signaling in vascular endothelium. *Arterioscler Thromb Vasc Biol* 33:1788-1794.
236. Petoumenos, V., G. Nickenig, and N. Werner. 2009. High-density lipoprotein exerts vasculoprotection via endothelial progenitor cells. *J Cell Mol Med* 13:4623-4635.
237. Sumi, M., M. Sata, S. Miura, K. A. Rye, N. Toya, Y. Kanaoka, K. Yanaga, T. Ohki, K. Saku, and R. Nagai. 2007. Reconstituted high-density lipoprotein stimulates differentiation of endothelial progenitor cells and enhances ischemia-induced angiogenesis. *Arterioscler Thromb Vasc Biol* 27:813-818.
238. Zhang, Q., H. Yin, P. Liu, H. Zhang, and M. She. 2010. Essential role of HDL on endothelial progenitor cell proliferation with PI3K/Akt/cyclin D1 as the signal pathway. *Exp Biol Med (Maywood)* 235:1082-1092.
239. Mineo, C., and P. W. Shaul. 2007. Role of high-density lipoprotein and scavenger receptor B type I in the promotion of endothelial repair. *Trends Cardiovasc Med* 17:156-161.
240. Naqvi, T. Z., P. K. Shah, P. A. Ivey, M. D. Molloy, A. M. Thomas, S. Panicker, A. Ahmed, B. Cercek, and S. Kaul. 1999. Evidence that high-density lipoprotein cholesterol is an independent predictor of acute platelet-dependent thrombus formation. *Am J Cardiol* 84:1011-1017.
241. Doggen, C. J., N. L. Smith, R. N. Lemaitre, S. R. Heckbert, F. R. Rosendaal, and B. M. Psaty. 2004. Serum lipid levels and the risk of venous thrombosis. *Arterioscler Thromb Vasc Biol* 24:1970-1975.
242. Deguchi, H., N. M. Pecheniuk, D. J. Elias, P. M. Averell, and J. H. Griffin. 2005. High-density lipoprotein deficiency and dyslipoproteinemia associated with venous thrombosis in men. *Circulation* 112:893-899.
243. Calkin, A. C., B. G. Drew, A. Ono, S. J. Duffy, M. V. Gordon, S. M. Schoenwaelder, D. Sviridov, M. E. Cooper, B. A. Kingwell, and S. P. Jackson. 2009. Reconstituted high-density lipoprotein attenuates platelet function in individuals with type 2 diabetes mellitus by promoting cholesterol efflux. *Circulation* 120:2095-2104.
244. Li, D., S. Weng, B. Yang, D. S. Zander, T. Saldeen, W. W. Nichols, S. Khan, and J. L. Mehta. 1999. Inhibition of arterial thrombus formation by ApoA1 Milano. *Arterioscler Thromb Vasc Biol* 19:378-383.
245. Murphy, A. J., N. Bijl, L. Yvan-Charvet, C. B. Welch, N. Bhagwat, A. Reheman, Y. Wang, J. A. Shaw, R. L. Levine, H. Ni, A. R. Tall, and N. Wang. 2013. Cholesterol efflux

in megakaryocyte progenitors suppresses platelet production and thrombocytosis. *Nat Med* 19:586-594.

246. Brodde, M. F., S. J. Korporaal, G. Herminghaus, M. Fobker, T. J. Van Berkel, U. J. Tietge, H. Robenek, M. Van Eck, B. E. Kehrel, and J. R. Nofer. 2011. Native high-density lipoproteins inhibit platelet activation via scavenger receptor BI: role of negatively charged phospholipids. *Atherosclerosis* 215:374-382.
247. Brill, A., A. Yesilaltay, S. F. De Meyer, J. Kisucka, T. A. Fuchs, O. Kocher, M. Krieger, and D. D. Wagner. 2012. Extrahepatic high-density lipoprotein receptor SR-BI and apoA-I protect against deep vein thrombosis in mice. *Arterioscler Thromb Vasc Biol* 32:1841-1847.
248. Zhang, Q. H., X. Y. Zu, R. X. Cao, J. H. Liu, Z. C. Mo, Y. Zeng, Y. B. Li, S. L. Xiong, X. Liu, D. F. Liao, and G. H. Yi. 2012. An involvement of SR-B1 mediated PI3K-Akt-eNOS signaling in HDL-induced cyclooxygenase 2 expression and prostacyclin production in endothelial cells. *Biochem Biophys Res Commun* 420:17-23.
249. Liu, D., L. Ji, X. Tong, B. Pan, J. Y. Han, Y. Huang, Y. E. Chen, S. Pennathur, Y. Zhang, and L. Zheng. 2011. Human apolipoprotein A-I induces cyclooxygenase-2 expression and prostaglandin I-2 release in endothelial cells through ATP-binding cassette transporter A1. *Am J Physiol Cell Physiol* 301:C739-748.
250. Deguchi, H., S. Yegneswaran, and J. H. Griffin. 2004. Sphingolipids as bioactive regulators of thrombin generation. *J Biol Chem* 279:12036-12042.
251. Williams, K. J., and I. Tabas. 1995. The response-to-retention hypothesis of early atherogenesis. *Arterioscler Thromb Vasc Biol* 15:551-561.
252. Stocker, R., and J. F. Keaney, Jr. 2004. Role of oxidative modifications in atherosclerosis. *Physiol Rev* 84:1381-1478.
253. Navab, M., S. Y. Hama, G. M. Anantharamaiah, K. Hassan, G. P. Hough, A. D. Watson, S. T. Reddy, A. Sevanian, G. C. Fonarow, and A. M. Fogelman. 2000. Normal high density lipoprotein inhibits three steps in the formation of mildly oxidized low density lipoprotein: steps 2 and 3. *J Lipid Res* 41:1495-1508.
254. Navab, M., S. Y. Hama, C. J. Cooke, G. M. Anantharamaiah, M. Chaddha, L. Jin, G. Subbanagounder, K. F. Faull, S. T. Reddy, N. E. Miller, and A. M. Fogelman. 2000. Normal high density lipoprotein inhibits three steps in the formation of mildly oxidized low density lipoprotein: step 1. *J Lipid Res* 41:1481-1494.
255. Garner, B., A. R. Waldeck, P. K. Witting, K. A. Rye, and R. Stocker. 1998. Oxidation of high density lipoproteins. II. Evidence for direct reduction of lipid hydroperoxides by methionine residues of apolipoproteins AI and AII. *J Biol Chem* 273:6088-6095.
256. Liu, Y., B. Mackness, and M. Mackness. 2008. Comparison of the ability of paraoxonases 1 and 3 to attenuate the in vitro oxidation of low-density lipoprotein and reduce macrophage oxidative stress. *Free Radic Biol Med* 45:743-748.
257. Watson, A. D., J. A. Berliner, S. Y. Hama, B. N. La Du, K. F. Faull, A. M. Fogelman, and M. Navab. 1995. Protective effect of high density lipoprotein associated paraoxonase. Inhibition of the biological activity of minimally oxidized low density lipoprotein. *J Clin Invest* 96:2882-2891.
258. Tward, A., Y. R. Xia, X. P. Wang, Y. S. Shi, C. Park, L. W. Castellani, A. J. Lusis, and D. M. Shih. 2002. Decreased atherosclerotic lesion formation in human serum paraoxonase transgenic mice. *Circulation* 106:484-490.
259. Shih, D. M., L. Gu, Y. R. Xia, M. Navab, W. F. Li, S. Hama, L. W. Castellani, C. E. Furlong, L. G. Costa, A. M. Fogelman, and A. J. Lusis. 1998. Mice lacking serum paraoxonase are susceptible to organophosphate toxicity and atherosclerosis. *Nature* 394:284-287.
260. Watson, A. D., M. Navab, S. Y. Hama, A. Sevanian, S. M. Prescott, D. M. Stafforini, T. M. McIntyre, B. N. Du, A. M. Fogelman, and J. A. Berliner. 1995. Effect of platelet

activating factor-acetylhydrolase on the formation and action of minimally oxidized low density lipoprotein. *The Journal of clinical investigation* 95:774-782.

261. Noto, H., M. Hara, K. Karasawa, O. N. Iso, H. Satoh, M. Togo, Y. Hashimoto, Y. Yamada, T. Kosaka, M. Kawamura, S. Kimura, and K. Tsukamoto. 2003. Human plasma platelet-activating factor acetylhydrolase binds to all the murine lipoproteins, conferring protection against oxidative stress. *Arterioscler Thromb Vasc Biol* 23:829-835.
262. Sabatine, M. S., D. A. Morrow, M. O'Donoghue, K. A. Jablonksi, M. M. Rice, S. Solomon, Y. Rosenberg, M. J. Domanski, and J. Hsia. 2007. Prognostic utility of lipoprotein-associated phospholipase A2 for cardiovascular outcomes in patients with stable coronary artery disease. *Arterioscler Thromb Vasc Biol* 27:2463-2469.
263. Brilakis, E. S., J. P. McConnell, R. J. Lennon, A. A. Elesber, J. G. Meyer, and P. B. Berger. 2005. Association of lipoprotein-associated phospholipase A2 levels with coronary artery disease risk factors, angiographic coronary artery disease, and major adverse events at follow-up. *Eur Heart J* 26:137-144.
264. Koenig, W., N. Khuseyinova, H. Lowel, G. Trischler, and C. Meisinger. 2004. Lipoprotein-associated phospholipase A2 adds to risk prediction of incident coronary events by C-reactive protein in apparently healthy middle-aged men from the general population: results from the 14-year follow-up of a large cohort from southern Germany. *Circulation* 110:1903-1908.
265. Tellis, C. C., and A. D. Tselepis. 2009. The role of lipoprotein-associated phospholipase A2 in atherosclerosis may depend on its lipoprotein carrier in plasma. *Biochim Biophys Acta* 1791:327-338.
266. Rallidis, L. S., C. C. Tellis, J. Lekakis, I. Rizos, C. Varounis, A. Charalampopoulos, M. Zolindaki, N. Dagres, M. Anastasiou-Nana, and A. D. Tselepis. 2012. Lipoprotein-associated phospholipase A(2) bound on high-density lipoprotein is associated with lower risk for cardiac death in stable coronary artery disease patients: a 3-year follow-up. *J Am Coll Cardiol* 60:2053-2060.
267. Vohl, M. C., T. A. Neville, R. Kumarathasan, S. Braschi, and D. L. Sparks. 1999. A novel lecithin-cholesterol acyltransferase antioxidant activity prevents the formation of oxidized lipids during lipoprotein oxidation. *Biochemistry* 38:5976-5981.
268. Mertens, A., P. Verhamme, J. K. Bielicki, M. C. Phillips, R. Quarck, W. Verreth, D. Stengel, E. Ninio, M. Navab, B. Mackness, M. Mackness, and P. Holvoet. 2003. Increased low-density lipoprotein oxidation and impaired high-density lipoprotein antioxidant defense are associated with increased macrophage homing and atherosclerosis in dyslipidemic obese mice: LCAT gene transfer decreases atherosclerosis. *Circulation* 107:1640-1646.
269. Yvan-Charvet, L., T. Pagler, E. L. Gautier, S. Avagyan, R. L. Siry, S. Han, C. L. Welch, N. Wang, G. J. Randolph, H. W. Snoeck, and A. R. Tall. 2010. ATP-binding cassette transporters and HDL suppress hematopoietic stem cell proliferation. *Science* 328:1689-1693.
270. Westerterp, M., S. Gourion-Arsiquaud, A. J. Murphy, A. Shih, S. Cremers, R. L. Levine, A. R. Tall, and L. Yvan-Charvet. 2012. Regulation of hematopoietic stem and progenitor cell mobilization by cholesterol efflux pathways. *Cell Stem Cell* 11:195-206.
271. Bursill, C. A., M. L. Castro, D. T. Beattie, S. Nakhla, E. van der Vorst, A. K. Heather, P. J. Barter, and K. A. Rye. 2010. High-density lipoproteins suppress chemokines and chemokine receptors in vitro and in vivo. *Arterioscler Thromb Vasc Biol* 30:1773-1778.

272. Spirig, R., A. Schaub, A. Kropf, S. Miescher, M. O. Spycher, and R. Rieben. 2013. Reconstituted high-density lipoprotein modulates activation of human leukocytes. *PLoS One* 8:e71235.
273. Tolle, M., A. Pawlak, M. Schuchardt, A. Kawamura, U. J. Tietge, S. Lorkowski, P. Keul, G. Assmann, J. Chun, B. Levkau, M. van der Giet, and J. R. Nofer. 2008. HDL-associated lysosphingolipids inhibit NAD(P)H oxidase-dependent monocyte chemoattractant protein-1 production. *Arterioscler Thromb Vasc Biol* 28:1542-1548.
274. Murphy, A. J., K. J. Woollard, A. Hoang, N. Mukhamedova, R. A. Stirzaker, S. P. McCormick, A. T. Remaley, D. Sviridov, and J. Chin-Dusting. 2008. High-density lipoprotein reduces the human monocyte inflammatory response. *Arterioscler Thromb Vasc Biol* 28:2071-2077.
275. Shaw, J. A., A. Bobik, A. Murphy, P. Kanellakis, P. Blombery, N. Mukhamedova, K. Woollard, S. Lyon, D. Sviridov, and A. M. Dart. 2008. Infusion of reconstituted high-density lipoprotein leads to acute changes in human atherosclerotic plaque. *Circulation research* 103:1084-1091.
276. Cockerill, G. W., T. Y. Huehns, A. Weerasinghe, C. Stocker, P. G. Lerch, N. E. Miller, and D. O. Haskard. 2001. Elevation of plasma high-density lipoprotein concentration reduces interleukin-1-induced expression of E-selectin in an in vivo model of acute inflammation. *Circulation* 103:108-112.
277. Ashby, D. T., K. A. Rye, M. A. Clay, M. A. Vadas, J. R. Gamble, and P. J. Barter. 1998. Factors influencing the ability of HDL to inhibit expression of vascular cell adhesion molecule-1 in endothelial cells. *Arterioscler Thromb Vasc Biol* 18:1450-1455.
278. Clay, M. A., D. H. Pyle, K. A. Rye, M. A. Vadas, J. R. Gamble, and P. J. Barter. 2001. Time sequence of the inhibition of endothelial adhesion molecule expression by reconstituted high density lipoproteins. *Atherosclerosis* 157:23-29.
279. Nicholls, S. J., G. J. Dusting, B. Cutri, S. Bao, G. R. Drummond, K. A. Rye, and P. J. Barter. 2005. Reconstituted high-density lipoproteins inhibit the acute pro-oxidant and proinflammatory vascular changes induced by a periarterial collar in normocholesterolemic rabbits. *Circulation* 111:1543-1550.
280. Puranik, R., S. Bao, E. Nobecourt, S. J. Nicholls, G. J. Dusting, P. J. Barter, D. S. Celermajer, and K. A. Rye. 2008. Low dose apolipoprotein A-I rescues carotid arteries from inflammation in vivo. *Atherosclerosis* 196:240-247.
281. Nofer, J. R., S. Geigenmuller, C. Gopfert, G. Assmann, E. Buddecke, and A. Schmidt. 2003. High density lipoprotein-associated lysosphingolipids reduce E-selectin expression in human endothelial cells. *Biochem Biophys Res Commun* 310:98-103.
282. Kimura, T., H. Tomura, C. Mogi, A. Kuwabara, A. Damirin, T. Ishizuka, A. Sekiguchi, M. Ishiwara, D. S. Im, K. Sato, M. Murakami, and F. Okajima. 2006. Role of scavenger receptor class B type I and sphingosine 1-phosphate receptors in high density lipoprotein-induced inhibition of adhesion molecule expression in endothelial cells. *J Biol Chem* 281:37457-37467.
283. Xia, P., M. A. Vadas, K. A. Rye, P. J. Barter, and J. R. Gamble. 1999. High density lipoproteins (HDL) interrupt the sphingosine kinase signaling pathway. A possible mechanism for protection against atherosclerosis by HDL. *J Biol Chem* 274:33143-33147.
284. Park, S. H., J. H. Park, J. S. Kang, and Y. H. Kang. 2003. Involvement of transcription factors in plasma HDL protection against TNF-alpha-induced vascular cell adhesion molecule-1 expression. *Int J Biochem Cell Biol* 35:168-182.
285. McGrath, K. C., X. H. Li, R. Puranik, E. C. Liong, J. T. Tan, V. M. Dy, B. A. DiBartolo, P. J. Barter, K. A. Rye, and A. K. Heather. 2009. Role of 3beta-hydroxysteroid-delta 24 reductase in mediating antiinflammatory effects of high-density lipoproteins in endothelial cells. *Arterioscler Thromb Vasc Biol* 29:877-882.

286. Wu, B. J., K. Chen, S. Shrestha, K. L. Ong, P. J. Barter, and K. A. Rye. 2013. High-density lipoproteins inhibit vascular endothelial inflammation by increasing 3beta-hydroxysteroid-Delta24 reductase expression and inducing heme oxygenase-1. *Circulation research* 112:278-288.
287. Tabet, F., K. C. Vickers, L. F. Cuesta Torres, C. B. Wiese, B. M. Shoucri, G. Lambert, C. Catherinet, L. Prado-Lourenco, M. G. Levin, S. Thacker, P. Sethupathy, P. J. Barter, A. T. Remaley, and K. A. Rye. 2014. HDL-transferred microRNA-223 regulates ICAM-1 expression in endothelial cells. *Nat Commun* 5:3292.
288. Norata, G. D., A. Pirillo, E. Ammirati, and A. L. Catapano. 2012. Emerging role of high density lipoproteins as a player in the immune system. *Atherosclerosis* 220:11-21.
289. Norata, G. D., A. Pirillo, and A. L. Catapano. 2011. HDLs, immunity, and atherosclerosis. *Curr Opin Lipidol* 22:410-416.
290. Iwasaki, A., and R. Medzhitov. 2015. Control of adaptive immunity by the innate immune system. *Nat Immunol* 16:343-353.
291. Shiflett, A. M., J. R. Bishop, A. Pahwa, and S. L. Hajduk. 2005. Human high density lipoproteins are platforms for the assembly of multi-component innate immune complexes. *J Biol Chem* 280:32578-32585.
292. Beck, W. H., C. P. Adams, I. M. Biglang-Awa, A. B. Patel, H. Vincent, E. J. Haas-Stapleton, and P. M. Weers. 2013. Apolipoprotein A-I binding to anionic vesicles and lipopolysaccharides: role for lysine residues in antimicrobial properties. *Biochim Biophys Acta* 1828:1503-1510.
293. Mathison, J. C., and R. J. Ulevitch. 1979. The clearance, tissue distribution, and cellular localization of intravenously injected lipopolysaccharide in rabbits. *J Immunol* 123:2133-2143.
294. Levine, D. M., T. S. Parker, T. M. Donnelly, A. Walsh, and A. L. Rubin. 1993. In vivo protection against endotoxin by plasma high density lipoprotein. *Proc Natl Acad Sci U S A* 90:12040-12044.
295. Wang, Y., X. Zhu, G. Wu, L. Shen, and B. Chen. 2008. Effect of lipid-bound apoA-I cysteine mutants on lipopolysaccharide-induced endotoxemia in mice. *J Lipid Res* 49:1640-1645.
296. Jiao, Y. L., and M. P. Wu. 2008. Apolipoprotein A-I diminishes acute lung injury and sepsis in mice induced by lipoteichoic acid. *Cytokine* 43:83-87.
297. Triantafilou, M., K. Miyake, D. T. Golenbock, and K. Triantafilou. 2002. Mediators of innate immune recognition of bacteria concentrate in lipid rafts and facilitate lipopolysaccharide-induced cell activation. *J Cell Sci* 115:2603-2611.
298. Smythies, L. E., C. R. White, A. Maheshwari, M. N. Palgunachari, G. M. Anantharamaiah, M. Chaddha, A. R. Kurundkar, and G. Datta. 2010. Apolipoprotein A-I mimetic 4F alters the function of human monocyte-derived macrophages. *Am J Physiol Cell Physiol* 298:C1538-1548.
299. Cheng, A. M., P. Handa, S. Tateya, J. Schwartz, C. Tang, P. Mitra, J. F. Oram, A. Chait, and F. Kim. 2012. Apolipoprotein A-I attenuates palmitate-mediated NF-kappaB activation by reducing Toll-like receptor-4 recruitment into lipid rafts. *PLoS One* 7:e33917.
300. Murphy, A. J., K. J. Woollard, A. Suhartoyo, R. A. Stirzaker, J. Shaw, D. Sviridov, and J. P. Chin-Dusting. 2011. Neutrophil activation is attenuated by high-density lipoprotein and apolipoprotein A-I in in vitro and in vivo models of inflammation. *Arterioscler Thromb Vasc Biol* 31:1333-1341.
301. Randolph, G. J., C. Jakubzick, and C. Qu. 2008. Antigen presentation by monocytes and monocyte-derived cells. *Curr Opin Immunol* 20:52-60.
302. van Niel, G., R. Wubbolts, and W. Stoorvogel. 2008. Endosomal sorting of MHC class II determines antigen presentation by dendritic cells. *Curr Opin Cell Biol* 20:437-444.

303. Catapano, A. L., A. Pirillo, F. Bonacina, and G. D. Norata. 2014. HDL in innate and adaptive immunity. *Cardiovascular research* 103:372-383.
304. Liu, G., and H. Yang. 2013. Modulation of macrophage activation and programming in immunity. *J Cell Physiol* 228:502-512.
305. Yan, Z. Q., and G. K. Hansson. 2007. Innate immunity, macrophage activation, and atherosclerosis. *Immunol Rev* 219:187-203.
306. Medzhitov, R., and T. Horng. 2009. Transcriptional control of the inflammatory response. *Nat Rev Immunol* 9:692-703.
307. Sanson, M., E. Distel, and E. A. Fisher. 2013. HDL induces the expression of the M2 macrophage markers arginase 1 and Fizz-1 in a STAT6-dependent process. *PLoS One* 8:e74676.
308. Hughes, J. E., S. Srinivasan, K. R. Lynch, R. L. Proia, P. Ferdek, and C. C. Hedrick. 2008. Sphingosine-1-phosphate induces an antiinflammatory phenotype in macrophages. *Circulation research* 102:950-958.
309. Suzuki, M., D. K. Pritchard, L. Becker, A. N. Hoofnagle, N. Tanimura, T. K. Bammler, R. P. Beyer, R. Bumgarner, T. Vaisar, M. C. de Beer, F. C. de Beer, K. Miyake, J. F. Oram, and J. W. Heinecke. 2010. High-density lipoprotein suppresses the type I interferon response, a family of potent antiviral immunoregulators, in macrophages challenged with lipopolysaccharide. *Circulation* 122:1919-1927.
310. De Nardo, D., L. I. Labzin, H. Kono, R. Seki, S. V. Schmidt, M. Beyer, D. Xu, S. Zimmer, C. Lahrmann, F. A. Schildberg, J. Vogelhuber, M. Kraut, T. Ulas, A. Kerksiek, W. Krebs, N. Bode, A. Grebe, M. L. Fitzgerald, N. J. Hernandez, B. R. Williams, P. Knolle, M. Kneilling, M. Rocken, D. Lutjohann, S. D. Wright, J. L. Schultze, and E. Latz. 2014. High-density lipoprotein mediates anti-inflammatory reprogramming of macrophages via the transcriptional regulator ATF3. *Nature immunology* 15:152-160.
311. Koseki, M., K. Hirano, D. Masuda, C. Ikegami, M. Tanaka, A. Ota, J. C. Sandoval, Y. Nakagawa-Toyama, S. B. Sato, T. Kobayashi, Y. Shimada, Y. Ohno-Iwashita, F. Matsuura, I. Shimomura, and S. Yamashita. 2007. Increased lipid rafts and accelerated lipopolysaccharide-induced tumor necrosis factor-alpha secretion in Abca1-deficient macrophages. *J Lipid Res* 48:299-306.
312. Zhu, X., J. Y. Lee, J. M. Timmins, J. M. Brown, E. Boudyguina, A. Mulya, A. K. Gebre, M. C. Willingham, E. M. Hiltbold, N. Mishra, N. Maeda, and J. S. Parks. 2008. Increased cellular free cholesterol in macrophage-specific Abca1 knock-out mice enhances pro-inflammatory response of macrophages. *J Biol Chem* 283:22930-22941.
313. Zhu, X., J. S. Owen, M. D. Wilson, H. Li, G. L. Griffiths, M. J. Thomas, E. M. Hiltbold, M. B. Fessler, and J. S. Parks. 2010. Macrophage ABCA1 reduces MyD88-dependent Toll-like receptor trafficking to lipid rafts by reduction of lipid raft cholesterol. *J Lipid Res* 51:3196-3206.
314. Yvan-Charvet, L., C. Welch, T. A. Pagler, M. Ranalletta, M. Lamkanfi, S. Han, M. Ishibashi, R. Li, N. Wang, and A. R. Tall. 2008. Increased inflammatory gene expression in ABC transporter-deficient macrophages: free cholesterol accumulation, increased signaling via toll-like receptors, and neutrophil infiltration of atherosclerotic lesions. *Circulation* 118:1837-1847.
315. Guermonprez, P., J. Valladeau, L. Zitvogel, C. Thery, and S. Amigorena. 2002. Antigen presentation and T cell stimulation by dendritic cells. *Annu Rev Immunol* 20:621-667.
316. Veldhoen, M., R. J. Hocking, C. J. Atkins, R. M. Locksley, and B. Stockinger. 2006. TGFbeta in the context of an inflammatory cytokine milieu supports de novo differentiation of IL-17-producing T cells. *Immunity* 24:179-189.

317. Nurieva, R., X. O. Yang, G. Martinez, Y. Zhang, A. D. Panopoulos, L. Ma, K. Schluns, Q. Tian, S. S. Watowich, A. M. Jetten, and C. Dong. 2007. Essential autocrine regulation by IL-21 in the generation of inflammatory T cells. *Nature* 448:480-483.
318. Afkarian, M., J. R. Sedy, J. Yang, N. G. Jacobson, N. Cereb, S. Y. Yang, T. L. Murphy, and K. M. Murphy. 2002. T-bet is a STAT1-induced regulator of IL-12R expression in naive CD4+ T cells. *Nat Immunol* 3:549-557.
319. Kim, K. D., H. Y. Lim, H. G. Lee, D. Y. Yoon, Y. K. Choe, I. Choi, S. G. Paik, Y. S. Kim, Y. Yang, and J. S. Lim. 2005. Apolipoprotein A-I induces IL-10 and PGE2 production in human monocytes and inhibits dendritic cell differentiation and maturation. *Biochem Biophys Res Commun* 338:1126-1136.
320. Perrin-Cocon, L., O. Diaz, M. Carreras, S. Dollet, A. Guironnet-Paquet, P. Andre, and V. Lotteau. 2012. High-density lipoprotein phospholipids interfere with dendritic cell Th1 functional maturation. *Immunobiology* 217:91-99.
321. Eren, E., J. Yates, K. Cwynarski, S. Preston, R. Dong, C. Germain, R. Lechler, R. Huby, M. Ritter, and G. Lombardi. 2006. Location of major histocompatibility complex class II molecules in rafts on dendritic cells enhances the efficiency of T-cell activation and proliferation. *Scand J Immunol* 63:7-16.
322. Wang, S. H., S. G. Yuan, D. Q. Peng, and S. P. Zhao. 2012. HDL and ApoA-I inhibit antigen presentation-mediated T cell activation by disrupting lipid rafts in antigen presenting cells. *Atherosclerosis* 225:105-114.
323. Schaper, K., M. Kietzmann, and W. Baumer. 2014. Sphingosine-1-phosphate differently regulates the cytokine production of IL-12, IL-23 and IL-27 in activated murine bone marrow derived dendritic cells. *Mol Immunol* 59:10-18.
324. Gupta, N., and A. L. DeFranco. 2007. Lipid rafts and B cell signaling. *Semin Cell Dev Biol* 18:616-626.
325. Kabouridis, P. S., and E. C. Jury. 2008. Lipid rafts and T-lymphocyte function: implications for autoimmunity. *FEBS Lett* 582:3711-3718.
326. Dykstra, M. L., R. Longnecker, and S. K. Pierce. 2001. Epstein-Barr virus coopts lipid rafts to block the signaling and antigen transport functions of the BCR. *Immunity* 14:57-67.
327. Flores-Borja, F., P. S. Kabouridis, E. C. Jury, D. A. Isenberg, and R. A. Mageed. 2005. Decreased Lyn expression and translocation to lipid raft signaling domains in B lymphocytes from patients with systemic lupus erythematosus. *Arthritis and rheumatism* 52:3955-3965.
328. Wilhelm, A. J., M. Zabalawi, J. M. Grayson, A. E. Weant, A. S. Major, J. Owen, M. Bharadwaj, R. Walzem, L. Chan, K. Oka, M. J. Thomas, and M. G. Sorci-Thomas. 2009. Apolipoprotein A-I and its role in lymphocyte cholesterol homeostasis and autoimmunity. *Arterioscler Thromb Vasc Biol* 29:843-849.
329. Wilhelm, A. J., M. Zabalawi, J. S. Owen, D. Shah, J. M. Grayson, A. S. Major, S. Bhat, D. P. Gibbs, Jr., M. J. Thomas, and M. G. Sorci-Thomas. 2010. Apolipoprotein A-I modulates regulatory T cells in autoimmune LDLr-/-, ApoA-I-/- mice. *The Journal of biological chemistry* 285:36158-36169.
330. Bensinger, S. J., M. N. Bradley, S. B. Joseph, N. Zelcer, E. M. Janssen, M. A. Hausner, R. Shih, J. S. Parks, P. A. Edwards, B. D. Jamieson, and P. Tontonoz. 2008. LXR signaling couples sterol metabolism to proliferation in the acquired immune response. *Cell* 134:97-111.
331. Mandala, S., R. Hajdu, J. Bergstrom, E. Quackenbush, J. Xie, J. Milligan, R. Thornton, G. J. Shei, D. Card, C. Keohane, M. Rosenbach, J. Hale, C. L. Lynch, K. Rupprecht, W. Parsons, and H. Rosen. 2002. Alteration of lymphocyte trafficking by sphingosine-1-phosphate receptor agonists. *Science* 296:346-349.

332. Liu, G., K. Yang, S. Burns, S. Shrestha, and H. Chi. 2010. The S1P(1)-mTOR axis directs the reciprocal differentiation of T(H)1 and T(reg) cells. *Nat Immunol* 11:1047-1056.
333. Weigert, A., N. Weis, and B. Brune. 2009. Regulation of macrophage function by sphingosine-1-phosphate. *Immunobiology* 214:748-760.
334. Ammirati, E., D. Cianflone, M. Banfi, V. Vecchio, A. Palini, M. De Metrio, G. Marenzi, C. Panciroli, G. Tumminello, A. Anzuini, A. Palloshi, L. Grigore, K. Garlaschelli, S. Tramontana, D. Tavano, F. Airoldi, A. A. Manfredi, A. L. Catapano, and G. D. Norata. 2010. Circulating CD4+CD25hiCD127lo regulatory T-Cell levels do not reflect the extent or severity of carotid and coronary atherosclerosis. *Arterioscler Thromb Vasc Biol* 30:1832-1841.
335. Charles-Schoeman, C., J. Watanabe, Y. Y. Lee, D. E. Furst, S. Amjadi, D. Elashoff, G. Park, M. McMahon, H. E. Paulus, A. M. Fogelman, and S. T. Reddy. 2009. Abnormal function of high-density lipoprotein is associated with poor disease control and an altered protein cargo in rheumatoid arthritis. *Arthritis and rheumatism* 60:2870-2879.
336. McMahon, M., J. Grossman, J. FitzGerald, E. Dahlin-Lee, D. J. Wallace, B. Y. Thong, H. Badsha, K. Kalunian, C. Charles, M. Navab, A. M. Fogelman, and B. H. Hahn. 2006. Proinflammatory high-density lipoprotein as a biomarker for atherosclerosis in patients with systemic lupus erythematosus and rheumatoid arthritis. *Arthritis and rheumatism* 54:2541-2549.
337. Petri, M., S. Perez-Gutthann, D. Spence, and M. C. Hochberg. 1992. Risk factors for coronary artery disease in patients with systemic lupus erythematosus. *The American journal of medicine* 93:513-519.
338. Shoenfeld, Y., R. Gerli, A. Doria, E. Matsuura, M. M. Cerinic, N. Ronda, L. J. Jara, M. Abu-Shakra, P. L. Meroni, and Y. Sherer. 2005. Accelerated atherosclerosis in autoimmune rheumatic diseases. *Circulation* 112:3337-3347.
339. Cederholm, A., E. Svenungsson, D. Stengel, G. Z. Fei, A. G. Pockley, E. Ninio, and J. Frostegard. 2004. Platelet-activating factor-acetylhydrolase and other novel risk and protective factors for cardiovascular disease in systemic lupus erythematosus. *Arthritis and rheumatism* 50:2869-2876.
340. van Leuven, S. I., R. Hezemans, J. H. Levels, S. Snoek, P. C. Stokkers, G. K. Hovingh, J. J. Kastelein, E. S. Stroes, E. de Groot, and D. W. Hommes. 2007. Enhanced atherogenesis and altered high density lipoprotein in patients with Crohn's disease. *J Lipid Res* 48:2640-2646.
341. Sappati Biyyani, R. S., B. S. Putka, and K. D. Mullen. 2010. Dyslipidemia and lipoprotein profiles in patients with inflammatory bowel disease. *J Clin Lipidol* 4:478-482.
342. Pan, B., Y. Ma, H. Ren, Y. He, Y. Wang, X. Lv, D. Liu, L. Ji, B. Yu, Y. E. Chen, S. Pennathur, J. D. Smith, G. Liu, and L. Zheng. 2012. Diabetic HDL is dysfunctional in stimulating endothelial cell migration and proliferation due to down regulation of SR-BI expression. *PLoS One* 7:e48530.
343. Kruit, J. K., L. R. Brunham, C. B. Verchere, and M. R. Hayden. 2010. HDL and LDL cholesterol significantly influence beta-cell function in type 2 diabetes mellitus. *Curr Opin Lipidol* 21:178-185.
344. Norata, G. D., and A. L. Catapano. 2012. HDL and adaptive immunity: a tale of lipid rafts. *Atherosclerosis* 225:34-35.
345. Yunt, Z. X., and J. J. Solomon. 2015. Lung Disease in Rheumatoid Arthritis. *Rheum Dis Clin North Am* 41:225-236.
346. Vuilleumier, N., S. Bas, S. Pagano, F. Montecucco, P. A. Guerne, A. Finckh, C. Lovis, F. Mach, D. Hochstrasser, P. Roux-Lombard, and C. Gabay. 2010. Anti-apolipoprotein A-

1 IgG predicts major cardiovascular events in patients with rheumatoid arthritis. *Arthritis and rheumatism* 62:2640-2650.

347. McInnes, I. B., and G. Schett. 2007. Cytokines in the pathogenesis of rheumatoid arthritis. *Nat Rev Immunol* 7:429-442.
348. Robertson, J., M. J. Peters, I. B. McInnes, and N. Sattar. 2013. Changes in lipid levels with inflammation and therapy in RA: a maturing paradigm. *Nature reviews. Rheumatology* 9:513-523.
349. Watanabe, J., C. Charles-Schoeman, Y. Miao, D. Elashoff, Y. Y. Lee, G. Katselis, T. D. Lee, and S. T. Reddy. 2012. Proteomic profiling following immunoaffinity capture of high-density lipoprotein: association of acute-phase proteins and complement factors with proinflammatory high-density lipoprotein in rheumatoid arthritis. *Arthritis and rheumatism* 64:1828-1837.
350. Ronda, N., E. Favari, M. O. Borghi, F. Ingegnoli, M. Gerosa, C. Chighizola, F. Zimetti, M. P. Adorni, F. Bernini, and P. L. Meroni. 2014. Impaired serum cholesterol efflux capacity in rheumatoid arthritis and systemic lupus erythematosus. *Annals of the rheumatic diseases* 73:609-615.
351. Charles-Schoeman, C., Y. Y. Lee, V. Grijalva, S. Amjadi, J. FitzGerald, V. K. Ranganath, M. Taylor, M. McMahon, H. E. Paulus, and S. T. Reddy. 2012. Cholesterol efflux by high density lipoproteins is impaired in patients with active rheumatoid arthritis. *Annals of the rheumatic diseases* 71:1157-1162.
352. Charles-Schoeman, C., M. L. Banquerigo, S. Hama, M. Navab, G. S. Park, B. J. Van Lenten, A. C. Wagner, A. M. Fogelman, and E. Brahn. 2008. Treatment with an apolipoprotein A-1 mimetic peptide in combination with pravastatin inhibits collagen-induced arthritis. *Clinical immunology* 127:234-244.
353. Wu, B. J., K. L. Ong, S. Shrestha, K. Chen, F. Tabet, P. J. Barter, and K. A. Rye. 2014. Inhibition of arthritis in the Lewis rat by apolipoprotein A-I and reconstituted high-density lipoproteins. *Arterioscler Thromb Vasc Biol* 34:543-551.
354. Skeoch, S., and I. N. Bruce. 2015. Atherosclerosis in rheumatoid arthritis: is it all about inflammation? *Nature reviews. Rheumatology*.
355. Khovidhunkit, W., M. S. Kim, R. A. Memon, J. K. Shigenaga, A. H. Moser, K. R. Feingold, and C. Grunfeld. 2004. Effects of infection and inflammation on lipid and lipoprotein metabolism: mechanisms and consequences to the host. *J Lipid Res* 45:1169-1196.
356. Navab, M., S. T. Reddy, B. J. Van Lenten, and A. M. Fogelman. 2011. HDL and cardiovascular disease: atherogenic and atheroprotective mechanisms. *Nat Rev Cardiol* 8:222-232.
357. Van Lenten, B. J., S. Y. Hama, F. C. de Beer, D. M. Stafforini, T. M. McIntyre, S. M. Prescott, B. N. La Du, A. M. Fogelman, and M. Navab. 1995. Anti-inflammatory HDL becomes pro-inflammatory during the acute phase response. Loss of protective effect of HDL against LDL oxidation in aortic wall cell cocultures. *The Journal of clinical investigation* 96:2758-2767.
358. Annema, W., N. Nijstad, M. Tolle, J. F. de Boer, R. V. Buijs, P. Heeringa, M. van der Giet, and U. J. Tietge. 2010. Myeloperoxidase and serum amyloid A contribute to impaired in vivo reverse cholesterol transport during the acute phase response but not group IIA secretory phospholipase A(2). *J Lipid Res* 51:743-754.
359. Chiba, T., M. Y. Chang, S. Wang, T. N. Wight, T. S. McMillen, J. F. Oram, T. Vaisar, J. W. Heinecke, F. C. De Beer, M. C. De Beer, and A. Chait. 2011. Serum amyloid A facilitates the binding of high-density lipoprotein from mice injected with lipopolysaccharide to vascular proteoglycans. *Arterioscler Thromb Vasc Biol* 31:1326-1332.

360. Vuilleumier, N., J. M. Dayer, A. von Eckardstein, and P. Roux-Lombard. 2013. Pro- or anti-inflammatory role of apolipoprotein A-1 in high-density lipoproteins? *Swiss Med Wkly* 143:w13781.
361. Fisher, E. A., J. E. Feig, B. Hewing, S. L. Hazen, and J. D. Smith. 2012. High-density lipoprotein function, dysfunction, and reverse cholesterol transport. *Arterioscler Thromb Vasc Biol* 32:2813-2820.
362. Daugherty, A., J. L. Dunn, D. L. Rateri, and J. W. Heinecke. 1994. Myeloperoxidase, a catalyst for lipoprotein oxidation, is expressed in human atherosclerotic lesions. *The Journal of clinical investigation* 94:437-444.
363. Shao, B. 2012. Site-specific oxidation of apolipoprotein A-I impairs cholesterol export by ABCA1, a key cardioprotective function of HDL. *Biochim Biophys Acta* 1821:490-501.
364. Brennan, M. L., M. S. Penn, F. Van Lente, V. Nambi, M. H. Shishehbor, R. J. Aviles, M. Goormastic, M. L. Pepoy, E. S. McErlean, E. J. Topol, S. E. Nissen, and S. L. Hazen. 2003. Prognostic value of myeloperoxidase in patients with chest pain. *The New England journal of medicine* 349:1595-1604.
365. Rudolph, V., T. Keller, A. Schulz, F. Ojeda, T. K. Rudolph, S. Tzikas, C. Bickel, T. Meinertz, T. Munzel, S. Blankenberg, and S. Baldus. 2012. Diagnostic and prognostic performance of myeloperoxidase plasma levels compared with sensitive troponins in patients admitted with acute onset chest pain. *Circ Cardiovasc Genet* 5:561-568.
366. Zheng, L., B. Nukuna, M. L. Brennan, M. Sun, M. Goormastic, M. Settle, D. Schmitt, X. Fu, L. Thomson, P. L. Fox, H. Ischiropoulos, J. D. Smith, M. Kinter, and S. L. Hazen. 2004. Apolipoprotein A-I is a selective target for myeloperoxidase-catalyzed oxidation and functional impairment in subjects with cardiovascular disease. *The Journal of clinical investigation* 114:529-541.
367. Wang, Z., S. J. Nicholls, E. R. Rodriguez, O. Kummu, S. Horkko, J. Barnard, W. F. Reynolds, E. J. Topol, J. A. DiDonato, and S. L. Hazen. 2007. Protein carbamylation links inflammation, smoking, uremia and atherogenesis. *Nat Med* 13:1176-1184.
368. Holzer, M., M. Gauster, T. Pfeifer, C. Wadsack, G. Fauler, P. Stiegler, H. Koefeler, E. Beubler, R. Schuligoi, A. Heinemann, and G. Marsche. 2011. Protein carbamylation renders high-density lipoprotein dysfunctional. *Antioxid Redox Signal* 14:2337-2346.
369. Bergt, C., S. Pennathur, X. Fu, J. Byun, K. O'Brien, T. O. McDonald, P. Singh, G. M. Anantharamaiah, A. Chait, J. Brunzell, R. L. Geary, J. F. Oram, and J. W. Heinecke. 2004. The myeloperoxidase product hypochlorous acid oxidizes HDL in the human artery wall and impairs ABCA1-dependent cholesterol transport. *Proc Natl Acad Sci U S A* 101:13032-13037.
370. Pennathur, S., C. Bergt, B. Shao, J. Byun, S. Y. Kassim, P. Singh, P. S. Green, T. O. McDonald, J. Brunzell, A. Chait, J. F. Oram, K. O'Brien, R. L. Geary, and J. W. Heinecke. 2004. Human atherosclerotic intima and blood of patients with established coronary artery disease contain high density lipoprotein damaged by reactive nitrogen species. *J Biol Chem* 279:42977-42983.
371. Hazell, L. J., L. Arnold, D. Flowers, G. Waeg, E. Malle, and R. Stocker. 1996. Presence of hypochlorite-modified proteins in human atherosclerotic lesions. *The Journal of clinical investigation* 97:1535-1544.
372. Zheng, L., M. Settle, G. Brubaker, D. Schmitt, S. L. Hazen, J. D. Smith, and M. Kinter. 2005. Localization of nitration and chlorination sites on apolipoprotein A-I catalyzed by myeloperoxidase in human atheroma and associated oxidative impairment in ABCA1-dependent cholesterol efflux from macrophages. *J Biol Chem* 280:38-47.
373. Wu, Z., M. A. Wagner, L. Zheng, J. S. Parks, J. M. Shy, 3rd, J. D. Smith, V. Gogonea, and S. L. Hazen. 2007. The refined structure of nascent HDL reveals a key functional domain for particle maturation and dysfunction. *Nat Struct Mol Biol* 14:861-868.

374. Shao, B., G. Cavigiolio, N. Brot, M. N. Oda, and J. W. Heinecke. 2008. Methionine oxidation impairs reverse cholesterol transport by apolipoprotein A-I. *Proc Natl Acad Sci U S A* 105:12224-12229.
375. Undurti, A., Y. Huang, J. A. Lupica, J. D. Smith, J. A. DiDonato, and S. L. Hazen. 2009. Modification of high density lipoprotein by myeloperoxidase generates a pro-inflammatory particle. *J Biol Chem* 284:30825-30835.
376. Fogelman, A. M. 2004. When good cholesterol goes bad. *Nat Med* 10:902-903.
377. Shao, B., S. Pennathur, and J. W. Heinecke. 2012. Myeloperoxidase targets apolipoprotein A-I, the major high density lipoprotein protein, for site-specific oxidation in human atherosclerotic lesions. *J Biol Chem* 287:6375-6386.
378. Shao, B., C. Tang, A. Sinha, P. S. Mayer, G. D. Davenport, N. Brot, M. N. Oda, X. Q. Zhao, and J. W. Heinecke. 2014. Humans with atherosclerosis have impaired ABCA1 cholesterol efflux and enhanced high-density lipoprotein oxidation by myeloperoxidase. *Circulation research* 114:1733-1742.
379. Shao, B., C. Bergt, X. Fu, P. Green, J. C. Voss, M. N. Oda, J. F. Oram, and J. W. Heinecke. 2005. Tyrosine 192 in apolipoprotein A-I is the major site of nitration and chlorination by myeloperoxidase, but only chlorination markedly impairs ABCA1-dependent cholesterol transport. *J Biol Chem* 280:5983-5993.
380. Shao, B., M. N. Oda, C. Bergt, X. Fu, P. S. Green, N. Brot, J. F. Oram, and J. W. Heinecke. 2006. Myeloperoxidase impairs ABCA1-dependent cholesterol efflux through methionine oxidation and site-specific tyrosine chlorination of apolipoprotein A-I. *J Biol Chem* 281:9001-9004.
381. Hawkins, C. L., D. I. Pattison, and M. J. Davies. 2003. Hypochlorite-induced oxidation of amino acids, peptides and proteins. *Amino Acids* 25:259-274.
382. Levine, R. L., L. Mosoni, B. S. Berlett, and E. R. Stadtman. 1996. Methionine residues as endogenous antioxidants in proteins. *Proc Natl Acad Sci U S A* 93:15036-15040.
383. Aulchenko, Y. S., S. Ripatti, I. Lindqvist, D. Boomsma, I. M. Heid, P. P. Pramstaller, B. W. Penninx, A. C. Janssens, J. F. Wilson, T. Spector, N. G. Martin, N. L. Pedersen, K. O. Kyvik, J. Kaprio, A. Hofman, N. B. Freimer, M. R. Jarvelin, U. Gyllensten, H. Campbell, I. Rudan, A. Johansson, F. Marroni, C. Hayward, V. Vitart, I. Jonasson, C. Pattaro, A. Wright, N. Hastie, I. Pichler, A. A. Hicks, M. Falchi, G. Willemsen, J. J. Hottenga, E. J. de Geus, G. W. Montgomery, J. Whitfield, P. Magnusson, J. Saharinen, M. Perola, K. Silander, A. Isaacs, E. J. Sijbrands, A. G. Uitterlinden, J. C. Witteman, B. A. Oostra, P. Elliott, A. Ruokonen, C. Sabatti, C. Gieger, T. Meitinger, F. Kronenberg, A. Doring, H. E. Wichmann, J. H. Smit, M. I. McCarthy, C. M. van Duijn, and L. Peltonen. 2009. Loci influencing lipid levels and coronary heart disease risk in 16 European population cohorts. *Nat Genet* 41:47-55.
384. Kathiresan, S., C. J. Willer, G. M. Peloso, S. Demissie, K. Musunuru, E. E. Schadt, L. Kaplan, D. Bennett, Y. Li, T. Tanaka, B. F. Voight, L. L. Bonnycastle, A. U. Jackson, G. Crawford, A. Surti, C. Guiducci, N. P. Burtt, S. Parish, R. Clarke, D. Zelenika, K. A. Kubalanza, M. A. Morken, L. J. Scott, H. M. Stringham, P. Galan, A. J. Swift, J. Kuusisto, R. N. Bergman, J. Sundvall, M. Laakso, L. Ferrucci, P. Scheet, S. Sanna, M. Uda, Q. Yang, K. L. Lunetta, J. Dupuis, P. I. de Bakker, C. J. O'Donnell, J. C. Chambers, J. S. Kooner, S. Hercberg, P. Meneton, E. G. Lakatta, A. Scuteri, D. Schlessinger, J. Tuomilehto, F. S. Collins, L. Groop, D. Altshuler, R. Collins, G. M. Lathrop, O. Melander, V. Salomaa, L. Peltonen, M. Orho-Melander, J. M. Ordovas, M. Boehnke, G. R. Abecasis, K. L. Mohlke, and L. A. Cupples. 2009. Common variants at 30 loci contribute to polygenic dyslipidemia. *Nat Genet* 41:56-65.
385. Kathiresan, S., O. Melander, C. Guiducci, A. Surti, N. P. Burtt, M. J. Rieder, G. M. Cooper, C. Roos, B. F. Voight, A. S. Havulinna, B. Wahlstrand, T. Hedner, D. Corella, E. S. Tai, J. M. Ordovas, G. Berglund, E. Vartiainen, P. Jousilahti, B. Hedblad, M. R.

Taskinen, C. Newton-Cheh, V. Salomaa, L. Peltonen, L. Groop, D. M. Altshuler, and M. Orho-Melander. 2008. Six new loci associated with blood low-density lipoprotein cholesterol, high-density lipoprotein cholesterol or triglycerides in humans. *Nat Genet* 40:189-197.

386. Willer, C. J., S. Sanna, A. U. Jackson, A. Scuteri, L. L. Bonnycastle, R. Clarke, S. C. Heath, N. J. Timpson, S. S. Najjar, H. M. Stringham, J. Strait, W. L. Duren, A. Maschio, F. Busonero, A. Mulas, G. Albai, A. J. Swift, M. A. Morken, N. Narisu, D. Bennett, S. Parish, H. Shen, P. Galan, P. Meneton, S. Hercberg, D. Zelenika, W. M. Chen, Y. Li, L. J. Scott, P. A. Scheet, J. Sundvall, R. M. Watanabe, R. Nagaraja, S. Ebrahim, D. A. Lawlor, Y. Ben-Shlomo, G. Davey-Smith, A. R. Shuldiner, R. Collins, R. N. Bergman, M. Uda, J. Tuomilehto, A. Cao, F. S. Collins, E. Lakatta, G. M. Lathrop, M. Boehnke, D. Schlessinger, K. L. Mohlke, and G. R. Abecasis. 2008. Newly identified loci that influence lipid concentrations and risk of coronary artery disease. *Nat Genet* 40:161-169.

387. Teslovich, T. M., K. Musunuru, A. V. Smith, A. C. Edmondson, I. M. Stylianou, M. Koseki, J. P. Pirruccello, S. Ripatti, D. I. Chasman, C. J. Willer, C. T. Johansen, S. W. Fouchier, A. Isaacs, G. M. Peloso, M. Barbalic, S. L. Ricketts, J. C. Bis, Y. S. Aulchenko, G. Thorleifsson, M. F. Feitosa, J. Chambers, M. Orho-Melander, O. Melander, T. Johnson, X. Li, X. Guo, M. Li, Y. Shin Cho, M. Jin Go, Y. Jin Kim, J. Y. Lee, T. Park, K. Kim, X. Sim, R. Twee-Hee Ong, D. C. Croteau-Chonka, L. A. Lange, J. D. Smith, K. Song, J. Hua Zhao, X. Yuan, J. Luan, C. Lamina, A. Ziegler, W. Zhang, R. Y. Zee, A. F. Wright, J. C. Witteman, J. F. Wilson, G. Willemsen, H. E. Wichmann, J. B. Whitfield, D. M. Waterworth, N. J. Wareham, G. Waeber, P. Vollenweider, B. F. Voight, V. Vitart, A. G. Uitterlinden, M. Uda, J. Tuomilehto, J. R. Thompson, T. Tanaka, I. Surakka, H. M. Stringham, T. D. Spector, N. Soranzo, J. H. Smit, J. Sinisalo, K. Silander, E. J. Sijbrands, A. Scuteri, J. Scott, D. Schlessinger, S. Sanna, V. Salomaa, J. Saharinen, C. Sabatti, A. Ruokonen, I. Rudan, L. M. Rose, R. Roberts, M. Rieder, B. M. Psaty, P. P. Pramstaller, I. Pichler, M. Perola, B. W. Penninx, N. L. Pedersen, C. Pattaro, A. N. Parker, G. Pare, B. A. Oostra, C. J. O'Donnell, M. S. Nieminen, D. A. Nickerson, G. W. Montgomery, T. Meitinger, R. McPherson, M. I. McCarthy, W. McArdle, D. Masson, N. G. Martin, F. Marroni, M. Mangino, P. K. Magnusson, G. Lucas, R. Luben, R. J. Loos, M. L. Lokki, G. Lettre, C. Langenberg, L. J. Launer, E. G. Lakatta, R. Laaksonen, K. O. Kyvik, F. Kronenberg, I. R. Konig, K. T. Khaw, J. Kaprio, L. M. Kaplan, A. Johansson, M. R. Jarvelin, A. C. Janssens, E. Ingelsson, W. Igl, G. Kees Hovingh, J. J. Hottenga, A. Hofman, A. A. Hicks, C. Hengstenberg, I. M. Heid, C. Hayward, A. S. Havulinna, N. D. Hastie, T. B. Harris, T. Haritunians, A. S. Hall, U. Gyllensten, C. Guiducci, L. C. Groop, E. Gonzalez, C. Gieger, N. B. Freimer, L. Ferrucci, J. Erdmann, P. Elliott, K. G. Ejebe, A. Doring, A. F. Dominiczak, S. Demissie, P. Deloukas, E. J. de Geus, U. de Faire, G. Crawford, F. S. Collins, Y. D. Chen, M. J. Caulfield, H. Campbell, N. P. Burtt, L. L. Bonnycastle, D. I. Boomsma, S. M. Boekholdt, R. N. Bergman, I. Barroso, S. Bandinelli, C. M. Ballantyne, T. L. Assimes, T. Quertermous, D. Altshuler, M. Seielstad, T. Y. Wong, E. S. Tai, A. B. Feranil, C. W. Kuzawa, L. S. Adair, H. A. Taylor, Jr., I. B. Borecki, S. B. Gabriel, J. G. Wilson, H. Holm, U. Thorsteinsdottir, V. Gudnason, R. M. Krauss, K. L. Mohlke, J. M. Ordovas, P. B. Munroe, J. S. Kooner, A. R. Tall, R. A. Hegele, J. J. Kastelein, E. E. Schadt, J. I. Rotter, E. Boerwinkle, D. P. Strachan, V. Mooser, K. Stefansson, M. P. Reilly, N. J. Samani, H. Schunkert, L. A. Cupples, M. S. Sandhu, P. M. Ridker, D. J. Rader, C. M. van Duijn, L. Peltonen, G. R. Abecasis, M. Boehnke, and S. Kathiresan. 2010. Biological, clinical and population relevance of 95 loci for blood lipids. *Nature* 466:707-713.

388. Ku, C. S., E. Y. Loy, Y. Pawitan, and K. S. Chia. 2010. The pursuit of genome-wide association studies: where are we now? *J Hum Genet* 55:195-206.

389. Tai, E. S., X. L. Sim, T. H. Ong, T. Y. Wong, S. M. Saw, T. Aung, S. Kathiresan, M. Orho-Melander, J. M. Ordovas, J. T. Tan, and M. Seielstad. 2009. Polymorphisms at newly identified lipid-associated loci are associated with blood lipids and cardiovascular disease in an Asian Malay population. *J Lipid Res* 50:514-520.
390. Polgar, N., L. Jaromi, V. Csongei, A. Maasz, C. Sipeky, E. Safrany, M. Szabo, and B. Melegh. 2010. Triglyceride level modifying functional variants of GALTN2 and MLXIPL in patients with ischaemic stroke. *Eur J Neurol* 17:1033-1039.
391. White, T., E. P. Bennett, K. Takio, T. Sorensen, N. Bonding, and H. Clausen. 1995. Purification and cDNA cloning of a human UDP-N-acetyl-alpha-D-galactosamine:polypeptide N-acetylgalactosaminyltransferase. *J Biol Chem* 270:24156-24165.
392. Ten Hagen, K. G., T. A. Fritz, and L. A. Tabak. 2003. All in the family: the UDP-GalNAc:polypeptide N-acetylgalactosaminyltransferases. *Glycobiology* 13:1R-16R.
393. Breton, C., J. Mucha, and C. Jeanneau. 2001. Structural and functional features of glycosyltransferases. *Biochimie* 83:713-718.
394. Vaith, P., G. Assmann, and G. Uhlenbruck. 1978. Characterization of the oligosaccharide side chain of apolipoprotein C-III from human plasma very low density lipoproteins. *Biochim Biophys Acta* 541:234-240.
395. Magrane, J., R. P. Casaroli-Marano, M. Reina, M. Gafvels, and S. Vilaro. 1999. The role of O-linked sugars in determining the very low density lipoprotein receptor stability or release from the cell. *FEBS Lett* 451:56-62.
396. Schindler, P. A., C. A. Settineri, X. Collet, C. J. Fielding, and A. L. Burlingame. 1995. Site-specific detection and structural characterization of the glycosylation of human plasma proteins lecithin:cholesterol acyltransferase and apolipoprotein D using HPLC/electrospray mass spectrometry and sequential glycosidase digestion. *Protein Sci* 4:791-803.
397. Goldstein, J. L., M. S. Brown, R. G. Anderson, D. W. Russell, and W. J. Schneider. 1985. Receptor-mediated endocytosis: concepts emerging from the LDL receptor system. *Annu Rev Cell Biol* 1:1-39.
398. Holleboom, A. G., H. Karlsson, R. S. Lin, T. M. Beres, J. A. Sierts, D. S. Herman, E. S. Stroes, J. M. Aerts, J. J. Kastelein, M. M. Motazacker, G. M. Dallinga-Thie, J. H. Levels, A. H. Zwinderman, J. G. Seidman, C. E. Seidman, S. Ljunggren, D. J. Lefeber, E. Morava, R. A. Wevers, T. A. Fritz, L. A. Tabak, M. Lindahl, G. K. Hovingh, and J. A. Kuivenhoven. 2011. Heterozygosity for a loss-of-function mutation in GALNT2 improves plasma triglyceride clearance in man. *Cell metabolism* 14:811-818.
399. Shimizugawa, T., M. Ono, M. Shimamura, K. Yoshida, Y. Ando, R. Koishi, K. Ueda, T. Inaba, H. Minekura, T. Kohama, and H. Furukawa. 2002. ANGPTL3 decreases very low density lipoprotein triglyceride clearance by inhibition of lipoprotein lipase. *J Biol Chem* 277:33742-33748.
400. Shimamura, M., M. Matsuda, H. Yasumo, M. Okazaki, K. Fujimoto, K. Kono, T. Shimizugawa, Y. Ando, R. Koishi, T. Kohama, N. Sakai, K. Kotani, R. Komuro, T. Ishida, K. Hirata, S. Yamashita, H. Furukawa, and I. Shimomura. 2007. Angiopoietin-like protein3 regulates plasma HDL cholesterol through suppression of endothelial lipase. *Arterioscler Thromb Vasc Biol* 27:366-372.
401. Schjoldager, K. T., M. B. Vester-Christensen, E. P. Bennett, S. B. Levery, T. Schwientek, W. Yin, O. Blixt, and H. Clausen. 2010. O-glycosylation modulates proprotein convertase activation of angiopoietin-like protein 3: possible role of polypeptide GalNAc-transferase-2 in regulation of concentrations of plasma lipids. *J Biol Chem* 285:36293-36303.
402. Ono, M., T. Shimizugawa, M. Shimamura, K. Yoshida, C. Noji-Sakikawa, Y. Ando, R. Koishi, and H. Furukawa. 2003. Protein region important for regulation of lipid

metabolism in angiopoietin-like 3 (ANGPTL3): ANGPTL3 is cleaved and activated in vivo. *J Biol Chem* 278:41804-41809.

403. Keys, A. 1980. W. O. Atwater memorial lecture: overweight, obesity, coronary heart disease and mortality. *Nutr Rev* 38:297-307.
404. Vest, A. R., H. M. Heneghan, S. Agarwal, P. R. Schauer, and J. B. Young. 2012. Bariatric surgery and cardiovascular outcomes: a systematic review. *Heart* 98:1763-1777.
405. Kodama, S., S. Tanaka, K. Saito, M. Shu, Y. Sone, F. Onitake, E. Suzuki, H. Shimano, S. Yamamoto, K. Kondo, Y. Ohashi, N. Yamada, and H. Sone. 2007. Effect of aerobic exercise training on serum levels of high-density lipoprotein cholesterol: a meta-analysis. *Arch Intern Med* 167:999-1008.
406. Craig, W. Y., G. E. Palomaki, and J. E. Haddow. 1989. Cigarette smoking and serum lipid and lipoprotein concentrations: an analysis of published data. *BMJ* 298:784-788.
407. Barter, P. J., G. Brandrup-Wognsen, M. K. Palmer, and S. J. Nicholls. 2010. Effect of statins on HDL-C: a complex process unrelated to changes in LDL-C: analysis of the VOYAGER Database. *J Lipid Res* 51:1546-1553.
408. Khoury, N., and A. C. Goldberg. 2011. The use of fibric Acid derivatives in cardiovascular prevention. *Curr Treat Options Cardiovasc Med* 13:335-342.
409. Vega, G. L., and S. M. Grundy. 1994. Lipoprotein responses to treatment with lovastatin, gemfibrozil, and nicotinic acid in normolipidemic patients with hypoalphalipoproteinemia. *Arch Intern Med* 154:73-82.
410. Kastelein, J. J., S. I. van Leuven, L. Burgess, G. W. Evans, J. A. Kuivenhoven, P. J. Barter, J. H. Revkin, D. E. Grobbee, W. A. Riley, C. L. Shear, W. T. Duggan, and M. L. Bots. 2007. Effect of torcetrapib on carotid atherosclerosis in familial hypercholesterolemia. *The New England journal of medicine* 356:1620-1630.
411. Schwartz, G. G., A. G. Olsson, M. Abt, C. M. Ballantyne, P. J. Barter, J. Brumm, B. R. Chaitman, I. M. Holme, D. Kallend, L. A. Leiter, E. Leitersdorf, J. J. McMurray, H. Mundl, S. J. Nicholls, P. K. Shah, J. C. Tardif, and R. S. Wright. 2012. Effects of dalcetrapib in patients with a recent acute coronary syndrome. *The New England journal of medicine* 367:2089-2099.
412. Cannon, C. P., S. Shah, H. M. Dansky, M. Davidson, E. A. Brinton, A. M. Gotto, M. Stepanavage, S. X. Liu, P. Gibbons, T. B. Ashraf, J. Zafarino, Y. Mitchel, and P. Barter. 2010. Safety of anacetrapib in patients with or at high risk for coronary heart disease. *The New England journal of medicine* 363:2406-2415.
413. Henry, R. R., A. M. Lincoff, S. Mudaliar, M. Rabbia, C. Chognot, and M. Herz. 2009. Effect of the dual peroxisome proliferator-activated receptor-alpha/gamma agonist aleglitazar on risk of cardiovascular disease in patients with type 2 diabetes (SYNCHRONY): a phase II, randomised, dose-ranging study. *Lancet* 374:126-135.
414. Fruchart, J. C. 2013. Selective peroxisome proliferator-activated receptor alpha modulators (SPPARMalpha): the next generation of peroxisome proliferator-activated receptor alpha-agonists. *Cardiovasc Diabetol* 12:82.
415. Terasaka, N., A. Hiroshima, T. Koieyama, N. Ubukata, Y. Morikawa, D. Nakai, and T. Inaba. 2003. T-0901317, a synthetic liver X receptor ligand, inhibits development of atherosclerosis in LDL receptor-deficient mice. *FEBS Lett* 536:6-11.
416. Joseph, S. B., E. McKilligin, L. Pei, M. A. Watson, A. R. Collins, B. A. Laffitte, M. Chen, G. Noh, J. Goodman, G. N. Hagger, J. Tran, T. K. Tippin, X. Wang, A. J. Lusis, W. A. Hsueh, R. E. Law, J. L. Collins, T. M. Willson, and P. Tontonoz. 2002. Synthetic LXR ligand inhibits the development of atherosclerosis in mice. *Proc Natl Acad Sci U S A* 99:7604-7609.

417. Joseph, S. B., A. Castrillo, B. A. Laffitte, D. J. Mangelsdorf, and P. Tontonoz. 2003. Reciprocal regulation of inflammation and lipid metabolism by liver X receptors. *Nat Med* 9:213-219.
418. Zelcer, N., N. Khanlou, R. Clare, Q. Jiang, E. G. Reed-Geaghan, G. E. Landreth, H. V. Vinters, and P. Tontonoz. 2007. Attenuation of neuroinflammation and Alzheimer's disease pathology by liver x receptors. *Proc Natl Acad Sci U S A* 104:10601-10606.
419. Calkin, A. C., and P. Tontonoz. 2012. Transcriptional integration of metabolism by the nuclear sterol-activated receptors LXR and FXR. *Nat Rev Mol Cell Biol* 13:213-224.
420. Graham, M. J., R. G. Lee, T. A. Bell, 3rd, W. Fu, A. E. Mullick, V. J. Alexander, W. Singleton, N. Viney, R. Geary, J. Su, B. F. Baker, J. Burkey, S. T. Crooke, and R. M. Crooke. 2013. Antisense oligonucleotide inhibition of apolipoprotein C-III reduces plasma triglycerides in rodents, nonhuman primates, and humans. *Circulation research* 112:1479-1490.
421. Kastelein, J. J., M. K. Wedel, B. F. Baker, J. Su, J. D. Bradley, R. Z. Yu, E. Chuang, M. J. Graham, and R. M. Crooke. 2006. Potent reduction of apolipoprotein B and low-density lipoprotein cholesterol by short-term administration of an antisense inhibitor of apolipoprotein B. *Circulation* 114:1729-1735.
422. Raal, F. J., R. D. Santos, D. J. Blom, A. D. Marais, M. J. Charng, W. C. Cromwell, R. H. Lachmann, D. Gaudet, J. L. Tan, S. Chasan-Taber, D. L. Tribble, J. D. Flaim, and S. T. Crooke. 2010. Mipomersen, an apolipoprotein B synthesis inhibitor, for lowering of LDL cholesterol concentrations in patients with homozygous familial hypercholesterolaemia: a randomised, double-blind, placebo-controlled trial. *Lancet* 375:998-1006.
423. Sehgal, A., A. Vaishnaw, and K. Fitzgerald. 2013. Liver as a target for oligonucleotide therapeutics. *J Hepatol* 59:1354-1359.
424. Rottiers, V., S. Obad, A. Petri, R. McGarrah, M. W. Lindholm, J. C. Black, S. Sinha, R. J. Goody, M. S. Lawrence, A. S. deLemos, H. F. Hansen, S. Whittaker, S. Henry, R. Brookes, S. H. Najafi-Shoushtari, R. T. Chung, J. R. Whetstine, R. E. Gerszten, S. Kauppinen, and A. M. Naar. 2013. Pharmacological inhibition of a microRNA family in nonhuman primates by a seed-targeting 8-mer antimiR. *Sci Transl Med* 5:212ra162.
425. de Aguiar Vallim, T. Q., E. J. Tarling, T. Kim, M. Civelek, A. Baldan, C. Esau, and P. A. Edwards. 2013. MicroRNA-144 regulates hepatic ATP binding cassette transporter A1 and plasma high-density lipoprotein after activation of the nuclear receptor farnesoid X receptor. *Circulation research* 112:1602-1612.
426. Wang, D., M. Xia, X. Yan, D. Li, L. Wang, Y. Xu, T. Jin, and W. Ling. 2012. Gut microbiota metabolism of anthocyanin promotes reverse cholesterol transport in mice via repressing miRNA-10b. *Circulation research* 111:967-981.
427. Catapano, A. L., and N. Papadopoulos. 2013. The safety of therapeutic monoclonal antibodies: implications for cardiovascular disease and targeting the PCSK9 pathway. *Atherosclerosis* 228:18-28.
428. Thomas, L. J., R. A. Hammond, E. M. Forsberg, K. M. Geoghegan-Barek, B. H. Karalius, H. C. Marsh, Jr., and C. W. Rittershaus. 2009. Co-administration of a CpG adjuvant (VaxImmune, CPG 7909) with CETP vaccines increased immunogenicity in rabbits and mice. *Hum Vaccin* 5:79-84.
429. Kramer, W. 2013. Novel drug approaches in development for the treatment of lipid disorders. *Exp Clin Endocrinol Diabetes* 121:567-580.
430. Jin, W., J. S. Millar, U. Broedl, J. M. Glick, and D. J. Rader. 2003. Inhibition of endothelial lipase causes increased HDL cholesterol levels in vivo. *The Journal of clinical investigation* 111:357-362.

431. Navab, M., G. M. Anantharamaiah, S. Hama, D. W. Garber, M. Chaddha, G. Hough, R. Lallone, and A. M. Fogelman. 2002. Oral administration of an Apo A-I mimetic Peptide synthesized from D-amino acids dramatically reduces atherosclerosis in mice independent of plasma cholesterol. *Circulation* 105:290-292.
432. Navab, M., G. M. Anantharamaiah, S. T. Reddy, S. Hama, G. Hough, V. R. Grijalva, A. C. Wagner, J. S. Frank, G. Datta, D. Garber, and A. M. Fogelman. 2004. Oral D-4F causes formation of pre-beta high-density lipoprotein and improves high-density lipoprotein-mediated cholesterol efflux and reverse cholesterol transport from macrophages in apolipoprotein E-null mice. *Circulation* 109:3215-3220.
433. Bloedon, L. T., R. Dunbar, D. Duffy, P. Pinell-Salles, R. Norris, B. J. DeGroot, R. Movva, M. Navab, A. M. Fogelman, and D. J. Rader. 2008. Safety, pharmacokinetics, and pharmacodynamics of oral apoA-I mimetic peptide D-4F in high-risk cardiovascular patients. *J Lipid Res* 49:1344-1352.
434. Watson, C. E., N. Weissbach, L. Kjems, S. Ayalasomayajula, Y. Zhang, I. Chang, M. Navab, S. Hama, G. Hough, S. T. Reddy, D. Soffer, D. J. Rader, A. M. Fogelman, and A. Schecter. 2011. Treatment of patients with cardiovascular disease with L-4F, an apo-A1 mimetic, did not improve select biomarkers of HDL function. *J Lipid Res* 52:361-373.
435. Chattopadhyay, A., M. Navab, G. Hough, F. Gao, D. Meriwether, V. Grijalva, J. R. Springstead, M. N. Palgnachari, R. Namiri-Kalantari, F. Su, B. J. Van Lenten, A. C. Wagner, G. M. Anantharamaiah, R. Farias-Eisner, S. T. Reddy, and A. M. Fogelman. 2013. A novel approach to oral apoA-I mimetic therapy. *J Lipid Res* 54:995-1010.
436. Navab, M., G. Hough, G. M. Buga, F. Su, A. C. Wagner, D. Meriwether, A. Chattopadhyay, F. Gao, V. Grijalva, J. S. Danciger, B. J. Van Lenten, E. Org, A. J. Lusis, C. Pan, G. M. Anantharamaiah, R. Farias-Eisner, S. S. Smyth, S. T. Reddy, and A. M. Fogelman. 2013. Transgenic 6F tomatoes act on the small intestine to prevent systemic inflammation and dyslipidemia caused by Western diet and intestinally derived lysophosphatidic acid. *J Lipid Res* 54:3403-3418.
437. Remaley, A. T., F. Thomas, J. A. Stonik, S. J. Demosky, S. E. Bark, E. B. Neufeld, A. V. Bocharov, T. G. Vishnyakova, A. P. Patterson, T. L. Eggerman, S. Santamarina-Fojo, and H. B. Brewer. 2003. Synthetic amphipathic helical peptides promote lipid efflux from cells by an ABCA1-dependent and an ABCA1-independent pathway. *J Lipid Res* 44:828-836.
438. Sethi, A. A., J. A. Stonik, F. Thomas, S. J. Demosky, M. Amar, E. Neufeld, H. B. Brewer, W. S. Davidson, W. D'Souza, D. Sviridov, and A. T. Remaley. 2008. Asymmetry in the lipid affinity of bihelical amphipathic peptides. A structural determinant for the specificity of ABCA1-dependent cholesterol efflux by peptides. *J Biol Chem* 283:32273-32282.
439. Amar, M. J., W. D'Souza, S. Turner, S. Demosky, D. Sviridov, J. Stonik, J. Luchoomun, J. Voogt, M. Hellerstein, and A. T. Remaley. 2010. 5A apolipoprotein mimetic peptide promotes cholesterol efflux and reduces atherosclerosis in mice. *J Pharmacol Exp Ther* 334:634-641.
440. Bielicki, J. K., H. Zhang, Y. Cortez, Y. Zheng, V. Narayanaswami, A. Patel, J. Johansson, and S. Azhar. 2010. A new HDL mimetic peptide that stimulates cellular cholesterol efflux with high efficiency greatly reduces atherosclerosis in mice. *J Lipid Res* 51:1496-1503.
441. Di Bartolo, B. A., L. Z. Vanags, J. T. Tan, S. Bao, K. A. Rye, P. J. Barter, and C. A. Bursill. 2011. The apolipoprotein A-I mimetic peptide, ETC-642, reduces chronic vascular inflammation in the rabbit. *Lipids Health Dis* 10:224.
442. Di Bartolo, B. A., S. J. Nicholls, S. Bao, K. A. Rye, A. K. Heather, P. J. Barter, and C. Bursill. 2011. The apolipoprotein A-I mimetic peptide ETC-642 exhibits anti-

inflammatory properties that are comparable to high density lipoproteins. *Atherosclerosis* 217:395-400.

443. Iwata, A., S. Miura, B. Zhang, S. Imaizumi, Y. Uehara, M. Shiomi, and K. Saku. 2011. Antiatherogenic effects of newly developed apolipoprotein A-I mimetic peptide/phospholipid complexes against aortic plaque burden in Watanabe-heritable hyperlipidemic rabbits. *Atherosclerosis* 218:300-307.
444. Badimon, J. J., L. Badimon, A. Galvez, R. Dische, and V. Fuster. 1989. High density lipoprotein plasma fractions inhibit aortic fatty streaks in cholesterol-fed rabbits. *Lab Invest* 60:455-461.
445. Badimon, J. J., L. Badimon, and V. Fuster. 1990. Regression of atherosclerotic lesions by high density lipoprotein plasma fraction in the cholesterol-fed rabbit. *The Journal of clinical investigation* 85:1234-1241.
446. Miyazaki, A., S. Sakuma, W. Morikawa, T. Takiue, F. Miake, T. Terano, M. Sakai, H. Hakamata, Y. Sakamoto, M. Natio, and et al. 1995. Intravenous injection of rabbit apolipoprotein A-I inhibits the progression of atherosclerosis in cholesterol-fed rabbits. *Arterioscler Thromb Vasc Biol* 15:1882-1888.
447. Ibanez B, G. C., Cimmino G, Santos-Gallego CG, Alique M, Pinero A, Vilahur G, Fuster V, Badimon L, Badimon JJ. 2012. Recombinant HDL(Milano) exerts greater antiinflammatory and plaque stabilizing properties than HDL(wild-type). *Atherosclerosis* 220:72-77.
448. Ameli, S., A. Hultgardh-Nilsson, B. Cercek, P. K. Shah, J. S. Forrester, H. Ageland, and J. Nilsson. 1994. Recombinant apolipoprotein A-I Milano reduces intimal thickening after balloon injury in hypercholesterolemic rabbits. *Circulation* 90:1935-1941.
449. Chiesa, G., E. Monteggia, M. Marchesi, P. Lorenzon, M. Laucello, V. Lorusso, C. Di Mario, E. Karvouni, R. S. Newton, C. L. Bisgaier, G. Franceschini, and C. R. Sirtori. 2002. Recombinant apolipoprotein A-I(Milano) infusion into rabbit carotid artery rapidly removes lipid from fatty streaks. *Circulation research* 90:974-980.
450. Shah, P. K., J. Nilsson, S. Kaul, M. C. Fishbein, H. Ageland, A. Hamsten, J. Johansson, F. Karpe, and B. Cercek. 1998. Effects of recombinant apolipoprotein A-I(Milano) on aortic atherosclerosis in apolipoprotein E-deficient mice. *Circulation* 97:780-785.
451. Shah, P. K., J. Yano, O. Reyes, K. Y. Chyu, S. Kaul, C. L. Bisgaier, S. Drake, and B. Cercek. 2001. High-dose recombinant apolipoprotein A-I(milano) mobilizes tissue cholesterol and rapidly reduces plaque lipid and macrophage content in apolipoprotein e-deficient mice. Potential implications for acute plaque stabilization. *Circulation* 103:3047-3050.
452. Soma, M. R., E. Donetti, C. Parolini, C. R. Sirtori, R. Fumagalli, and G. Franceschini. 1995. Recombinant apolipoprotein A-IMilano dimer inhibits carotid intimal thickening induced by perivascular manipulation in rabbits. *Circulation research* 76:405-411.
453. Nissen, S. E., T. Tsunoda, E. M. Tuzcu, P. Schoenhagen, C. J. Cooper, M. Yasin, G. M. Eaton, M. A. Lauer, W. S. Sheldon, C. L. Grines, S. Halpern, T. Crowe, J. C. Blankenship, and R. Kerensky. 2003. Effect of recombinant ApoA-I Milano on coronary atherosclerosis in patients with acute coronary syndromes: a randomized controlled trial. *JAMA* 290:2292-2300.
454. Easton, R., A. Gille, D. D'Andrea, R. Davis, S. D. Wright, and C. Shear. 2013. A multiple ascending dose study of CSL112, an infused formulation of ApoA-I. *J Clin Pharmacol* 54:301-310.
455. Goffinet M, T. C., Bluteau A, Boubekeur N, Baron R, Keyserling C, Barbaras R, Lalwani N, Dasseux J. 2012. Anti-atherosclerotic effect of CER-001, an engineered HDL-mimetic, in the high-fat diet-fed LDLr knock-out mouse. *Circulation* 126.

456. Sacks, F. M., L. L. Rudel, A. Conner, H. Akeefe, G. Kostner, T. Baki, G. Rothblat, M. de la Llera-Moya, B. Asztalos, T. Perlman, C. Zheng, P. Alaupovic, J. A. Maltais, and H. B. Brewer. 2009. Selective delipidation of plasma HDL enhances reverse cholesterol transport in vivo. *J Lipid Res* 50:894-907.
457. Luo, J., Z. L. Deng, X. Luo, N. Tang, W. X. Song, J. Chen, K. A. Sharff, H. H. Luu, R. C. Haydon, K. W. Kinzler, B. Vogelstein, and T. C. He. 2007. A protocol for rapid generation of recombinant adenoviruses using the AdEasy system. *Nat Protoc* 2:1236-1247.
458. Chroni, A., H. Y. Kan, K. E. Kypreos, I. N. Gorshkova, A. Shkodrani, and V. I. Zannis. 2004. Substitutions of glutamate 110 and 111 in the middle helix 4 of human apolipoprotein A-I (apoA-I) by alanine affect the structure and in vitro functions of apoA-I and induce severe hypertriglyceridemia in apoA-I-deficient mice. *Biochemistry* 43:10442-10457.
459. Matz, C. E., and A. Jonas. 1982. Micellar complexes of human apolipoprotein A-I with phosphatidylcholines and cholesterol prepared from cholate-lipid dispersions. *J Biol Chem* 257:4535-4540.
460. Laccotripe, M., S. C. Makrides, A. Jonas, and V. I. Zannis. 1997. The carboxyl-terminal hydrophobic residues of apolipoprotein A-I affect its rate of phospholipid binding and its association with high density lipoprotein. *J Biol Chem* 272:17511-17522.
461. Freeman, L. A. 2013. Native-native 2D gel electrophoresis for HDL subpopulation analysis. *Methods Mol Biol* 1027:353-367.
462. Lutz, M. B., N. Kukutsch, A. L. Ogilvie, S. Rossner, F. Koch, N. Romani, and G. Schuler. 1999. An advanced culture method for generating large quantities of highly pure dendritic cells from mouse bone marrow. *J Immunol Methods* 223:77-92.
463. Zal, T., A. Volkmann, and B. Stockinger. 1994. Mechanisms of tolerance induction in major histocompatibility complex class II-restricted T cells specific for a blood-borne self-antigen. *J Exp Med* 180:2089-2099.
464. Yan, C., R. H. Costa, J. E. Darnell, Jr., J. D. Chen, and T. A. Van Dyke. 1990. Distinct positive and negative elements control the limited hepatocyte and choroid plexus expression of transthyretin in transgenic mice. *EMBO J* 9:869-878.
465. Georgopoulos, S., A. McKee, H. Y. Kan, and V. I. Zannis. 2002. Generation and characterization of two transgenic mouse lines expressing human ApoE2 in neurons and glial cells. *Biochemistry* 41:9293-9301.
466. McNeish, J., R. J. Aiello, D. Guyot, T. Turi, C. Gabel, C. Aldinger, K. L. Hoppe, M. L. Roach, L. J. Royer, J. de Wet, C. Broccardo, G. Chimini, and O. L. Francone. 2000. High density lipoprotein deficiency and foam cell accumulation in mice with targeted disruption of ATP-binding cassette transporter-1. *Proc Natl Acad Sci U S A* 97:4245-4250.
467. Rigotti, A., B. L. Trigatti, M. Penman, H. Rayburn, J. Herz, and M. Krieger. 1997. A targeted mutation in the murine gene encoding the high density lipoprotein (HDL) receptor scavenger receptor class B type I reveals its key role in HDL metabolism. *Proc Natl Acad Sci U S A* 94:12610-12615.
468. Nishina, P. M., J. Verstuyft, and B. Paigen. 1990. Synthetic low and high fat diets for the study of atherosclerosis in the mouse. *J Lipid Res* 31:859-869.
469. Havel, R. J., H. A. Eder, and J. H. Bragdon. 1955. The distribution and chemical composition of ultracentrifugally separated lipoproteins in human serum. *The Journal of clinical investigation* 34:1345-1353.
470. Li, X., H. Y. Kan, S. Lavrentiadou, M. Krieger, and V. Zannis. 2002. Reconstituted discoidal ApoE-phospholipid particles are ligands for the scavenger receptor BI. The amino-terminal 1-165 domain of ApoE suffices for receptor binding. *J Biol Chem* 277:21149-21157.

471. Fielding, C. J., and P. E. Fielding. 1996. Two-dimensional nondenaturing electrophoresis of lipoproteins: applications to high-density lipoprotein speciation. *Methods Enzymol* 263:251-259.
472. Tsimihodimos, V., S. A. Karabina, A. P. Tambaki, E. Bairaktari, J. A. Goudevenos, M. J. Chapman, M. Elisaf, and A. D. Tselepis. 2002. Atorvastatin preferentially reduces LDL-associated platelet-activating factor acetylhydrolase activity in dyslipidemias of type IIA and type IIB. *Arterioscler Thromb Vasc Biol* 22:306-311.
473. Navab, M., S. Y. Hama, G. P. Hough, G. Subbanagounder, S. T. Reddy, and A. M. Fogelman. 2001. A cell-free assay for detecting HDL that is dysfunctional in preventing the formation of or inactivating oxidized phospholipids. *J Lipid Res* 42:1308-1317.
474. Williamson, R., D. Lee, J. Hagaman, and N. Maeda. 1992. Marked reduction of high density lipoprotein cholesterol in mice genetically modified to lack apolipoprotein A-I. *Proc Natl Acad Sci U S A* 89:7134-7138.
475. Iliopoulos, D., M. Kavousanaki, M. Ioannou, D. Boumpas, and P. Verginis. The negative costimulatory molecule PD-1 modulates the balance between immunity and tolerance via miR-21. *Eur J Immunol* 41:1754-1763.
476. van den Berg, W. B., L. A. Joosten, and P. L. van Lent. 2007. Murine antigen-induced arthritis. *Methods Mol Med* 136:243-253.
477. Hahn, B. H., J. Grossman, B. J. Ansell, B. J. Skaggs, and M. McMahon. 2008. Altered lipoprotein metabolism in chronic inflammatory states: proinflammatory high-density lipoprotein and accelerated atherosclerosis in systemic lupus erythematosus and rheumatoid arthritis. *Arthritis research & therapy* 10:213.
478. Lubberts, E., M. I. Koenders, and W. B. van den Berg. 2005. The role of T-cell interleukin-17 in conducting destructive arthritis: lessons from animal models. *Arthritis research & therapy* 7:29-37.
479. Schulze-Koops, H., and J. R. Kalden. 2001. The balance of Th1/Th2 cytokines in rheumatoid arthritis. *Best Pract Res Clin Rheumatol* 15:677-691.
480. Banchereau, J., and R. M. Steinman. 1998. Dendritic cells and the control of immunity. *Nature* 392:245-252.
481. Takeda, K., and S. Akira. 2004. TLR signaling pathways. *Semin Immunol* 16:3-9.
482. Mineo, C., and P. W. Shaul. 2013. Regulation of signal transduction by HDL. *Journal of lipid research* 54:2315-2324.
483. Yvan-Charvet, L., N. Wang, and A. R. Tall. 2010. Role of HDL, ABCA1, and ABCG1 transporters in cholesterol efflux and immune responses. *Arteriosclerosis, thrombosis, and vascular biology* 30:139-143.
484. Shah, A. S., L. Tan, J. L. Long, and W. S. Davidson. 2013. Proteomic diversity of high density lipoproteins: our emerging understanding of its importance in lipid transport and beyond. *J Lipid Res* 54:2575-2585.
485. Gordon, D. J., and B. M. Rifkind. 1989. High-density lipoprotein--the clinical implications of recent studies. *The New England journal of medicine* 321:1311-1316.
486. Gordon, T., W. P. Castelli, M. C. Hjortland, W. B. Kannel, and T. R. Dawber. 1977. High density lipoprotein as a protective factor against coronary heart disease. The Framingham Study. *The American journal of medicine* 62:707-714.
487. Riwanto, M., and U. Landmesser. 2013. High density lipoproteins and endothelial functions: mechanistic insights and alterations in cardiovascular disease. *Journal of lipid research* 54:3227-3243.
488. Sorci-Thomas, M. G., and M. J. Thomas. High density lipoprotein biogenesis, cholesterol efflux, and immune cell function. *Arteriosclerosis, thrombosis, and vascular biology* 32:2561-2565.

489. Besler, C., T. F. Luscher, and U. Landmesser. 2012. Molecular mechanisms of vascular effects of High-density lipoprotein: alterations in cardiovascular disease. *EMBO molecular medicine* 4:251-268.
490. Luscher, T. F., U. Landmesser, A. von Eckardstein, and A. M. Fogelman. 2014. High-density lipoprotein: vascular protective effects, dysfunction, and potential as therapeutic target. *Circulation research* 114:171-182.
491. Tall, A. R., L. Yvan-Charvet, N. Terasaka, T. Pagler, and N. Wang. 2008. HDL, ABC transporters, and cholesterol efflux: implications for the treatment of atherosclerosis. *Cell metabolism* 7:365-375.
492. Holy, E. W., C. Besler, M. F. Reiner, G. G. Camici, J. Manz, J. H. Beer, T. F. Luscher, U. Landmesser, and F. C. Tanner. 2014. High-density lipoprotein from patients with coronary heart disease loses anti-thrombotic effects on endothelial cells: impact on arterial thrombus formation. *Thrombosis and haemostasis* 112.
493. Sorrentino, S. A., C. Besler, L. Rohrer, M. Meyer, K. Heinrich, F. H. Bahlmann, M. Mueller, T. Horvath, C. Doerries, M. Heinemann, S. Flemmer, A. Markowski, C. Manes, M. J. Bahr, H. Haller, A. von Eckardstein, H. Drexler, and U. Landmesser. 2010. Endothelial-vasoprotective effects of high-density lipoprotein are impaired in patients with type 2 diabetes mellitus but are improved after extended-release niacin therapy. *Circulation* 121:110-122.
494. Vaziri, N. D., M. Navab, and A. M. Fogelman. 2010. HDL metabolism and activity in chronic kidney disease. *Nature reviews. Nephrology* 6:287-296.
495. Meune, C., E. Touze, L. Trinquart, and Y. Allanore. 2009. Trends in cardiovascular mortality in patients with rheumatoid arthritis over 50 years: a systematic review and meta-analysis of cohort studies. *Rheumatology* 48:1309-1313.
496. Park, Y. B., S. K. Lee, W. K. Lee, C. H. Suh, C. W. Lee, C. H. Lee, C. H. Song, and J. Lee. 1999. Lipid profiles in untreated patients with rheumatoid arthritis. *The Journal of rheumatology* 26:1701-1704.
497. van Halm, V. P., M. M. Nielen, M. T. Nurmohamed, D. van Schaardenburg, H. W. Reesink, A. E. Voskuyl, J. W. Twisk, R. J. van de Stadt, M. H. de Koning, M. R. Habibuw, I. E. van der Horst-Bruinsma, and B. A. Dijkmans. 2007. Lipids and inflammation: serial measurements of the lipid profile of blood donors who later developed rheumatoid arthritis. *Annals of the rheumatic diseases* 66:184-188.
498. Park, Y. B., H. K. Choi, M. Y. Kim, W. K. Lee, J. Song, D. K. Kim, and S. K. Lee. 2002. Effects of antirheumatic therapy on serum lipid levels in patients with rheumatoid arthritis: a prospective study. *The American journal of medicine* 113:188-193.
499. Lee, H. K., L. M. Mattei, B. E. Steinberg, P. Alberts, Y. H. Lee, A. Chervonsky, N. Mizushima, S. Grinstein, and A. Iwasaki. In vivo requirement for Atg5 in antigen presentation by dendritic cells. *Immunity* 32:227-239.
500. Trombetta, E. S., and I. Mellman. 2005. Cell biology of antigen processing in vitro and in vivo. *Annu Rev Immunol* 23:975-1028.
501. Muller, C., R. Salvayre, A. Negre-Salvayre, and C. Vindis. HDLs inhibit endoplasmic reticulum stress and autophagic response induced by oxidized LDLs. *Cell Death Differ* 18:817-828.
502. Menges, M., S. Rossner, C. Voigtlander, H. Schindler, N. A. Kukutsch, C. Bogdan, K. Erb, G. Schuler, and M. B. Lutz. 2002. Repetitive injections of dendritic cells matured with tumor necrosis factor alpha induce antigen-specific protection of mice from autoimmunity. *The Journal of experimental medicine* 195:15-21.
503. Verginis, P., H. S. Li, and G. Carayanniotis. 2005. Tolerogenic semimature dendritic cells suppress experimental autoimmune thyroiditis by activation of thyroglobulin-specific CD4+CD25+ T cells. *J Immunol* 174:7433-7439.

504. Ehrenstein, M. R., J. G. Evans, A. Singh, S. Moore, G. Warnes, D. A. Isenberg, and C. Mauri. 2004. Compromised function of regulatory T cells in rheumatoid arthritis and reversal by anti-TNFalpha therapy. *The Journal of experimental medicine* 200:277-285.
505. Korn, T., J. Reddy, W. Gao, E. Bettelli, A. Awasthi, T. R. Petersen, B. T. Backstrom, R. A. Sobel, K. W. Wucherpfennig, T. B. Strom, M. Oukka, and V. K. Kuchroo. 2007. Myelin-specific regulatory T cells accumulate in the CNS but fail to control autoimmune inflammation. *Nat Med* 13:423-431.
506. Hoekstra, M., M. Van Eck, and S. J. Korporaal. 2012. Genetic studies in mice and humans reveal new physiological roles for the high-density lipoprotein receptor scavenger receptor class B type I. *Current opinion in lipidology* 23:127-132.
507. Poti, F., M. Simoni, and J. R. Nofer. 2014. Atheroprotective role of high-density lipoprotein (HDL)-associated sphingosine-1-phosphate (S1P). *Cardiovascular research* 103:395-404.
508. Suzuki, M., D. K. Pritchard, L. Becker, A. N. Hoofnagle, N. Tanimura, T. K. Bammler, R. P. Beyer, R. Bumgarner, T. Vaisar, M. C. de Beer, F. C. de Beer, K. Miyake, J. F. Oram, and J. W. Heinecke. High-density lipoprotein suppresses the type I interferon response, a family of potent antiviral immunoregulators, in macrophages challenged with lipopolysaccharide. *Circulation* 122:1919-1927.
509. Horejsi, V., and M. Hrdinka. Membrane microdomains in immunoreceptor signaling. *FEBS Lett* 588:2392-2397.
510. Smythies, L. E., C. R. White, A. Maheshwari, M. N. Palgunachari, G. M. Anantharamaiah, M. Chaddha, A. R. Kurundkar, and G. Datta. Apolipoprotein A-I mimetic 4F alters the function of human monocyte-derived macrophages. *Am J Physiol Cell Physiol* 298:C1538-1548.
511. Al-Jarallah, A., and B. L. Trigatti. A role for the scavenger receptor, class B type I in high density lipoprotein dependent activation of cellular signaling pathways. *Biochimica et biophysica acta* 1801:1239-1248.
512. Tang, C., Y. Liu, P. S. Kessler, A. M. Vaughan, and J. F. Oram. 2009. The macrophage cholesterol exporter ABCA1 functions as an anti-inflammatory receptor. *The Journal of biological chemistry* 284:32336-32343.
513. Navab, M., J. A. Berliner, G. Subbanagounder, S. Hama, A. J. Lusis, L. W. Castellani, S. Reddy, D. Shih, W. Shi, A. D. Watson, B. J. Van Lenten, D. Vora, and A. M. Fogelman. 2001. HDL and the inflammatory response induced by LDL-derived oxidized phospholipids. *Arterioscler Thromb Vasc Biol* 21:481-488.
514. de la Llera-Moya, M., D. Drazul-Schrader, B. F. Asztalos, M. Cuchel, D. J. Rader, and G. H. Rothblat. 2010. The ability to promote efflux via ABCA1 determines the capacity of serum specimens with similar high-density lipoprotein cholesterol to remove cholesterol from macrophages. *Arterioscler Thromb Vasc Biol* 30:796-801.
515. Larrede, S., C. M. Quinn, W. Jessup, E. Frisdal, M. Olivier, V. Hsieh, M. J. Kim, M. Van Eck, P. Couvert, A. Carrie, P. Giral, M. J. Chapman, M. Guerin, and W. Le Goff. 2009. Stimulation of cholesterol efflux by LXR agonists in cholesterol-loaded human macrophages is ABCA1-dependent but ABCG1-independent. *Arterioscler Thromb Vasc Biol* 29:1930-1936.
516. Kawasaki, K., R. S. Smith, Jr., C. M. Hsieh, J. Sun, J. Chao, and J. K. Liao. 2003. Activation of the phosphatidylinositol 3-kinase/protein kinase Akt pathway mediates nitric oxide-induced endothelial cell migration and angiogenesis. *Mol Cell Biol* 23:5726-5737.
517. Ishida, B. Y., P. J. Blanche, A. V. Nichols, M. Yashar, and B. Paigen. 1991. Effects of atherogenic diet consumption on lipoproteins in mouse strains C57BL/6 and C3H. *J Lipid Res* 32:559-568.

518. Schaefer, E. J., P. Anthanont, and B. F. Asztalos. 2014. High-density lipoprotein metabolism, composition, function, and deficiency. *Curr Opin Lipidol* 25:194-199.
519. Karlsson, H., A. Kontush, and R. W. James. 2015. Functionality of HDL: Antioxidation and Detoxifying Effects. *Handb Exp Pharmacol* 224:207-228.
520. Meurs, I., M. Van Eck, and T. J. Van Berkel. 2010. High-density lipoprotein: key molecule in cholesterol efflux and the prevention of atherosclerosis. *Curr Pharm Des* 16:1445-1467.
521. Riwanto, M., L. Rohrer, A. von Eckardstein, and U. Landmesser. 2015. Dysfunctional HDL: From Structure-Function-Relationships to Biomarkers. *Handb Exp Pharmacol* 224:337-366.
522. Cunningham, K. S., and A. I. Gotlieb. 2005. The role of shear stress in the pathogenesis of atherosclerosis. *Lab Invest* 85:9-23.
523. Ross, R. 1993. The pathogenesis of atherosclerosis: a perspective for the 1990s. *Nature* 362:801-809.
524. Rossig, L., S. Dimmeler, and A. M. Zeiher. 2001. Apoptosis in the vascular wall and atherosclerosis. *Basic Res Cardiol* 96:11-22.
525. Werner, N., S. Junk, U. Laufs, A. Link, K. Walenta, M. Bohm, and G. Nickenig. 2003. Intravenous transfusion of endothelial progenitor cells reduces neointima formation after vascular injury. *Circulation research* 93:e17-24.
526. Perez-Mendez, O., H. G. Pacheco, C. Martinez-Sanchez, and M. Franco. 2014. HDL-cholesterol in coronary artery disease risk: function or structure? *Clin Chim Acta* 429:111-122.
527. Pirillo, A., G. D. Norata, and A. L. Catapano. 2013. Treating high density lipoprotein cholesterol (HDL-C): quantity versus quality. *Curr Pharm Des* 19:3841-3857.
528. Nicholls, S. J., L. Zheng, and S. L. Hazen. 2005. Formation of dysfunctional high-density lipoprotein by myeloperoxidase. *Trends Cardiovasc Med* 15:212-219.
529. He, T. C., S. Zhou, L. T. da Costa, J. Yu, K. W. Kinzler, and B. Vogelstein. 1998. A simplified system for generating recombinant adenoviruses. *Proc Natl Acad Sci U S A* 95:2509-2514.
530. Georgopoulos, S., H. Y. Kan, C. Reardon-Alulis, and V. Zannis. 2000. The SP1 sites of the human apoCIII enhancer are essential for the expression of the apoCIII gene and contribute to the hepatic and intestinal expression of the apoA-I gene in transgenic mice. *Nucleic Acids Res* 28:4919-4929.

The Journal of Immunology

High-Density Lipoprotein Attenuates Th1 and Th17 Autoimmune Responses by Modulating Dendritic Cell Maturation and Function

Ioanna Tiniakou, Elias Drakos, Vaios Sinatkas, Miranda Van Eck, Vassilis I. Zannis, Dimitrios Boumpas, Panayotis Verginis and Dimitris Kardassis

J Immunol 2015; 194:4676-4687; Prepublished online 13 April 2015;
doi: 10.4049/jimmunol.1402870
http://www.jimmunol.org/content/194/10/4676

The Journal of Immunology is published twice each month by
The American Association of Immunologists, Inc.,
9650 Rockville Pike, Bethesda, MD 20814-3994.

Print ISSN: 0022-1767 Online ISSN: 1550-6606.

High-Density Lipoprotein Attenuates Th1 and Th17 Autoimmune Responses by Modulating Dendritic Cell Maturation and Function

Ioanna Tiniakou,*,† Elias Drakos,‡ Vaios Sinatkas,‡ Miranda Van Eck,§ Vassilis I. Zannis,*,¶ Dimitrios Boumpas,‖ Panayotis Verginis,‖,1 and Dimitris Kardassis*,†,1

Aberrant levels and function of the potent anti-inflammatory high-density lipoprotein (HDL) and accelerated atherosclerosis have been reported in patients with autoimmune inflammatory diseases. Whether HDL affects the development of an autoimmune response remains elusive. In this study, we used apolipoprotein A-I–deficient (apoA-I$^{-/-}$) mice, characterized by diminished circulating HDL levels, to delineate the role of HDL in autoimmunity. ApoA-I$^{-/-}$ mice exhibited increased severity of Ag-induced arthritis compared with wild-type mice, and this was associated with elevated Th1 and Th17 cell reactivity in the draining lymph nodes. Furthermore, reconstituted HDL (rHDL) attenuated IFN-γ and IL-17 secretion by Ag-specific T cells upon stimulation of draining lymph nodes in vitro. The suppressive effects of rHDL were mediated through modulation of dendritic cell (DC) function. Specifically, rHDL-treated DCs demonstrated an immature phenotype characterized by downregulated costimulatory molecules, the release of low amounts of proinflammatory cytokines, and failure to promote T cell proliferation in vitro. The mechanism of action involved the inhibition of NF-κB nuclear translocation and the decrease of *Myd88* mRNA levels by rHDL. Finally, modulation of DC function by rHDL was critically dependent on the presence of scavenger receptor class B type I and ATP Binding Cassette Transporter A1, but not the ATP Binding Cassette Transporter G1. These findings reveal a novel role of HDL in the regulation of adaptive inflammatory responses through suppression of DC function that could be exploited therapeutically in autoimmune inflammatory diseases. ***The Journal of Immunology*****, 2015, 194: 4676–4687.**

High-density lipoprotein (HDL) constitutes a heterogeneous population of particles that is characterized by great complexity in terms of structure and functionality (1). Although it has been best recognized for its inverse correlation with cardiovascular events (2, 3), accumulating evidence has revealed novel roles of HDL in cholesterol metabolism, endothelial integrity, and inflammation (4, 5). HDL metabolism entails the successive interactions of apolipoprotein A-I (apoA-I), the major protein component of HDL, with the ATP binding cassette transporters (ABC) ABCA1, ABCG1, and the scavenger receptor class B type I (SR-BI) (6). Numerous studies have implicated each of these transporters in HDL's antiatherogenic actions involving mechanisms such as cholesterol efflux and activation of HDL-induced signaling pathways (7–9). However, under certain conditions, HDL can become functionally defective. In fact, the protective functions of HDL are compromised in patients with coronary heart disease, diabetes, and autoimmune diseases (10–12).

Rheumatoid arthritis (RA) is a chronic inflammatory autoimmune disease manifested by leukocyte infiltration into the synovial lining leading to cartilage destruction and bone erosion (13, 14). RA pathology is critically dependent on the presence of autoreactive IFN-γ–producing Th1 and IL-17–releasing Th17 CD4$^+$ cell subsets, and proinflammatory cytokines such as TNF-α, IL-1β, and IL-6 (15). RA is associated with increased cardiovascular morbidity and mortality, and the majority of these patients are dyslipidemic (16). Interestingly, although HDL-cholesterol (HDL-c) levels are decreased, the levels of proinflammatory HDL are increased in RA patients (17). In support, antirheumatic drugs improve both HDL functionality and cholesterol levels (16). In vivo studies using animal models of arthritis have suggested a protective role of apoA-I and reconstituted HDL (rHDL). Particularly, treatment of rats with an apoA-I mimetic peptide inhibited collagen-induced arthritis and reduced inflammatory cytokine levels (18). Moreover, administration of apoA-I or rHDL attenuated peptidoglycan-polysaccharide–induced arthritis in Lewis female rats in an

*Laboratory of Biochemistry, Department of Basic Sciences, University of Crete Medical School, 71003 Heraklion, Crete, Greece; †Institute of Molecular Biology and Biotechnology, Foundation for Research and Technology–Hellas, 70013 Heraklion, Crete, Greece; ‡Department of Pathology, University of Crete Medical School, 71003 Heraklion, Crete, Greece; §Division of Biopharmaceutics, Leiden Academic Centre for Drug Research, 2333 Leiden, the Netherlands; ¶Whitaker Cardiovascular Institute, Boston University School of Medicine, Boston, MA 02118; and ‖Biomedical Research Foundation, Academy of Athens, 11527 Athens, Greece

[1]P.V. and D.K. contributed equally to this work.

Received for publication November 12, 2014. Accepted for publication March 16, 2015.

This work was supported by the Greek General Secretariat of Research and Technology (SYNERGASIA Grant 09SYN-12-897 and ARISTEIA II Grant 4220 to D.K.), the European Union project Innovative Medicine Initiative 6 ("Be The Cure," Contract 115142-2 to P.V. and D.B.), the National Institutes of Health (Grant HL48739 to V.I.Z.), and the Netherlands Organization for Scientific Research (VICI Grant 91813603 to M.V.E.). M.V.E. is an Established Investigator of the Netherlands Heart Foundation (Grant 2007T056).

Address correspondence and reprint requests to Dr. Dimitris Kardassis or Dr. Panayotis Verginis, Laboratory of Biochemistry, Department of Basic Sciences, University of Crete Medical School and Institute of Molecular Biology and Biotechnology, Foundation for Research and Technology of Hellas, 71003 Heraklion, Greece (D.K.) or Division of Immunology and Transplantation, Biomedical Research Foundation, Academy of Athens, 11527 Athens, Greece (P.V.). E-mail addresses: kardasis@imbb.forth.gr (D.K.) or pverginis@bioacademy.gr (P.V.)

Abbreviations used in this article: ABC, ATP binding cassette transporter; AIA, Ag-induced arthritis; apoA-I, apolipoprotein A-I; ATF3, activating transcription factor 3; BMDC, bone marrow–derived DC; C_t, cycle threshold; DC, dendritic cell; dLN, draining lymph node; dLNC, dLN cell; HDL, high-density lipoprotein; HDL-c, HDL-cholesterol; i.a., intra-articularly; mBSA, methylated BSA; MHC-II, MHC class II; PON-1, paraoxonase 1; RA, rheumatoid arthritis; rHDL, reconstituted HDL; SR-BI, scavenger receptor class B type I; Treg, regulatory T cell; TRIF, TIR domain–containing adapter-inducing IFN-β; WT, wild-type.

www.jimmunol.org/cgi/doi/10.4049/jimmunol.1402870

ABCA1-dependent manner (19). Although studies have shown that HDL can modulate the activity of various immune cell subsets (12), the mechanism through which HDL regulates autoreactive T cell responses in vivo remains elusive.

Dendritic cells (DCs) are professional APCs that carry Ags in the draining lymph nodes (dLNs) and promote the activation, differentiation, and polarization of naive T cells into effector Th cell subsets (20). Specifically, mature DCs present the Ag in the context of MHC and provide costimulatory signals that are required for efficient activation and priming of T cells. Furthermore, through secretion of proinflammatory cytokines, DCs direct the polarization of T cell toward the different T cell lineages. Ag recognition in the presence of IL-12 favors the generation of Th1 cells, whereas IL-6 and IL-23 drive the generation of Th17 effector cells (21–23). Because Th1 and Th17 cells and proinflammatory cytokines orchestrate the autoimmune responses in RA, strategies aiming at modulation of DC function and subsequent suppression of autoreactive Th1/Th17 responses might provide novel targets in the design of therapeutic protocols for the treatment of this disease.

In this study, we show that rHDL exerts its anti-inflammatory actions through modulation of DC maturation and function, and that rHDL-exposed DCs suppress T cell proliferation in vitro. Of interest, apoA-I$^{-/-}$ mice that lack conventional HDL develop severe arthritis and elevated Th1 and Th17 cell responses. Finally, our findings support a critical role of SR-BI and ABCA1 transporters in the rHDL-mediated anti-inflammatory function of DCs.

Materials and Methods

Animals

Wild-type (WT) C57BL/6 and apoA-I$^{-/-}$ (ApoA1^{tm1Unc}) mice on a C57BL/6 background were obtained from the specific pathogen-free animal facility of the Institute of Molecular Biology and Biotechnology (Heraklion, Greece). Mice were maintained on a 12-h light/dark cycle and fed standard rodent chow. Femurs and tibias were obtained from ABCA1$^{-/-}$ (24), ABCG1$^{-/-}$ (Deltagen, San Carlos, CA), and SR-BI$^{-/-}$ mice (25). All experimental protocols were in accordance with institutional guidelines and were approved by the Greek Federal Veterinary Office.

Reagents

Cell cultures were maintained in complete medium consisting of DMEM (Invitrogen), supplemented with 10% FBS (Biochrom) and antibiotic-antimycotic solution (Invitrogen). For flow-cytometric analysis, the following fluorescent-conjugated Abs were used: anti-CD11b (M1/70) and anti–MHC class II (MHC-II; AF6-120.1) were purchased from BD Biosciences. Abs against CD3 (145-2C11), CD4 (RM4-5), CD8a (53-6.7), CD44 (IM7), CD45R/B220 (RA3-6B2), Ly-6G/Ly-6C (Gr-1) (RB6-8C5), CD11c (N418), CD40 (3/23), CD80 (16-10A1), and CD86 (GL-1) were all purchased from Biolegend.

Induction of arthritis and clinical assessment

Mice were immunized s.c. at the base of the tail with 100 μg methylated BSA (mBSA; Sigma-Aldrich) in 50 μl PBS emulsified with equal volume of CFA (Sigma-Aldrich). On day 21 postimmunization, mice were injected intra-articularly (i.a.) with 50 μg mBSA in 20 μl PBS into the left knee joint. The swelling of the joint was evaluated by daily measurement (days 21–30) of the knee diameter (mm) using a digital vernier caliper (Cocraft). Nine days after i.a. injection (day 30), mice were euthanized and blood and tissues were collected.

Histological grading

Tissues were fixed in 3.7% formaldehyde for 24 h, and legs were decalcified in Schaefer solution for 2–3 d. Tissues were embedded in paraffin, and 4-μm-thick sections were stained with H&E. Specimens were blindly evaluated by two pathologists. Histological grade of arthritis was determined as follows: 0 = normal knee joint, 1 = normal synovium or mild synovial reaction with scarce inflammatory cells, 2 = moderate synovial reaction and moderate density of inflammatory cells, 3 = severe synovial hyperplasia and dense population of inflammatory cells, and 4 = pannus formation associated with articular cartilage erosion. The extent of skin inflammation was evaluated by scoring samples separately for the following parameters: severity of inflammation, extent of epidermal changes, and size of abscesses. A total histological score was assessed by summing the scores (0 = normal, 1 = mild, 2 = moderate, 3 = severe) for each parameter. The range of possible score was 0–9. Histopathology images were captured using a Nikon Eclipse E-400 microscope and Nikon Digital sight, DS-SM, photographic system. Images were autocorrected in Windows Photo Manager.

Serum HDL preparation and cholesterol measurement

Mice were euthanized and blood was collected by cardiac puncture after a 4-h fast. Serum was isolated, and an aliquot was used for HDL preparation. In brief, equal volumes of dextran sulfate (MP Biomedicals) and $MgCl_2$ stock solutions were mixed to produce the precipitation solution consisting of 10 g/l dextran sulfate and 0.5 M $MgCl_2$. Serum samples were mixed thoroughly with precipitation solution at a volume ratio of 10:1 and incubated for 10 min at room temperature. The mixture was centrifuged for 40 min at 14,000 × *g* at 4°C, and the HDL-containing supernatant was collected for determination of cholesterol levels and functionality assays. Total cholesterol and HDL-c were measured using a commercially available assay (Thermo Scientific) according to the manufacturer's recommendations.

Paraoxonase-1 activity assay

Paraoxonase-1 (PON-1) activity was determined in HDL preparations from mouse serum using paraoxon as substrate. In brief, 5 μl HDL was added in 245 μl buffer (100 mM Tris-HCl, pH 8.0, and 2 mM $CaCl_2$) containing 1.1 mM paraoxon (Sigma-Aldrich), and the absorbance at 405 nm was measured every 40 s for 20 min at room temperature in a microplate spectrophotometer. The rate of p-nitrophenol formed by the hydrolysis of paraoxon was determined by monitoring the increase in absorbance. PON-1 activity was expressed as units per liter (U/l) of HDL with 1 U defined as the activity that catalyzes the formation of 1 μmol p-nitrophenol per minute.

Preparation of rHDL containing apoA-I

Recombinant apoA-I was produced and purified from the culture medium of adenovirus-infected HTB-13 cells as previously described (26). rHDL particles were prepared by the sodium cholate dialysis method (27) using POPC/cholesterol/apoA-I/sodium cholate in a molar ratio of 100:10:1:100 as previously described (28). The rHDL preparation was extensively dialyzed against PBS, and the formation of apolipoprotein–lipid complexes was verified by two-dimensional gel electrophoresis (29, 30). Concentration of rHDL was based on apoA-I content and was determined by DC Protein Assay (Bio-Rad).

In vitro proliferation of dLN cells

Female mice (8–10 wk old) were immunized s.c. at the base of the tail with 100 μg OVA (Sigma-Aldrich) emulsified in equal volume of CFA. dLNs were excised 9 d later and single-cell suspensions were prepared. dLN cells (dLNCs) were cultured in flat-bottom, 96-well plates (5×10^5 cells/well) in the presence of OVA (15 μg/ml) and/or increasing concentrations of rHDL (1 μM = 28 μg/ml) for 72 h. Cells were then pulsed with 1 μCi [^{3}H]thymidine (TRK120; Amersham Biosciences) for 18 h, and the incorporated radioactivity was measured using a Beckman beta counter. Cytokine levels in culture supernatants were determined by ELISA and cells were analyzed by flow cytometry after 48 h of stimulation.

Generation of mouse bone marrow–derived DCs

Bone marrow–derived DCs (BMDCs) were generated from bone marrow progenitors, as previously described (31). In brief, bone marrow was isolated from femurs and tibias of female mice, treated with RBC lysis buffer (155 mM NH_4Cl, 10 mM $KHCO_3$, 0.1 mM Na_2EDTA), and plated at 2.5×10^6 cells per 100-mm cell culture dish in complete medium supplemented with 20% supernatant from a murine GM-CSF–secreting cell line (X63Ag8; kindly provided by B. Stockinger, National Institute of Medical Research, London, U.K.) (32). The culture medium was half-renewed on days 3, 6, and 8. On day 9, nonadherent cells were collected and cultured in 24-well tissue culture plates (1×10^6 cells/well) in the presence of either 0.5 μg/ml LPS from *Escherichia coli* O111: B4 (Calbiochem) or 20 μg/ml zymosan (Invivogen) and/or 4 μM rHDL. BMDCs were harvested as indicated for RNA, Western blot, and FACS analysis. Culture supernatants were collected at 12 or 18 h for cytokine analysis by ELISA.

Cocultures

BMDCs from WT mice were stimulated with 0.25 μg/ml LPS and pulsed with 20 μg/ml OVA in the presence or absence of 4 μM rHDL for 12 h.

Cells were collected and washed to remove excess LPS, OVA, and rHDL, and were cocultured with dLNCs isolated from OVA-immunized mice (9 d postimmunization) as described earlier. Culture supernatants were harvested 48 h later.

ELISA

Cytokine levels in culture supernatants were measured by ELISA kits following the manufacturer's recommendations. Mouse IL-17, IFN-γ, IL-12 p70, IL-8, IL-6, and TNF-α were purchased from R&D Systems. Mouse IL-23 and IL-2 were obtained from eBioscience, and IL-10 from Biolegend.

Flow cytometry

Cells were stained by incubation with fluorescent-conjugated Abs for 20 min at 4°C in PBS/5% FBS. Intracellular Foxp3 staining was performed using the Alexa Fluor 488 anti-mouse Foxp3 Ab (Biolegend) and the Foxp3/Transcription Factor Staining Buffer Set (eBioscience), according to the manufacturer's protocol. Cells were acquired on a FACSCalibur (BD Biosciences), and data were analyzed using the FlowJo software (Tree Star).

RNA isolation and quantitative PCR

Total RNA was prepared from mouse BMDCs using TRIzol reagent according to the manufacturer's protocol (Invitrogen). For each sample, 1 μg isolated RNA was used for cDNA synthesis with SuperScript II Reverse Transcriptase (Invitrogen). Quantitative PCR was performed on a StepOnePlus Real-Time PCR system (Applied Biosystems) using KAPA SYBR FAST qPCR Master Mix (Kapa Biosystems). The primer sequences were as follows: mouse *Hprt*, forward 5′-CGAAGTGTTGGATACAGGCC-3′ and reverse 5′-GGCAACATCAACAGGACTCC-3′; mouse *Myd88*, forward 5′-CCACCCTTGATGACCCCCTA-3′ and reverse 5′-TGCGGCGACACCTTTTCTC-3′; mouse *Trif*, forward 5′-TCTACCAGCTCAAGACCCCT-3′ and reverse 5′-GTCAGCCTGTCCCTTTCCAA-3′; mouse *Atf3*, forward 5′-GAGCTGAGATTCGCCATCCA-3′ and reverse 5′-CCGCCTCCTTTTCCTCTCAT-3′. Melting curve analysis was performed to ensure primer specificity. The expression of the target genes was normalized to the expression of the housekeeping gene, *Hprt*, and the normalized threshold cycle (C_t) values were calibrated against the control condition (untreated BMDCs) for each sample. The relative gene expression levels were determined using the relative standard curve method and the comparative C_t method ($\Delta\Delta C_t$ method) as described in Applied Biosystems Guide.

Western blot analysis

BMDCs were lysed on ice for 30 min in radioimmunoprecipitation assay lysis buffer (50 mM Tris-HCl pH 8.0, 150 mM NaCl, 1% Triton X-100, 0.1% SDS, and 0.5% sodium deoxycholate) supplemented with cOmplete Proteade Inhibitor Cocktail (Roche), 5 mM NaF, 1 mM Na_3VO_4, and centrifuged at 13,000 × *g* for 30 min at 4°C. The supernatant was collected as total cell lysate, and protein concentration was determined by DC Protein Assay (Bio-Rad). Thirty micrograms total cell protein per sample were denatured by boiling for 10 min, loaded onto a 10.5% SDS polyacrylamide gel, and transferred to nitrocellulose membrane (GE Healthcare Life Sciences). Blots were incubated with primary Abs to anti–p-Stat3 (Tyr705; Cell Signaling) and anti-STAT3 (BD Biosciences). Anti-actin Ab (Merck Millipore) was used as loading control. After incubation with HRP-conjugated secondary Abs (Jackson Immunoresearch Laboratories), proteins were visualized on a ChemiDoc XRS+ imaging system (BioRad), and band intensities were quantified using the Image Lab Software (BioRad).

Immunofluorescence

BMDCs were seeded onto poly-L-lysine (Sigma-Aldrich)–coated coverslips in 24-well tissue culture plates (1×10^6 cells/well). Twenty-four hours later, cells were stimulated with 0.5 μg/ml LPS and treated with 4 μM rHDL for 2 h. Cells were fixed with 4% paraformaldehyde (Sigma-Aldrich), permeabilized with PBS-Triton X-100 0.5%, and incubated with anti-p65 (sc-109; Santa Cruz Biotechnology). Alexa Fluor 555 Goat Anti-Rabbit IgG (Molecular Probes) was used as secondary Ab. DNA was stained with 1 μg/ml DAPI, and coverslips were mounted on Mowiol 4-88 (Sigma-Aldrich). Images were acquired using a confocal laser scanning microscope (TCS SP8; Leica Microsystems) and an HC PL APO CS2 40×/1.30 oil objective using identical settings within each experiment. Images were obtained using the LAS AF v3.3 software (Leica Microsystems) and processed with Adobe Photoshop 7.0 (Adobe Systems). A total of 100 cells from 4 different fields from each slide was analyzed for fluorescence intensity of nucleus and cytoplasm using the National Institutes of Health ImageJ software.

Statistical analysis

Data are expressed as mean ± SEM unless stated otherwise. Statistical significance was determined using two-tailed Student *t* test. The χ^2 test was used for categorical variables. For all results, $p < 0.05$ was considered statistically significant. Analysis was performed using GraphPad Prism software (version 5.00; GraphPad).

Results

Increased severity of Ag-induced arthritis in apoA-I$^{-/-}$ mice

HDL-c levels are significantly reduced in various autoimmune conditions such as RA (16); however, whether there is a role for HDL in induction and perpetuation of the autoimmune response remains elusive. We investigated the development of Ag-induced arthritis (AIA) in apoA-I$^{-/-}$ mice that are characterized by very low serum HDL-c levels (~25% of normal) (33). AIA is induced upon i.a. injection of mBSA in mBSA-sensitized animals (Fig. 1A) and serves as a model for RA (34, 35). Interestingly, apoA-I$^{-/-}$ mice developed increased severity of AIA compared with WT animals (Fig. 1B). This result correlated well with the histological examination of injected knee joints of apoA-I$^{-/-}$ mice, which developed extensive pannus formation (grade 4), contrary to WT mice, which exhibited moderate-to-severe inflammation (grades 2–3; $*p = 0.0393$ for pannus versus nonpannus; Fig. 1C, 1D). A striking observation was the extensive inflammatory reaction in the skin of apoA-I$^{-/-}$ mice 3 wk after immunization as opposed to WT mice (Fig. 1E), which was characterized by significant epidermis alterations at the site of the injection including ulceration, dense inflammation in the dermis with abundant neutrophil infiltration, and formation of large abscesses (Fig. 1F, 1G; data not shown). In contrast, WT mice showed moderate inflammatory reaction in the dermis and occasional small neutrophil aggregates (Fig. 1F, 1G). Collectively, these findings indicate that decreased levels of circulating HDL are associated with exacerbation of inflammatory arthritis and severe inflammatory reactions in the skin.

Anti-inflammatory functions of HDL are compromised in arthritic WT mice

We examined whether HDL-c levels were affected by the inflammatory response and whether HDL functionality was altered during AIA development. According to our results, total and HDL-c levels of both mBSA-immunized (day 21) and arthritic (day 30 i.a.) mice showed no significant differences as compared with naive WT mice (Fig. 2A). To assess the functional properties of HDL, we measured HDL-associated PON-1 activity at different time points during disease development. Our results indicated that there is a biphasic response of the immunized mice in terms of HDL activity: an early upregulation of HDL functionality (day 10) that could be accounted for by an early attempt to attenuate the inflammation followed by a gradual decline in HDL functionality as the inflammation resolves (days 21 and 30; Fig. 2B). Importantly, our data showed that upon the i.a. antigenic challenge, HDL functionality significantly decreased to even lower levels (day 21 versus day 30 i.a.; Fig. 2B). Although mice are still capable of responding to the i.a. mBSA challenge by increasing PON-1 activity (day 30 versus day 30 i.a.), this potential is markedly compromised compared with day 10 (Fig. 2B). Collectively, our results signify that although the HDL-c levels remained unaffected, the anti-inflammatory/antioxidant properties of circulating HDL were attenuated in an inflammatory environment.

ApoA-I$^{-/-}$ mice exhibit exacerbated OVA-specific Th1 and Th17 immune responses

Development and progression of arthritis depends on the generation of autoreactive Th1 and Th17 cells (36, 37). To monitor the in-

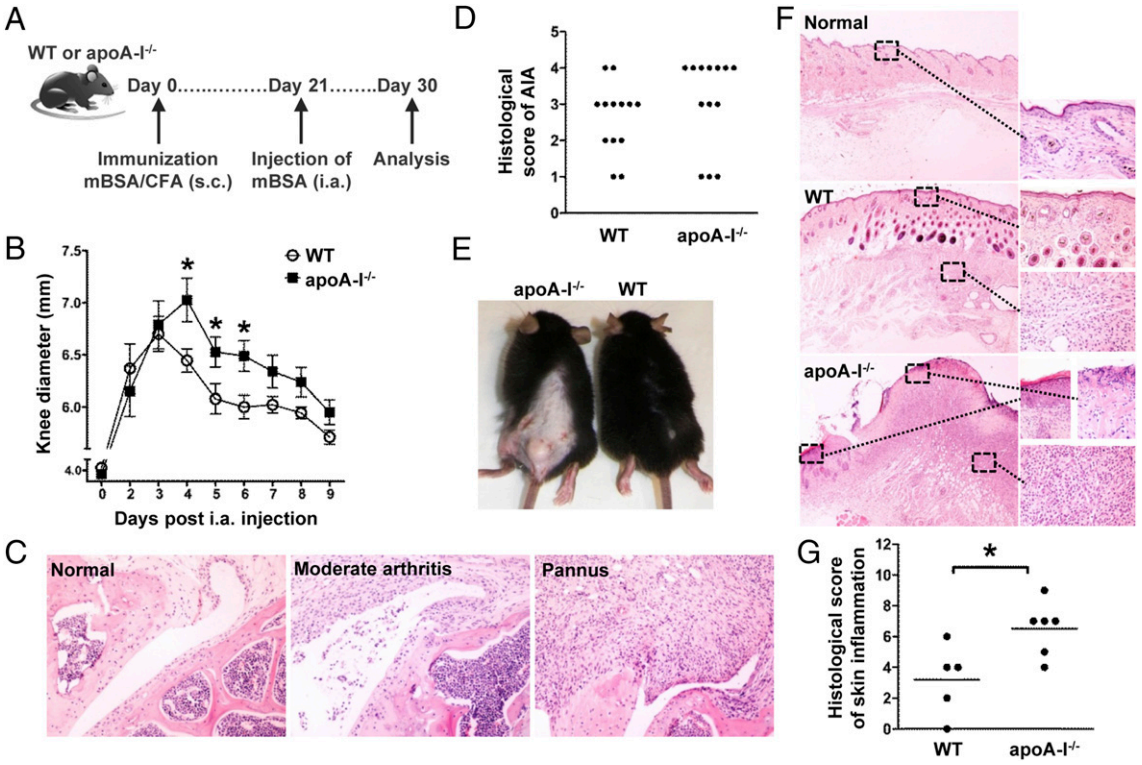

FIGURE 1. ApoA-I$^{-/-}$ mice demonstrate an aggravated AIA phenotype. (**A**) WT and apoA-I$^{-/-}$ mice (n = 13/group) were immunized s.c. with mBSA/CFA, and arthritis was induced upon i.a. injection of mBSA 21 d later. (**B**) Evaluation of arthritis by measurement of knee joint swelling daily after i.a. injection (n = 8–9/group; day 4: *p = 0.0233, day 5: *p = 0.0455, day 6: *p = 0.0182). Results are expressed as mean ± SEM. (**C**) Representative H&E-stained sections of inflamed joints from WT (moderate arthritis) and apoA-I$^{-/-}$ mice (pannus), as well as noninjected knee joint (normal), are shown (original magnification ×200). (**D**) Histological scores for AIA in WT and apoA-I$^{-/-}$ mice. The histopathologies of injected knee joints were scored as described in *Materials and Methods*; *p = 0.0393 for pannus versus nonpannus. (**E**) Photos of skin lesions in apoA-I$^{-/-}$ mice 21 d after mBSA immunization. (**F**) Representative H&E-stained sections of normal and inflamed skin (original magnification ×20 [*left panels*], ×400 [*right panels*]). (**G**) Histological grading of skin inflammation developed in WT and apoA-I$^{-/-}$ mice (*p = 0.0239). In all panels, data are from two independent experiments.

duction of T cell responses in apoA-I$^{-/-}$ mice, we first examined whether T cell lymphopoiesis was affected in these mice. Analysis of CD4$^+$ and CD8$^+$ T cell subsets in thymus and peripheral lymphoid organs revealed no differences between naive apoA-I$^{-/-}$ and WT mice, indicating that loss of apoA-I did not cause alterations in T cell development and homeostasis (Fig. 3A). In addition, the frequency of peripheral CD4$^+$Foxp3$^+$ regulatory T cells (Tregs) was similar in apoA-I$^{-/-}$ and WT mice (Fig. 3B). We next assessed whether decreased HDL levels could affect the induction of Ag-specific Th1 and Th17 responses. Interestingly, dLNs of apoA-I$^{-/-}$ mice showed increased cellularity 9 d after the antigenic challenge compared with WT mice (53.5 ± 2.5 versus 42.1 ± 2.0 × 10^6 cells; Fig. 4A). Detailed analysis of the dLNs for the different cells subsets revealed a significant increase of CD11c$^+$ DCs in apoA-I$^{-/-}$ mice, 3.5 and 9 d after the antigenic challenge, compared with WT mice, and to a lesser extent of CD4$^+$ T cells (Fig. 4B). Notably, no significant differences were observed in the frequencies of B220$^+$ B cells and CD11b$^+$ macrophages, whereas CD8$^+$ T cells were slightly decreased in dLNs of apoA-I$^{-/-}$ mice (Fig. 4B). Moreover, the absolute numbers of CD4$^+$Foxp3$^+$ Tregs were significantly increased in immunized apoA-I$^{-/-}$ mice (Fig. 4B). Although both groups of mice exhibited similar frequencies of activated CD3$^+$CD4$^+$CD44$^+$ T cells after in vitro restimulation with OVA (Fig. 4C), dLNCs from apoA-I$^{-/-}$ mice exhibited increased proliferation as indicated by IL-2 levels (181.3 ± 14.1 versus 74.7 ± 7.9; Fig. 4D). This finding was accompanied by markedly increased production of both IL-17 (773.1 ± 105.9 versus 292.5 ± 85.8; Fig. 4E) and IFN-γ (708.9 ± 114.8 versus 172.4 ± 40.0; Fig. 4F) in apoA-I$^{-/-}$ OVA-stimulated dLNC supernatants, whereas IL-10 was undetectable (data not shown). Taken together, these data demonstrate that apoA-I deficiency promotes T cell proliferation and enhances Ag-specific Th1 and Th17 immune responses.

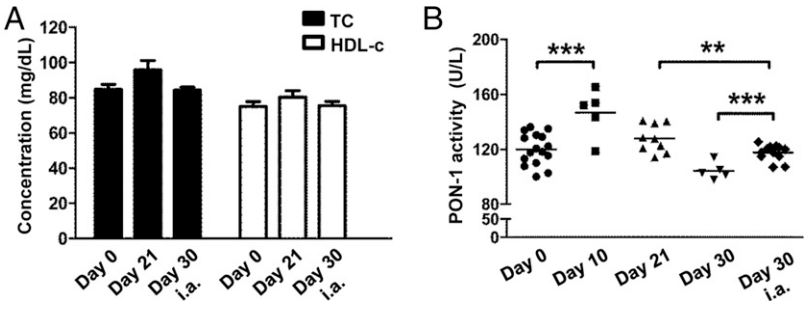

FIGURE 2. HDL functionality is altered during AIA in WT mice. (**A**) Total (TC) and HDL-c levels in serum of naive mice (day 0), mBSA-immunized mice (day 21), and arthritic mice (day 30 i.a.). (**B**) Characterization of HDL antioxidant/anti-inflammatory properties by assessment of HDL-associated PON-1 activity (**p = 0.0084, ***$p \leq 0.0007$). Results are expressed as mean ± SEM; data are combined from two independent experiments; n = 5–16/group.

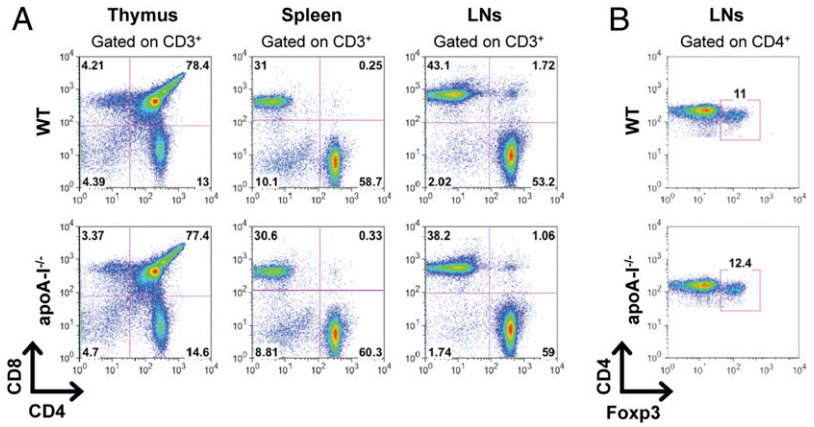

FIGURE 3. T cell development and homeostasis is not affected in apoA-I$^{-/-}$ mice. (**A** and **B**) Flow-cytometric analysis of thymocytes, splenocytes, and lymph node cells from naive WT and apoA-I$^{-/-}$ mice (n = 3/group) is shown. Gates were set as indicated. Data are representative of two independent experiments.

rHDL inhibits Ag-specific Th1 and Th17 immune responses in vitro

Next, we examined whether HDL could directly affect the induction of Th1 and Th17 immune responses. To address this, we performed in vitro restimulation assays of dLNCs from OVA-immunized WT animals in the presence of titrating amounts of rHDL. Treatment with rHDL led to impaired proliferation of OVA-specific T cells as a response to the antigenic stimulus (Fig. 4G). In support, IL-2 secretion was decreased in culture supernatants of rHDL-treated dLNCs (Fig. 4H). Furthermore, decreased proliferation of dLNCs in the presence of rHDL was accompanied by a dose-dependent decrease in secretion of IL-17 (Fig. 4I) and IFN-γ (Fig. 4J). Overall, these results provide direct evidence for a potent role of rHDL in the suppression of Th1 and Th17 immune responses in vitro.

rHDL downregulates costimulatory molecule expression and suppresses proinflammatory cytokine production in stimulated BMDCs

T cell activation, polarization, and proliferation in vivo require Ag presentation by professional APCs. DCs serve as the best candidate that upon maturation provide the necessary costimulatory molecules and secrete proinflammatory cytokines to instruct T cell responses (20, 38). We asked whether the suppressive effect of rHDL on T cell responses is mediated through modulation of DC function. To this end, we first examined the maturation status of DCs in dLNs and spleen of immunized apoA-I$^{-/-}$ and WT mice. Our findings demonstrated an increase of MHC-II and CD40 expression in CD11c^{+} DCs from apoA-I$^{-/-}$ compared with WT mice and a more prominent increase in the expression of the costimulatory molecule CD86 in both dLNs and spleen (Fig. 5). In contrast, no differences were observed in the expression levels of CD80 (Fig. 5). To examine a direct role of HDL on DC maturation, we generated BMDCs from WT mice and treated them with rHDL during LPS stimulation. As shown in Fig. 6A, treatment with rHDL led to downregulation of MHC-II, CD40, CD86, and CD80. To determine whether this effect was specific to the TLR4-mediated response in DCs, we stimulated BMDCs from WT mice with zymosan, a TLR2 ligand, and treated them with rHDL. Although expression of MHC-II was not altered, a significant downregulation of CD40, CD86, and CD80 expression was observed in rHDL-treated zymosan-activated BMDCs compared with zymosan alone (Fig. 6B). These results indicate that the suppressive effect of rHDL on DC maturation is not limited to TLR4-induced immune responses. Furthermore, secretion of proinflammatory cytokines IL-6, IL-12, IL-23, chemokine IL-8, and the anti-inflammatory cytokine IL-10 was reduced in rHDL-treated LPS-stimulated BMDCs, whereas TNF-α production was unaffected by rHDL treatment (Fig. 6C). Notably, rHDL suppressed the secretion of IL-6, IL-8, and TNF-α in immature DCs, indicating that the anti-inflammatory properties of rHDL could be exerted independent of LPS. Collectively, these data demonstrate an inhibitory effect of rHDL on activation and maturation of and cytokine secretion by DCs in vitro.

rHDL treatment of mature BMDCs suppresses Ag-specific T cell proliferation

To assess the functional importance of our findings, we performed coculture experiments with rHDL-treated OVA-pulsed BMDCs and OVA-primed dLNCs as shown in Fig. 7A. To this end, WT BMDCs were activated with LPS and pulsed with OVA in the presence or absence of rHDL for 12 h. BMDCs were then cocultured with dLNCs isolated from OVA-immunized WT syngeneic mice. Forty-eight hours later, culture supernatants were collected and IL-2 production was assessed. Interestingly, rHDL-treated OVA-pulsed BMDCs significantly reduced IL-2 production by OVA-primed dLNCs as compared with OVA-pulsed BMDCs (Fig. 7B). These findings provide evidence for the impaired capacity of rHDL-treated DCs to promote T cell proliferation.

rHDL prevents activation of the MyD88-dependent pathway in stimulated BMDCs

LPS binding to TLR4 leads to NF-κB nuclear translocation and induction of inflammatory cytokine gene transcription (39). To gain insights into the molecular events leading to HDL-mediated suppression of DC function, we examined whether rHDL suppressed LPS-induced proinflammatory cytokine secretion by interfering with the NF-κB pathway. To this end, we performed immunofluorescence studies to assess nuclear translocation of the p65 subunit of NF-κB in LPS-stimulated BMDCs. Our findings showed a marked increase in nuclear p65 compared with unstimulated cells, whereas LPS-induced translocation of p65 to the nucleus was impaired after rHDL treatment (Fig. 8A, 8B). In TLR4 signaling, activation of NF-κB is initiated by interactions with either MyD88 or TIR domain–containing adapter-inducing IFN-β (TRIF) adaptor protein (39). To determine whether these two pathways were disrupted by rHDL, we assessed mRNA levels in LPS-stimulated BMDCs. We found that rHDL decreased *Myd88* mRNA levels in LPS-stimulated BMDCs after 18 h of treatment (Fig. 8C). In contrast, rHDL treatment did not affect *Trif* expression neither at an early nor at a later time point (Fig. 8D). These data suggest a role for rHDL in modulating inflammatory responses through interference with the MyD88-dependent TLR4 signaling pathway.

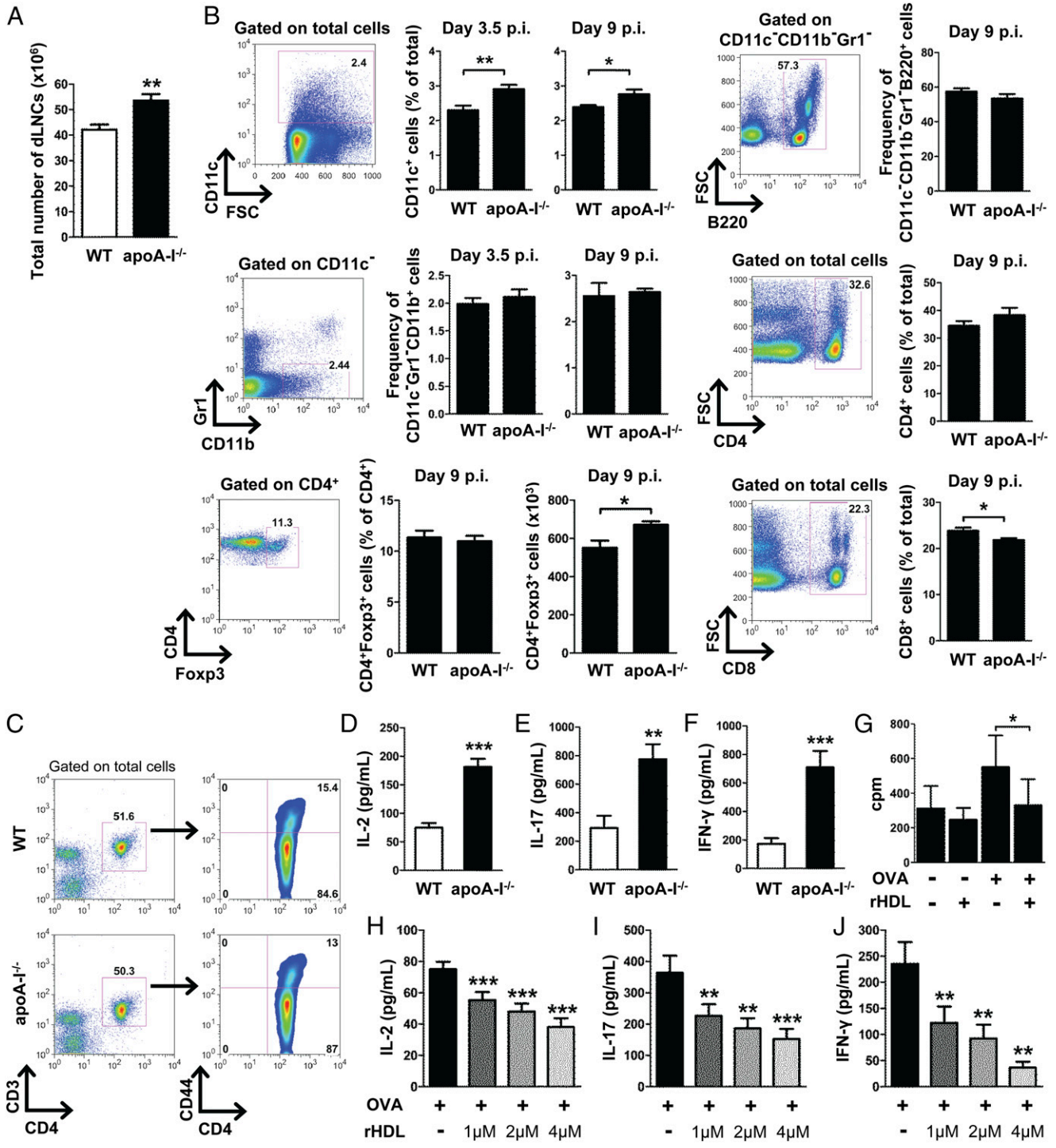

FIGURE 4. OVA-specific Th1 and Th17 immune responses are modulated by HDL. (**A**) LN cellularity in WT and apoA-I$^{-/-}$ mice (n = 12–13/group) 9 d after OVA immunization (**p = 0.0018). Results are expressed as mean ± SEM; data are combined from five independent experiments. (**B**) dLNCs from WT and apoA-I$^{-/-}$ mice (n = 4–6/group) were collected 3.5 and 9 d post OVA immunization (p.i.). Gating strategy and frequencies or absolute numbers of CD11c$^+$ DCs, B220$^+$ B cells, CD11b$^+$ macrophages, CD4$^+$ and CD8$^+$ T cells, and Foxp3$^+$ Tregs are shown. Numbers on the gates denote frequencies. Results are expressed as mean ± SEM. *$p \leq 0.0469$, **p = 0.0096. (**C**) Flow-cytometric analysis of OVA-primed dLNCs from WT and apoA-I$^{-/-}$ mice (n = 6/group) after in vitro restimulation with 15 μg/ml OVA for 48 h. Gates were set as indicated. Data are representative of three independent experiments. (**D**–**F**) Levels of IL-2 (***$p < 0.0001$), IL-17 (**p = 0.0055), and IFN-γ (***p = 0.0008) in culture supernatants of OVA-primed dLNCs are shown (n = 6–7/group). Results are expressed as mean ± SEM; data are combined from at least four independent experiments. (**G**) OVA-primed dLNCs from WT mice (n = 3/group) were restimulated with OVA (15 μg/ml) in vitro in the presence of rHDL (1 μM) for 72 h and then pulsed with 1 μCi [^{3}H]thymidine for 18 h. The incorporated radioactivity was measured. Results are expressed as mean ± SEM. *$p < 0.0367$. (**H**–**J**) dLNCs from OVA-immunized WT mice (n = 6–8/group) were cultured with increasing concentrations of rHDL in the presence of OVA (15 μg/ml). Levels of IL-2 (***$p \leq 0.0004$), IL-17 (**p = 0.001, ***p = 0.0006), and IFN-γ (**$p \leq 0.0081$) were determined in culture supernatants 48 h later. Results are expressed as mean ± SEM; data are combined from at least three independent experiments.

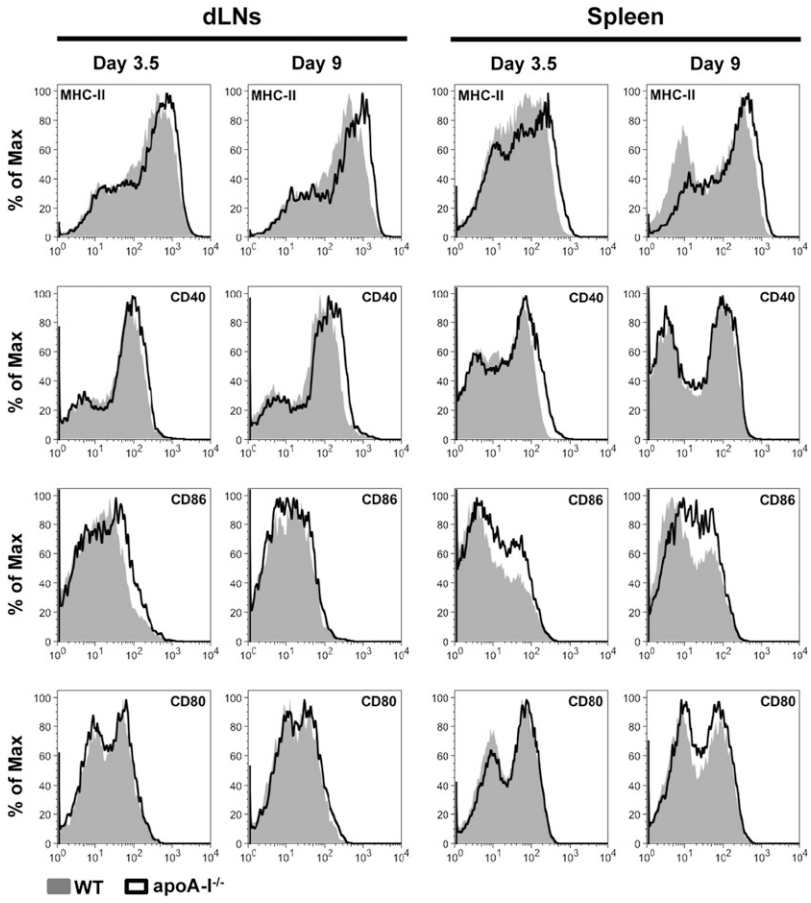

FIGURE 5. The expression of DC maturation markers is increased in immunized apoA-I$^{-/-}$ mice. dLNCs and splenocytes from WT and apoA-I$^{-/-}$ mice (n = 4–8/group) were collected 3.5 and 9 d post OVA immunization. Expression levels of MHC-II, CD40, CD86, and CD80 were evaluated by flow cytometry. Representative FACS histograms are shown. Gates were set on CD11c^{+} cells.

Recently, activating transcription factor 3 (ATF3), a transcriptional regulator that provides negative feedback on TLR-induced inflammation, was identified as a critical mediator of HDL's anti-inflammatory effects in macrophages (40). Thus, we assessed *Atf3* mRNA levels in rHDL-treated BMDCs. Indeed, after 4 h of treatment with rHDL, LPS-stimulated BMDCs demonstrated increased expression of *Atf3* compared with nontreated cells, whereas expression was decreased at 18 h (Fig. 8E). This finding suggests that an HDL-inducible, ATF3-dependent mechanism may operate in DCs, acting as a restrainer of the TLR-stimulated response by preventing excessive proinflammatory cytokine production.

Anti-inflammatory effects of rHDL on stimulated BMDCs are mediated through ABCA1 and SR-BI

It is well established that HDL exerts its pleiotropic functions through interactions with SR-BI, ABCA1, and ABCG1 transporters (7, 9). To investigate the contribution of each transporter in rHDL's anti-inflammatory effects on DCs, we assessed cytokine secretion in LPS-stimulated ABCG1$^{-/-}$, ABCA1$^{-/-}$, and SR-BI$^{-/-}$ BMDCs in the presence or absence of rHDL. Deficiency in any of these transporters in BMDCs did not affect their ability to efficiently secrete proinflammatory cytokines upon LPS stimulation (data not shown). Interestingly, rHDL suppressed the levels of IL-12, IL-8, or IL-23 in ABCG1$^{-/-}$ BMDCs as efficiently as in BMDCs from WT mice and to an even greater extent the secretion of IL-6, indicating that this transporter is not involved in the inhibitory effect of rHDL on DC activation (Fig. 9A). In contrast, rHDL was unable to efficiently impair proinflammatory cytokine secretion in ABCA1$^{-/-}$ and SR-BI$^{-/-}$ BMDCs, suggesting that rHDL-mediated modulation of DC function is ABCA1 and SR-BI dependent (Fig. 9A). Notably, the decrease in IL-10 levels that was observed upon rHDL treatment of LPS-stimulated WT BMDCs (34.5 ± 1.6%) was retained independent of ABCG1, ABCA1, or SR-BI deficiency (ABCG1$^{-/-}$: 30.5 ± 1.2%; ABCA1$^{-/-}$: 38.0 ± 1.4%; SR-BI$^{-/-}$: 35.9 ± 2.6%; Fig. 9A). This result suggests either that the ABCG1 transporter does not contribute to rHDL's inhibitory actions or that in the case of IL-10 there is a redundancy in the functions of the three transporters.

Further support of these findings was obtained upon assessment of the effects of rHDL on signaling events downstream of the NF-κB pathway in BMDCs from WT mice or mice deficient for any of the above transporters. Upon LPS stimulation, STAT3 signaling, as indicated by increased STAT3 phosphorylation, was efficiently induced in BMDCs from all groups as compared with non-stimulated cells (WT: 6.0 ± 0.8-fold; ABCG1$^{-/-}$: 4.3 ± 0.5-fold; ABCA1$^{-/-}$: 4.2 ± 0.5-fold; SR-BI$^{-/-}$: 3.9 ± 0.5-fold; Fig. 9B, 9C), and treatment with rHDL was able to diminish STAT3 activation in WT (4.5 ± 0.7-fold; *p = 0.0283) and ABCG1$^{-/-}$ BMDCs (2.5 ± 0.2-fold; *p = 0.0127). However, rHDL-treated ABCA1$^{-/-}$ and SR-BI$^{-/-}$ BMDCs demonstrated similar levels of LPS-induced STAT3 phosphorylation (ABCA1$^{-/-}$: 3.9 ± 0.7-fold; SR-BI$^{-/-}$: 4.2 ± 0.7-fold; Fig. 9B, 9C) as compared with cells treated with LPS alone. Overall, our data provide evidence for an important role of ABCA1 and SR-BI, but not ABCG1, in the HDL-mediated anti-inflammatory function on DCs.

Discussion

Although numerous studies have reported the anti-inflammatory properties of HDL, the mechanisms involved in HDL-mediated suppression of autoimmune inflammatory responses are not well understood. Our results demonstrate that HDL suppresses the activation, maturation of, and cytokine secretion by DCs resulting in the establishment of a "semimature phenotype" of these cells. To this end, treatment of BMDCs with rHDL resulted in reduced

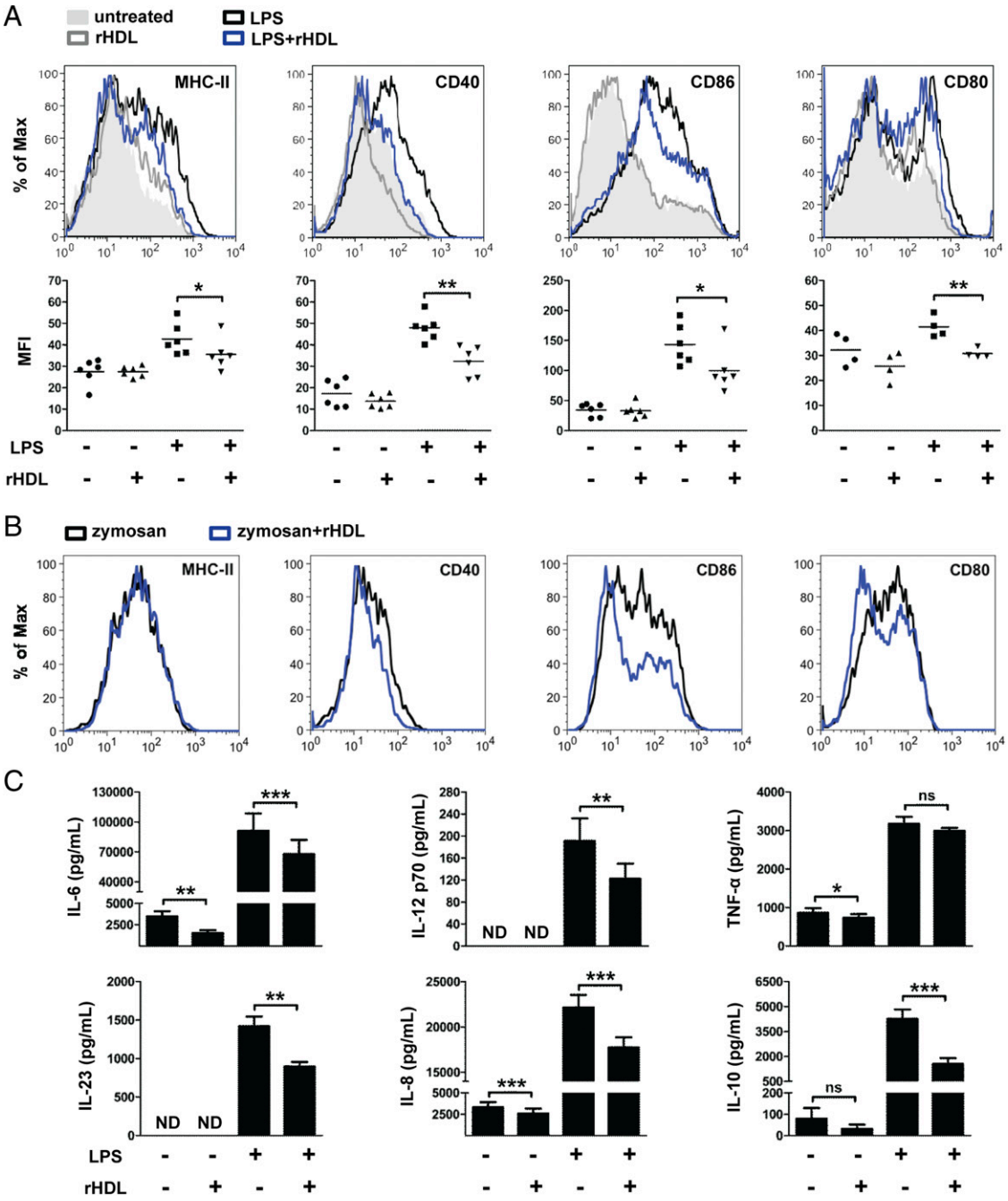

FIGURE 6. rHDL prevents activation and maturation of BMDCs. BMDCs from WT mice (n = 2–6) were stimulated with LPS (0.5 μg/ml) or zymosan (20 μg/ml) and treated with 4 μM rHDL for 18 h. (**A**) Expression levels of MHC-II (*p = 0.026), CD40 (**p = 0.0076), CD86 (*p = 0.0226), and CD80 (**p = 0.0047) were evaluated by flow cytometry. Representative FACS histograms are shown. Gates were set on CD11c$^+$ cells. Dot plots represent the averages of the geometric mean fluorescence intensity (MFI) of at least two independent experiments. (**B**) Expression levels of MHC-II, CD40, CD86, and CD80 were evaluated by flow cytometry. Representative FACS histograms are shown. Gates were set on CD11c$^+$ cells. (**C**) Levels of IL-6, IL-23, IL-12 p70, IL-8, IL-10, and TNF-α in culture supernatants were measured by ELISA. Results are expressed as mean ± SEM; data are combined from three independent experiments; *p = 0.0229, **$p \leq 0.0038$, ***$p \leq 0.0008$. ND, not detectable; ns, not significantly different.

expression of MHC-II and costimulatory molecules that are required for efficient Ag presentation and activation of T lymphocytes. This is in line with previous reports revealing a role of HDL and apoA-I on human DC differentiation and function (41, 42). Ag loading to MHC-II is mediated either through the classical or via the autophagy pathway (43, 44). Recent data suggest that HDL inhibits autophagy induced by oxidized low-density lipoproteins in endothelial cells (45). Whether HDL could suppress the induction of autophagy in DCs and delivery of Ags to MHC loading compartments remains to be shown.

The functional importance of the anti-inflammatory effects of HDL on DCs is demonstrated by the decreased ability of rHDL-treated BMDCs to promote T cell proliferation in vitro. DCs with a "semimature phenotype" have the ability to downregulate immune responses and to ameliorate autoimmunity upon adoptive transfer in vivo (46, 47). In particular, it was shown that TNF-α–treated DCs are tolerogenic and suppress experimental autoimmune thyroiditis through induction of CD4$^+$CD25$^+$ Tregs in vivo and in vitro (47). Because Tregs play a prominent role in the re-establishment but also maintenance of self-tolerance, it remains to

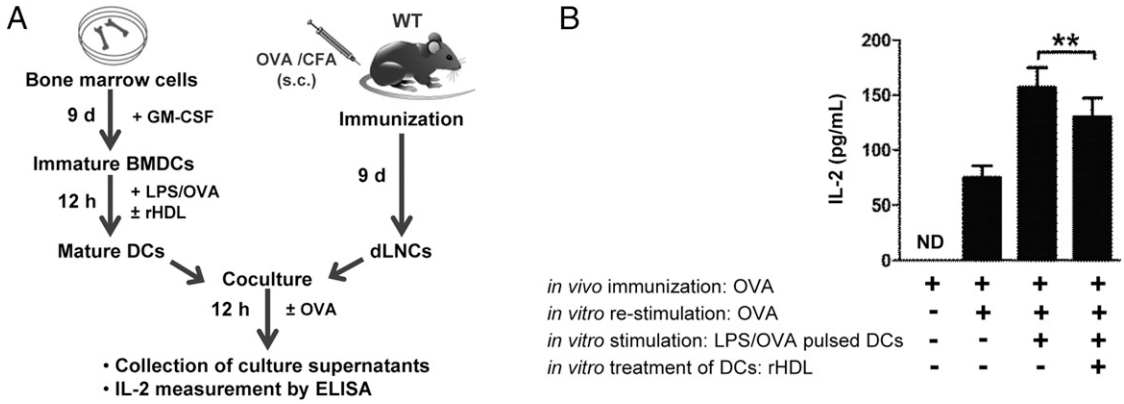

FIGURE 7. rHDL-treated DCs suppress Ag-specific T cell proliferation in vitro. (**A**) Outline of the coculture experimental setup. LPS-stimulated, OVA-pulsed BMDCs from WT mice (n = 5/experiment) were treated with rHDL for 12 h and cocultured with OVA-primed dLNCs. Cells were restimulated with OVA and 48 h later (**B**) IL-2 secretion in culture supernatants was assessed by ELISA. Results are expressed as mean ± SEM; data are combined from two independent experiments (**p = 0.005).

be examined whether rHDL-treated BMDCs possess the ability to induce and/or expand Tregs in vivo. Interestingly, absolute numbers of $CD4^+Foxp3^+$ Tregs in the dLNs of immunized apoA-$I^{-/-}$ were increased compared with WT mice. However, the suppressive potential of $Foxp3^+$ Tregs in an inflammatory environment is currently under debate (48, 49).

According to our data, absence of apoA-I in mice resulted in exacerbated inflammation in the knee joints during AIA and caused extensive inflammatory reactions in the skin. These findings are in line with previous studies demonstrating that lack of apoA-I in low-density lipoprotein receptor–deficient mice fed with high-fat diet was associated with skin lesion development due to enlarged skin dLNs that contained expanded populations of cholesterol-enriched lymphocytes including T cells, B cells, and DCs (50). Moreover, when fed an atherogenic diet, these double-knockout mice exhibited increased T cell activation, proliferation, and production of autoantibodies in the plasma. Importantly, this autoimmune phenotype was restored after treatment of mice with either lipid-free apoA-I or adenovirus-mediated gene transfer of apoA-I (50, 51).

The capacity of HDL to bind LPS and neutralize its inflammatory activity has been demonstrated in multiple in vitro and in vivo studies (52, 53). Although this possibility cannot be excluded, the data presented in this study using BMDCs from ABCA1-, ABCG1-, or SR-BI–deficient mice do not support such a mechanism of action for rHDL. In our experiments, rHDL did not efficiently suppress LPS-induced secretion of IL-6, IL-12, or IL-23 in mice lacking ABCA1 or SR-BI, indicating that a specific interaction between rHDL and these transporters, rather than sequestration of LPS by rHDL, is responsible for its anti-inflammatory functions on BMDCs.

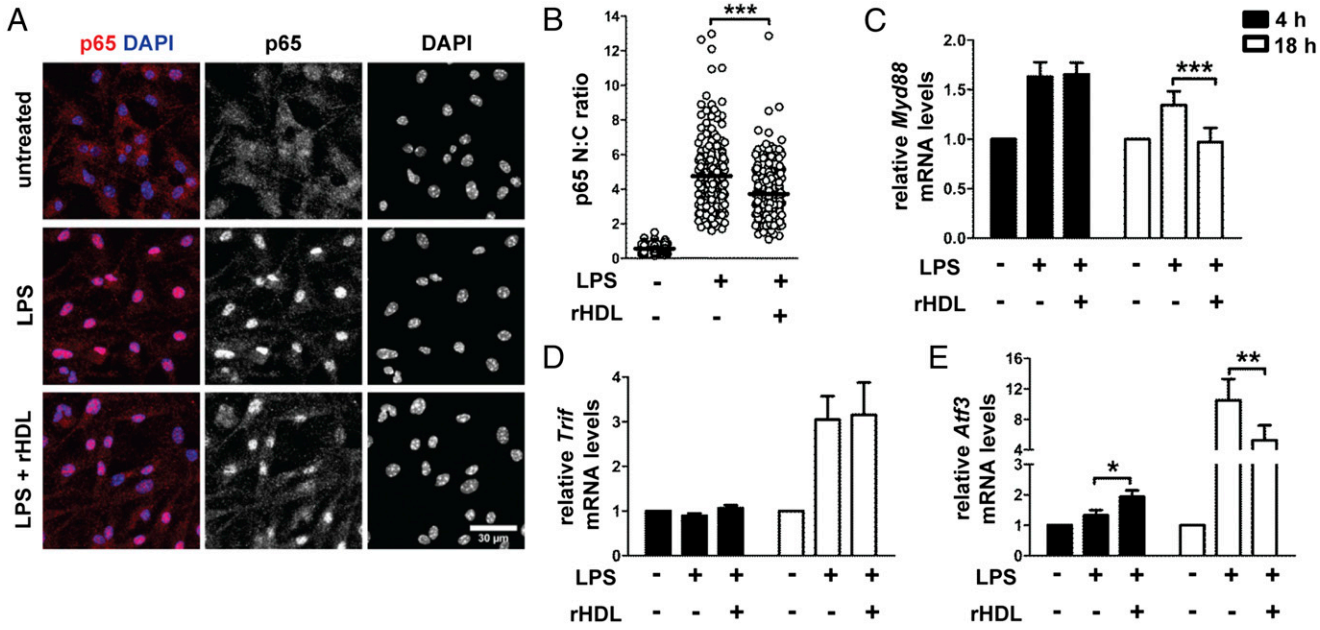

FIGURE 8. rHDL inhibits activation of BMDCs by interfering with the TLR4 pathway. WT BMDCs were stimulated with LPS (0.5 μg/ml) and treated with 4 μM rHDL for the indicated time periods. (**A**) Confocal immunofluorescence microscopy for p65 (red) translocation into the nucleus (DAPI stained, blue) in BMDCs stimulated with LPS for 2 h. Maximum projections of image stacks are shown; representative of two independent experiments. (**B**) Quantification of p65 cell distribution by determining nuclear/cytoplasmic (N:C) ratios of signal intensity at single-cell level. Data are combined of two independent experiments; ***$p < 0.0001$. (**C**–**E**) Relative mRNA levels of *Myd88* (***p = 0.0004), *Trif*, and *Atf3* (*p = 0.0177, **p = 0.0016) after treatment of WT BMDCs (n = 6–8) with rHDL for 4 and 18 h. Results are expressed as mean ± SEM; data are combined from at least three independent experiments.

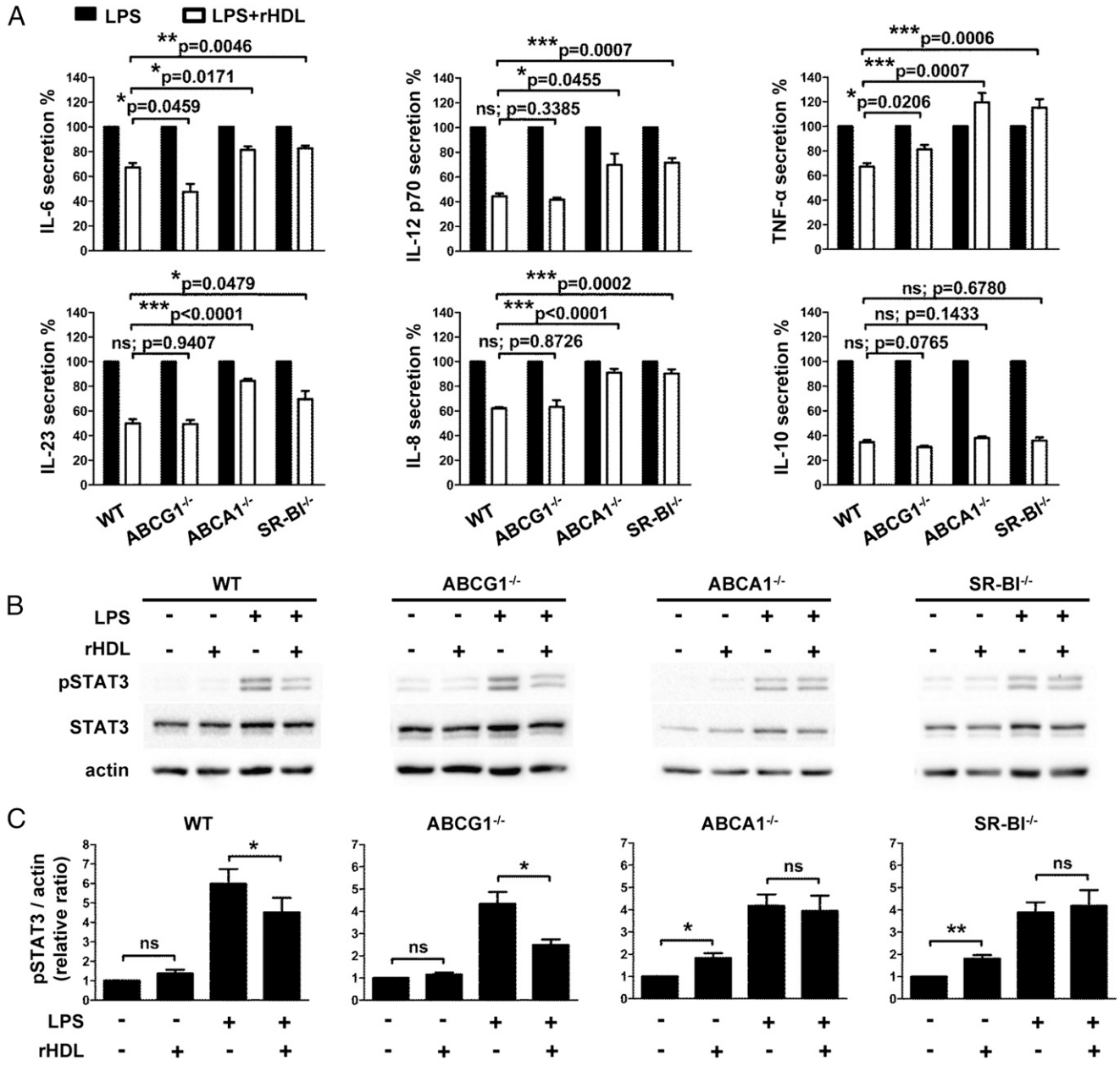

FIGURE 9. The suppressive effect of rHDL on BMDCs activation is dependent on ABCA1 and SR-BI. BMDCs from WT, ABCG1$^{-/-}$, ABCA1$^{-/-}$, and SR-BI$^{-/-}$ mice (n = 4–6/group) were stimulated with LPS (0.5 μg/ml) and treated with 4 μM rHDL for 12 h. (**A**) Levels of IL-6, IL-12 p70, TNF-α, IL-23, IL-8, and IL-10 in culture supernatants of stimulated BMDCs. Percentages of cytokine secretion are shown for LPS-stimulated BMDCs after treatment with rHDL, normalized against untreated LPS-stimulated BMDCs of the same genotype. (**B**) Representative Western blot images of pSTAT3, total STAT3, and actin are shown for each genotype. (**C**) Levels of pSTAT3 and actin were quantified by densitometry and the pSTAT3/actin ratio was calculated. (A and C) Results are expressed as mean ± SEM; data are combined from at least two independent experiments. *$p < 0.05$, **$p < 0.01$, ***$p < 0.001$. ns, not significantly different.

LPS stimulation of DCs activates NF-κB, via either the MyD88- or the TRIF-dependent pathway, which is then recruited to the nucleus to induce inflammatory cytokine gene transcription (39). Our data demonstrate that the anti-inflammatory effects of rHDL on LPS-stimulated BMDCs are mediated through interference with the MyD88/NF-κB pathway. Although the inhibitory actions of apoA-I and HDL on TLR signaling have been previously reported (19, 54), a mechanism by which HDL selectively impedes the MyD88-dependent signaling in DCs has not yet been established. Based on our findings, we speculate that interaction of apoA-I on HDL with cell-surface lipid transporters such as ABCA1 or SR-BI leads to changes in downstream signaling events that, in turn, compromise NF-κB activation and transcriptional upregulation of *Myd88* by LPS. This could be mediated via two alternative, but not necessarily mutually exclusive pathways. One mechanism could involve depletion of lipid rafts from plasma membranes as a result of cholesterol efflux initiated by apoA-I/ABCA1 or apoA-I/SR-BI interactions. Lipid rafts are dynamic structures that have been critically implicated in a variety of cellular processes including signal transduction, endocytosis, vesicular transport, and immunoregulation (55). Treatment of APCs with either HDL or apoA-I has been associated with cholesterol depletion and lipid raft disruption leading to suppressed T cell activation and downregulation of proinflammatory cytokine secretion (56, 57). The second mechanism could involve activation of ABCA1- or SR-BI–induced signaling that results in inhibition

of the TLR-induced response. According to previous studies, interaction of HDL or apoA-I with SR-BI present on endothelial cells activates downstream signaling cascades stimulating a variety of protective cellular responses (58). In addition, apoA-I binding to ABCA1 activates the JAK2/STAT3 pathway in macrophages leading to suppression of LPS-induced inflammatory cytokine production through the action of the mRNA-destabilizing protein, tristetraprolin (59). To date, no signaling events have been reported as a result of interactions between apoA-I or HDL and ABCG1, a transporter known to greatly contribute to the cholesterol efflux process in macrophages. Notably, in our study, the inhibitory properties of rHDL on BMDCs were found to be independent of ABCG1. These data argue against the hypothesis that the anti-inflammatory effects of rHDL on BMDCs are due to cholesterol depletion leading to lipid raft remodeling and favor a model that implicates transporter-specific downstream signaling events.

In a recent study, ATF3, a transcriptional repressor of TLR-stimulated inflammation, was identified as an HDL-inducible target gene that mediated HDL's anti-inflammatory actions in macrophages (40). It was shown that the protective effects of HDL on TLR responses were fully dependent on ATF3 in vitro and in vivo. We show in this study that treatment of LPS-stimulated BMDCs with rHDL caused an upregulation in *Atf3* expression. These data support the notion that an ATF3-dependent mechanism may also be activated by HDL in DCs to constrain the inflammatory response.

In summary, our findings provide evidence for a novel role of HDL in shaping the autoimmune responses both in vivo and in vitro. HDL suppresses adaptive T cell responses by modulating the proinflammatory function of DCs, in an ABCA1- and SR-BI–dependent fashion. The results presented in this article shed light on the mechanism underlying the anti-inflammatory properties of HDL that could aid the development of new therapeutic approaches for autoimmune and other inflammatory diseases.

Acknowledgments

We thank members of the Kardassis and Verginis laboratories for discussions and technical assistance, Prof. Joanna Moschandreas for assistance with biostatistical analyses (University of Crete Medical School), Dr. Joanna Charlton for flow cytometry Abs (Institute of Molecular Biology and Biotechnology), Dr. Panagiotis Fotakis (University of Crete Medical School), Christina Gkolfinopoulou and Dr. Angeliki Chroni (both at Demokritos National Center for Scientific Research) for production and purification of human apoA-I and for protocols, and Ronald van der Sluis and Mara Kröner (Leiden Academic Centre for Drug Research) for preparing bone samples from ABCA1$^{-/-}$, ABCG1$^{-/-}$, and SR-BI$^{-/-}$ mice.

Disclosures

The authors have no financial conflicts of interest.

References

1. Shah, A. S., L. Tan, J. L. Long, and W. S. Davidson. 2013. Proteomic diversity of high density lipoproteins: our emerging understanding of its importance in lipid transport and beyond. *J. Lipid Res.* 54: 2575–2585.
2. Gordon, D. J., and B. M. Rifkind. 1989. High-density lipoprotein—the clinical implications of recent studies. *N. Engl. J. Med.* 321: 1311–1316.
3. Gordon, T., W. P. Castelli, M. C. Hjortland, W. B. Kannel, and T. R. Dawber. 1977. High density lipoprotein as a protective factor against coronary heart disease. The Framingham Study. *Am. J. Med.* 62: 707–714.
4. Riwanto, M., and U. Landmesser. 2013. High density lipoproteins and endothelial functions: mechanistic insights and alterations in cardiovascular disease. *J. Lipid Res.* 54: 3227–3243.
5. Sorci-Thomas, M. G., and M. J. Thomas. 2012. High density lipoprotein biogenesis, cholesterol efflux, and immune cell function. *Arterioscler. Thromb. Vasc. Biol.* 32: 2561–2565.
6. Zannis, V. I., A. Chroni, and M. Krieger. 2006. Role of apoA-I, ABCA1, LCAT, and SR-BI in the biogenesis of HDL. *J. Mol. Med.* 84: 276–294.
7. Yvan-Charvet, L., N. Wang, and A. R. Tall. 2010. Role of HDL, ABCA1, and ABCG1 transporters in cholesterol efflux and immune responses. *Arterioscler. Thromb. Vasc. Biol.* 30: 139–143.
8. Hoekstra, M., M. Van Eck, and S. J. Korporaal. 2012. Genetic studies in mice and humans reveal new physiological roles for the high-density lipoprotein receptor scavenger receptor class B type I. *Curr. Opin. Lipidol.* 23: 127–132.
9. Mineo, C., and P. W. Shaul. 2013. Regulation of signal transduction by HDL. *J. Lipid Res.* 54: 2315–2324.
10. Lüscher, T. F., U. Landmesser, A. von Eckardstein, and A. M. Fogelman. 2014. High-density lipoprotein: vascular protective effects, dysfunction, and potential as therapeutic target. *Circ. Res.* 114: 171–182.
11. Hahn, B. H., J. Grossman, B. J. Ansell, B. J. Skaggs, and M. McMahon. 2008. Altered lipoprotein metabolism in chronic inflammatory states: proinflammatory high-density lipoprotein and accelerated atherosclerosis in systemic lupus erythematosus and rheumatoid arthritis. *Arthritis Res. Ther.* 10: 213.
12. Catapano, A. L., A. Pirillo, F. Bonacina, and G. D. Norata. 2014. HDL in innate and adaptive immunity. *Cardiovasc. Res.* 103: 372–383.
13. Feldmann, M., F. M. Brennan, and R. N. Maini. 1996. Rheumatoid arthritis. *Cell* 85: 307–310.
14. Firestein, G. S. 2003. Evolving concepts of rheumatoid arthritis. *Nature* 423: 356–361.
15. McInnes, I. B., and G. Schett. 2007. Cytokines in the pathogenesis of rheumatoid arthritis. *Nat. Rev. Immunol.* 7: 429–442.
16. Robertson, J., M. J. Peters, I. B. McInnes, and N. Sattar. 2013. Changes in lipid levels with inflammation and therapy in RA: a maturing paradigm. *Nat Rev Rheumatol* 9: 513–523.
17. Charles-Schoeman, C., J. Watanabe, Y. Y. Lee, D. E. Furst, S. Amjadi, D. Elashoff, G. Park, M. McMahon, H. E. Paulus, A. M. Fogelman, and S. T. Reddy. 2009. Abnormal function of high-density lipoprotein is associated with poor disease control and an altered protein cargo in rheumatoid arthritis. *Arthritis Rheum.* 60: 2870–2879.
18. Charles-Schoeman, C., M. L. Banquerigo, S. Hama, M. Navab, G. S. Park, B. J. Van Lenten, A. C. Wagner, A. M. Fogelman, and E. Brahn. 2008. Treatment with an apolipoprotein A-1 mimetic peptide in combination with pravastatin inhibits collagen-induced arthritis. *Clin. Immunol.* 127: 234–244.
19. Wu, B. J., K. L. Ong, S. Shrestha, K. Chen, F. Tabet, P. J. Barter, and K. A. Rye. 2014. Inhibition of arthritis in the Lewis rat by apolipoprotein A-I and reconstituted high-density lipoproteins. *Arterioscler. Thromb. Vasc. Biol.* 34: 543–551.
20. Guermonprez, P., J. Valladeau, L. Zitvogel, C. Théry, and S. Amigorena. 2002. Antigen presentation and T cell stimulation by dendritic cells. *Annu. Rev. Immunol.* 20: 621–667.
21. Afkarian, M., J. R. Sedy, J. Yang, N. G. Jacobson, N. Cereb, S. Y. Yang, T. L. Murphy, and K. M. Murphy. 2002. T-bet is a STAT1-induced regulator of IL-12R expression in naïve CD4+ T cells. *Nat. Immunol.* 3: 549–557.
22. Nurieva, R., X. O. Yang, G. Martinez, Y. Zhang, A. D. Panopoulos, L. Ma, K. Schluns, Q. Tian, S. S. Watowich, A. M. Jetten, and C. Dong. 2007. Essential autocrine regulation by IL-21 in the generation of inflammatory T cells. *Nature* 448: 480–483.
23. Veldhoen, M., R. J. Hocking, C. J. Atkins, R. M. Locksley, and B. Stockinger. 2006. TGFbeta in the context of an inflammatory cytokine milieu supports de novo differentiation of IL-17-producing T cells. *Immunity* 24: 179–189.
24. McNeish, J., R. J. Aiello, D. Guyot, T. Turi, C. Gabel, C. Aldinger, K. L. Hoppe, M. L. Roach, L. J. Royer, J. de Wet, et al. 2000. High density lipoprotein deficiency and foam cell accumulation in mice with targeted disruption of ATP-binding cassette transporter-1. *Proc. Natl. Acad. Sci. USA* 97: 4245–4250.
25. Rigotti, A., B. L. Trigatti, M. Penman, H. Rayburn, J. Herz, and M. Krieger. 1997. A targeted mutation in the murine gene encoding the high density lipoprotein (HDL) receptor scavenger receptor class B type I reveals its key role in HDL metabolism. *Proc. Natl. Acad. Sci. USA* 94: 12610–12615.
26. Chroni, A., H. Y. Kan, K. E. Kypreos, I. N. Gorshkova, A. Shkodrani, and V. I. Zannis. 2004. Substitutions of glutamate 110 and 111 in the middle helix 4 of human apolipoprotein A-I (apoA-I) by alanine affect the structure and in vitro functions of apoA-I and induce severe hypertriglyceridemia in apoA-I-deficient mice. *Biochemistry* 43: 10442–10457.
27. Matz, C. E., and A. Jonas. 1982. Micellar complexes of human apolipoprotein A-I with phosphatidylcholines and cholesterol prepared from cholate-lipid dispersions. *J. Biol. Chem.* 257: 4535–4540.
28. Laccotripe, M., S. C. Makrides, A. Jonas, and V. I. Zannis. 1997. The carboxyl-terminal hydrophobic residues of apolipoprotein A-I affect its rate of phospholipid binding and its association with high density lipoprotein. *J. Biol. Chem.* 272: 17511–17522.
29. Asztalos, B. F., C. H. Sloop, L. Wong, and P. S. Roheim. 1993. Two-dimensional electrophoresis of plasma lipoproteins: recognition of new apo A-I-containing subpopulations. *Biochim. Biophys. Acta* 1169: 291–300.
30. Freeman, L. A. 2013. Native-native 2D gel electrophoresis for HDL subpopulation analysis. *Methods Mol. Biol.* 1027: 353–367.
31. Lutz, M. B., N. Kukutsch, A. L. Ogilvie, S. Rössner, F. Koch, N. Romani, and G. Schuler. 1999. An advanced culture method for generating large quantities of highly pure dendritic cells from mouse bone marrow. *J. Immunol. Methods* 223: 77–92.
32. Zal, T., A. Volkmann, and B. Stockinger. 1994. Mechanisms of tolerance induction in major histocompatibility complex class II-restricted T cells specific for a blood-borne self-antigen. *J. Exp. Med.* 180: 2089–2099.
33. Williamson, R., D. Lee, J. Hagaman, and N. Maeda. 1992. Marked reduction of high density lipoprotein cholesterol in mice genetically modified to lack apolipoprotein A-I. *Proc. Natl. Acad. Sci. USA* 89: 7134–7138.
34. Iliopoulos, D., M. Kavousanaki, M. Ioannou, D. Boumpas, and P. Verginis. 2011. The negative costimulatory molecule PD-1 modulates the balance between immunity and tolerance via miR-21. *Eur. J. Immunol.* 41: 1754–1763.

35. van den Berg, W. B., L. A. Joosten, and P. L. van Lent. 2007. Murine antigen-induced arthritis. *Methods Mol. Med.* 136: 243–253.
36. Lubberts, E., M. I. Koenders, and W. B. van den Berg. 2005. The role of T-cell interleukin-17 in conducting destructive arthritis: lessons from animal models. *Arthritis Res. Ther.* 7: 29–37.
37. Schulze-Koops, H., and J. R. Kalden. 2001. The balance of Th1/Th2 cytokines in rheumatoid arthritis. *Best Pract. Res. Clin. Rheumatol.* 15: 677–691.
38. Banchereau, J., and R. M. Steinman. 1998. Dendritic cells and the control of immunity. *Nature* 392: 245–252.
39. Takeda, K., and S. Akira. 2004. TLR signaling pathways. *Semin. Immunol.* 16: 3–9.
40. De Nardo, D., L. I. Labzin, H. Kono, R. Seki, S. V. Schmidt, M. Beyer, D. Xu, S. Zimmer, C. Lahrmann, F. A. Schildberg, et al. 2014. High-density lipoprotein mediates anti-inflammatory reprogramming of macrophages via the transcriptional regulator ATF3. *Nat. Immunol.* 15: 152–160.
41. Kim, K. D., H. Y. Lim, H. G. Lee, D. Y. Yoon, Y. K. Choe, I. Choi, S. G. Paik, Y. S. Kim, Y. Yang, and J. S. Lim. 2005. Apolipoprotein A-I induces IL-10 and PGE2 production in human monocytes and inhibits dendritic cell differentiation and maturation. *Biochem. Biophys. Res. Commun.* 338: 1126–1136.
42. Perrin-Cocon, L., O. Diaz, M. Carreras, S. Dollet, A. Guironnet-Paquet, P. André, and V. Lotteau. 2012. High-density lipoprotein phospholipids interfere with dendritic cell Th1 functional maturation. *Immunobiology* 217: 91–99.
43. Lee, H. K., L. M. Mattei, B. E. Steinberg, P. Alberts, Y. H. Lee, A. Chervonsky, N. Mizushima, S. Grinstein, and A. Iwasaki. 2010. In vivo requirement for Atg5 in antigen presentation by dendritic cells. *Immunity* 32: 227–239.
44. Trombetta, E. S., and I. Mellman. 2005. Cell biology of antigen processing in vitro and in vivo. *Annu. Rev. Immunol.* 23: 975–1028.
45. Muller, C., R. Salvayre, A. Nègre-Salvayre, and C. Vindis. 2011. HDLs inhibit endoplasmic reticulum stress and autophagic response induced by oxidized LDLs. *Cell Death Differ.* 18: 817–828.
46. Menges, M., S. Rössner, C. Voigtländer, H. Schindler, N. A. Kukutsch, C. Bogdan, K. Erb, G. Schuler, and M. B. Lutz. 2002. Repetitive injections of dendritic cells matured with tumor necrosis factor alpha induce antigen-specific protection of mice from autoimmunity. *J. Exp. Med.* 195: 15–21.
47. Verginis, P., H. S. Li, and G. Carayanniotis. 2005. Tolerogenic semimature dendritic cells suppress experimental autoimmune thyroiditis by activation of thyroglobulin-specific CD4+CD25+ T cells. *J. Immunol.* 174: 7433–7439.
48. Ehrenstein, M. R., J. G. Evans, A. Singh, S. Moore, G. Warnes, D. A. Isenberg, and C. Mauri. 2004. Compromised function of regulatory T cells in rheumatoid arthritis and reversal by anti-TNFalpha therapy. *J. Exp. Med.* 200: 277–285.
49. Korn, T., J. Reddy, W. Gao, E. Bettelli, A. Awasthi, T. R. Petersen, B. T. Bäckström, R. A. Sobel, K. W. Wucherpfennig, T. B. Strom, et al. 2007. Myelin-specific regulatory T cells accumulate in the CNS but fail to control autoimmune inflammation. *Nat. Med.* 13: 423–431.
50. Wilhelm, A. J., M. Zabalawi, J. M. Grayson, A. E. Weant, A. S. Major, J. Owen, M. Bharadwaj, R. Walzem, L. Chan, K. Oka, et al. 2009. Apolipoprotein A-I and its role in lymphocyte cholesterol homeostasis and autoimmunity. *Arterioscler. Thromb. Vasc. Biol.* 29: 843–849.
51. Wilhelm, A. J., M. Zabalawi, J. S. Owen, D. Shah, J. M. Grayson, A. S. Major, S. Bhat, D. P. Gibbs, Jr., M. J. Thomas, and M. G. Sorci-Thomas. 2010. Apolipoprotein A-I modulates regulatory T cells in autoimmune LDLr$^{-/-}$, ApoA-I$^{-/-}$ mice. *J. Biol. Chem.* 285: 36158–36169.
52. Levine, D. M., T. S. Parker, T. M. Donnelly, A. Walsh, and A. L. Rubin. 1993. In vivo protection against endotoxin by plasma high density lipoprotein. *Proc. Natl. Acad. Sci. USA* 90: 12040–12044.
53. Wang, Y., X. Zhu, G. Wu, L. Shen, and B. Chen. 2008. Effect of lipid-bound apoA-I cysteine mutants on lipopolysaccharide-induced endotoxemia in mice. *J. Lipid Res.* 49: 1640–1645.
54. Suzuki, M., D. K. Pritchard, L. Becker, A. N. Hoofnagle, N. Tanimura, T. K. Bammler, R. P. Beyer, R. Bumgarner, T. Vaisar, M. C. de Beer, et al. 2010. High-density lipoprotein suppresses the type I interferon response, a family of potent antiviral immunoregulators, in macrophages challenged with lipopolysaccharide. *Circulation* 122: 1919–1927.
55. Horejsi, V., and M. Hrdinka. 2014. Membrane microdomains in immunoreceptor signaling. *FEBS Lett.* 588: 2392–2397.
56. Smythies, L. E., C. R. White, A. Maheshwari, M. N. Palgunachari, G. M. Anantharamaiah, M. Chaddha, A. R. Kurundkar, and G. Datta. 2010. Apolipoprotein A-I mimetic 4F alters the function of human monocyte-derived macrophages. *Am. J. Physiol. Cell Physiol.* 298: C1538–C1548.
57. Wang, S. H., S. G. Yuan, D. Q. Peng, and S. P. Zhao. 2012. HDL and ApoA-I inhibit antigen presentation-mediated T cell activation by disrupting lipid rafts in antigen presenting cells. *Atherosclerosis* 225: 105–114.
58. Al-Jarallah, A., and B. L. Trigatti. 2010. A role for the scavenger receptor, class B type I in high density lipoprotein dependent activation of cellular signaling pathways. *Biochim. Biophys. Acta* 1801: 1239–1248.
59. Tang, C., Y. Liu, P. S. Kessler, A. M. Vaughan, and J. F. Oram. 2009. The macrophage cholesterol exporter ABCA1 functions as an anti-inflammatory receptor. *J. Biol. Chem.* 284: 32336–32343.